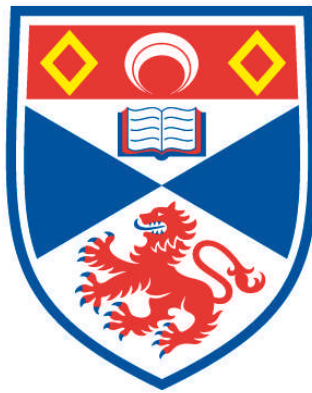


**GEOLOGY OF THE ORDOVICIAN ROCKS BETWEEN
LEADHILLS AND ABINGTON, LANARKSHIRE**

Barry C. Hepworth

**A Thesis Submitted for the Degree of PhD
at the
University of St Andrews**



1981

**Full metadata for this item is available in
Research@StAndrews:FullText
at:**

<http://research-repository.st-andrews.ac.uk/>

Please use this identifier to cite or link to this item:

<http://hdl.handle.net/10023/7132>

This item is protected by original copyright

GEOLOGY OF THE ORDOVICIAN
ROCKS BETWEEN LEADHILLS
AND ABINGTON, LANARKSHIRE.

by

Barry C. Hepworth

Thesis presented for the degree of Doctor of Philosophy in the
Faculty of Science of the University of St. Andrews.



November, 1981

To Jane and my parents

Only let the source be pure.

Béla Bartók

ABSTRACT

NE-SW faults in the Abington area of the Northern Belt of the Southern Uplands define blocks up to 3.2 km wide. The strata, folded and locally overturned, young predominantly to the NW but blocks to the SW contain younger sequences. Analogous configurations occur in modern accretionary margins. The oldest rocks, generally of pelagic and hemipelagic origin, are Arenig basalts, dolerites, cherts and brown mudstones underlying red mudstones, possibly Llanvirn, and black fossiliferous mudstones and cherts of Llandeilo and Caradoc age.

Trench sediments overlying pelagic sequences represent a range of depositional mechanisms. Rudites and associated fine-grained lithologies of lateral origin relate to a lower trench-slope canyon system, whilst axially transported sands, originating on the lower trench slope, were deposited by turbidity currents and related flows. Sandstone petrography varies markedly across strike, with quartz-rich compositions suggesting a recycled orogen source, and ferromagnesian-rich compositions a dissected magmatic arc provenance.

Faults, initially low-angle thrusts, facilitated thrust nappe formation; faults and bedding were rotated through the vertical within the accretionary complex, predating or accompanying slaty cleavage development. Soft sediment

deformation, two fold phases and a kink-band set are recognised. Imbricate fault zones, located in incompetent pelagic sequences, are equated with tectonic mélange of other accretionary complexes.

Index minerals, illite crystallinity and 'vitrinite' reflectance establish metamorphic grade as prehnite-pumpellyite facies.

CONTENTS

LIST OF FIGURES
LIST OF TABLES
LIST OF PLATES
LIST OF APPENDICES

	<u>Page</u>
CHAPTER 1: INTRODUCTION	1
1.1 LOCATION OF AREA	1
1.2 HISTORY OF PREVIOUS RESEARCH IN THE SOUTHERN UPLANDS	2
1.3 PREVIOUS RESEARCH IN THE ABINGTON DISTRICT	7
CHAPTER 2: STRATIGRAPHY	12
2.1 INTRODUCTION	12
2.1.1 General stratigraphy	14
2.2 MILL BURN BLOCK	15
2.2.1 Mill Burn Member	16
2.2.2 Haggis Rock	17
2.2.3 Relationship between major litho- stratigraphical units	18
2.2.4 Local correlations	18
2.3 CRAWFORDJOHN BLOCK	19
2.3.1 Lithologies of the Shield Burn Imbricate Zone	19
2.3.2 Crawfordjohn Formation	23
2.3.3 Relationship between major litho- stratigraphical units	24
2.3.4 Local correlations	24
2.4 ABINGTON BLOCK	25
2.4.1 Raven Gill Formation	27
2.4.2 Kirkton beds	31
2.4.3 Moffat Shales	33
2.4.4 Abington Formation	36
2.4.5 Relationships among major litho- stratigraphical units	37
2.4.6 Local and regional correlations	37
2.5 ELVANFOOT BLOCK	39
2.5.1 Moffat Shales	40
2.5.2 Elvan Formation	41
2.5.3 Glencaple Formation	42
2.5.4 Relationships among major litho- stratigraphical units	42

	<u>Page</u>
2.5.5 Local and regional correlations	44
2.6 DISCUSSION	44
2.6.1 General	44
2.6.2 West Nithsdale succession	46
2.6.3 Clydesdale succession	49
 CHAPTER 3: SANDSTONE PETROGRAPHY	 51
3.1 INTRODUCTION	51
3.2 MODAL ANALYSIS	51
3.2.1 Results	53
3.3 SUMMARY OF PETROGRAPHY OF THE LITHO- STRATIGRAPHICAL UNITS	57
3.3.1 Haggis Rock	57
3.3.2 Crawfordjohn Formation	58
3.3.3 Abington Formation	58
3.3.4 Glencaple Formation	59
3.3.5 Elvan Formation	59
3.4 COMPARISON WITH OTHER AREAS	60
 CHAPTER 4: SEDIMENTOLOGY	 63
4.1 INTRODUCTION	63
4.2 DESCRIPTION AND INTERPRETATION OF SEDIMENTARY FACIES	65
4.2.1 Cobbly siltstones	65
4.2.2 Disorganised conglomerates	67
4.2.3 Organised pebbly and granular sandstones	69
4.2.4 Ungraded sandstones	72
4.2.5 Graded sandstones	77
4.2.6 'Base-missing' sandstones	80
4.2.7 Laminites	81
4.2.8 Mudstones	83
4.2.9 Cherts	84
4.2.10 Disturbed beds	88
4.3 STRATIGRAPHICAL DISTRIBUTION OF FACIES	92
4.3.1 Mill Burn Block	92
4.3.2 Crawfordjohn Block	92
4.3.3 Abington Block	93
4.3.4 Elvanfoot Block	94
4.4 PALAEOCURRENT ANALYSIS	95
 CHAPTER 5: STRUCTURAL GEOLOGY	 99
5.1 PRIMARY DEFORMATION (D ₁)	99

	<u>Page</u>
5.1.1 S ₁ cleavage	99
5.1.2 F ₁ folds	102
5.2 SECONDARY DEFORMATION (D ₂)	108
5.3 KINK-BANDS (D ₃)	109
5.4 FAULTING	110
5.4.1 Leadhills Imbricate Zone	111
5.4.2 Shield Burn Imbricate Zone	115
5.4.3 Fardingmullach Imbricate Zone	116
5.4.4 Lateral continuation of imbricate zones	117
5.4.5 Wrench faults	119
5.4.6 Minor faults	120
5.4.7 Joints	123
5.5 STRUCTURAL INTERPRETATION OF MOFFAT SHALE INLIERS	123
5.6 DEFORMATIONAL HISTORY	127
 CHAPTER 6: METAMORPHISM	 130
6.1 PETROGRAPHY	130
6.1.1 Sandstones	130
6.1.2 Fine-grained sediments	134
6.1.3 Metadolerites, spilites and lithic tuffs	136
6.2 X-RAY DIFFRACTION STUDIES OF SHEET SILICATES	137
6.2.1 Sheet silicate assemblages	138
6.2.2 10Å mica	138
6.2.3 Chlorite	141
6.2.4 Illite crystallinity: methods	142
6.2.5 Illite crystallinity: results	146
6.3 MINERAL CHEMISTRY	148
6.4 GRAPTOLITE REFLECTANCE	154
6.4.1 Introduction	154
6.4.2 Results	156
6.5 DISCUSSION	158
6.5.1 Correlation of techniques used for establishing metamorphic grade	158
6.5.2 Physiochemical conditions of meta- morphism	159
6.5.3 Comparison with other areas	161
 CHAPTER 7: DISCUSSION	 165
7.1 PLATE TECTONIC FRAMEWORK	165

	<u>Page</u>
7.2 PETROGRAPHIC COMPARISONS WITH MODERN AND ANCIENT FORE-ARC REGIONS	166
7.3 TRENCH SEDIMENTATION	173
7.4 FORE-ARC TECTONICS AND LOW-GRADE METAMORPHISM	183
7.5 ABSTRACT	188
ACKNOWLEDGEMENTS	190
REFERENCES	192
APPENDICES	

LIST OF FIGURES

	<u>Between pages</u>
1 Location of the Leadhills-Abington district	1-2
2 Correlation of Ordovician series boundaries	13-14
3 Major structural features	14-15
4 Distribution of formations	14-15
5 Lithostratigraphy of the fault blocks	15-16
6 Correlation of lithostratigraphical units used by previous authors in the Northern Belt	19-20
7 Ordovician stratigraphical sequences within fault blocks from the Northern Belt	47-48
8 Point count data: Qm-F-Lt plot	54-55
9 Point count data: Q-F-L plot	55-56
10 Point count data: Q-M-F plot	55-56
11 Point count data: Qm-F-FM plot	56-57
12 Point count data: Qm-P-K plot	56-57
13 Point count data: Lm-Lv-Ls plot	57-58
14 Point count data: Qp-Lvm-Lsm plot	57-58
15 Bed thickness data: (a) Crawfordjohn and Abington Formations (log./log. plot) (b) Abington Formation, very thick- and thick-bedded facies (log./log. plot) (c) Abington Formation (probability plot)	92-93
16 Bed thickness data: (a) Elvan and Glencaple formations (b) Glencaple Formation (c) Elvan Formation. Log./log. plots.	94-95
17 Stereograms of poles to bedding: (a) Abington and Elvanfoot Blocks (b) Mill Burn structural subarea	103-104
18 Stereograms of fold data, Abington Block: (a) F1 fold plunges (b) F1 fold plunges (contoured) (c) poles to F1 axial surfaces (d) Elvanfoot Block: poles to F1 axial surfaces and fold plunges	103-104

19	Stereograms of fold data, Mill Burn structural subarea: (a) F1 fold plunges (b) F1 fold plunges (contoured) (c) poles to F1 axial surfaces (d) poles to F1 axial surfaces (contoured)	103-104
20	Structural section in Glencaple Burn	104-105
21	Stereograms of cleavage data: (a) poles to S1. Bedding/cleavage intersection lineations (stereographically derived) (b) SE-younging beds (c) NW-younging beds	105-106
22	Stereogram of F2 folds (a) Abington Block (b) Mill Burn subarea	108-109
23	Geometrical configuration of conjugate kink-band system	109-110
24	Distribution of stratigraphical units within the Leadhills Imbricate Zone	Back cover pocket
25	Composite structural profile across the Leadhills Imbricate Zone	111-112
26	Stereograms: (a) poles to fault planes, entire area (b) poles to fault planes with known sense of displacement	121-122
27	Stereograms of slickensides on: (a) strike-parallel faults (b) joint-parallel faults (c) faults at high angles to bedding	121-122
28	Stereograms of poles to fault planes: (a) Abington Block (b) Leadhills Imbricate Zone (c) Elvanfoot Block (excluding Fardingmullach IZ).	122-123
29	Stereogram of poles to joint planes, entire area	122-123
30	Schematic diagram illustrating possible structural locations at which imbricate zones could form.	125-126
31	Metamorphic map of the Abington district	130-131
32	X.R.D. scan of -2 μ m fraction of mudstone, dry run, random orientation	138-139
33	(a) X.R.D. scans of mudstone, showing the effects of different treatments (b) Scan of well orientated mudstone, showing illite (002) peak	138-139

Between pages

34	(a) Histogram of d(002)2M spacing (b) Histogram of <u>b</u> parameter of illites	139-140
35	Definition of parameters used in text with reference to illite	143-144
36	Esquevin diagram showing illite crystallinity results	146-147
37	Effects of depth of burial on clay mineral assemblages	148-149
38	Pumpellyite analyses: Al ³⁺ , Mg ²⁺ , Fetot ²⁺ cation proportions	149-150
39	Pumpellyite analyses: wt % Fetot against wt % Al ₂ O ₃	149-150
40	Prehnite analyses: Al ³⁺ , Ca ²⁺ , Fetot ³⁺ cation proportions	150-151
41	Chlorite analyses plotted on Hey diagram	150-151
42	Plagioclase analyses: Na ⁺ , Ca ²⁺ , K ⁺ cation proportions	151-152
43	Pyroxene analyses plotted on part of the pyroxene quadrilateral	152-153
44	Classification of amphiboles in Elvan Formation sandstones	153-154
45	Representative chart recordings of graptolite reflectance measurements from three localities	156-157
46	Chart recording of reflectance measurements on graptolite rotated through 360°: (a) section of graptolite perpendicular to bedding (b) section parallel to bedding	156-157
47	Comparison of point count results with compositional means of modern deep-sea sands from known tectonic environments: (a) Qm-F-Lt plot (b) Q-F-L plot	167-168
48	Compositional plots for mean framework modes for sandstones from different tectonic environments: (a) Q-F-L plot (b) Qm-F-Lt plot (c) Qp-Lvm-Lsm plot	168-169

- 49 Possible ocean/continent configurations to account for petrographic provinces: (a) marginal ocean basin (b) passive margin with seamount (c) remnant ocean basin 169-170
- 50 Schematic diagram of the distribution of sedimentary facies within the Abington area 178-179

LIST OF TABLES

	<u>Between pages</u>
1 Comparison of greywacke formation means	60-61
2 Summary of sedimentological characteristics of lithostratigraphical units	92-93
3 Current data	96-97
4 Facing directions of bedding on cleavage for each structural block	105-106
5 Summary of deformational history	127-128
6 Comparison between means of runs of Kübler standards made at Neuchâtel and St. Andrews	145-146
7 Illite crystallinity results as measured using Kübler and Weber indices	146-147
8 Correlation of anchizone limits defined by previous authors	146-147
9 Summary of microprobe analyses of metamorphic minerals	148-149
10 Variable statistics for maximum reflectance values for sample 29	157-158
11 Graptolite reflectance values from Moffat Shales in the Leadhills Imbricate Zone	157-158

LIST OF PLATES

	<u>Between pages</u>
1 Interbedded chert and brown mudstone, Raven Gill Formation	27-28
2 Massive lava and brown mudstone, Raven Gill Formation	27-28
3 Brown mudstone interbedded with chert, Raven Gill Formation	30-31
4 Black mudstone interbedded with pervasively veined radiolarian chert (photomicrograph)	30-31
5 Black mudstones of <u>D. clingani</u> age	34-35
6 Thin ash band within black mudstone sequence	34-35
7 Black cherts with thin ?ash bands	35-36
8 Transition zone between black cherts and black mudstones	35-36
9 Tae turbidites of the Abington Formation	37-38
10 Thick-bedded, massive sandstone of the Elvan Formation	37-38
11 Conformable contact between Moffat Shale and the Elvan Formation	44-45
12 Parallel-laminated sandstone clast in cobble siltstone, Glencaple Formation	65-66
13 Disorganised conglomerate, Haggis Rock Member	65-66
14 Delayed grading at base of organised granule sandstone, Glencaple Formation	70-71
15 Thick-bedded, organised, pebbly sandstone, Glencaple Formation	70-71
16 'Base-missing' sandstone, Abington Formation	80-81
17 Disturbed facies, Glencaple Formation	80-81
18 Disturbed facies, Glencaple Formation	90-91
19 Ball-and-pillow structure in disrupted sandstone bed, Glencaple Formation	90-91

Between pages

20	Thinning and fining upwards sequence in sandstones, Abington Formation	94-95
21	Strong S1 cleavage in basal Elvan Formation sandstone	100-101
22	Grumous texture in chert in the vicinity of the Raven Gill Fault	100-101
23	F1 fold, Mill Burn subarea	106-107
24	Downward facing bedding/cleavage relationships, Mill Burn subarea	106-107
25	Pumpellyite-albite amygdale, Raven Gill Formation	136-137

LIST OF APPENDICES

- 1 List of graptolite specimens and zone identification
- 2 Four stratigraphical sections through the Raven Gill Formation in Raven Gill
- 3 Stratigraphical log of the Raven Gill Formation in Glencaple Burn
- 4 Sandstone point count data
- 5 Petrography and stratigraphical distribution of sandstone clasts
- 6 Sedimentological profile of the Abington Formation in Craighead Quarry
- 7 Field map of structures in Mill Burn
- 8 Structural profile through part of the Leadhills Imbricate Zone in Cleuch Burn
- 9 Structural profile through part of the Leadhills Imbricate Zone in Bellgill Burn and Middle Grain
- 10 Structural profile through part of the Leadhills Imbricate Zone in Kirk Gill
- 11 Preparation of $-2\mu\text{m}$ fraction for X-ray diffraction studies
- 12 Instrumental conditions used for clay mineral determinations
- 13 $d(002)2M$, $d(060)$ and b values of illite
- 14 Location of first four basal reflections of chlorite and peak position of (001) after ethylene glycol and heat treatment
- 15 Chlorite species, as inferred from intensity ratios of (001) to (005) basal reflections
- 16 Illite crystallinity: experimental methods and factors controlling half-peak width
- 17 Emplacement of wedge-shaped standard (Kübler 33) on specimen holder
- 18 Measurement of illite crystallinity
- 19 Accuracy and precision of electron microprobe data
- 20 Pumpellyite analyses (electron microprobe)
- 21 Prehnite analyses (electron microprobe)

- 22 Chlorite analyses (electron microprobe)
- 23 Plagioclase feldspar analyses (electron microprobe)
- 24 Pyroxene analyses (electron microprobe)
- 25 Amphibole analyses (electron microprobe)
- 26 Phengite analyses (electron microprobe)
- 27 Sample preparation techniques for graptolite reflectance study

CHAPTER 1: INTRODUCTION

1.1 LOCATION OF AREA

Lying entirely within the Northern Belt of the Southern Uplands (Peach & Horne 1899), the area studied occupies some 60 sq. km of hilly moorland in the southern part of Lanark District (Strathclyde Region). The approximate limits of the study area (Fig. 1) are:

- to the north: Southern Uplands Fault (NS862236-914266),
- to the east: the A74 trunk road and in part the 1976 British Gas pipeline section (NS914266-943163),
- to the south: Windgate and Lead Burns (NS943163-902134),
- to the west: the Leadhills-Crawfordjohn road (NS943163-862236).

Relief varies from a minimum of 236 m in the NE of the area up to a maximum elevation of 553 m on Wellgrain Dod (NS902179). Heather and glacial drift largely obscure the rocks, and exposure is restricted principally to stream sections which are small, few in number and often deeply weathered.

Ordovician basic igneous rocks, cherts, mudstones and sandstones form the bulk of the succession, and were

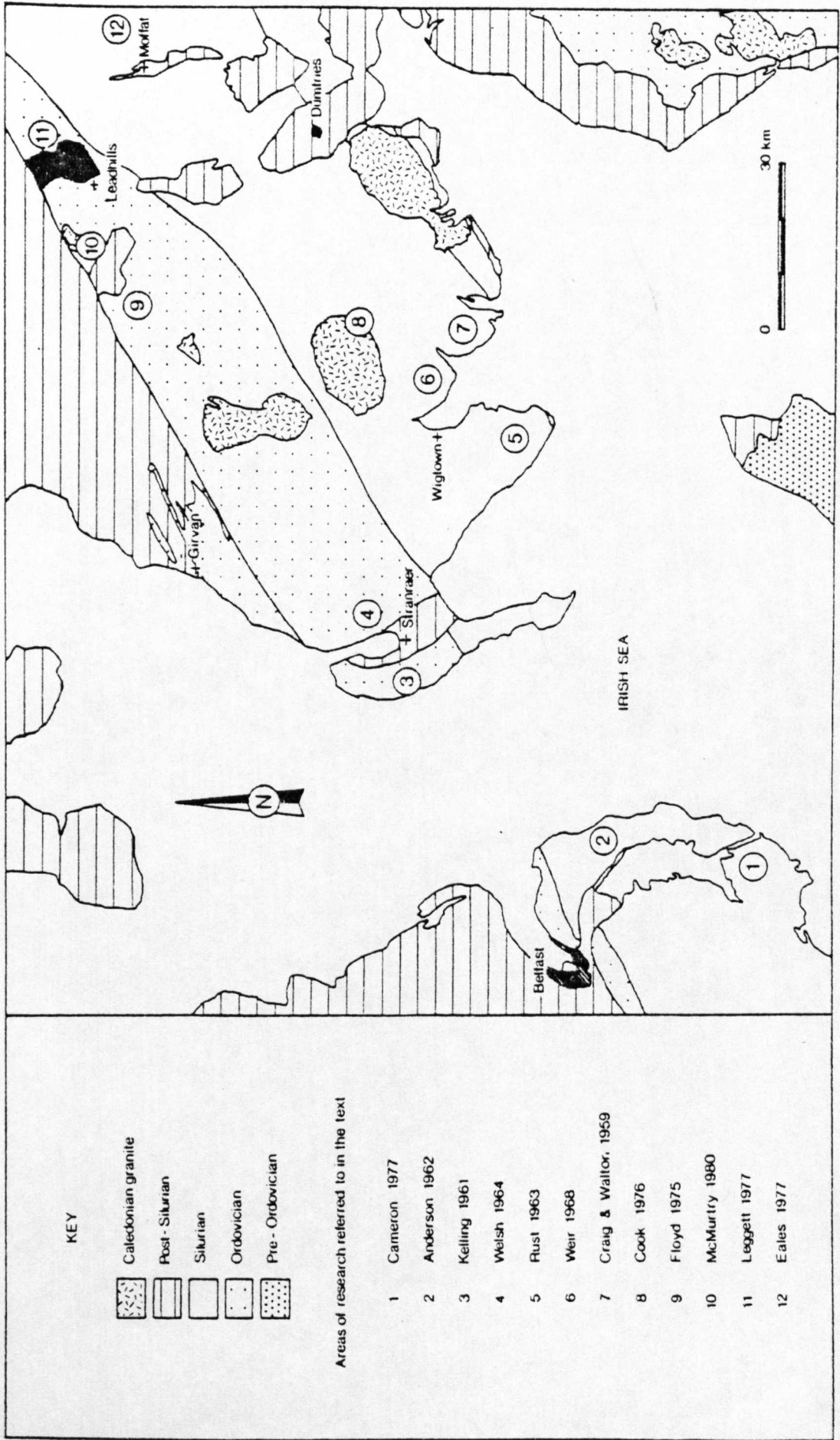


Fig. 1: Location of the Leadhills-Abington district (shaded in black) showing areas of previous research

deformed during the Caledonian orogeny into the present NE-SW strike and vertical orientation. Problems dealt with in the following text include:

- the stratigraphy of the part of the Northern Belt examined,
- clastic sedimentation accompanying the development of an accretionary fore-arc complex,
- the deformational mechanisms and structure of the area, in particular the nature of the Leadhills 'Line',
- regional metamorphism above an ancient subduction zone.

All of these are pertinent to the understanding of the Southern Uplands within the framework of plate tectonic theory.

Grid references should be prefixed by the letters NS unless stated.

1.2 HISTORY OF PREVIOUS RESEARCH IN THE SOUTHERN UPLANDS

The Southern Uplands have been an area of active research since the later years of the eighteenth century when Hutton ('Theory of the Earth', 1795) recognised them as being a tract of schistose mountains wherein strata are highly inclined or vertical.

Attempts to unravel the complex stratigraphy were made by such distinguished workers as Nicol (1848), Sedgwick (1850), Harkness (1851), Murchison (1851), Geikie (1871) and Lapworth (1874). These pioneers regarded the thick greywacke sequences of the central Southern Uplands ('Hawick Rocks') as being the oldest rock unit, overlain by at least two separate units of Moffat Shales and further greywackes - this interpretation necessitated the presence of a 'great anticline' (cf. Harkness 1856), extending between Berwick and Dumfries with the Hawick Rocks occupying the anticlinal core.

Modern understanding of the stratigraphy of the Southern Uplands owes most to the endeavours of Lapworth who established the internal stratigraphy of the Moffat Shales, using graptolites as the main tool of subdivision. He substantially modified the notion of a 'great anticline', regarding the Moffat Shales as the lowest stratigraphical unit in the Southern Uplands and placing the Hawick Rocks above the Moffat Shales conformably below upper Silurian strata (Lapworth 1876). The linear outcrop belt of Moffat Shales extending from Portpatrick through Leadhills to the Lammermuirs, termed the Leadhills Line (Lapworth 1889, p. 62), was therefore believed to be a narrow inlier forming the core of a large-scale tightly folded anticline (endocline or anticlinorium) with a corresponding syncline (exocline or

synclinatorium) to the SE. The Leadhills Line separated a northern area, within which axial planes dipped predominantly southwards, from the area to the south of generally northerly dipping axial planes.

Lapworth (1878) also noted the progressive disappearance of graptolite zones of the black shales passing NW from Moffatdale, until only a "degenerated representative of the Hartfell-Glenkiln division" is present along the northern edge of the Southern Uplands.

By 1889 Lapworth had sufficient confidence in his structural model to write, "...underlying all these stratigraphical complexities, there is, in reality, a broad tectonic structure of great simplicity".

The Geological Survey began the re-examination of the Moffat Series of the Southern Uplands in 1889 and this work culminated eleven years later in the publication of the first volume of the Silurian Rocks of Britain (Peach & Horne 1899).

The stratigraphy of Peach & Horne largely followed that of Lapworth, differing principally in the recognition of pre-Moffat Shale sediments and volcanics. The proposed succession consisted of Arenig volcanics and associated basic intrusives (150 m) conformably overlain by a continuous stratigraphical sequence of mudstones (1.2 m), radiolarian cherts (21.3 m), black shales and greywackes (270-365 m),

black shales with cherty bands (2.45-3.65 m) and black shales with flinty bands (12 m) of lower Hartfell (C. wilsoni to P. linearis) age. The upper black shales were considered to pass up into volcanic rocks and the Lowther Shales (D. complanatus to D. anceps zones). Lapworth's interpretation of the structure of the Southern Uplands was confirmed and extended by Peach & Horne. It is a tribute to the endeavour and knowledge of the Geological Survey team that modern workers continue to draw data from the memoir of 1899.

Little re-interpretation of the anticlinorium-synclinorium model was possible until advances in sedimentological knowledge enabled attention to be focussed on the sandstone sequences which constitute the bulk of the Southern Uplands. The use of 'way-up' criteria and study of petrographical differences between greywacke sequences (Walton 1955, 1956; Craig & Walton 1959; Kelling 1961) resulted in major revisions to the earlier stratigraphical and structural interpretations. Lithostratigraphical subdivisions of the greywackes were made, although interpretation of the relationships between the Moffat Shales and the greywackes remained unchanged. The structure was envisaged as consisting of major monoclinal folds of Caledonoid trend, with subvertical northern limbs and tightly-folded southern limbs, each unit being separated

by faults, principally steep thrust faults.

Mackay (1958) re-interpreted the Leadhills Line as a NW-dipping thrust zone, with Lowther greywackes overridden by a block mainly of Arenig and Llandeilo lithologies, a view adopted by Kelling (1961) for the continuation of the structure in the Rhinns of Galloway (Killantringan thrust).

Toghill (1970) interpreted the south-east limit of the Moffat Shales in the Ettrick Valley as a major strike-parallel dislocation (Ettrick Valley Fault), with Moffat Shales being thrust over younger greywackes to the south. Repetition of Moffat Shales across strike was attributed to imbrication of the succession by high angle reverse faults.

Following advances in theories of plate tectonics, workers in the 1970s incorporated the general ideas of Wilson (1966) and Dewey (1969a, 1969b) in relating the structure(s) of the Southern Uplands to those formed in oceanic sediments above subduction zones. Mitchell (1974) compared the structural style of the Southern Uplands with modern and ancient examples from the Pacific and Caribbean, inherently suggesting north-westward subduction of an oceanic plate beneath the site of the present Midland Valley.

Floyd (1975) introduced the term Fardingmullach Line to describe a narrow linear outcrop-belt of Moffat Shales to the south of the Leadhills Line; both lines were recognised as complex fault-zones, probably with overall reverse movement.

Working along strike from Toghill (1970) in Selcoth Burn and Craigmichan Scaurs, Fyfe & Weir (1976) demonstrated the presence of schuppen repeating Moffat Shale bands, related to and overlying a basal thrust (Ettrick Valley Thrust). This idea was extended across the Southern Uplands as a whole by McKerrow et al. (1977), and the regional structure as envisaged by Mitchell was interpreted as an accretionary prism.

The Leadhills Line was renamed the Leadhills Imbricate Zone by Leggett et al. (1979).

1.3 PREVIOUS RESEARCH IN THE ABINGTON DISTRICT

In their "Explanation of Sheet 15" (1871), the Geological Survey of Scotland recognised the following stratigraphy in the Abington district:

Caradoc Beds:	Caradoc Group of Duntercleuch and Glendowran (520 m)
Llandeilo Beds:	{ Black Shale Group (1040 m) Lowther Group (1500 m) Haggis Rock Group (550 m)

Haggis Rock, outcropping near Crawfordjohn, was correlated with quartz and shale pebble conglomerates on Louise Wood Law (932158), separated by the intervening and younger Lowther and Black Shale Groups; thus a "great synclinal fold" was recognised

(with several minor synclinal and anticlinal "curves") extending from Crawfordjohn south-eastwards to the valley of Potrail Water (941110).

The feldspathic nature of the blue greywackes of the Lowther Group was described, and it was noted that feldspathic greywackes, which extend from St. Abb's Head to Portpatrick, preferentially display effects of metamorphic recrystallisation in contrast to more quartzose rocks.

Lapworth (1876) observed that no Birkhill Shales occur in the Leadhills district, the highest black shales present being the top zones of the Hartfell Shales. The lower Moffat Shales were found to be represented by siliceous flagstones.

Hinde (1890) compared cherts from the Abington area with Tertiary rocks on Barbados and the Nicobar Islands, and suggested a deep-sea origin as a radiolarian ooze at depths greater than 3650 m. Associated fine-grained beds of red and green mudstones supported this interpretation. Peach & Horne (1899) recorded the presence of rocks of Arenig-Caradoc age in the Leadhills district. Their stratigraphical sequence consisted of Arenig volcanics (lavas, agglomerates and tuffs, including those of Bail Hill) cut by dolerites and gabbros of intrusive origin and overlain by mid-Arenig fossiliferous mudstones. These in turn were considered to be succeeded by cherts and mudstones (late Arenig to mid-Llandeilo) which were grouped into three subzones - red or chocolate-coloured cherts embedded in a fine

ashy matrix forming the lower unit, the middle and upper zones consisting of green and grey nodular cherts respectively.

Moffat Shales (with graptolites from the zones of Nemagraptus gracilis through to Dicranograptus clingani) and Caradoc greywackes and grits complete the succession.

The Arenig lithologies were inferred to occupy anticlinal cores, flanked on either side by the radiolarian cherts, Moffat Shales and Caradoc greywackes. The repetition of black shales and cherts in stream sections south of Glengonnar Water was attributed to continuous isoclinal folding. Such stratigraphical repetition was not recognisable in the Caradoc grits. However, Peach & Horne suggested, "It is possible, if not certain, that the upper series (i.e. Caradoc) is as much folded as the lower" (p. 289).

The general structure of the Leadhills-Abington district was considered to be, "a striking example of a 'fan structure', where in the centre of the primary fold the strata are folded on vertical axes while the axial planes dip inwards on the north-west and south-east sides, thus producing a pseudo-syncline...strata not exceeding from 200 to 300 feet in thickness have been compressed as to form continuous outcrops more than a mile across" (p. 74).

Ritchie & Eckford (1935) recognised three rudaceous horizons (Haggis Rock, Calcareous conglomerates and shaly breccias) of Hartfell age which were interpreted to pass

through the Leadhills district. Of these, only Haggis Rock has been found in the study area. On the basis of a correlation of trachyte fragments displaying fluidal feldspars in the Haggis Rock with similar lithologies in the Tweeddale lavas, Ritchie & Eckford assigned a lower Hartfell (post-D. clingani zone) age to the Haggis Rock. Other volcanic rock fragments were interpreted to be derived from the Bail Hill complex. The variously coloured shales, mudstones, cherts and greywackes, forming approximately 80% of the fragmentary material, were regarded as having a local source. It was noted that shale clasts showed a low grade of metamorphism.

Ritchie & Eckford followed Peach & Horne (1899) in proposing an unconformity below the Haggis Rock, the former authors suggesting the presence of a ridge of uplifted sea-floor south of the present outcrops, with processes of tidal scour in operation.

The fossiliferous succession in Raven Gill was re-examined by Lamont & Lindström (1957). From the descriptions given, it appears that they were unsuccessful in the attempt to locate the black shale band from which Peach & Horne found Arenig graptolites; however, the stratigraphical conclusions of the latter authors were confirmed using conodont evidence from brown mudstones at the same locality.

Mackay (1958) noted that most lithological contacts were tectonic (mostly reverse faults) rather than stratigraphical and regarded the isoclinal model of Peach & Horne not to be applicable to the Leadhills area.

Based on unpublished company reports by J. Mitchell (c. 1930), Mackay agreed with the suggestion that a low-angle reverse fault or zone of movement dipping towards the NW at angles between 30-40° thrust Arenig and Llandeilo rocks over an area mainly of Lowther greywackes. This structure was regarded as being the major control on mineralisation in the Leadhills-Wanlockhead mining district. Mackay refused to publish the data from which his conclusions were drawn, with the prospect of economic exploitation of the orefield.

Although focussing primarily on the 1976 British Gas pipeline section (which was taken to be the eastern extremity of the mapping area by the present author), Leggett et al. (1979) examined sections in northward-flowing tributaries of Glengonnar Water. Raven Gill was chosen to demonstrate a succession of basalts (volcanic) overlain by 1 m mudstone (Arenig) and cherts. Oliver & Leggett (1980) demonstrated prehnite-pumpellyite facies metamorphism from dolerites in the Leadhills Imbricate Zone.

CHAPTER 2: STRATIGRAPHY

2.1 INTRODUCTION

The sedimentary rocks are divided into lithostratigraphical units following the procedures recommended by Holland et al. (1978). Terms established for many years, such as 'Moffat Shale' (Lapworth 1878) and 'Haggis Rock' (Peach & Horne 1899; Ritchie & Eckford 1935) are retained. Haggis Rock only occurs in a small series of exposures in one stream-cutting in the area (see 2.2.2) and is accorded the status of member.

The utilisation of biostratigraphy is restricted to brown mudstones and Moffat Shales within the Leadhills Imbricate Zone. The Moffat Shales also occur within the Fardingmullach Imbricate Zone to the SE. These strata are lithologically distinct and easily recognisable even where fossils are absent. Unless stated in the following descriptions, it can be assumed that lithostratigraphical units have not yielded any fossils and are uncertain in age.

The stratigraphical nomenclature of Williams et al. (1976) is followed throughout unless stated; chronostratigraphical terms used by other authors which differ from

this scheme henceforth are always underlined (cf. Fig. 2). Where indistinguishable, the graptolite zones of Climacograptus peltifer and C. wilsoni are replaced by the single zone of Diplograptus multidentis (Skevington 1969).

Arenaceous and rudaceous sedimentary rocks observed in the field are generally prefixed using terms from the combined size-grade scale of Udden (1898) and Wentworth (1922). Use of the term greywacke, describing a poorly sorted arenaceous rock (e.g. Pettijohn 1957), is restricted to petrographical descriptions in the following account.

The development of a cleavage precludes use of the classification scheme of mudrocks based on the presence or absence of fissility (Blatt et al. 1972). A more recent work (Spears 1980) expands the Blatt et al. classification by subdividing fissile and nonfissile mudrocks into classes based on the percentage of quartz - this scheme is not used by the present author as it equates composition (in percentage of quartz in the rock) directly with a size-grade scale based on terms similar to those used by Udden (op. cit.). The term laminites describes lithologies consisting of alternate mudstone and siltstone laminae less than 1 cm thick. Mudstone is used to describe a nonlaminated rock of clay and silt-size material; it is not possible to establish whether the rock was massive or fissile prior to tectonic

	(i) Graptolite Zone	(ii) Conodont Zone	(iii)	(iv)	(v)	(vi)
	anceps	?		A S H G I L L	A S H G I L L	A S H G L
	complanatus	Am. ordovicicus				
	linearis					
	clingani	Am. superbus		C A R A D O C	C A R A D O C	C A R A D O C
multidens	wilsoni	----- ? -----				
	peltifer	Am. tvaerensis				
	gracilis			L D	L L D O	L L D
	teretiusculus	P. anserinus	L L D O	L L A N V R N	L L A N V	L L A N V
	murchisoni	P. serrus				
	bifidus					
	hirundo					
D. extensus	gibberulus			A R E N I G	A R E N I G	A R E N I G
	nitidus					
	deflexus					
	(approximatus)					

Fig. 2: Correlation of Ordovician series boundaries used by previous authors, with graptolite and conodont zones. Columns after: (i) Williams et al. 1976; (ii) Bergström 1971; (iii) Lamont & Lindström 1957; (iv) Bergström 1971; (v) Williams et al. 1976; (vi) Churkin et al. 1977. Correlation of graptolite and conodont zones after Bergström 1971.

deformation and cleavage development. Bed thickness terminology is after Reineck & Singh (1975, Fig. 136).

Separated by major faults, a series of NE-SW orientated structural blocks (cf. Anderson & Cameron, 1979) has been recognised, which are (from NE to SW):-

- 1) Mill Burn Block
- 2) Crawfordjohn Block
- 3) Abington Block
- 4) Elvanfoot Block

Each of the fault-blocks (Fig. 3) consists of two or more lithostratigraphical units which are usually formations; the distribution of the major formations is shown in Fig. 4.

Imbricate zones form the southern margin of structural blocks. More complete descriptions of sedimentary facies within formations are given in Chapter 4.

2.1.1 General stratigraphy

Deeply weathered basic lavas in Raven Gill are associated with cherts and fossiliferous brown mudstones which contain Lower Arenig graptolites and conodonts (Peach & Horne 1899; Lamont & Lindström 1957). These are interpreted to underlie unfossiliferous sequences of cherts and mudstones which possibly range in age from Upper Arenig through to

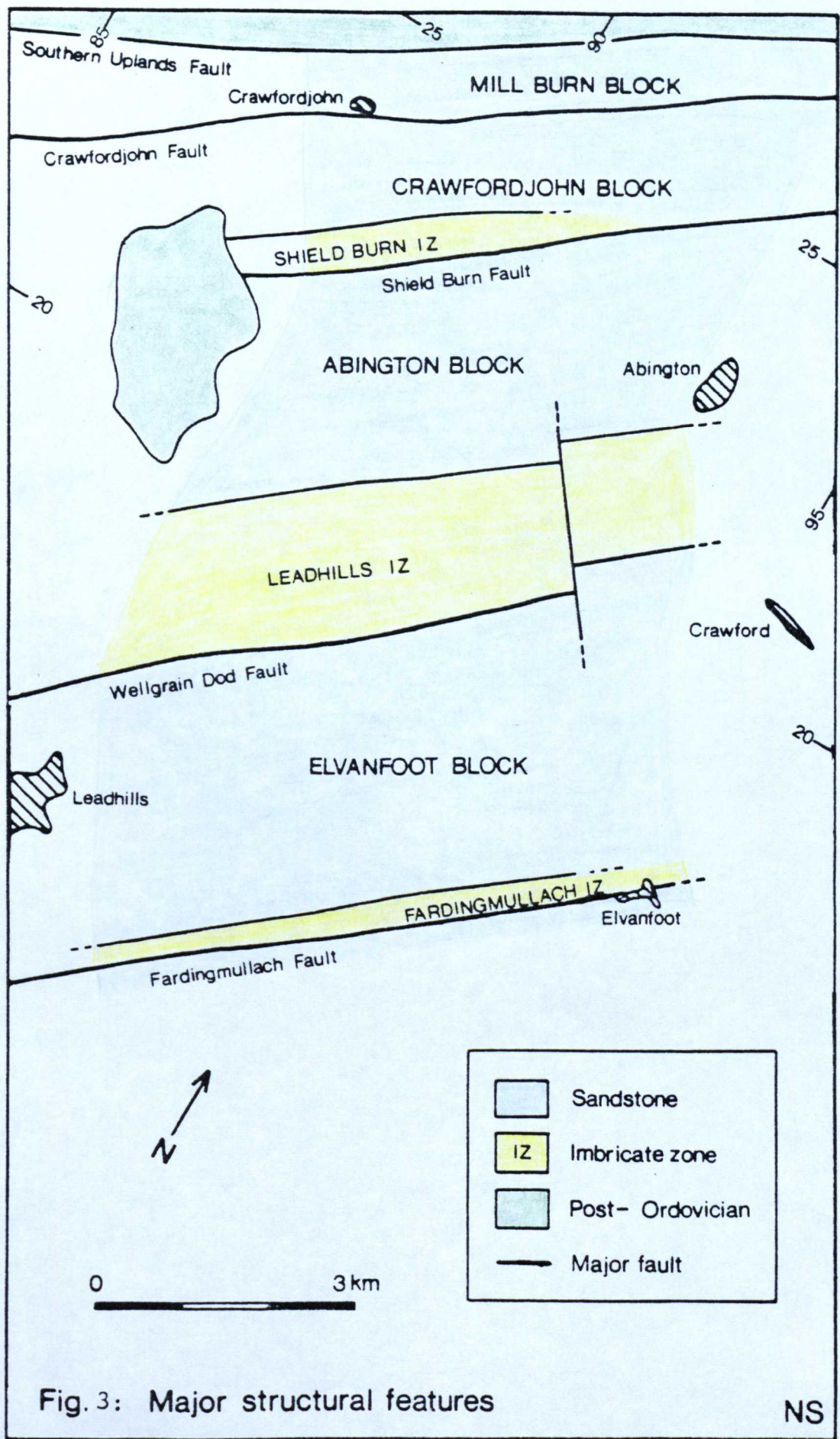
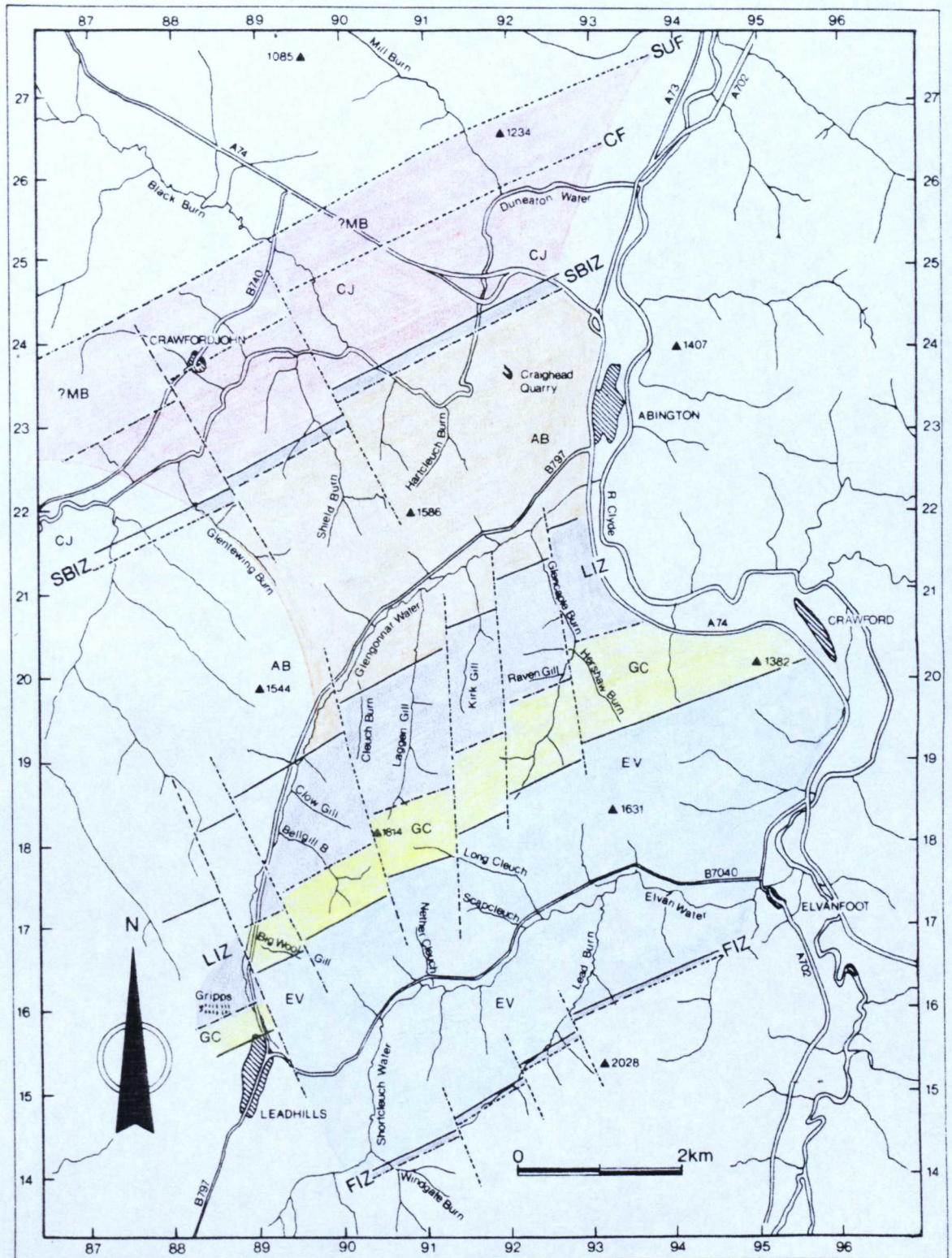


Fig. 3: Major structural features

NS

Fig. 4: Distribution of formations



- | | | | |
|---|------------------------|---|-------------------------------|
| MB | ? Marchburn Formation | SUF | Southern Uplands Fault |
| CJ | Crawfordjohn Formation | CF | Crawfordjohn Fault |
| AB | Abington Formation | SBIZ | Shield Burn Imbricate Zone |
| GC | Glencaple Formation | LIZ | Leadhills Imbricate Zone |
| EV | Elvan Formation | FIZ | Fardingmullach Imbricate Zone |
| IZ | Imbricate Zone | | Stratigraphical boundary |
| | Fault | | |

Lower Llandeilo (Fig. 5, Abington Block).

The Moffat Shales, formed principally of black mudstones and cherts, contain graptolites which give Upper Llandeilo to upper Caradoc ages (zones of N. gracilis to D. clingani, see Appendix 1) and are therefore inferred to overlie the previous strata. The total thickness of pre-upper Caradoc lithologies is probably less than 180 m.

It is inferred from graptolite evidence that the onset of sandstone sedimentation occurred in the Upper Llandeilo or lower Caradoc in the north of the area, whilst in the south this took place later, in the upper Caradoc (Fig. 5). The sandstones conformably overlie the Moffat Shales in the Elvanfoot Block. In contrast to the thinly developed, fine-grained lithologies, the sandstones form successions which have a present-day thickness of up to 3200 m.

2.2 MILL BURN BLOCK

The Mill Burn Block occupies the low-lying ground extending for 950 m south-eastwards from the Lower Old Red Sandstone conglomerates in the extreme north of the area. Recognition of this fault-block is based upon a suggested lateral continuation of the Carcow Fault of Floyd (1975). It is the most poorly exposed of all the structural blocks, outcrop being essentially restricted to one stream section in Mill Burn (917262). The Mill Burn Block is inferred to

NW

SE

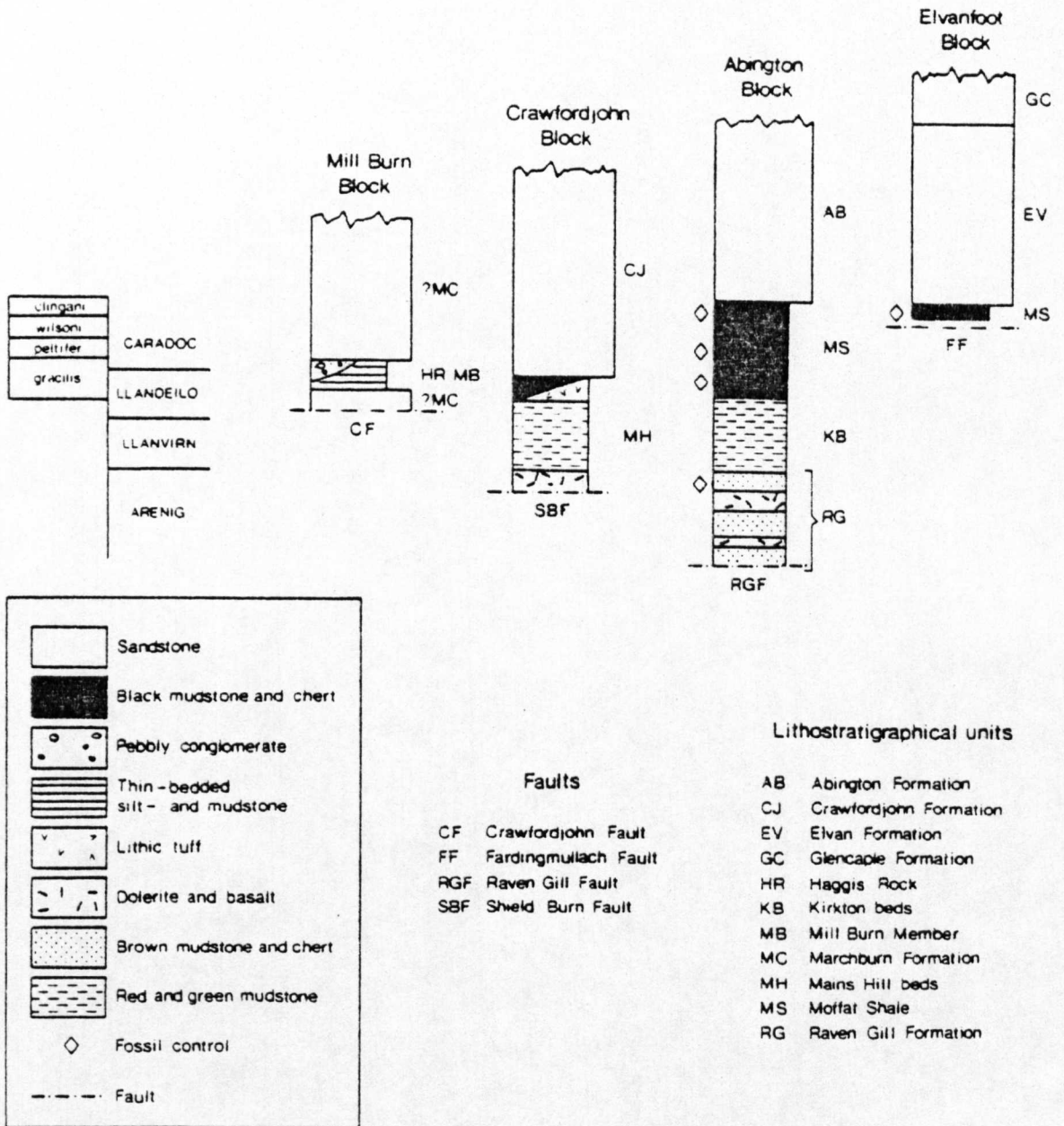


Fig. 5: Lithostratigraphy of the fault-blocks (diagrammatic). See Section 7.3 for discussion on the upper age limit of sandstone formations.

be truncated by two strike-parallel faults, the Southern Uplands Fault to the NW and the Crawfordjohn Fault to the SE.

In Mill Burn the dominant lithology consists of laminites with subordinate sandstones (Mill Burn Member) and conglomerates ('Haggis Rock' of Peach & Horne 1899 and Ritchie & Eckford 1935). Due to the paucity of exposure none of these lithologies can be traced laterally, hence the term formation is not applicable to descriptions of this block.

2.2.1 Mill Burn Member

(i) Characteristic lithologies

Lithologies of this member consist of laminites (sometimes calcareous), siltstones and subordinate sandstones which form a tightly folded unit with an across-strike outcrop width of 300 m. Laminites are the dominant lithology, although multiple siltstone and very fine sandstone beds may form packets in excess of 30 cm thick. Individual siltstone/very fine sandstone layers range from less than a millimetre to 15 cm in thickness. Most are laterally continuous on the scale of tens of centimetres and few show marked lenticularity.

Coarser-grained sandstones form less than 10% of the total exposure; these are generally well graded, blue-grey and medium-grained showing bedding units 20-25 cm thick. The sandstone units are amalgamated. Quartz is the dominant detrital component.

2.2.2 Haggis Rock

(i) Characteristic lithologies

A few scrappy exposures of Haggis Rock occur in Mill Burn (917262). The lithologies of this member are medium to small pebble conglomerates, and granule to very coarse sandstones. They represent the coarsest-grained sedimentary rocks in the area (Plate 13).

Bedding units are not generally distinguishable, but some are in excess of 60 cm thick. Internal sedimentary structures such as grading and lamination have not been observed except for a granule sandstone bed which displays parallel orientation of lithic fragments. The clasts may or may not be supported by a sandy matrix.

The Haggis Rock is polymictic. Sediments are the most common rock fragment, forming up to 60% of the total clast content; the remainder consists of fine-grained ?lavas (25%), acid igneous (10%) and metamorphic rocks (5%). Monomineralic grains of quartz, mica and plagioclase feldspar dominate the sand component.

Fragments in the rudites have a maximum diameter of 14 mm and tend to be angular sedimentary rock clasts (cherts, shales and mudstones) of low sphericity. Acidic igneous fragments contrast in showing greater roundness (generally

subangular to subrounded) and higher sphericity (estimated using charts of Powers 1953).

2.2.3 Relationship between major lithostratigraphical units

The Haggis Rock occurs to the north of the Mill Burn Member, separated by a gap of over 40 m which precludes the direct establishment of age relationships between the two members.

2.2.4 Local correlations

The Mill Burn Member and Haggis Rock are comparable with the Marchburn Formation of west Nithsdale (Floyd 1975). No fossils have been found in the Marchburn Formation. However, correlations with the Corsewall (Kelling 1961), Glen App (Walton 1961) and Tappins (Peach & Horne 1899) "Groups" on the coast south of Girvan enabled Floyd to suggest that it is of lower Glenkiln (N. gracilis) age.

The lowest part of the Marchburn Formation consists of thin-bedded sandstones, shales and isolated, massive, quartzose sandstones, which equate with the Mill Burn Member. The chert and volcanic sequences of the Marchburn Formation do not outcrop in the Crawfordjohn-Elvanfoot area. In view of poor exposure in the northern part of the area, it is probable that Marchburn Formation sandstones are the dominant lithology in the Mill Burn Block. Both the Mill

Burn Block and the Marchburn Formation occur immediately SE of the Southern Uplands Fault (Fig. 6).

2.3 CRAWFORDJOHN BLOCK

Occupying the 1300 m wide tract of land to the SE of the Mill Burn Block, the Crawfordjohn Block is bounded to the NW by the inferred Crawfordjohn Fault, and to the SE by the Shield Burn Imbricate Zone.

Sandstones of the Crawfordjohn Formation constitute the greater part of the block; at the south-eastern margin of the block in the Shield Burn Imbricate Zone, lithic tuffs, dolerites and cherts generally crop out as isolated exposures.

2.3.1 Lithologies of the Shield Burn Imbricate Zone

Descriptions of rock units are given in order of presumed stratigraphical position (Fig. 5), based on local and regional lithological correlations (Section 2.3.4).

(i) Characteristic lithologies

'Dolerite': A 3.5 m thick, dark grey-green coloured 'dolerite' was observed in Shield Burn at 89402313 in contact with enclosing light green siliceous mudstones and trending parallel to the regional strike. The 'dolerite' is massive, occasionally containing irregularly distributed vesicles or amygdales up to 2 mm in diameter.

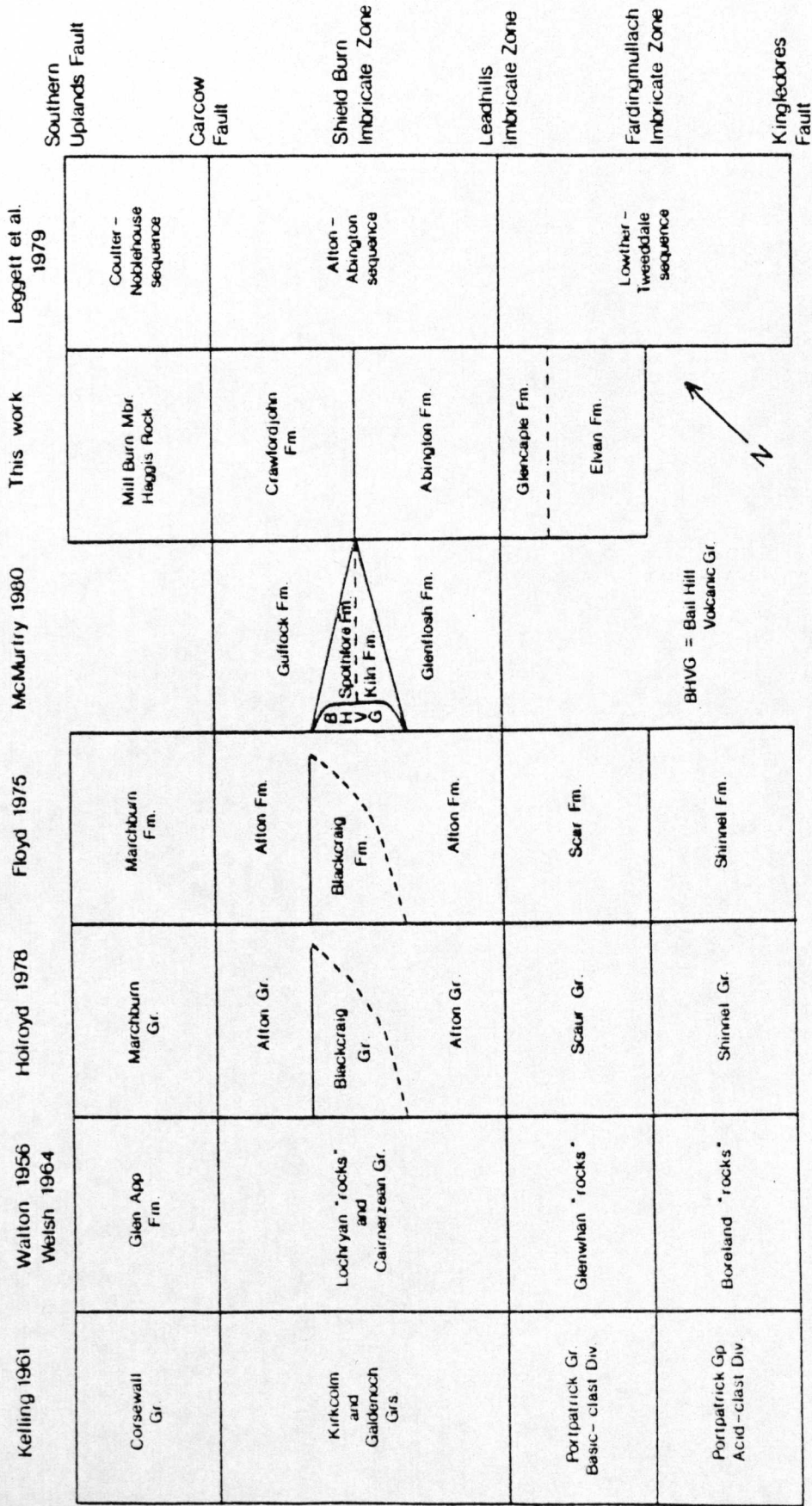


Fig. 6: Correlation of lithostratigraphical units used by previous authors in the Northern Belt. Solid horizontal line = faulted contact; dotted line = stratigraphical contact. Location of Southern Uplands Fault north of the Corsewall Group after Leggett et al. 1979.

In thin section the 'dolerite' is medium-grained (crystals less than 2.2 mm in length), aphyric and consists principally of feldspar, with chlorite, carbonate and iron oxides. No variation in grain-size was observed between the 'dolerite' at both north-western and south-eastern contacts with the enclosing sediments, and at the centre of the igneous body.

Feldspars are andesine in composition, but all show some degree of alteration to carbonate and, more rarely, to chlorite. Dark green clots occur interstitially to the feldspar, and comprise subcircular aggregates of radiating sheaves of fibrous chlorite which probably represent recrystallised glass. Brown mica has also been observed with the chlorite aggregates. Carbonate occurs as veins and irregularly shaped pools throughout the 'dolerite'. There is no evidence to suggest the former presence of phenocryst phases.

Green mudstones (Mains Hill beds): Strata of uncertain stratigraphical position within the Shield Burn Imbricate Zone are informally named the Mains Hill beds. More complete descriptions of green mudstones lithologically comparable to the Mains Hill beds are given in Section 2.4.2. In the Shield Burn Imbricate Zone the green mudstones have a

maximum observed thickness of 2.5 m. The mudstones are siliceous and locally show intercalations of light green cherts 6-7 cm thick or thin silt laminae. Thicker, light green and massive chert sequences up to 1.5 m thick occur in Shield Burn and are also assigned to the Mains Hill beds.

Lithic tuffs: An isolated exposure of lithic tuff is exposed in Shield Burn (89472308) near the south-eastern margin of the Shield Burn Imbricate Zone. The exposure is 2 m wide across strike, although internally faulted. Bedding is not visible; the exposures indicate that units are in excess of 50 cm thick. There is no evidence of any inter-bedded sediment.

The lithic tuffs consist of poorly sorted rock and mineral fragments 0.2-22.0 mm in diameter which form a clast-supported framework. The composition of the interstices is largely indeterminate but does include some opaque material. Clasts are subangular to angular in outline.

The dominant lithology of the clasts is porphyritic lava, containing phenocrysts of amphibole, plagioclase feldspar, biotite/phlogopite and apatite. The subhedral amphibole is completely replaced by secondary minerals - largely by chlorite, with subordinate carbonate and iron oxides. The characteristic amphibole cleavage persists due to selective

replacement by carbonate along former cleavage cracks. It is common for amphibole to be absent from the clasts. Feldspars are turbid in appearance due to partial replacement, principally by carbonate or, more rarely, by white mica. Andesine/oligoclase compositions suggest the lavas are hawaiites and mugearites (cf. McMurtry 1980a).

Biotite/phlogopite phenocrysts contain lenses of ?prehnite which have grown along the cleavage. Apatite is a common accessory mineral, commonly showing euhedral form. A few siltstone clasts have also been recognised.

Pools of calcite are distributed randomly throughout the groundmass, and also replace plagioclase feldspar.

Black cherts: Road cuttings along the Leadhills-Crawfordjohn road afford scrappy exposures of black chert within the Shield Burn Imbricate Zone. The cherts are well bedded (although faulted) and have a minimum thickness of 6 m. This lithology is also described in greater detail below, with Moffat Shales of the Abington Block (Section 2.4.3).

(ii) Field relations

The relationships among lithologies within the imbricate zone are difficult to determine due to poor and isolated exposures, which in addition are badly weathered.

The 'dolerites' are seen to be intercalated within a 6 m thick green siliceous mudstone and laminite sequence. However, the nature of the igneous/sediment contact is equivocal and it is not known whether the juxtaposition reflects original igneous or subsequent tectonic emplacement. Grain-size does not vary across the igneous body from the centre to the contacts with the surrounding sediments, precluding recognition of the chilled margin(s). The presence of vesicles suggests emplacement of the 'dolerite' at a high structural level, either as a sill or lava flow.

The relationships among the lithic tuffs, green mudstones and black cherts are not known.

2.3.2 Crawfordjohn Formation

The Crawfordjohn Formation is the most poorly exposed of the sandstone formations, occupying a tract of land over 900 m in width. Exposures occur east of Crawfordjohn in Shield Burn (89472304 to 89162386) and also in Duneaton Water (86782218).

(i) Characteristic lithologies

Typical sandstones of the Crawfordjohn Formation are dark grey in colour, bedded in units 25-50 cm thick, rarely in excess of 1 m. Grain-size is medium to coarse sand, and many beds grade upwards into fine sandstones,

laminites or mudstones. No other internal sedimentary structures have been recorded. Sandstone bases only rarely show sole markings.

Laminites and mudstones interbedded with the sandstones attain a maximum observed thickness of 40 cm. Fresh exposures of mudstones are dark grey, weathering to dark green.

The Crawfordjohn Formation sandstones are quartz-rich and poor in feldspar (Table 1).

2.3.3 Relationship between major lithostratigraphical units

The Crawfordjohn Formation lies to the NW of the Shield Burn Imbricate Zone. By comparison with other parts of the Crawfordjohn-Elvanfoot area (Section 2.5.4), it is suggested that the Crawfordjohn Formation conformably overlies black mudstones and cherts.

2.3.4 Local correlations

It is tentatively suggested that the 'dolerites' correlate with those of the Raven Gill Formation in the Abington Block to the SE. Green mudstones (Mains Hill beds) and black cherts also crop out in the Leadhills Imbricate Zone near the base of the Abington Block. The Mains Hill beds are the presumed equivalent of the Kirkton beds in the Abington Block (i.e. post-Lower Arenig, pre-Moffat Shale).

McMurtry (1980a) recognised four separate tuff members outcropping NE along strike from the Bail Hill Volcanic Group. Of the petrographic descriptions given by McMurtry, that of the Stoodfold Member is most closely comparable in terms of phenocryst mineralogies and plagioclase composition with the lithic tuff unit in Shield Burn. Graptolites found in the Stoodfold Member are from the N. gracilis zone.

No fossils have been recovered from the Crawfordjohn Formation; however, it is in lateral continuity with the Guffock (McMurtry 1980a) and Afton (North) (Floyd 1975) Formations. All three formations are characteristically quartz-rich. Graptolites from the N. gracilis zone have been recovered from black shales associated with the Guffock and Afton (North) Formations (Peach & Horne 1899, pp. 370-1; Floyd 1975; McMurtry 1980a), and the Crawfordjohn Formation is therefore considered to be at least as old.

2.4 ABINGTON BLOCK

Streams flowing north or north-westwards off the dissected plateau-land south of Glengonnar Water and north of Elvan Water afford some of the better outcrops in the area, including exposures of basal lithologies of the 4250 m wide Abington Block. Between streams the terrain is heather- and peat-covered moorland and little or no exposure is seen.

The Abington Block is inferred to be faulted against the Crawfordjohn Block to the NW along the Shield Burn Imbricate Zone. Forming the southerly margin of the Abington Block, the Leadhills Imbricate Zone has an across-strike outcrop width of 1800 m and separates the Abington Block from the Elvanfoot Block to the SE. The Abington Block comprises three formations and one less well defined stratigraphical unit, all of which occur in the Leadhills Imbricate Zone. These are, from oldest (1) to youngest (4):-

- 4) Abington Formation
- 3) Moffat Shales
- 2) Kirkton beds
- 1) Raven Gill Formation.

The Abington Formation is the only formation exposed between the Leadhills and Shield Burn Imbricate Zones. The Raven Gill Formation is the oldest stratigraphical unit yet recognised in the Southern Uplands, and is fault-bounded at the base. This contact, however, does not define the base of the Abington Block, which continues south-eastwards from the base of the Raven Gill Formation for a further 280 m where it is faulted against the Elvanfoot Block to the SE along the Wellgrain Dod Fault (Fig. 24).

2.4.1 Raven Gill Formation

The lithologically diverse Raven Gill Formation outcrops near the south-eastern margin of the Abington Block. At the type section at the head of Raven Gill (92041989) this formation has a minimum thickness of 55 m. It is also well exposed in Glencaple Burn (92212146) and may be recognised in Cleuch Burn, Windgate Burn and on Craigdod Hill.

(i) Characteristic lithologies in Raven Gill

The succession consists of intercalated red and light grey cherts, brown mudstones, dolerites and spilites (Appendix 2).

Cherts: The cherts (Plate 1) are light grey in colour, with small, dark grey radiolaria visible to the naked eye. Bedding is well developed with units 4-6 cm thick, forming packets up to 2.6 m; the packets vary in thickness along the length of an outcrop.

One small outcrop of black chert with red staining occurs near the base of the Raven Gill Formation (92051984). The chert has developed a grumous texture (cf. Spry 1969) as a result of metamorphic recrystallisation, with circular clots of unaltered chert surrounded by more coarsely crystalline quartz grains less than 0.6 mm in diameter.

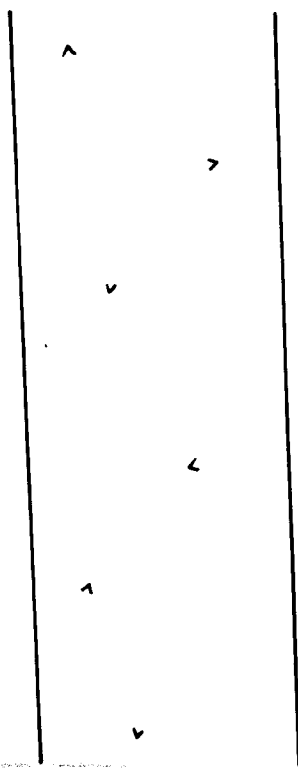




Plate 1: Interbedded chert (massive) and brown mudstone (cleaved); Raven Gill Formation, type section.



Plate 2: Massive lava unit (delineated) interbedded with brown mudstones; Raven Gill Formation, type section.



Plate 1: Interbedded chert (massive) and brown mudstone (cleaved); Raven Gill Formation, type section.



Plate 2: Massive lava unit (delineated) interbedded with brown mudstones; Raven Gill Formation, type section.

Iron oxide coats the quartz grain boundaries, giving the red coloration. This chert is discussed further in Section 6.1.2.

Brown mudstones: The brown mudstones are bedded in units 2-180 cm thick, and internally are massive, well cleaved and locally siliceous (Plates 1 & 2). The mudstones weather to an olive-green colour.

Dolerites: Dolerites are the dominant lithology forming the interfluvium between the two scours at the head of Raven Gill (92051988). The dark green, massive dolerites form units 50-400 cm thick which possess a sheet-like geometry parallel to the strike of the encompassing sediments. Vesicles up to 2 mm in diameter are locally abundant.

The dolerites are fine- to medium-grained, aphyric and consist of plagioclase, chlorite, carbonate, sphene and iron oxides; clinopyroxene is sometimes present ophitically intergrown with plagioclase. Metamorphic index minerals are also developed, including prehnite and pumpellyite.

Clinopyroxenes are present as subhedral, rounded grains. Elsewhere pyroxenes occur as feathery radiating aggregates, suggesting a more rapid cooling history than the dolerites with ophitic textures (C. H. Donaldson, pers. comm. 1980). Electron microprobe analyses show salite and augite

compositions. A feature of the Raven Gill pyroxenes is the presence of Cr_2O_3 and the lack of Na_2O , also an attribute of the Bail Hill Volcanic Group pyroxenes (McMurtry 1980a). Feldspars show a high degree of alteration, usually to white mica; probe analyses of feldspar remnants consistently show albitic compositions. Irregularly shaped patches of fibrous and variolitic chlorite occupy the interstices between feldspar and clinopyroxene grains, and locally replace the feldspar. Chlorite also occurs as a fine crystalline mass within amygdales, resulting from recrystallisation of glassy material.

Spilites: The spilites are dark green, fine-grained lavas in units 50-180 cm thick. Laths of sodic plagioclase (albite) up to 0.8 mm in length are set in a finer-grained matrix of chlorite and iron oxide (recrystallised glass). A trachytic texture is shown by the feldspar laths. Vesicles up to 3 mm in diameter are usually present.

(ii) Characteristic lithologies in Glencaple Burn

In addition to the lithologies described from the type locality, the section through the Raven Gill Formation in Glencaple Burn displays relatively thick brown mudstones containing chert nodules (Appendix 3). These beds are

0.8-4.6 m thick and consist predominantly of brown mudstones which form between 75 and 95% of the total; dark grey, lenticular chert nodules (0.5-20 cm in diameter) form the remainder. Individual nodules tend to be randomly distributed throughout the brown mudstones although they may coalesce to form a more persistent bed (Plate 3).

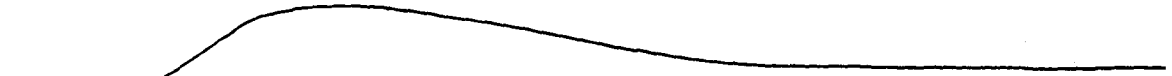
Well bedded, light grey radiolarian cherts 20-200 cm thick are interbedded with the nodular brown mudstones. A massive dolerite forms the northernmost 38 m of the outcrop in Glencaple Burn.

No fossils have yet been retrieved from the Glencaple succession. However, it is suggested that it stratigraphically overlies the Raven Gill sequence, and may thus extend into the Arenig or Llanvirn.

(iii) Field relations

The cherts and brown mudstones are demonstrably interbedded in the north scarp of Raven Gill (92021989) where thin intercalations of spilites are also seen. These show no evidence of faulting or chilled margins and are interpreted as lava flows. The dolerites are more enigmatic as no evidence has yet been found to distinguish their mode of emplacement either as sills or lava flows. The presence of vesicles, however, suggests that emplacement occurred at a

Mudstone



Chert

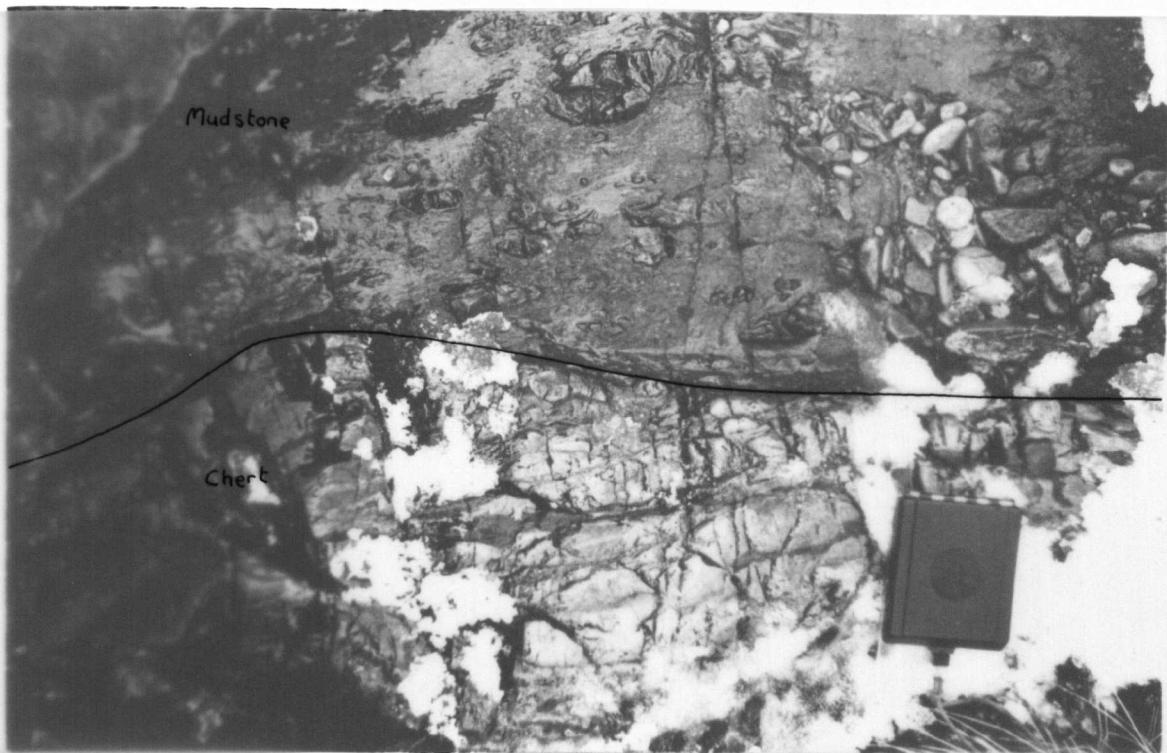


Plate 3: Brown mudstones with chert nodules interbedded with chert (beneath compass). Raven Gill Formation, Glencaple Burn (923214).

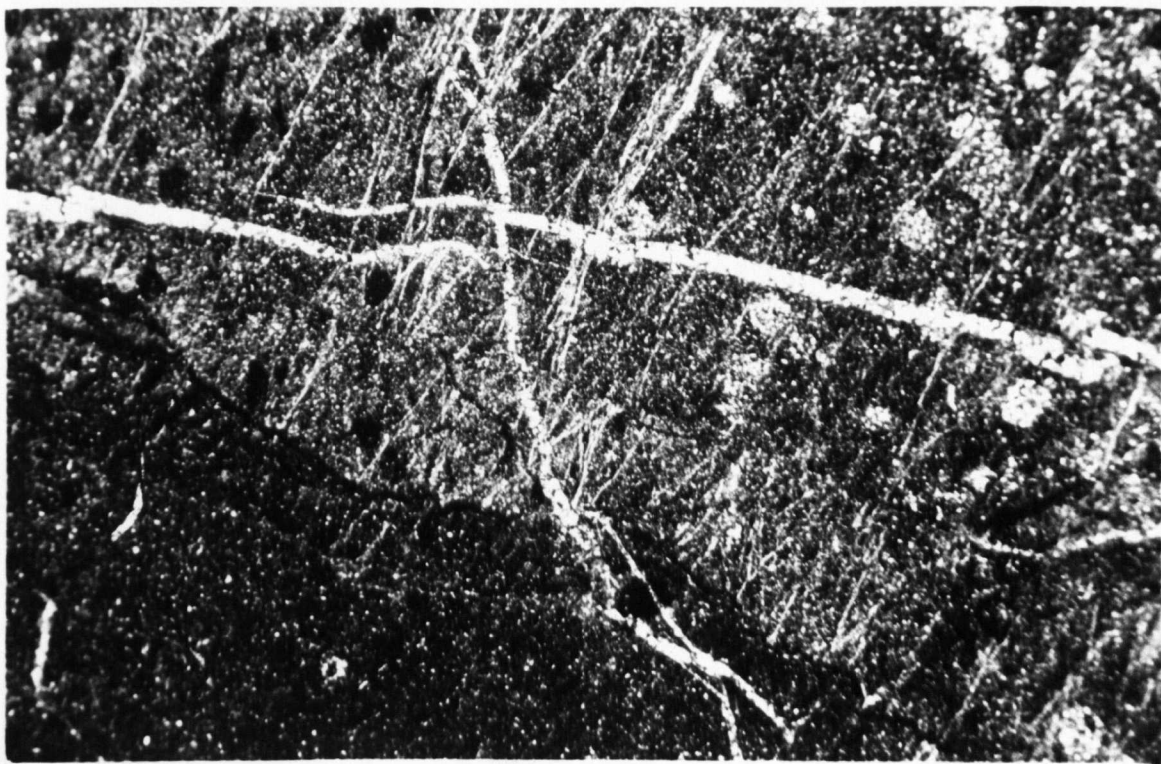


Plate 4: Black mudstone interbedded with pervasively veined radiolarian chert. Photomicrograph; scale bar represents 1.0 mm.



Plate 3: Brown mudstones with chert nodules interbedded with chert (beneath compass). Raven Gill Formation, Glencaple Burn (923214).

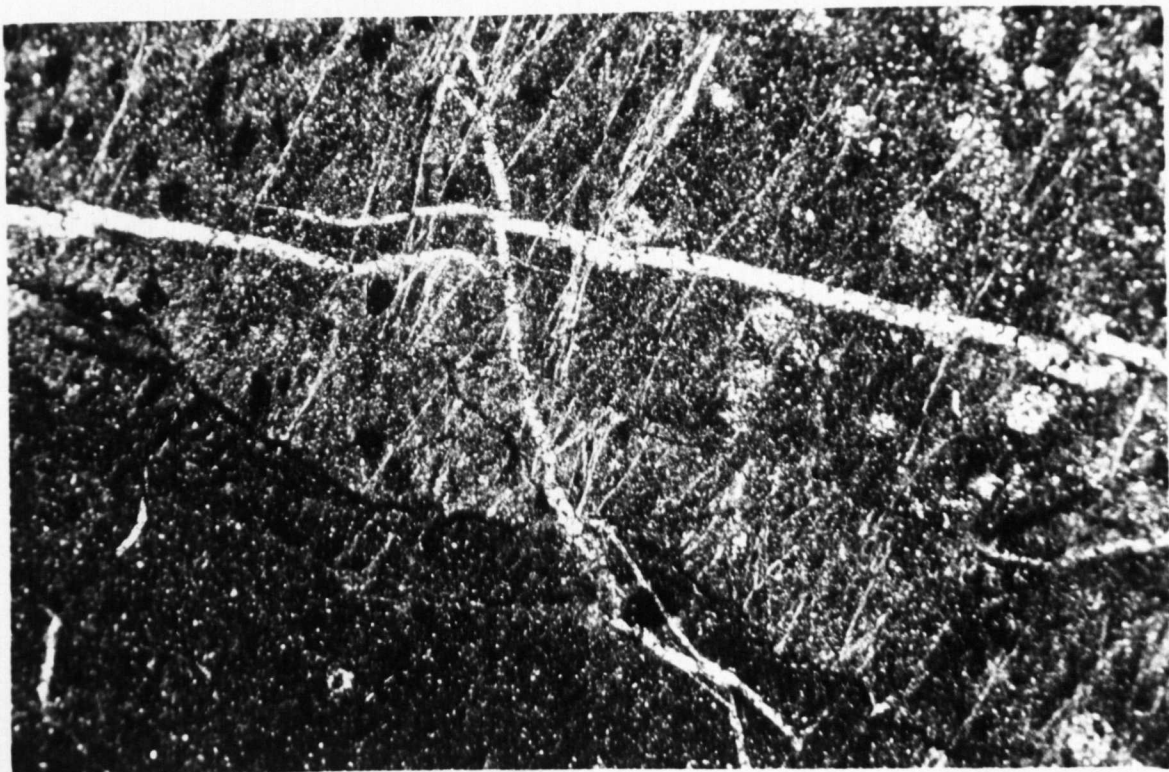


Plate 4: Black mudstone interbedded with pervasively veined radiolarian chert. Photomicrograph; scale bar represents 1.0 mm.

close to surface.

(iv) Age

Peach & Horne (1899) collected a fauna from a thin seam of black shales 'overlying' the lavas in Raven Gill including the graptolites Tetragraptus fruticosus and T. quadribranchiatus, which were interpreted to be of middle Arenig age. From mudstones overlying the black shales a more diverse fauna containing inarticulate brachiopods, sponge fragments and annelid jaws was reported by Peach & Horne. More recently, Lamont & Lindström (1957) collected a rich conodont fauna equivalent to the graptolite zone of Phyllograptus densus in Sweden, and a small sample of conodonts from the slightly lower stratigraphical level of the T. approximatus zone. The fauna was equated with parts of the British Lower Arenig graptolite zone of Dichograptus and Didymograptus extensus (referred to as Didymograptus extensus in Williams et al. 1976), agreeing with the conclusions drawn by Peach & Horne.

Search by the present author did not produce any further evidence of a graptolitic fauna.

2.4.2 Kirkton beds

The Kirkton beds consist of strata of uncertain stratigraphical position, which are inferred to occur between the Raven Gill Formation and the Moffat Shales in the Leadhills

Imbricate Zone. For reasons of brevity, discussion is restricted to unfossiliferous strata which are common in occurrence or significant in terms of their sedimentology, allowing regional lithostratigraphical correlations to be made.

(i) Lithologies

Green siliceous mudstones: outcrop along all streams which expose sections of the Leadhills Imbricate Zone. Thicknesses up to 7 m have been measured, although their frequency of occurrence would suggest the sequence to be thicker. Green cherts, bedded on the scale of a few centimetres, locally occur within the mudstones, as do more thinly bedded (1-15 mm thick) siltstone laminae.

The mudstones show a compositional spectrum, with micaceous (white mica and chlorite) and siliceous (less than 5% detrital mica and quartz) end members. The former are best described as mudstones, the latter as silty cherts. The silty cherts may contain ovate chert nodules (maximum diameter 0.1-10 mm) which form 5-40% of the total lithology. Grain-size of the mudstones ranges between very fine and medium silt.

Red mudstones: In Glencaple Burn (92521988) an outcrop of massive red mudstones occurs within a discontinuous 80 m

thick (faulted) succession of green siliceous and nodular mudstones. The red mudstone has a thickness in excess of 4 m and consists of fine and medium silts. White mica and quartz are the dominant detrital components; the red coloration is derived from amorphous iron oxides.

(ii) Field relations

No sedimentary contact is seen between the red and green mudstones. The red mudstones are bounded both to the NW and SE by the green mudstones, and it is tentatively suggested that the two are interbedded.

2.4.3 Moffat Shales

The Moffat Shales crop out near, and sometimes at, the southern margin of the Abington Block.

(i) Characteristic lithologies

The dominant lithology consists of black mudstones and cherts, although laminites, siltstones, thin sandstones and green mudstones occur as ribs within the mudstones.

Black mudstones: Thick black mudstone sequences occur in Gripps (88091507-88181510), unnamed tributaries of Bellgill Burn (89381794-89291782), Cleuch Burn (90221931-90091942) and Kirk Gill (91501961-91341972). Scattered exposures are

seen in all the northward flowing streams south of Glengonnar Water. The original thickness of the black mudstones is not known as all the well exposed outcrops show strike-parallel faults which could have produced considerable repetition of strata. The maximum outcrop width observed is 170 m in a tributary near the head of Kirk Gill although a considerable proportion of interbedded grey mudstones is also present; the exposures in Gripps and the tributary of Bellgill Burn are 35 m thick across strike and this value is probably closer to the original postcompactional thickness.

The typical lithology consists of flaggy black mudstones which weather to a distinctive light grey colour (Plate 5). Siliceous black mudstones containing pyrite are also common. Internally the mudstones are generally massive, although thin silt beds a few mm thick locally comprise up to 40% of the total lithology. The siliceous black mudstones contain thin chert beds or nodules (Plate 4). Evidence for contemporaneous volcanism includes interbedded ash bands (?metabentonites) (Plate 6) and rare pumice fragments less than 1 cm in diameter.

(ii) Age

Peach & Horne (1899) obtained graptolites from black mudstones at ten localities near the southern margin of the



Plate 5: Well bedded black mudstones of D. clingani age. Overcleuch (921202).



Plate 6: Thin ash band within black mudstone sequence. Dry Cleuch (923205).

Abington Block ranging in age from the Nemagraptus gracilis to the Dicranograptus clingani zone. The author has collected further material from some of the localities listed in Peach & Horne (1899) and in addition has found some new graptolite localities (Appendix 1). Faunas from the N. gracilis, Diplograptus multidentis and the D. clingani zones have been identified, supporting the conclusions of Peach & Horne (1899). Siliceous mudstones tend to be of N. gracilis age, whilst the flaggy mudstones differ by containing D. multidentis and D. clingani faunas.

Cherts: The geographical distribution of cherts is similar to that of the black mudstones. The thickest chert sequence (internally faulted and folded) occurs in Gripps (88281712-88381711) and has an outcrop width of over 30 m across strike.

Black radiolarian cherts predominate, generally well bedded with units typically 5-10 cm thick. Beds of black chert may alternate with light to dark grey coloured, nodular or well bedded chert, dark grey mudstone, light green or black siliceous mudstones and yellow claystone horizons interpreted as metabentonites (Plate 7).

(iii) Field relations

In the Gripps, cherts pass transitionally through a

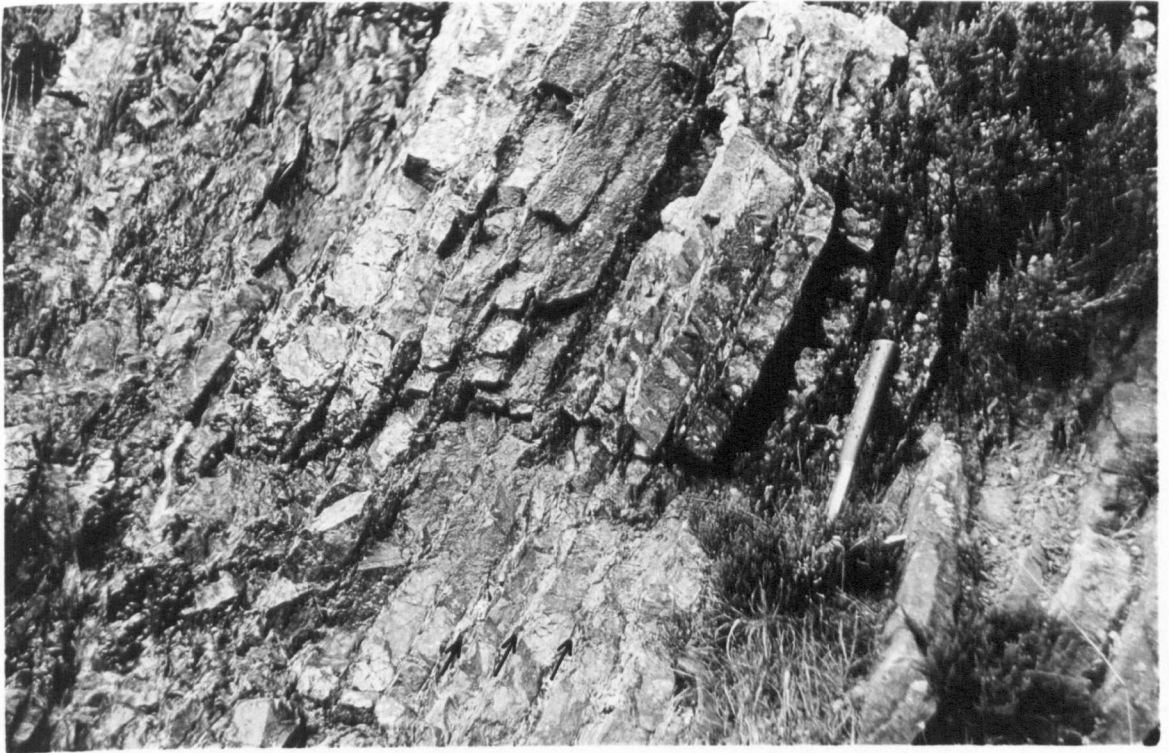


Plate 7: Well bedded black cherts with thin ash bands (arrowed). Gripps (882171).



Plate 8: Transition zone between black cherts (left of rucksack) and flaggy black mudstones (right of rucksack); cherts situated SE from the mudstones. Gripps (882171).

2 m wide zone into a thick sequence of black mudstones to the NW (Plate 8); both are undated in the Gripps and yield no 'way-up' criteria, precluding the establishment of age relationships. Elsewhere in the Leadhills Imbricate Zone the cherts and mudstones are commonly seen to be interbedded (Plate 4), with the exception of the relatively unsiliceous flaggy mudstone units which are lithologically homogenous.

2.4.4 Abington Formation

The Abington Formation has type sections in road cuttings alongside the A74 north of Abington (93042428-92932447) and in Craighead Quarry (91902378). Although this formation is 2800 m thick, it is largely concealed beneath heather- and peat-covered moorland; exposures are small and scattered.

(i) Characteristic lithologies

The typical lithology consists of quartz-rich, medium to coarse sandstones with bed thickness generally varying from 15-40 cm, although beds up to 405 cm have been recorded. The sandstones are characteristically interbedded with varying thicknesses of laminites and mudstones; amalgamated sandstone units are locally developed. Grain-size is always less than very fine pebble-grade, apart from sporadic mudstone clasts which attain a maximum size of 30 x 6 cm.

The lack of good exposures precludes the recognition of fine sedimentary structures, although normal grading is frequently seen (Plate 9).

2.4.5 Relationships among major lithostratigraphical units

The Abington Formation sandstones generally young towards the NW, and are thus interpreted to lie above the rocks of the Leadhills Imbricate Zone. By comparison with strata in the Fardingmullach Imbricate Zone the Moffat Shale/sandstone contact is probably conformable (Section 2.5.4).

2.4.6 Local and regional correlations

The distribution of the Raven Gill Formation appears to be restricted to the central part of the Northern Belt in the Crawfordjohn-Elvanfoot area, in contrast to the red and green mudstones which apparently are regional in development. Lamont & Lindström (1957) described light green or yellow chert beds from Normangill Burn in the Leadhills Imbricate Zone NE of Crawford (NS 971241) which contain conodonts of pre-N. gracilis (Llandeilo) age. Red shales at Morroch Bay in the Rhinns of Galloway also yield a pre-N. gracilis (Upper Llandeilo) fauna.

The red shale and cherts occur in close proximity to black graptolitic shale with N. gracilis faunas, and indeed in Normangill, Lamont & Lindström interpreted green cherts



Plate 9: Tae turbidites of the Abington Formation, younging right to left. The two central units are each approximately 40 cm thick. A74, north of Abington (930244).



Plate 10: Typical thick-bedded, massive sandstone of the Elvan Formation. A74, Crawford.

to be in normal stratigraphical contact with black shales. Kelling (1961) considered the red mudstones in Morroch Bay to lie immediately under black shales with chert ribs carrying Glenkiln graptolites.

The red and green mudstones (Kirkton beds) in the Abington area are accordingly correlated on lithological grounds with those described by Lamont & Lindström. Following the correlation scheme of Fig. 2, these mudstones are regarded as being at least as old as Lower Llandeilo, and are therefore inferred to succeed the Raven Gill Formation.

The Abington Formation is correlated with the Afton (South) and Glenfloss Formations in west and east Nithsdale respectively (Floyd 1975; McMurtry 1980a) where quartz-rich, medium-bedded sandstones are situated to the NW of the Leadhills Imbricate Zone (Fig. 6). Outcrop distribution of the three formations is broadly coincident along strike. Weir (1979) considered the Leadhills Line to extend north-eastwards from west Nithsdale continuing past Abington, a view supported by Leggett *et al.* (1979). Along this 36 km belt graptolites from the zones of N. gracilis through to D. clingani are represented (Peach & Horne 1899; Floyd 1975).

The equivalent quartz-rich unit in the Rhinns of Galloway (Kelling 1961) is the Kirkcolm Group, although the latter is more thickly bedded (1-2 m) than the Abington Formation. No fossils younger than Glenkiln were found

within the imbricate zone immediately SE of the Kirkcolm Group in the Portslogan coastal section, and all descriptions are of N. gracilis faunas.

2.5 ELVANFOOT BLOCK

The Elvanfoot Block is the most southerly of the fault-blocks examined. The area is heather-covered moorland, with rock exposures seen principally in tributaries north and south of the Elvan Water, and road and railway cuttings between Leadhills and Elvanfoot.

The block comprises three formations, which are, from NW to SE:

- 3) Glencaple Formation
- 2) Elvan Formation
- 1) Moffat Shales.

The Moffat Shales are believed to be fault-bounded at the base against unmapped sediments to the SE along the postulated Lead Burn Fault. The top of the Glencaple Formation is faulted to the NW against a variety of lithologies of the Abington Block incorporated into the Leadhills Imbricate Zone.

2.5.1 Moffat Shales

(i) Characteristic lithologies

Black mudstones and associated cherts crop out along the south-eastern margin of the area and have a maximum observed thickness of 20 m. Recognition of bedding in the mudstones is often precluded by the presence of shearing throughout entire exposures. Where unfaulted, mudstones are typically dark grey to black in colour, often contain pyrite and are commonly siliceous.

Nodular cherts, bedded cherts and sandstones are interbedded with the mudstones. The cherts attain a maximum observed thickness of 1 m and show bedding units generally less than 6 cm thick. The sandstones are thin (5-40 cm) isolated ribs, occurring near the top of the siliceous mudstone succession and are very coarse sand-grade or less.

The siliceous black mudstones and cherts are overlain by flaggy, steel-blue grey mudstones which weather to a distinctive rusty-orange colour. These mudstones form the top of the Moffat Shale sequence in Lead Burn (91961512). However, in a tributary of Windgate Burn (90321393) a band of grey mudstones (120 cm thick) separates black mudstones from sandstones of the Elvan Formation to the NW.

(ii) Age

Graptolite assemblages characteristic of the D. clingani zone have been recovered from near the base of a 20 m thick siliceous black Moffat Shale succession in Windgate Burn (90231389).

2.5.2 Elvan Formation

The Elvan Formation has an across-strike width of 2500 m. The type section is in Long Cleuch (91201768 to 92141716); sections showing typical lithological characteristics are also seen in Scapcleuch Burn (91251697 to 91931683) and Nether Cleuch (90591682 to 90811634), both of which are tributaries of the Elvan Water after which the formation is named. Exposure of this formation is generally poor and restricted to discontinuous stream sections.

(i) Characteristic lithology

Throughout the formation the dominant lithology consists of dark blue-grey, very fine pebble and granule sandstones. Beds range in thickness from 0.4 to over 4.0 m, though are generally 0.8-1.2 m thick (Plate 10). Internally the beds are apparently structureless and graded bedding is rare. Amalgamation of sandstone beds is common. Petrographically the sandstones are relatively quartz-poor and feldspar-rich, with pyroxene and amphibole consistently present.

2.5.3 Glencaple Formation

The type section of this formation is exposed in Glencaple Burn (from 91921842 to 92491974). Other exposures are found in Hershaw Burn and Bellgill Burn and its tributaries Well Grain, Middle Grain and Rushy Grain. The outcrop width of the formation is 1100 m.

(i) Characteristic lithology

This formation is distinct in the area as internal sedimentary structures are well developed and diverse in character. Interbedded sandstones, siltstones, laminites and mudstones are all common with thickness of sandstone layers typically being about 30 cm, individual beds varying from 8-150 cm. The colour of the sandstones is light blue-grey.

Grading is commonly seen in the sandstones, though other sedimentary structures include parallel, cross and convolute laminations.

The Glencaple Formation is relatively quartz-poor and feldspar-rich and differs from the Elvan Formation as pyroxene and amphibole are not always present in thin section.

Although common, the laminites and mudstones are subordinate in development to the sandstones.

2.5.4 Relationships among major lithostratigraphical units

The base of the Moffat Shale sequence is not seen. The

contact between the Moffat Shales and the Elvan Formation is seen to be conformable in a tributary of Windgate Burn (90321393) and Lead Burn, where the contact is traceable for a distance of over 500 m in discontinuous exposure (91961511 to 91601477, Plate 11). Sedimentary younging evidence from within both the Moffat Shales and adjacent sandstones of the Elvan Formation to the NW indicates that the former are older than the latter.

The sandstones at the base of the Elvan Formation overlie different Moffat Shale lithologies in different parts of the area. In Lead Burn black mudstones underlie the sandstones, whilst in Windgate Burn grey mudstones are sandwiched between the black mudstones and the sandstones. The lowermost 30 m of the sandstone succession is more thinly bedded than the rest of the Elvan Formation, consisting of beds less than 20 cm thick interbedded with mudstones 5-500 cm in thickness.

Occurrences within the Glencaple Formation of massive lithologies and petrographies more appropriate to the Elvan Formation indicate a conformable transition between the two units.

No fossils have been found in the sandstone sequences and the age of the base of the Elvan Formation can only be described as post-D. clingani. The age of the upper contact of the Glencaple Formation is discussed in Section 7.3.

2.5.5 Local and regional correlations

Coarse-grained and massive sandstones, relatively rich in feldspar and poor in quartz, occur to the NW of Moffat Shales which extend up to the D. clingani zone in both west Clydesdale and west Nithsdale. Therefore, the Scar Formation (Floyd 1975) is correlated with the Elvan Formation and the Fardingmullach Line is considered to continue at least as far NE as Elvanfoot. Peach & Horne (1899) recorded graptolites from the zones of N. gracilis to D. clingani from Moffat Shales of the Fardingmullach Line.

Floyd (1975) described no lithologies which could be correlated with the Glencaple Formation; it is considered that this formation is laterally impersistent. To the SW in the Rhinns of Galloway, the Portpatrick Group Basic-clast division is lithologically and petrographically similar to the Elvan and Glencaple Formations. Shales at the base of the Portpatrick Group produced a zonally nondiagnostic fauna which resembles that at the base of the Elvan Formation in containing Orthograptus species in variety, which are locally abundant. Kelling interpreted the fauna to be of upper Glenkiln-lower Hartfell (i.e. D. multidentis) age.

2.6. DISCUSSION

2.6.1 General



Plate 11: Conformable contact in stream bed between Moffat Shale (by hammer head) and the Elvan Formation (top left). Contact is abrupt, although sandstone is more thinly bedded than the typical Elvan lithology.



Plate 11: Conformable contact in stream bed between Moffat Shale (by hammer head) and the Elvan Formation (top left). Contact is abrupt, although sandstone is more thinly bedded than the typical Elvan lithology.

The stratigraphical scheme proposed does not differ markedly from that of Peach & Horne (1899), with the exception that they distinguished a thick pre-N. gracilis succession of greywackes and shales (275-365 m), locally interbedded with Lower Llandeilo cherts which has not been recognised by the present author.

The fundamental differences between Peach & Horne's stratigraphy and the present scheme concern the size of the geographical area to which the stratigraphical column is applicable. This problem arises from contrasting views held on the structural evolution of the Southern Uplands. Lapworth (1878) and Peach & Horne (1899) envisaged regional deformation as occurring after the last greywacke unit had been deposited in the Southern Belt (post-Ludlow). In contrast, recent authors have proposed a regional south-eastward diachronism of both stratigraphical and structural events (e.g. McKerrow et al. 1977) - hence at any one place a complete succession of strata was never deposited. This precludes the use of a single lithostratigraphical column for the Southern Uplands and columns apply only to individual fault blocks (cf. McKerrow et al. op. cit., Fig. 2).

The distribution of graptolite zones in the Crawfordjohn-Elvanfoot area is also in broad agreement with results of previous workers (Lapworth 1878; Peach & Horne 1899; Kelling 1961; Walton 1965; Floyd 1975; McKerrow et al. 1977; Holroyd

1978; McMurtry 1980a), who found younger graptolite zones to crop out in successive Moffat Shale inliers to the SE.

The comparative age of onset of sandstone sedimentation as between the Abington and Elvan Formations presents a problem, as a 20 m thickness of unfossiliferous mudstones (possibly representing the D. complanatus zone of the Barren Mudstones) separates sandstones of the Elvan Formation from D. clingani mudstones (Section 2.5.1). The Abington Formation is inferred to rest on D. clingani mudstones; those underlying the Elvan Formation may belong to a higher level, even to a younger zone. In any event, it is argued (Section 7.3) that deposition of the sandstone formations in the area occurred within the time span of a single graptolite zone - thus the level of refinement of the zonation scheme in current use would preclude determination of the relative ages of both formations.

2.6.2 West Nithsdale succession

(i) Afton/Blackcraig Formation relations

Floyd (1975) regarded the Blackcraig Formation as having a broadly synclinal structure, occurring as an outlier within the Afton Formation. The Blackcraig Formation overlies the Afton Formation at the southern contact of the 'outlier' and the corresponding northern contact was interpreted as a fault. Interpretation of a synclinal structure was based

principally on the recognition of two extensive tracts of northward and southward dipping beds within the Blackcraig Formation separated by the large symmetrical syncline observed on Blackcraig Hill. However, the evidence does not support the suggestion of a southerly younging limb to the north of this syncline, as northerly younging limbs predominate in the ratio 3:2 (Floyd 1975, Fig. 8). It is suggested that the thick-bedded, locally conglomeratic southern part of the exposure forms a north-facing limb, separated by the syncline on Blackcraig Hill from more thinly bedded, and hence more tightly folded, lithologies to the north. The revised stratigraphical sequence north of the Leadhills Line would then consist of the Afton Formation (South) conformably overlain by the Blackcraig Formation; the age of both formations remains at least in the D. clingani zone if not higher, as proposed by Floyd (1975) (Fig. 7).

The Afton Formation (North) is older than the Afton Formation (South) on the basis of graptolite evidence (see Sections 2.3.4 and 2.4.6) and it is suggested that the Langlee Fault (Floyd 1975) is a major outcrop-controlling structure which is represented in the Abington area by the boundary fault of the Shield Burn Imbricate Zone.

(ii) Scar/Shinnel Formation relations

South of the Leadhills Line, Floyd (1975) recognised three lithostratigraphical units, which are, from NW to SE:-

TECTONIC UNIT	RHINNS OF GALLOWAY (Modified after Kelling 1961)	WEST NITHSDALE (Modified after Floyd 1975)	BAIL HILL (McMurtry 1980a)	ABINGTON (This work)
(unnamed)	Portpatrick Gr. Acid- clast Div. (?ur. Caradoc/lr. Ashgill)	Shinnel Fm. (?ur. Caradoc/lr. Ashgill)	-	-
ELVANFOOT BLOCK	Portpatrick Gr. Basic- clast Div. (ur. Caradoc) Moffat Shales (<u>gracilis-clingani</u>)	Scar Fm. (ur. Caradoc) Moffat Shales (<u>gracilis-clingani</u>)	-	Glencaple Fm. (?ur. Caradoc) Elvan Fm. (ur. Caradoc) Moffat Shales (<u>clingani</u>)
ABINGTON BLOCK	Galdenoch Gr. (?lr. Caradoc) Kirkcolm Gr. (?lr. Caradoc) Moffat Shales (<u>gracilis</u>)	Blackcraig Fm. (?ur. Caradoc) Afton Fm. South (ur. Caradoc) Moffat Shales (<u>gracilis-clingani</u>)	Glenflosch Fm. (ur. Caradoc) Moffat Shales (<u>gracilis-clingani</u>)	Abington Fm. (ur. Caradoc) Moffat Shales (<u>gracilis-clingani</u>) Kirkton Beds (Llandeilo) Raven Gill Fm. (Arenig)
CRAWFORDJOHN BLOCK	Corsewall Gr. (?Ur. Llandeilo/lr. Caradoc)	Afton Fm. North (lr. Caradoc) Moffat Shales (<u>gracilis</u>)	Guffock Fm. (lr. Caradoc) Moffat Shales (<u>gracilis</u>)	Crawfordjohn Fm. (?lr. Caradoc) Moffat Shales (?gracilis) Mains Hill beds (?Llandeilo)
MILL BURN BLOCK	Marchburn Fm. (?Ur. Llandeilo/lr. Caradoc)	Marchburn Fm. (?Ur. Llandeilo/lr. Caradoc)	-	Marchburn Fm./Haggis Rock Mbr. Mill Burn Mbr. (?Ur. Llandeilo/lr. Caradoc)

Fig. 7: Ordovician stratigraphical sequences within fault blocks from the Northern Belt; see text for discussion on age revisions. Tectono-stratigraphical positions of Galdenoch/Kirkcolm Groups uncertain.

- 1) Scar Formation
- 2) Moffat Shales
- 3) Shinnel Formation.

Floyd considered the Scar Formation to lie stratigraphically above the Shinnel Formation, with Moffat Shales of the Fardingmullach Line assumed to lie below the sediments of the Shinnel Formation. The general younging direction in both sandstone formations is towards the NW, generating the incongruous situation whereby north-westerly younging rocks have the oldest strata (Moffat Shale) exposed at the northernmost limits of one of the formations, no contact being observed between the Moffat Shales and the sandstones. Age relationships between lithostratigraphical units are more clear in west Clydesdale, where Moffat Shale (D. clingani zone) exposures, situated approximately north-eastwards along strike from the Fardingmullach Line in west Nithsdale, lie to the south of, and stratigraphically beneath, the Elvan Formation. This observation supports Holroyd (1978) who proposed the stratigraphical order of the Scar and Shinnel Formations to be reversed (Fig. 7). This interpretation leaves the Shinnel Formation undated. However, the Portpatrick Acid-clast Division in the Rhinns of Galloway, regarded as the lateral equivalent of the Shinnel Formation (Floyd 1975), contains a nonspecific graptolite fauna of Hartfell affinity

near the postulated Ordovician-Silurian boundary (Kelling 1961). The status of the Fardingmullach Line as an outcrop-controlling fault is thus not yet proven.

2.6.3 Clydesdale succession

In describing the stratigraphy of the Northern Belt in a north-south traverse in a pipe-line section immediately adjacent to the eastern boundary of the study area, McKerrow et al. (1977) and Leggett et al. (1979) recognised three sequences. These have been further subdivided by McMurtry (1980a), Hepworth et al. (1981) and the present author (Fig. 6). In the Afton-Abington sequence to the north of the Leadhills Imbricate Zone, Leggett et al. (op. cit.) proposed the succession basalts (Arenig), fault-bounded at the base, overlain by cherts (Arenig-Llandeilo), carbonaceous shales (lower-upper Caradoc) and greywackes (upper Caradoc-?Ashgill). The following are points concerning the age and age relationships of this sequence.

(i) The identification of a continuous chert succession from Arenig to Llandeilo remains as yet unproven as conodont evidence is incomplete. Lamont & Lindström (1957) described conodonts in the Northern Belt cherts from the zones of Pygodus anserinus and Bergström (1971) found the zonal form Pygodus serrus in the chert material dealt with by Lamont & Lindström. The P. serrus zone (Fig. 2) spans part of two

graptolite zones (D. murchisoni and G. teretiusculus) and hence parts of two Ordovician series (Llanvirn and Llandeilo). Thus the occurrence of Llanvirn strata is not yet proven.

(ii) It is suggested that the upper limit of the period of chert formation be extended from the Llandeilo to the Caradoc in accordance with the presence of black cherts interbedded with black mudstones which contain N. gracilis and D. clingani faunas.

(iii) The basalts are not invariably fault-bounded at the base and overlain by cherts to the NW, as both lithologies are intercalated in Raven Gill (Appendix 2). It is more accurate to describe the Raven Gill Formation as being fault-bounded at the base (to the SE).

(iv) Leggett et al. (op. cit.) state that the brown Lower Arenig mudstone separates the underlying basalts from younger cherts to the NW. The relationship between the basalts and the mudstone was used to advance the idea that the youngest basalts in the Afton-Abington sequence are older than those in the Coulter-Noblehouse sequence, which are overlain by P. serrus (Bergström 1971) and P. anserinus (Lamont & Lindström 1957) red cherts. Lying both to the NW and SE of the mudstones in Raven Gill, it is possible that the basalts extend into the Llanvirn or even the Llandeilo in the Afton-Abington sequence.

CHAPTER 3: SANDSTONE PETROGRAPHY

3.1 INTRODUCTION

In contrast to early workers, whose attention was directed towards the fossiliferous Moffat Shales, recent studies have concentrated on the thick sandstone sequences which form the bulk of the Ordovician succession. Variations in both sedimentology and petrography have enabled subdivision of the Northern Belt sandstones into Groups and Divisions (Kelling 1961, 1962) and Formations (Floyd 1975; McMurtry 1980a). Other studies (e.g. Crook 1974; Dickinson et al. 1979; Dickinson & Suczec 1979) have stressed the relationship between sandstone composition and tectonic environment. Petrographic analysis was carried out to supplement the stratigraphy, and to assist possibly in constructing a palaeotectonic and palaeogeographical setting for the Ordovician rocks of the Abington district.

3.2 MODAL ANALYSIS

The Abington, Glencaple and Elvan Formations have been extensively sampled; poor exposure precludes intensive collecting from the Crawfordjohn Formation, the Mill Burn Member and Haggis Rock. Beds with a maximum grain-size of coarse sand-grade were chosen preferentially for modal analysis, although medium sand- and very coarse sand-grade were

occasionally used.

Counts of 1000 points per sample, at point intervals of 0.3 mm, were carried out on successive traverses across thin sections for a total of 66 specimens. The constituents were grouped into nine categories, based on those of Kelling (1962), which are:

- Monocrystalline quartz,
- Feldspar,
- Mica,
- Ferromagnesian minerals (pyroxene, amphibole, olivine and epidote),
- Acid igneous clasts (leucocratic igneous rocks, principally polycrystalline quartz and granite),
- Basic igneous clasts (melanocratic igneous rocks, principally spilite and basalt),
- Sedimentary clasts (chert, mudstone, shale, siltstone and sandstone),
- Metamorphic clasts (principally slate, schist and quartzite),
- Matrix (including all material less than 0.01 mm, heavy minerals and amorphous material).

In addition numerical details were recorded of component variation within each category to enable the data to be replotted into classification schemes used by authors working

outwith the Southern Uplands (e.g. Dickinson 1970). Veins and secondary carbonate, mica and feldspar were excluded from point counts.

The principal sources of error (Floyd 1975) are the confusion of:

- fresh, untwinned alkali feldspar with quartz.
- deformed, fine-grained sedimentary fragments with matrix,
- chert with rhyolite and devitrified glass,
- unmetamorphosed argillite-shale with quartz-mica tectonite.

Other potential major error sources result from the effects of metamorphic recrystallisation, particularly important in the volcanigenic sandstones. Plagioclase commonly breaks down to sericite and/or carbonate, and this may be confused with the matrix; similar transformations are responsible for the destruction of sharp grain boundaries in melanocratic igneous clasts, and porphyritic plagioclase within such fragments may be mistakenly assigned to the 'feldspar' rather than the 'basic rock' component. Albitisation of plagioclase feldspar precludes the precise identification of original andesites and related rocks (cf. Kelling 1962; Floyd 1975; McMurtry 1980a).

3.2.1 Results

Point counting results are listed in Appendix 4 and

formation means are given in Table 1. A series of triangular compositional diagrams (Figs. 8-14) have been utilised to display the data. Most plots show at least two separate clusters of points; Haggis Rock, the Crawfordjohn Formation and Abington Formation form one field (referred to in the following descriptions as the 'quartzose' lithologies), and the Glencaple and Elvan Formations (referred to as the 'basic' lithologies) form the other.

Qm-F-Lt Fig. 8

This plot has been used to classify sandstones (Dott 1964; Pettijohn et al. 1972) and emphasises aspects of provenance (Graham et al. 1976). All sandstones from the Abington area contain between 15-75% matrix and are classified as wackes (Pettijohn et al. 1972). The Abington Formation, Crawfordjohn Formation and Haggis Rock form a quartz-rich field, composed largely of lithic greywackes with subordinate feldspathic greywackes.

Compositional fields for the Glencaple and Elvan Formations overlap; with decreasing quartz and increasing feldspar content the Glencaple field grades into the Elvan field. The Elvan Formation consists predominantly of feldspathic greywackes, whilst the Glencaple Formation consists equally of feldspathic and lithic greywackes. Both 'basic'

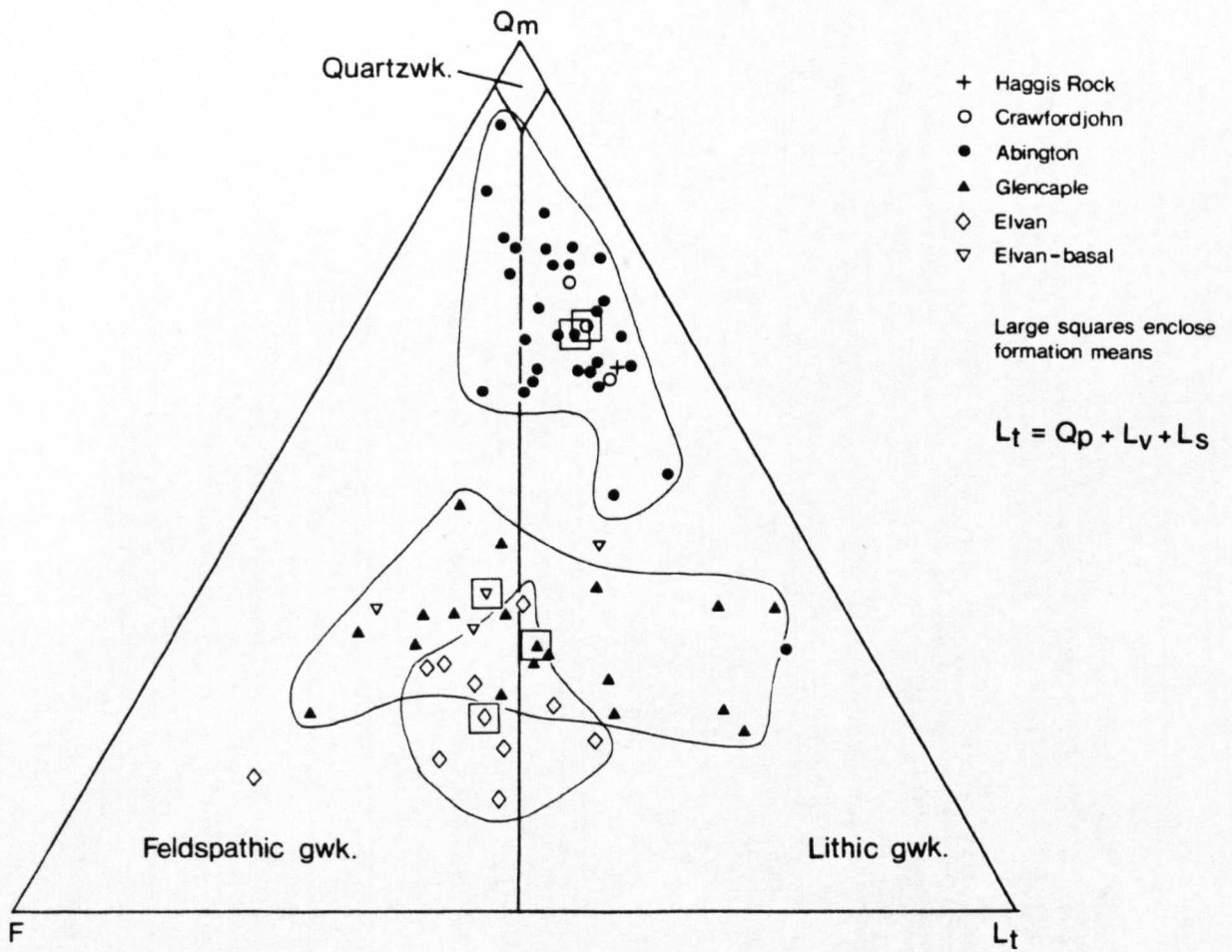


Fig. 8: Q_m -F- L_t plot

Q_m = monocrystalline quartz; F = total feldspar; L_t = polycrystalline quartzose fragments + carbonate + sedimentary frags. + metasedimentary frags. + volcanic frags. + metavolcanic frags. Fields of composition after Pettijohn *et al.* 1972, for matrix content between 15 - 75%. Compositional fields of Abington, Glencaple and Elvan Formations delineated.

formations show a greater proportion of lithic clasts than the Abington Formation.

Q-F-L Fig. 9

A plot which includes the total quartzose population (Q) emphasises aspects of maturity; again the compositional contrasts between the quartzose and 'basic' formations are seen. This scheme does not take into account ferromagnesian minerals, hence the fields of the Glencaple and Elvan Formations overlap.

Q-M-F Fig. 10

Despite metamorphic grade controlling the amount of matrix present in sandstones from any given area, this scheme has been used extensively in the Southern Uplands by previous authors and is provided for comparative purposes (Kelling 1962; Floyd 1975; McMurtry 1980a). However, the diagram illustrates that the Abington, Glencaple and Elvan Formations show comparable variations in the proportions of matrix, despite differing contents of stable (quartz) and unstable (feldspar) components. The compositional field of the Glencaple Formation is larger than that of the Elvan Formation.

Qm-F-FM Fig. 11

The Glencaple and Elvan Formations may be distinguished

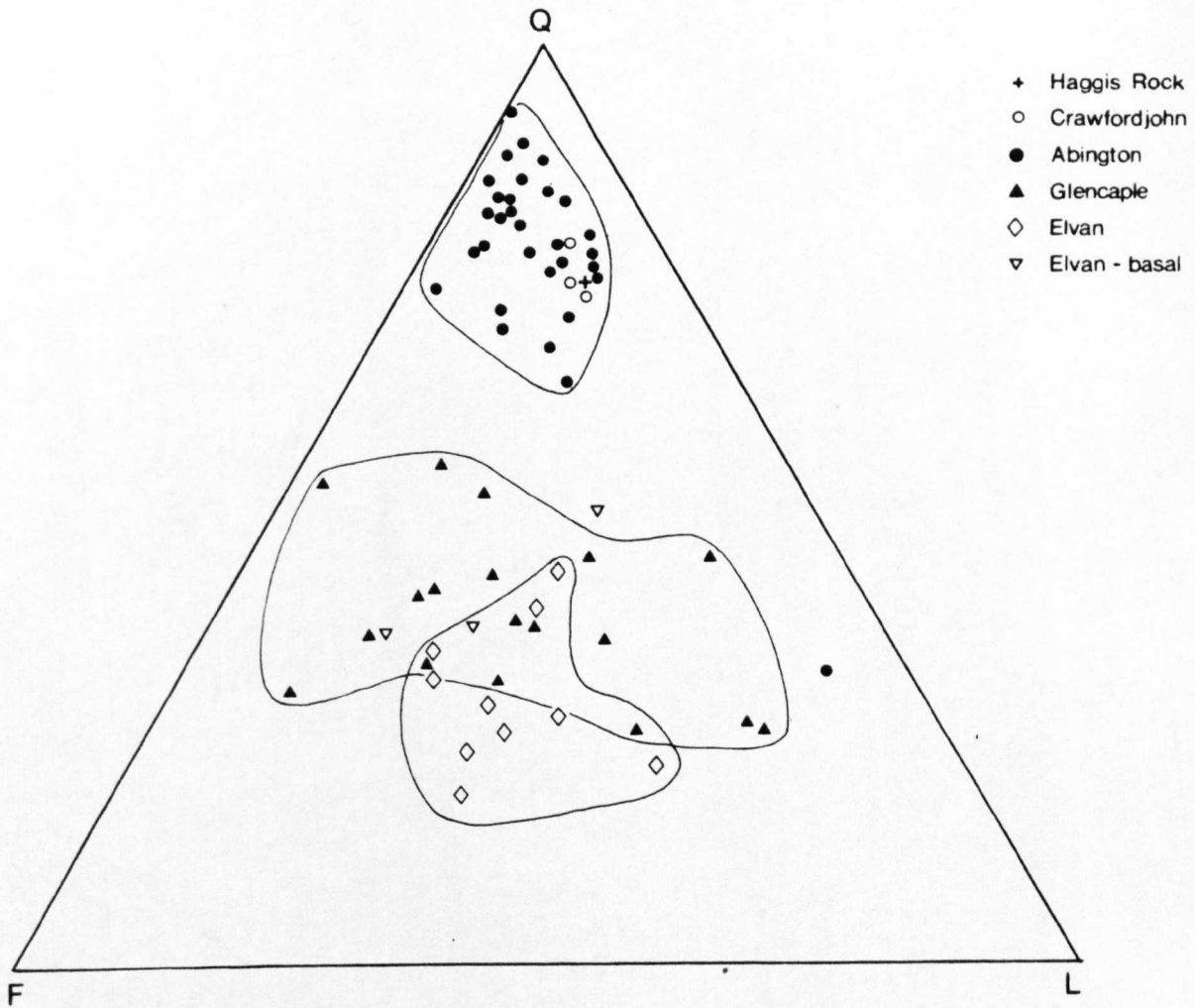


Fig. 9: Q-F-L plot

Q = Q_m (monocrystalline quartz) + Q_p (polycrystalline quartzose fragments, including chert, fine acid and quartzite fragments); F = total feldspar; L = total lithic fragments minus Q_p . Compositional fields of Abington, Glencaple and Elvan Formations delineated.

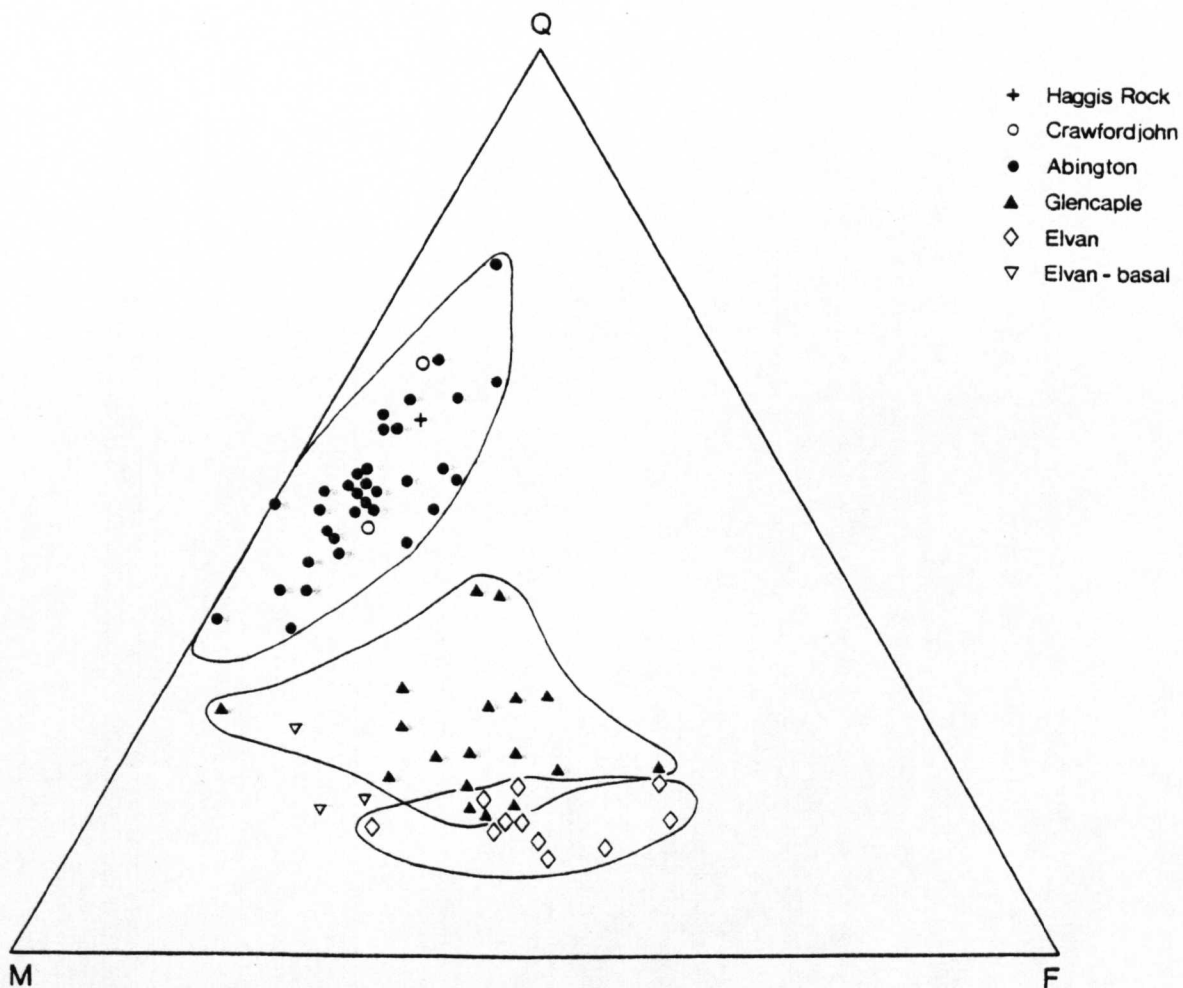


Fig. 10: Q-M-F plot

Q = quartz + acid igneous + metamorphic fragments; M = matrix + mica + sedimentary fragments; F = feldspar + amphibole + pyroxene + basic fragments. Compositional fields of Abington, Glencaple and Elvan Formations delineated.

using a ternary diagram which includes ferromagnesian minerals and micas at one pole. Although several thin sections of Glencaple Formation sandstones contain amounts of ferromagnesian minerals comparable with the Elvan Formation, the relative abundance of quartz in the former separates the compositional fields. The quartzose lithologies yield FM values comparable to those for the Glencaple Formation - this is attributed to the greater abundance of micas in the quartzose lithologies, rather than to particular abundance of amphiboles and pyroxenes.

Qm-P-K Fig. 12

This plot includes monocrystalline grains only. Despite inherent observational inaccuracies, due to the identification of feldspars by optical techniques using unstained thin sections, three clusters are recognised (Elvan Formation, Glencaple Formation and quartzose lithologies) which show approximately constant proportions of K- feldspar. Plagioclase increases in amount from the quartzose lithologies through the Glencaple Formation into the Elvan Formation.

Lm-Lv-Ls Fig. 13

The Abington Formation shows a compositional field elongated towards the sedimentary lithic fragment pole, maintaining similar proportions of metamorphic to volcanic

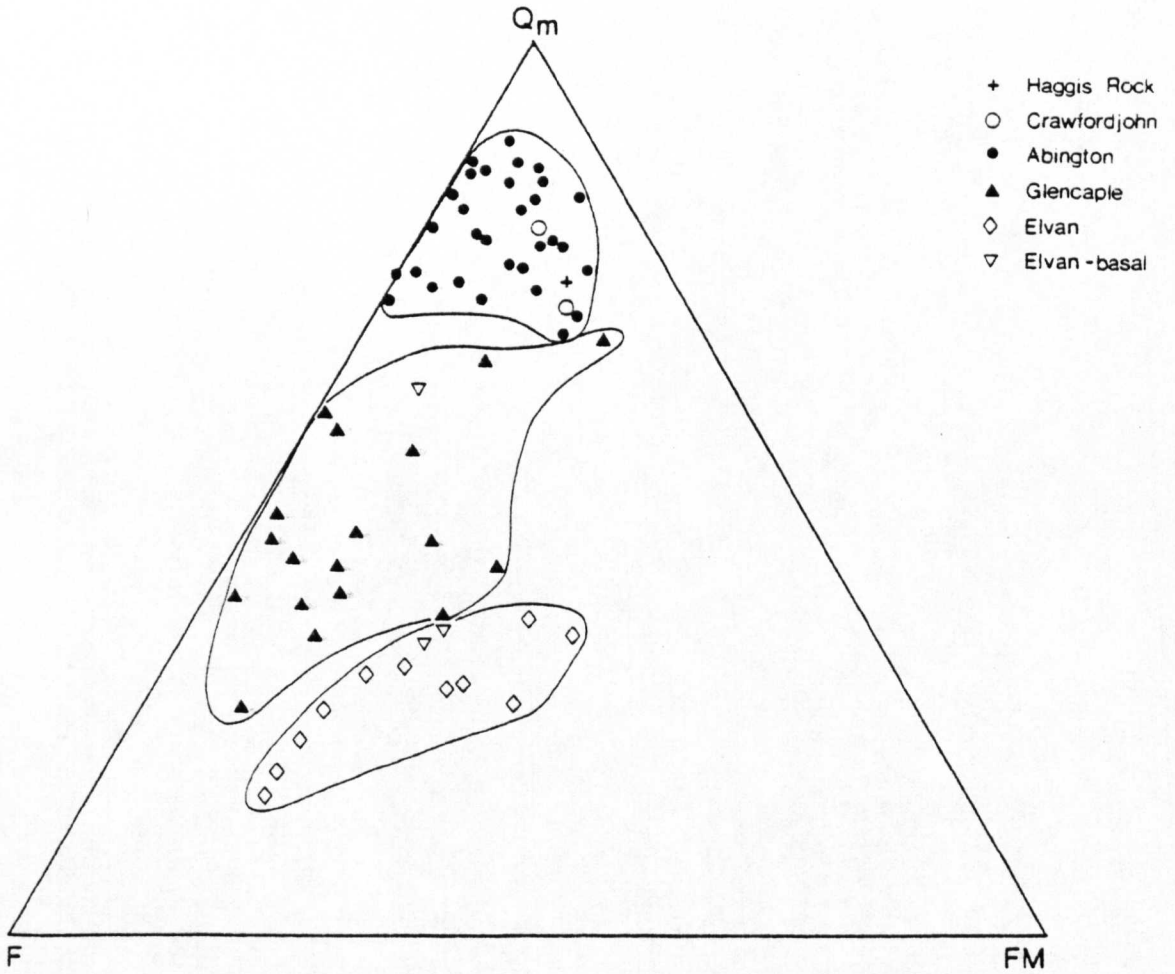


Fig. 11: Q_m -F-FM plot

Q_m = monocrystalline quartz; F = total feldspar; FM = ferromagnesian fragments (amphibole + pyroxene + olivine) + mica. Compositional fields of Abington, Glencaple and Elvan Formations delineated.

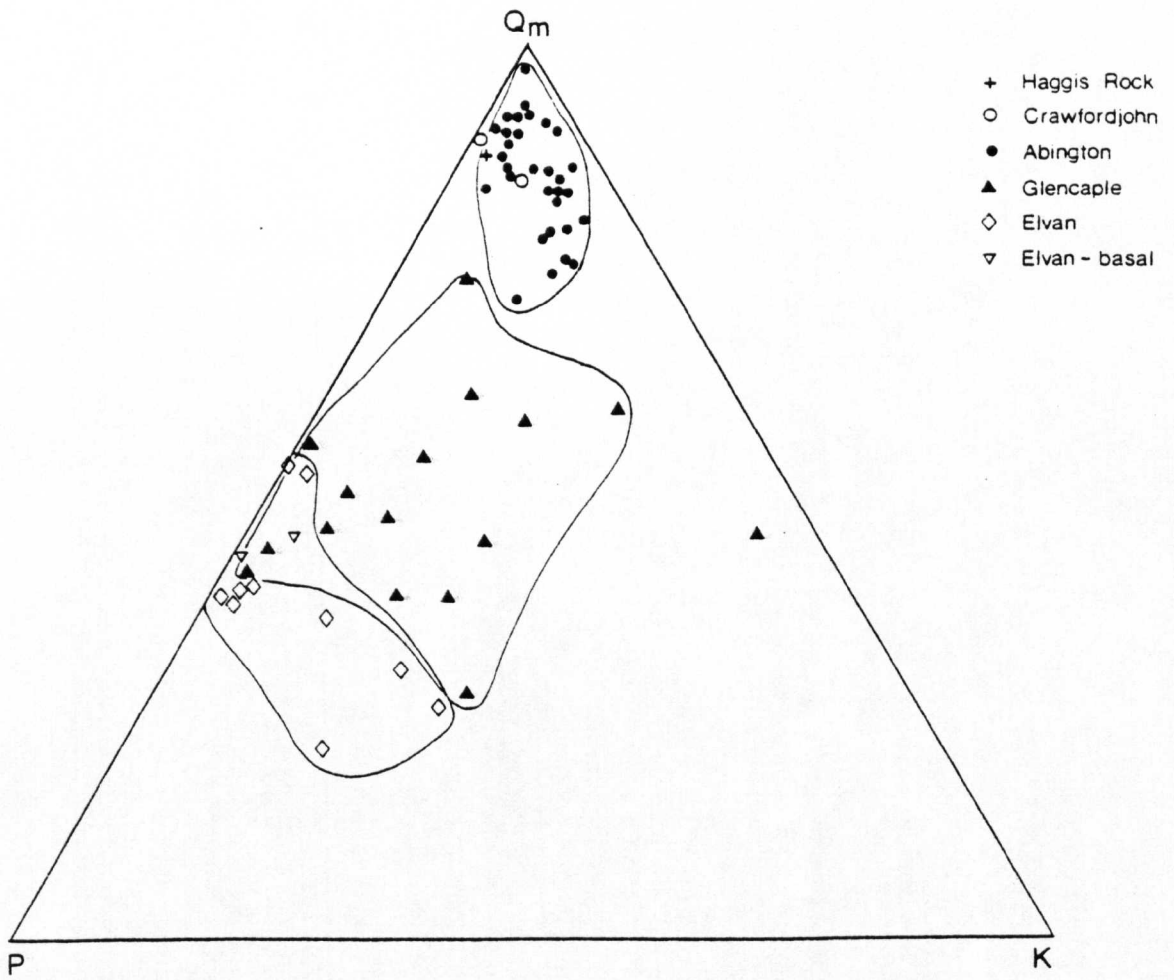


Fig. 12: Q_m -P-K plot

Q_m = monocrystalline quartz; P = plagioclase;
 K = K-feldspar. Compositional fields of
 Abington, Glencaple and Elvan Formations
 delineated.

fragments. The Elvan and Glencaple Formations are indistinguishable. However, by comparison with the Abington Formation they contain a smaller proportion of metamorphic and sedimentary clasts and are rich in volcanic/hypabyssal fragments.

Qp-Lvm-Lsm Fig. 14

Again emphasising the volcanoclastic nature of the Elvan and Glencaple Formations, this diagram shows the greater compositional variation in the proportions of sedimentary and polycrystalline quartzose fragments in the latter formation. The Crawfordjohn Formation is distinguished from the Abington Formation by containing smaller amounts of polycrystalline quartzose fragments.

3.3 SUMMARY OF PETROGRAPHY OF THE LITHOSTRATIGRAPHICAL UNITS

Details of the petrography of lithic clasts found within sandstones are presented in Appendix 5.

3.3.1 Haggis Rock

Lithic greywackes of this member are quartz-rich, feldspar-poor, very coarse sandstones with a significant mica contribution (10%). Acid igneous fragments are the dominant clast type, including quartz + muscovite, quartz + muscovite +

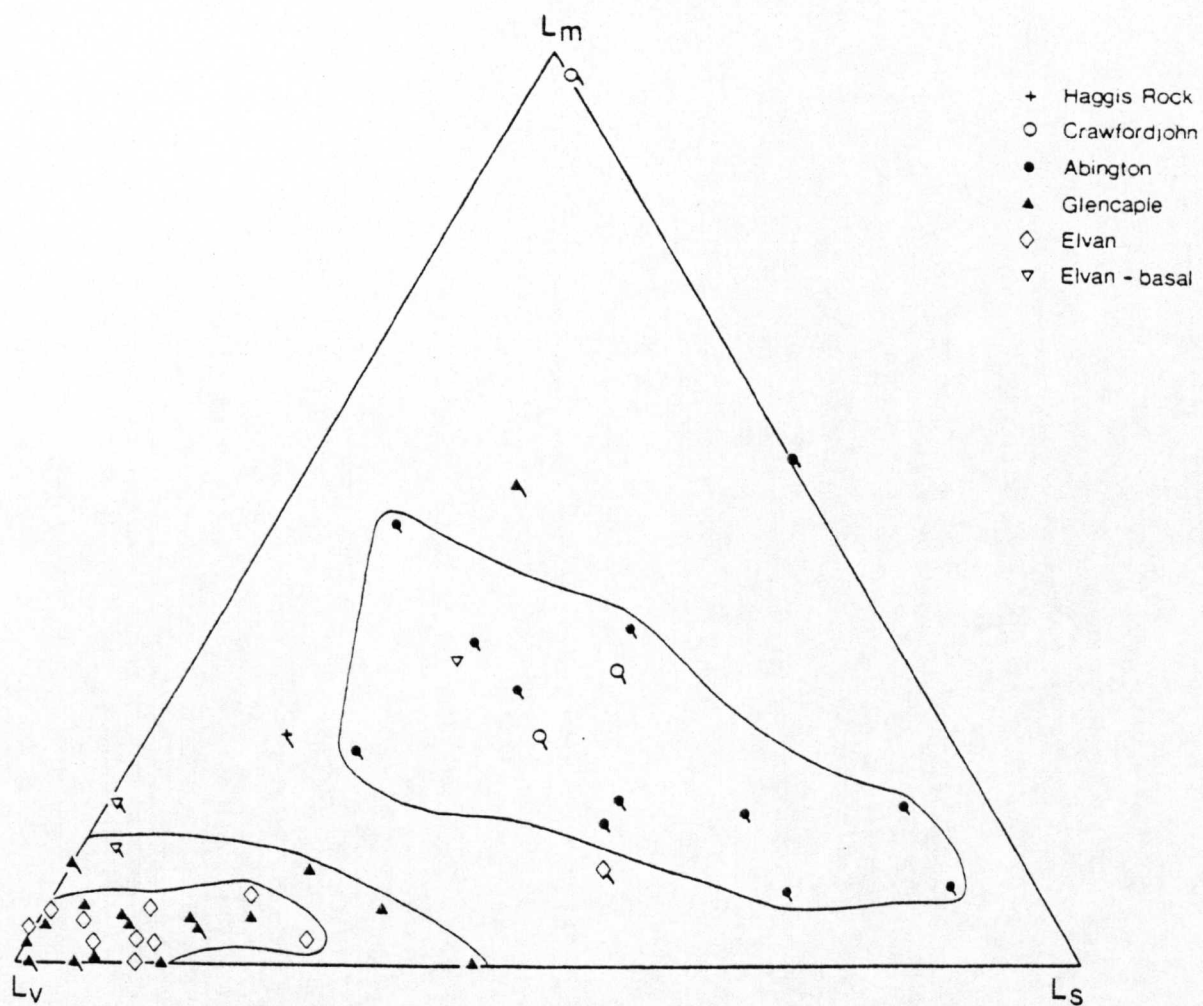


Fig. 13: L_m - L_v - L_s plot

L_m = metamorphic lithic fragments; L_v = volcanic/hypabyssal lithic fragments; L_s = sedimentary lithic fragments (minus chert).
 Modal analyses containing 5 - 10% lithic clasts indicated by tick on south-eastern side of symbol; other symbols represent >10% lithic clasts per thin section. Compositional fields of Abington, Glencaple and Elvan Formations delineated.

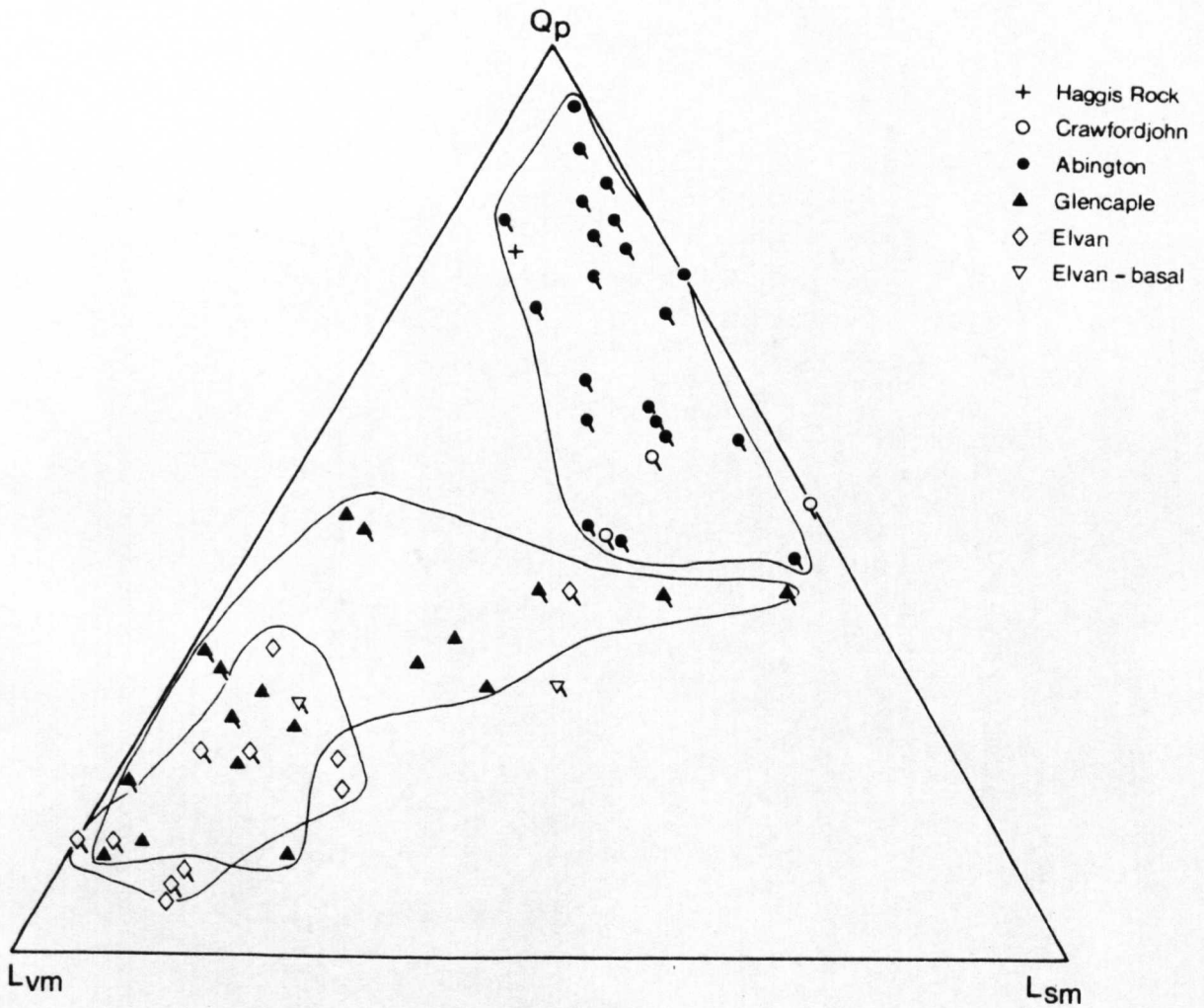


Fig. 14: $Q_p - L_{vm} - L_{sm}$ plot

Q_p = polycrystalline quartzose grains (including foliate metaquartzite, chert and aggregate quartz); L_{sm} = polycrystalline mica + quartz-mica tectonite + argillite shale; L_{vm} = volcanic/hypabyssal fragments. Modal analyses containing between 10 - 20% lithic clasts indicated by tick on south-eastern side of symbol. Compositional fields of Abington, Glencaple and Elvan Formations delineated.

biotite and quartz + albite microgranites. The low feldspar count is reflected by the low percentage of basic igneous clasts; spilite and 'intermediate' lavas with trachytic textures have been recognised, neither of which contains an appreciable content of ferromagnesian minerals.

3.3.2 Crawfordjohn Formation

Sandstones throughout this formation are quartz-rich, feldspar-poor, without a ferromagnesian contribution. Acid igneous fragments account for 6% and metamorphic fragments 4% of the total. The metamorphic clast assemblage is diverse (see Appendix 5) with muscovite schists predominant.

3.3.3 Abington Formation

Lithic and feldspathic greywackes of this formation are quartz-rich and feldspar-poor; ferromagnesian minerals (excluding biotite) are absent in all but one of the thin sections examined.

Acid igneous fragments are common and form, on average, 10% of the total. Sedimentary, metamorphic and basic igneous clasts occur less frequently. Detrital garnet and epidote have been recorded.

The Abington Formation is petrographically similar to the Crawfordjohn Formation, although the latter contains a significantly greater proportion of mica.

3.3.4 Glencaple Formation

The Glencaple Formation contains lower percentages of quartz (18%) and considerably more feldspar (19%) than the Abington Formation. Ferromagnesian minerals are generally absent or rare, although within this formation interbedded units occur which show the characteristics of the Elvan Formation i.e. lower quartz and higher ferromagnesian contents.

The clast population is dominated by melanocratic igneous fragments which only rarely bear ferromagnesian phases (see Appendix 5 - 'Intermediate' lavas) and form up to 19% of the total. Acid fragments average 5%, with metamorphic and sedimentary clasts together totalling less than 4%.

3.3.5 Elvan Formation

The Elvan Formation is petrographically related to the Glencaple Formation, as both have low quartz values and are relatively rich in feldspar detritus and basic igneous clasts. However, the Elvan Formation is distinguished by lower quartz percentages (11%), greater feldspar (22%), basic igneous and matrix contents and the ubiquitous presence of ferromagnesian minerals. Quartz values are the lowest of any formation - feldspar and matrix values are the highest. The ferromagnesian component includes clinopyroxene, clinoamphibole and rare olivine fragments.

Again 'intermediate' lavas are found, basalt/andesite fragments with pyroxene and amphibole phenocrysts being practically restricted to this formation. A single grain of glaucophane has been identified.

For a distance of a few tens of metres above the top of the underlying Moffat Shales, the Elvan Formation shows the petrographical characteristics of the Glencaple Formation; percentages of feldspar, ferromagnesian minerals and basic igneous fragments are lower, and quartz values are higher in the basal Elvan Formation (Appendix 4).

3.4 COMPARISON WITH OTHER AREAS

Petrological studies in the Northern Belt by previous authors have shown that sandstone composition varies across strike, and particular units or formations are continuous along strike for distances in excess of 90 km (Kelling 1962; Welsh 1964; Floyd 1975; McMurtry 1980a). Thus a classification scheme has already been established to which the arenite succession of the Abington area can be related. Only relative values of individual components are used for comparative purposes (Welsh 1967; Floyd 1975).

All authors who have collected samples between the Leadhills and Fardingmullach Lines or their equivalents (Kelling 1962; Welsh 1964; Floyd 1975) have described sandstones with ferromagnesian- and feldspar-rich compositions.

Table 1 (overleaf)

Comparison of greywacke formation means from point count analysis. Vertical columns indicate lithostratigraphical units in lateral continuity.

(a) HEPWORTH (this thesis: see Appendix 4 for full data)

Formation Means

Component	Crawfordjohn	Abington	Glencaple	Elvan
Quartz	40.7	41.3	17.7	11.2
Feldspar	6.5	7.2	19.1	21.8
Basic ig.	1.8	1.1	12.9	12.5
Acid ig.	6.1	9.6	5.2	2.6
Metamorphic	3.6	1.5	1.1	0.6
Sedimentary	2.5	1.7	2.1	2.6
Ferromags.	-	-	1.1	8.7
Matrix	38.8	37.6	40.8	40.0
n (61)	3	30	17	11

(b) MCMURTRY (1980a, Table 2)

	Guffock	Spothfore Matrix	Glenfloss
Quartz	30.1	27.3	41.2
Feldspar	17.4	16.6	6.9
Basic ig.	4.8	5.4	3.6
Acid ig.	2.4	2.4	1.2
Metamorphic	1.8	1.4	2.0
Sedimentary	3.9	5.0	5.3
Ferromags.	0.1	0.1	-
Matrix	39.5	41.8	39.8
n (40)	11	17	12

(c) FLOYD (1975, Table 5)

	Marchburn	Blackcraig	Afton	Scar
Quartz	14.9	33.4	48.3	20.3
Feldspar	44.3	15.8	14.1	49.5
Basic ig.	7.1	13.6	4.4	4.3
Acid ig.	3.5	2.6	0.9	2.3
Metamorphic	1.0	4.2	2.7	1.4
Sedimentary	1.6	1.3	1.4	1.5
Ferromags.	1.5	6.1	0.2	1.7
Matrix	26.1	23.0	28.0	19.0
n (122)	22	20	50	30

(d) WELSH (1964, Table 5)

	Cairnerzean	Lochryan	Glenwhan
Quartz	13.7	28.5	4.8
Feldspar	15.3	7.4	13.9
Basic ig.	27.7	18.7	47.5
Acid ig.	5.9	9.8	4.3
Metamorphic	10.0	9.6	2.2
Sedimentary	2.9	5.2	3.8
Ferromags.	7.1	-	5.4
Matrix	17.4	20.8	18.1
n (87)	27	39	21

(e) KELLING (1962, Tables 2 and 3)

	Corsewall	Galdenoch	Kirkcolm	Port. basic
Quartz	16.6	26.2	29.6	8.6
Feldspar	17.5	9.7	11.1	30.9
Basic ig.	17.7	10.2	9.0	29.4
Acid ig.	17.4	13.2	13.3	5.5
Metamorphic	0.8	2.8	4.8	0.6
Sedimentary	1.1	1.8	5.0	2.3
Ferromags.	10.3	7.8	0.6	13.4
Matrix	18.3	28.0	26.8	9.3
n (69)	24	3	37	5

n = number of specimens

However, within this structural block local variations in petrography occur; in the Rhinns of Galloway basal lithologies of the Portpatrick Group (the Acid-clast Division) are relatively depleted in ferromagnesian minerals, feldspar and basic fragments and are enriched in quartz and acid fragments, a composition compatible with that of the Elvan and basal Elvan Formation although acid fragments do not show such marked variation in the Abington district. The development of a ferromagnesian-poor (Glencaple) formation at the top of the sequence has not been described from this block anywhere else in the Northern Belt.

North of the Leadhills Line, quartz-rich sandstones are dominant. Kelling (1961) subdivided these on the basis of quartz and metamorphic clast percentages, whilst in east Nithsdale, McMurtry (1980a) recognised two formations (Guffock/Glenflossh) which have significantly different percentages of quartz from each other. Considerable fluctuations in the amounts of quartz and metamorphic fragments occur in the Abington area, but it is not possible to ascertain whether these form mappable sequences within the Crawfordjohn and Abington Formations or are isolated horizons of little vertical significance. Equivalents of the ferromagnesian-rich Galdenoch Group (Kelling 1961) and Blackcraig Formation (Floyd 1975) have not been recognised NE of the Sanquhar coal basin.

The northernmost fault block of the Northern Belt also contains ferromagnesian-rich sediments in the Rhinns of Galloway and west Nithsdale (Kelling 1961; Floyd 1975) which are not found in the poorly exposed Mill Burn Block. Although not point counted on account of their fine grain-size, sandstones of the Mill Burn Member are quartz-rich and feldspar-poor, and as such compare with descriptions of the lowest part of the Marchburn Formation (Floyd 1975).

CHAPTER 4: SEDIMENTOLOGY

4.1 INTRODUCTION

This chapter describes the sedimentary criteria by which facies and facies associations (Mutti & Ricci-Lucchi 1975) are recognised within the study area. Turbidite is used to describe the product of deposition from a turbidity current s.s. Where either the depositional mechanism is unclear or two or more distinct processes resulted in the formation of a single bed, the term sediment gravity flow is preferred. Proximal and distal are used in the sense of Kelling & Holroyd (1978), referring to distance from either source or point of input into the basin.

Reconstruction of flow dynamics is based on sedimentary structures. The dominant grain-support mechanisms of sediment gravity flows responsible for deposition of the bulk of lithologies observed at outcrop in the Abington district are (Middleton & Hampton 1973):-

Turbidity currents: The current contains particles which are maintained in suspension by turbulence and moves due to its density being greater than the ambient fluid.

Fluidised sediment flows: are produced by the expansion of a granular bed by an upward flow of fluid; the liquified

sand layer persists until the pore fluids are lost, in which case the flow 'freezes' from the bottom upwards (upward intergranular flow).

Grain flows: are supported by dispersive pressure (Bagnold 1954) acting upon cohesionless grains moving downslope in response to gravity. Modified grain flows maintain dispersion by the presence of a dense interstitial fluid, an overlying current or excess pore-fluid pressure; density-modified grain flows contain interstitial fluid, the density of which exceeds that of the ambient fluid (Lowe 1976).

Debris flow: Grain-support is achieved by clay minerals in the flow acting together as a single fluid possessing finite cohesion (matrix strength) and works in conjunction with buoyancy effects.

Each flow type is not necessarily characterised by a specific grain-support mechanism, hence grains in a dense, predominantly turbiditic suspension may also be supported by buoyancy and dispersive pressure.

The E division of a turbidite unit is used in the sense of van der Lingen (1969) and Hesse (1975) to describe mudstone of turbiditic origin; hemipelagic and pelagic background sedimentation (e.g. black mudstones and cherts) is termed the F division following the same scheme.

4.2 DESCRIPTION AND INTERPRETATION OF SEDIMENTARY FACIES

In this section, the sedimentary facies recognised in the area are organised, generally in order of decreasing grain-size. Implicit in this scheme is the gradual down-current evolution of flow parameters (hence the transitional nature among facies) and the increasingly distal character of finer-grained rocks. Where possible, facies are equated with those in existing classification schemes (e.g. Walker & Mutti 1973; Mutti & Ricci-Lucchi 1975) which are given at the end of each section. The stratigraphical occurrence of facies is included in the summary of sedimentological characteristics of each lithostratigraphical unit (Table 2).

4.2.1 Cobbly siltstones

This facies outcrops only in one stream section, Glencaple Burn (92461966). The distinguishing feature is the presence of large, elongate clasts of sandstone (4-20 cm in length) set in a matrix of massive siltstone. The clasts vary from rounded to subangular in outline. However, this variation may occur within a single clast (Plate 12). A variability in the sharpness of definition of clast margins is also evident; diffuse, wispy and sharp contacts with enclosing siltstones are all represented. Most clasts are structureless, although graded and parallel-laminated sandstones - all intrabasinal in origin - have been observed.



Plate 12: Parallel-laminated sandstone clast in cobble siltstone, Glencaple Formation.



Plate 13: Disorganised conglomerate, Haggis Rock Member.

Laminated clasts are juxtaposed laterally with nonlaminated clasts. Numerous veins pervade the clasts and are orientated at high angles to bedding (defined by the parallel orientation of the long axes of the clasts). The vein material is dark grey in colour, resembling the silt material of the matrix. The thickness of this unit is not known, but exceeds 50 cm.

The presence of veinlets of the encompassing silty sediment, the diffuse nature of boundaries and the variability of shape of the sandstone clasts taken together indicate that the clasts and matrix were semilithified during remobilisation - thus the density contrast between clasts and matrix was not significantly different. The low clast and high matrix content is interpreted to represent the result of emplacement by debris flow (Johnson 1970; Hampton 1972). Pierson (1981) summarised the dominant particle support mechanisms of debris flow as (1) cohesive strength of matrix (2) buoyancy (3) dispersive pressure (4) static grain-to-grain contact (5) turbulence. Static grain-to-grain contact requires grain concentrations in excess of 50% (Rodine & Johnson 1976); turbulence and dispersive pressure would produce forces tending to destroy semilithified clasts and these three mechanisms are therefore not considered applicable to this facies. In view of the low density contrast between clast

and matrix, a combination of cohesive matrix strength working with buoyancy effects probably maintained the clasts in suspension.

Rounding of the lateral margins of some clasts may have been achieved by the erosive effects of shearing within the flow. It is significant that finer-grained sandstones (parallel-laminated) have well rounded margins, in contrast to coarser sediments which have more diffuse contacts with the enclosing mudstone. Presumably this reflects greater cohesive strength of the former.

Subaerial debris flows have been observed to travel over slopes as low as 1 or 2 degrees (Sharp & Nobles 1953; Curry 1966); slopes, possibly exceeding these values, are therefore inferred for this facies.

Walker & Mutti (1973) Facies F; Mutti & Ricci-Lucchi (1975) Facies F.

4.2.2 Disorganised conglomerates

This facies comprises small and medium pebble, clast-supported conglomerates with fragments attaining a maximum diameter of 14 mm (see 2.2.2, Haggis Rock). Size distribution of sediment is strongly bimodal, with grain-size in the matrix ranging from fine to medium sand. The matrix forms 15-30% of

the rock. Within individual beds the clasts (as distinct from the sandy matrix) are well sorted (Plate 13). Modal clast size, however, varies between units.

Poor exposure precludes the determination of parameters such as bed thickness, lateral continuity and the nature of bed contacts. No internal sedimentary structures have been found, therefore this facies cannot be assigned to the Bouma sequence.

Clasts are mostly equant, although sedimentary fragments may be tabular or bladed (Zingg 1935). The short (c)-axes of tabular and bladed fragments lie at high angles to bedding, and a crude parallel arrangement of these fragments is discernible. Some clasts are orientated with their planes of maximum projection at angles as much as 45° to bedding. A preferred clast fabric (cf. Davies & Walker 1974) has not been recognised.

This facies is characterised by the absence of structures indicative of deposition from suspension or traction-load, suggesting emplacement either as a debris flow or density-modified grain flow. Previous literature studies (e.g. Rocheleau & Lajoie 1974) have been directed towards rudites showing the development of structures which can be interpreted hydrodynamically, with the consequent neglect in the understanding of structureless rudites. However, in

view of previous descriptions of rudites from the Northern Belt (Holroyd 1978; McMurtry 1980a), and the absence of sedimentary structures from which transportation involving dispersive pressures can be inferred (e.g. inverse graded bedding), it is tentatively suggested that debris flow was the dominant mechanism. The high clast-to-matrix ratio would allow grain collisions and hence dispersive pressures would contribute to sediment support within the flow. Such a mechanism corresponds to the term inertia flow (Sanders 1965; Carter 1975).

Sandstones (thicknesses of the order of a few tens of centimetres), occasionally interbedded with rudites, may reflect the development of a low density turbulent cloud eroded from the snout of the debris flow (Hampton 1972). Kelling and Holroyd (1978) described similar 'bipartite' beds from Corsewall in the Rhinns of Galloway.

Walker & Mutti (1973) Facies A₁; Mutti & Ricci-Lucchi (1975) Facies A₂.

4.2.3 Organised pebbly and granular sandstones

Units of this facies range from 45-405 cm (mean = 170 cm) and are of unknown lateral continuity. Basal contacts are sharp and planar, with little evidence of extensive scouring; upper contacts are diffuse or sharp. Sand:shale ratio tends

towards infinity as a result of frequent amalgamation.

Solemarks are restricted in development to rare flames.

Internal structures, usually defined by the coarsest grain-sizes (predominantly granule-grade), include normal, delayed and inverse grading and weak stratification - Bouma sequences may therefore be assigned to the T_a division with T_{b-f} absent (Plates 14 and 15). Coarse-tail grading predominates, although distribution grading also occurs.

A thin zone of inverse coarse-tail grading, a few centimetres thick, is sometimes present below the normally graded layer.

Pebbles rarely form more than 5% of a bed. Stratification is rare, consisting of diffuse trails of matrix-supported coarse sand to granule grains which are the thickness of a single grain or a few centimetres. Trails are laterally discontinuous and are developed near the base of sandstone units. Multiple trails within single beds have also been recognised; trails may be separated by up to 75 cm of ungraded and structureless sandstone, without any evidence of a break in sedimentation between the two layers. In one instance, the upper is coarser than the lower train. Stratification is also indicated by the parallel orientation of shale intraclasts. Erosion hollows at the base of beds may be filled by lenses of pebbles of irregular thickness. Where present, shale intraclasts are invariably larger than the modal class of quartz and feldspar pebbles.

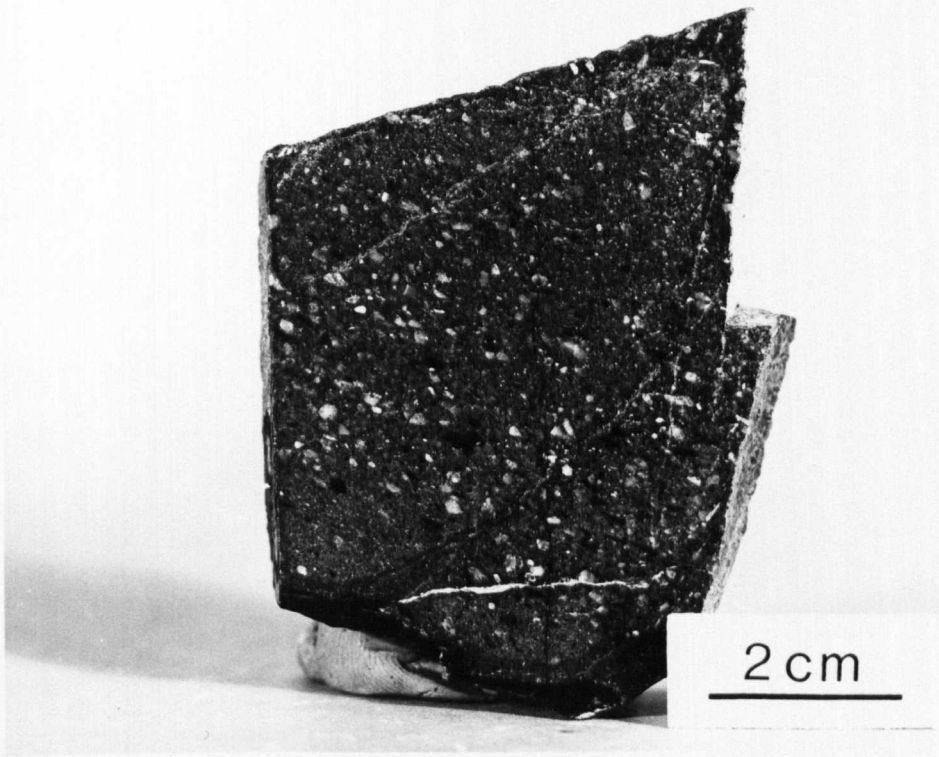


Plate 14: Delayed grading at base of organised granule sandstone, Glencaple Formation.

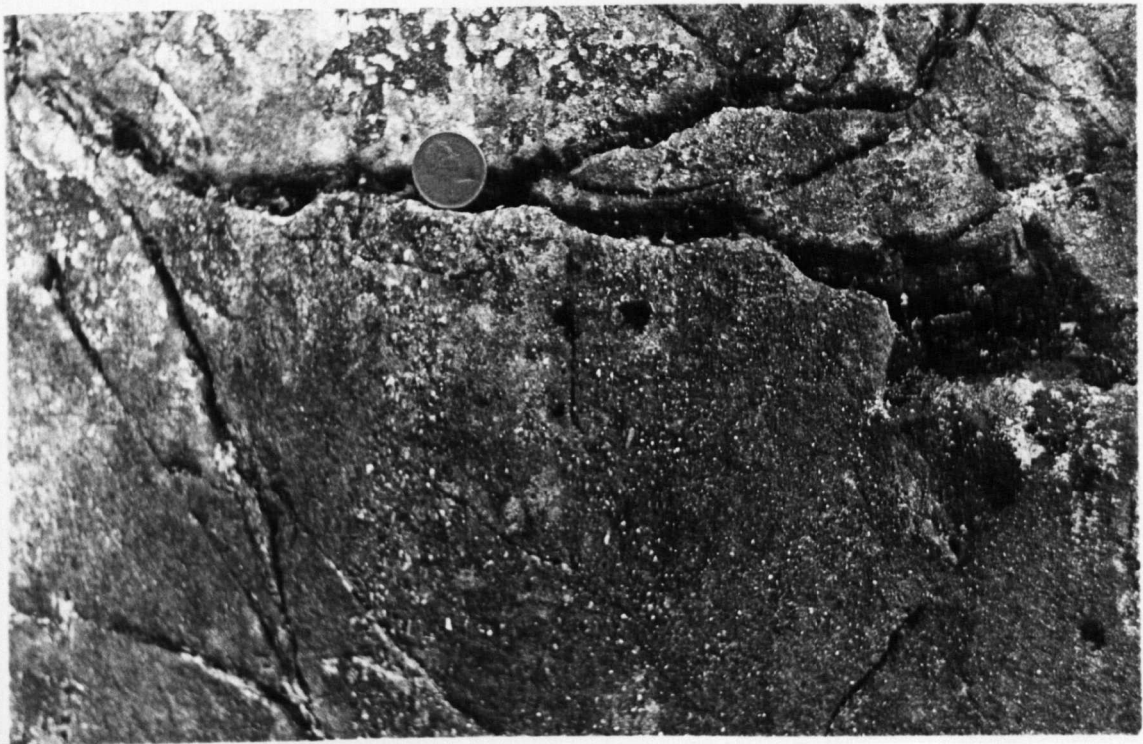


Plate 15: Thick-bedded, organised, pebbly sandstone, Glencaple Formation (younging left to right, vertical section). Zone of delayed grading above base (not seen) of bed; coarse-tail, normal grading towards top of unit. 1p coin for scale.

Penetration of intraclasts through former interstices within the sandstones indicates that the former were soft at the time of deposition. Scattered pebbles dispersed through the base of a sandstone bed have been considered by Walker & Mutti (1973) to represent the transition between ungraded sandstones and organised pebbly sandstones.

The characteristic features of this facies, namely apparently ungraded beds with the development of sedimentary structures restricted to the coarsest grain-sizes, indicate a depositional mechanism related to the ungraded sandstone facies - indeed, many arguments concerning the origin of the latter are applicable to organised pebbly sandstone facies (see section below on ungraded sandstones).

There is general agreement that inverse and normal grading of the coarse-tail fraction is produced by density flows of high concentration (Bagnold 1954; Middleton 1967; Fisher 1971; Middleton & Hampton 1973). Dispersive pressure (Bagnold 1954, 1968) and the "kinetic sieve" mechanism (Middleton 1970) have been invoked to explain inverse coarse-tail grading. Middleton (1967) produced normal coarse-tail grading experimentally from high concentration suspensions (greater than 30% grains by volume).

In view of the inferred rapid sedimentation of this facies, it is considered unlikely that granule trails were

formed by traction at the sediment/water interface. It is probable that the trails represent local granule concentrations within a complex flow.

This facies was therefore deposited by mechanisms ranging from high concentration, density-modified grain flows (ungraded portions of beds) to high concentration turbidity currents (graded divisions). The presence of semilithified clasts indicates the erosive capabilities of these currents. Smith (1972) concluded that most mud clasts in sedimentary rocks were deposited very close to their source (within a few tens or hundreds of metres) because of rapid rates of attrition of fragments.

Walker & Mutti (1973) Facies A₄; Mutti & Ricci-Lucchi (1975) Facies A₁.

4.2.4 Ungraded sandstones

Bed thickness of this facies ranges from 70-320 cm (mean = 115 cm). Beds are typically amalgamated, although in some instances they may overlie thin T_c, T_d or T_e sequences; bases of beds are sharp and planar at outcrop scale. Locally, currents have eroded a few centimetres down into the underlying sediment. Lack of outcrop precludes the determination of bed geometry; one exposure in Glencaple Burn (92441951) shows a bed with a convex upper surface. Sand:shale ratio

tends towards infinity over continuous sections in excess of 20 m thick (Plate 10).

These very coarse sandstones are poorly sorted and thin sections show a size range of monocrystalline quartz fragments from coarse silt- to coarse sand-grade. Being largely structureless, Bouma sequences are not generally applicable to this facies. Shale intraclasts attain a maximum size of 30 x 6 cm, typically occurring in the lower half of a bed. Rare and isolated pebbles of granule- and occasionally small pebble-grade show a similar distribution. T_c , T_d and convolute bedding have been recorded to overlie sharp tops of sandstone beds.

The massive sandstones have been metamorphosed under prehnite-pumpellyite conditions (Chapter 6), so that assessment of the original sedimentary microtectures, particularly the matrix content (important to the hydrodynamic interpretation) remains speculative. Any consideration of the flow dynamics must account for the following characteristics:

- lack of typical turbidite features
(especially grading),
- lack of traction-current structures,
- apparent absence of solemarks,
- presence of large intraclasts,

-sharp bounding surfaces to some bedding units.

The presence of large intraclasts and lack of grading and other associated structures eliminates the possibility of deposition of sediment from turbulent suspension in a turbidity current. These features also preclude grain-by-grain deposition by traction currents (Stauffer 1967). The poorly sorted nature of these deposits suggests deposition from relatively highly concentrated flows, as mechanical segregation of coarse from fine grains did not occur (Pettijohn 1950). This contention is supported by the absence of traction structures, indicating that grain movement under both upper flow (UFR) and lower flow (LFR) regimes was prevented by rapid burial following sedimentation (Middleton & Hampton 1973). In such conditions, fine-grained material may be passively trapped in the interstices between sand grains during deposition (Kuenen 1966).

The grain-support mechanism of this facies is poorly understood. Fluidised sediment flow (Middleton & Hampton 1973) is unlikely, given the lack of liquefaction features (e.g. injection and dish structures; diffuse plane lamination). Structureless beds have been explained as the products of grain flow, involving the support of cohesionless sand grains by dispersive pressure (Bagnold

1954; Stauffer 1967). Lowe (1976) has challenged this view, concluding that sedimentation units in excess of 5 cm thick are unlikely to be generated by such mechanism. However, the presence of dispersed fines interstitial to the coarser grains would allow flow over slopes substantially less than those required for movement of granular aggregates of corresponding sand-grade, due to: (1) reduction of the immersed weight of the larger grains and, therefore, the dispersive pressure to maintain dispersion (buoyancy effect) and (2) increasing the density contrast between flow and ambient fluid, thereby promoting higher velocities (Lowe 1976). Hampton (1972) has suggested that the presence of clay, forming less than 10% of a bed, is sufficient to maintain complete support of sand size material in a debris flow. The poor sorting of the ungraded sandstones suggests the presence of interstitial material. In the absence of turbulence, solemarks, such as flutes, would not be expected.

Middleton(1967) proposed an alternative explanation to account for the lack of traction structures, based on experimental observations. High concentration flows behaved as an expanded viscous fluid for a short period after rapid deposition, and waves, formed along the interface of the "quick" bed and overlying entrained layer, "churn" the sediment, with the consequent destruction of any lamination which may have previously formed by traction.

The lack of traction structures is further discussed in Section 4.2.5.

The sharp tops of some beds are not considered to be a primary feature, as some units, although ungraded and structureless for the bulk of their thickness, show a thin, transitional (graded) upper contact with the overlying sediment. This material is often thinly laminated (T_d division) and represents pulsatory deposition from low concentration suspensions. Together, the delayed grading and laminated divisions are inferred to be a product of dilute, but turbulent, suspensions in the entrained layer accompanying the sediment gravity flow. The absence of these layers from most ungraded units is attributed to basal erosion from the overlying flow. The high sand:shale ratio probably resulted from a combination of erosion of mud layers and rapid emplacement of successive flows which suppressed the development of sediments of low concentration turbiditic or hemipelagic origin. By-passing of the depositional site of the ungraded sandstones by finer-grained sediment may also account for the above features. Shale intraclasts, showing evidence of soft sediment deformation, indicate that flows were capable of erosion.

It is concluded that either high concentration, density-modified grain flows (Lowe 1976) or sandy debris flows (Hampton 1972) were responsible for deposition of the

ungraded sandstone facies, with sudden 'freezing' of the flow resulting from rapid decay of the current in a proximal environment. Energy was dissipated rapidly, either due to a sudden overbank discharge from a channel, or the marked decrease in gradient of the slope (Middleton & Hampton 1976). Postdepositional deformation may also have contributed to the destruction of internal sedimentary structures.

Walker & Mutti (1973) Facies B2.

4.2.5 Graded sandstones

This facies can be subdivided into two subfacies according to the relative development of Bouma sequences overlying the graded layer. These are respectively T_{ae} (centre-cutout) sequences and units corresponding broadly to complete T_{a-e} sequences.

T_{ae} Bouma sequences: are characterised by the presence of Bouma T_a and T_e units, with the exclusion of the intermediate T_b , T_c and T_d divisions (Plate 9). Unit thickness varies from 15-300 cm with a mean of 70 cm. Contacts between beds are sharp and usually parallel-sided at outcrop scale; basal surfaces rarely show evidence of scouring, save for minor local channels not exceeding a width of 50 cm and depth of 10 cm cut into an otherwise planar surface. Amalgamation

of bedding is common. Flame structures and load casts are sporadically developed.

Both coarse-tail and distribution grading are common, typically from very coarse sandstone at the base of the unit to fine sandstone at the top. In addition, the thickest beds also show a basal zone of inverse or delayed grading of varying thickness. The modal grain-size class incorporates both very coarse- and coarse sand-grades. With increasing grain-size this subfacies is transitional to the organised pebbly sandstone facies.

Walker & Mutti (1973) describe T_{ae} sandstones as, "the typical, classical proximal turbidite..., not an ABCDE bed". Deposition from an inertia-flow layer has been suggested to account for this facies (e.g. Bagnold 1941; 1954; 1956; Sanders 1965), with traction carpets and flowing grain layers moving concurrently with, and surrounded by, a zone of turbulent suspension. Middleton (1970) provided an alternative explanation, based on deposition from high concentration flows, namely, an increased rate of deposition once deposition starts. Within such flows, tractional movement would be suppressed, leading to the formation of a bed devoid of lamination (Walton 1967).

T_{a-e} Bouma sequences: In contrast to the T_{ae} Bouma sequences

this facies is defined by units which approximate to complete T_{a-e} sequences, although such have not, in fact, been recorded. Most permutations do occur, T_{ad} being the most common, with subsidiary T_{acde} and T_{ade} cycles and the T_b interval rarely developed. T_{ad} sequences are generally characteristic of thicker and coarser-grained beds. The facies is typically medium-bedded (mean thickness = 30 cm). Again beds are parallel-sided at outcrop scale, with no evidence of basal erosion, save minor flame structures. Load structures are developed where a sandstone layer immediately overlies mudstone.

The cross-laminated T_c division consists of solitary sets of small-scale ripples - sets of two ripples have only been observed in one instance. Convolute lamination is also a feature of the T_c division.

Distribution grading is ubiquitous in the T_a division and there is a direct relationship between grain-size at the base of such units and bed thickness. Amalgamation of sandstone beds is rare.

Deposition of this facies took place from waning turbidity currents. Development of relatively complete Bouma sequences reflects decreasing flow intensity (or flow regime), combined with a decreasing rate of deposition from suspension and increasing importance of traction upwards through the bed (Walker 1967). Distribution grading

indicates that the turbidity currents which produced this facies were of a lower density than those responsible for T_{ae} sequences.

Walker & Mutti (1973) Facies C; Mutti & Ricci-Lucchi (1975) Facies C_2 .

4.2.6 'Base-missing' sandstones

This facies is transitional between the T_{a-e} and the laminite facies (see 4.2.7). It is volumetrically insignificant, and consists of beds produced by a single depositional event, within which at least the lowest Bouma division is absent. Bed thickness is typically a few centimetres, with a range from 2-25 cm. Most units are lenticular at outcrop scale.

'Base-missing' Bouma sequences are predominantly medium to fine sandstones. A typical member of this facies would show T_{c-e} divisions, with no break in sedimentation up into the overlying mudstone (Plate 16). Where present, the T_b unit forms a thin veneer less than 1 cm thick below the cross-laminated division.

Ripple sets are usually solitary in occurrence and small-scale (3-20 mm in thickness). The lower bounding surface may be erosional or nonerosional (cf. Allen 1963).



Plate 16: 'Base-missing' sandstone, Abington Formation. Sharply overlying hemipelagic mudstone, the unit consists of Tc, Td and ?Te divisions. Climbing ripples in Tc units; flame structures on base of bed.

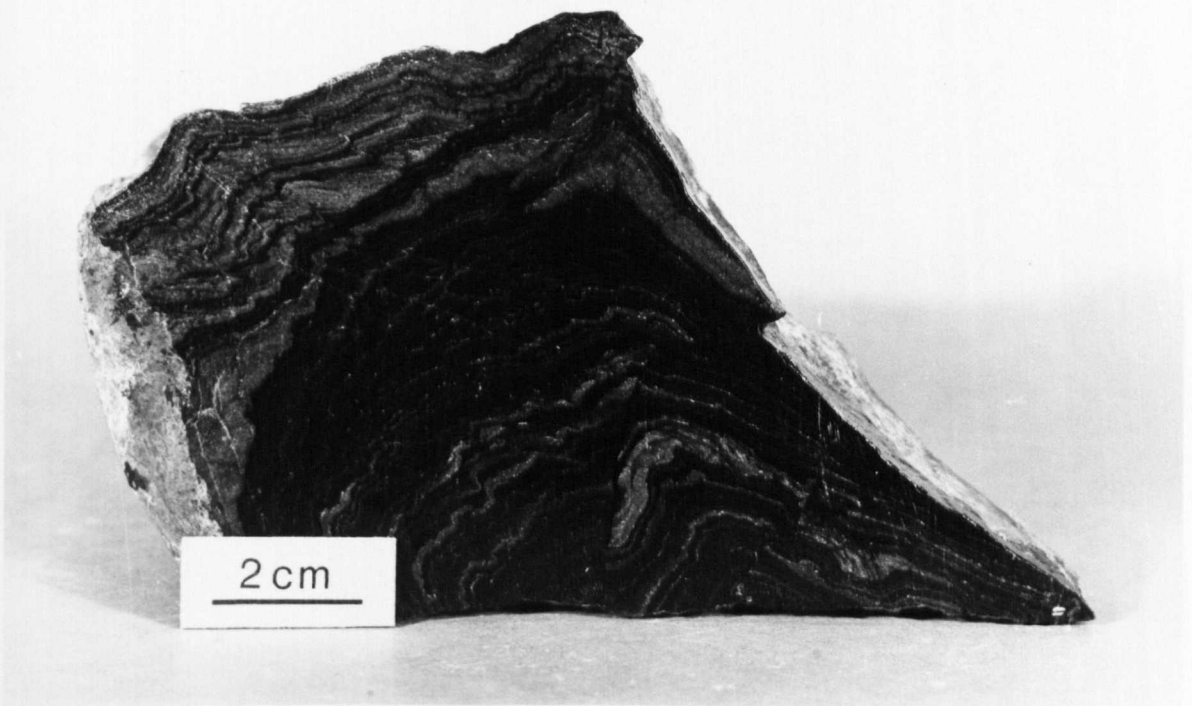


Plate 17: Disturbed facies, Glencaple Formation. Marked variations in bed thickness around fold.

Where the cross-stratified unit immediately overlies a T_b division, the bounding surface is always gradational. Climbing ripples preserve both stoss and lee laminae, and accordingly may be classified as Type 1 ripple laminae in-drift (Reineck & Singh 1973). The change in grain-size from sand- to silt- and mud-grade throughout the turbidite is normally accompanied by T_c , T_d and T_e Bouma intervals. However, instances occur where the T_c unit has a sharp and planar upper bounding surface overlain directly by the T_e division to the exclusion of the parallel-laminated T_d sequence.

Continuous T_{c-e} sequences suggest tractional reworking of material deposited initially from a relatively low density turbulent suspension under lower flow regime conditions. Higher rates of sedimentation are reflected by the development of climbing ripples. The absence of T_a and T_b intervals has been interpreted to indicate a distal environment of deposition (Walker 1967):

Walker & Mutti (1973) Facies D; Mutti & Ricci-Lucchi (1975) Facies D_1/D_2 .

4.2.7 Laminites

This facies consists of thin, alternating laminations of light (arenaceous) and dark (argillaceous) beds. The

former consists predominantly of quartz fragments of very fine sand-grade or less, contrasting with the darker bands which comprise silt-grade material generally micaceous in composition. Individual laminae are typically less than 2 mm in thickness; occasional laminae may attain 1 cm. Laminite packets have a maximum thickness of 12 m.

Lenticularity of bedding is almost ubiquitous, and most horizons are impersistent over the distance of a few centimetres. Within thicker laminae, small-scale, solitary sets of cross-lamination are the dominant structures, although convolute lamination also occurs. In contrast to the 'base-missing' Bouma sequences, both lower and upper contacts of sandstone laminae abut sharply against the enclosing siltstone. Other laminae are more persistent laterally, showing grading with no sharp break in sedimentation between the arenaceous and argillaceous material.

Graded units within this facies are believed to represent fallout from dilute suspensions, either from a turbidity current or a nepheloid layer. Lenticular and sharp-topped units were formed by traction of silt material over the underlying dark-grey siltstone. The latter is interpreted as the normal background sediment. It is not known whether the silt was brought to its present depositional site as a graded layer described above and

subsequently reworked, or as bedload accompanying other currents such as contourites (Bouma & Hollister 1973).

4.2.8 Mudstones

Mudstones (fissile and nonfissile) consist of silt- and clay-grade material forming sequences devoid of any lamination, up to 10 m thick. Contacts with other lithologies are sharp and planar. The range of colours (black, green, red and brown) reflects differing oxidation states or the presence of free carbon. Black mudstones are sometimes fossiliferous, containing graptolites and rare radiolaria; pyrite is a common mineral in this lithology. The parallel orientation of graptolite fragments, although rare, implies bottom-currents. Mudstones are commonly siliceous and with decreasing mica content grade into cherts. Chert nodules occur in brown and green mudstones (Plate 3).

The absence of lamination in this facies suggests deposition as hemipelagic fallout. Brown mudstones are interbedded with lavas and may thus be volcanic in origin (Walton 1965). Devitrification of volcanic glass may account for the release of silica to form chert nodules (see 4.2.9).

Walker & Mutti (1973) Facies G; Mutti & Ricci-Lucchi (1975) Facies G.

4.2.9 Cherts

This facies consists of two main types - black and grey cherts - which are distinguished by variations in colour first and also in the content of radiolaria, micas and quartz microveins.

Black cherts: are internally structureless and well bedded in units 5-10 cm thick. Bedding surfaces are generally persistent but many amalgamate laterally to produce beds of lenticular geometry. The maximum thickness of bedded black cherts is 30 m, although this sequence is internally faulted and may involve repetition of strata (see 2.4.3). The lithology consists of microcrystalline quartz in association with opaque material which may form up to 20% of the rock. Mica forms less than 1% of the total volume; pyrite cubes occur infrequently. Spherical aggregates of microcrystalline quartz (0.05-0.35 mm in diameter) are interpreted as the recrystallised remains of radiolaria. These are evenly distributed throughout each bed and comprise up to 60% of the rock. Two types of cavity-fill are recognised: (i) the cavity wall is coated by a

microcrystalline quartz aggregate several grains thick, and (ii) the centre of the cavity consists either of a cryptocrystalline quartz mosaic or fibrous chalcedony in radial arrangement - the latter producing extinction crosses when viewed under cross-polarised light.

Black cherts are invariably pervaded by microcrystalline quartz veins (generally orientated at high angles to bedding) of which three generations may be distinguished by mutual cross-cutting relationships. Four vein types have been recognised: (i) crystal size increases towards the centre of the vein, with no preferred orientation, (ii) crystal size increases towards the centre of the vein, with preferred orientation, (iii) vein walls are coated with fibrous chalcedony orientated perpendicularly to vein walls, the centre of the veins being filled by radiating aggregates of fibrous chalcedony which show extinction crosses. Anhydrous, opaque iron oxide in the centre of vein types (i) and (ii) is the last material to crystallise in the cavity-fill sequence. All three vein types have sharp walls and cross-cut another form, (iv), which has gradational contacts with the host rock, shows marked thickness variations and is more variable in orientation.

Whilst it is clear that types (i) to (iii) originated as the filling of brittle fractures, type (iv) may have formed during early diagenesis. The different vein

varieties indicate that silica, produced by thermal and pressure solution, remained a mobile phase from early diagenesis until after lithification.

Grey chert: Bedding characteristics of this subfacies are similar to those for black cherts. In addition, however, packets of grey cherts vary in thickness when traced along strike over large exposures (Appendix 2).

Thin sections show white mica (which may form up to 10% of the rock) and sporadic angular quartz fragments of fine sand-grade or less set in an otherwise cryptocrystalline matrix. In contrast to black cherts, radiolaria are fewer in number and a pervasive quartz vein system is not extensively developed.

The principal problem in explaining the formation of cherts concerns the origin of the silica, which is not precipitated at concentrations present in modern oceans (Krauskopf 1959; Siever 1962). Three alternative modes of origin have been proposed:

- (i) Formation from accumulations of siliceous organisms (e.g. radiolaria and diatoms) (Bramlette 1946).
- (ii) Direct inorganic precipitation of silica as a gel, either in restricted basins at high

pH values or in association with volcanic springs which produce concentrations of silica greater than the solubility of amorphous silica.

- (iii) Release of silica into solution accompanying the devitrification of volcanic glass, via the reactions of zeolite → montmorillonite → illite or kaolinite (Lancelot 1973).

In black cherts, the origin of silica is clear - namely, redistribution by partial dissolution of radiolarian tests. Precipitation of silica according to arguments (ii) and (iii) is not feasible as volcanic horizons are rarely associated with black cherts, neither do they contain significant proportions of clay minerals.

The origin of grey cherts is more obscure. They are associated with basalts and dolerites of possible volcanic origin in Raven Gill (see 2.4.1). These cherts contain sporadic radiolaria and are relatively rich in mica; hence none of the proposed mechanisms of chert formation may be dismissed as inapplicable. However, the presence of radiolarian ghosts may well indicate that many more existed in the original sediment than are presently preserved, the majority having been dissolved during

diagenesis and low-grade metamorphism (Wise & Weaver 1974). The cherts are thought to have formed in a restrictive basin, starved of all sediment save pelagic fallout.

4.2.10 Disturbed beds

This facies includes all lithologies which show evidence of deformation before sediment lithification (D_0). A variety of structures has been recognised, most frequently developed in laminites. Fold classification schemes of Ramsay (1967) and Rickard (1971) are followed. Load structures, although formed by soft sediment deformation, are described elsewhere along with descriptions of the facies in which they are found.

Folds: The identification of folds produced by soft sediment deformation is based on the following criteria:

- the occurrence of isolated folds in a sequence which faces in an otherwise uniform direction,
- an unfaulted angular disparity between either the upper or lower fold limb and enclosing sediment,
- marked variations in orthogonal thickness (t) of a single layer, or the presence in

a folded multilayer sequence of more than one fold class.

Folds are isolate and are only rarely present as complete fold pairs. Amplitude is of the order of a few centimetres. Upright horizontal folds (Rickard 1971) predominate, generally with tight to isoclinal limbs - open folds are rare. Both angular and rounded fold closures have been recorded. Axial surfaces are typically planar, but may show slight curvature.

Component beds thicken markedly around folds (Plate 17); mudstone laminae show a threefold increase in orthogonal bed thickness (t) when traced from limb to hinge. A synform in Bellgill Burn (89431770) has the geometry of a class 1C fold (Ramsay 1967). However, individual laminae within the fold show classes 1C, 2 and 3.

An important feature relevant to the genesis of these folds concerns the presence of angular discontinuities and décollement surfaces developed either on the lower or upper limbs. Folded lamination of the T_b division with part of the upper limb removed by erosion and directly overlain by a graded sandstone bed suggests that current-drag accompanying the turbidity current produced deformation of the T_b division prior to deposition of the sand load (Stewart 1961; McKee et al. 1962).

The occurrence of laminite units with part of the lower limb removed indicates another depositional mechanism. A pronounced angular discordance separates the lower fold limb from underlying sediment, and laminae within the former are smeared out and deformed into parasitic folds with anomalous vergence characteristics (Plate 18). Large flame structures are overturned in the same direction as the fold. Sediment immediately below the discontinuity differs from the folded laminite by showing pronounced lenticularity and unusually coarse grain-size (granule-grade) with respect to the very thin-bedded nature of the deposit - individual grains protrude into the overlying sediment.

This structure is interpreted as an allochthonous slump fold which originated on a palaeoslope. Curved axial surfaces may reflect either the original fold shape, or may indicate that deformation continued after emplacement.

Fragmentary bedding: This subfacies is characterised by fragmented and contorted sandstones enclosed within a matrix of structureless mudstone, which form units a few tens of centimetres thick. Two types are recognised, distinguished by the shape of sandstone fragments and the degree of preservation of original layering.

The first is characterised by inequidimensional,

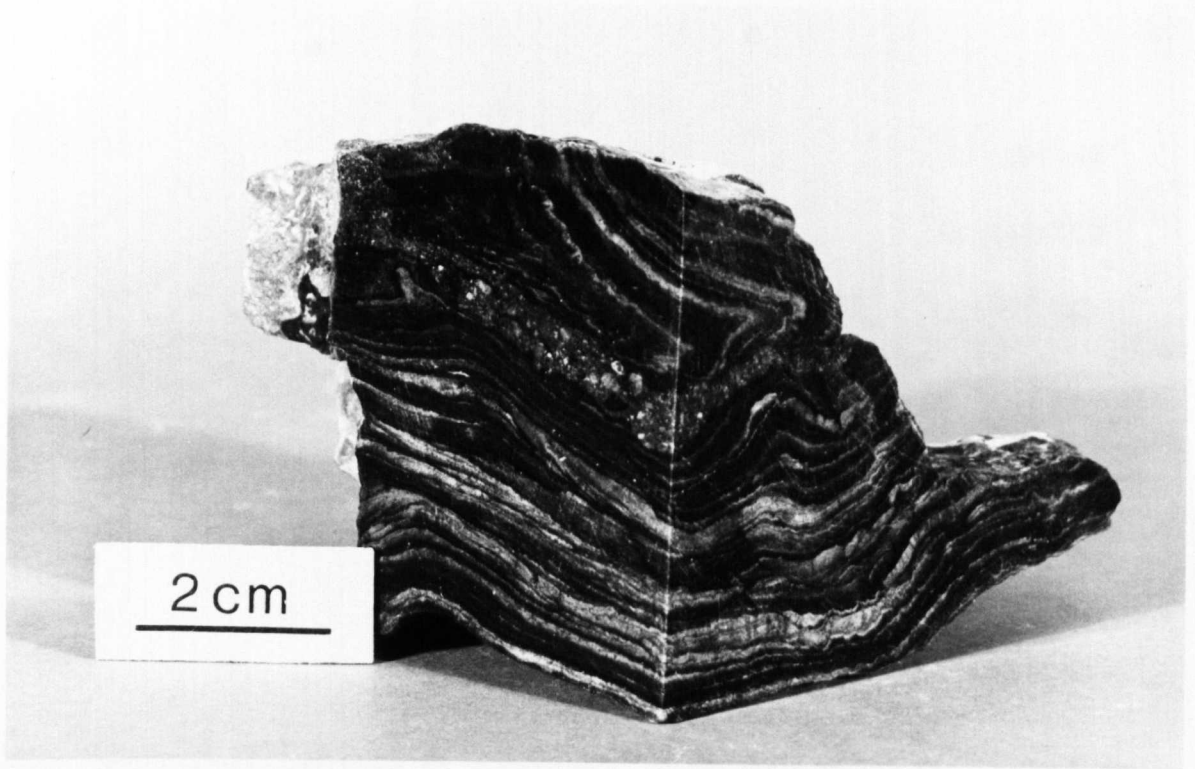


Plate 18: Disturbed facies, Glencaple Formation. Décollement surface developed along lower fold limb (see text for discussion).

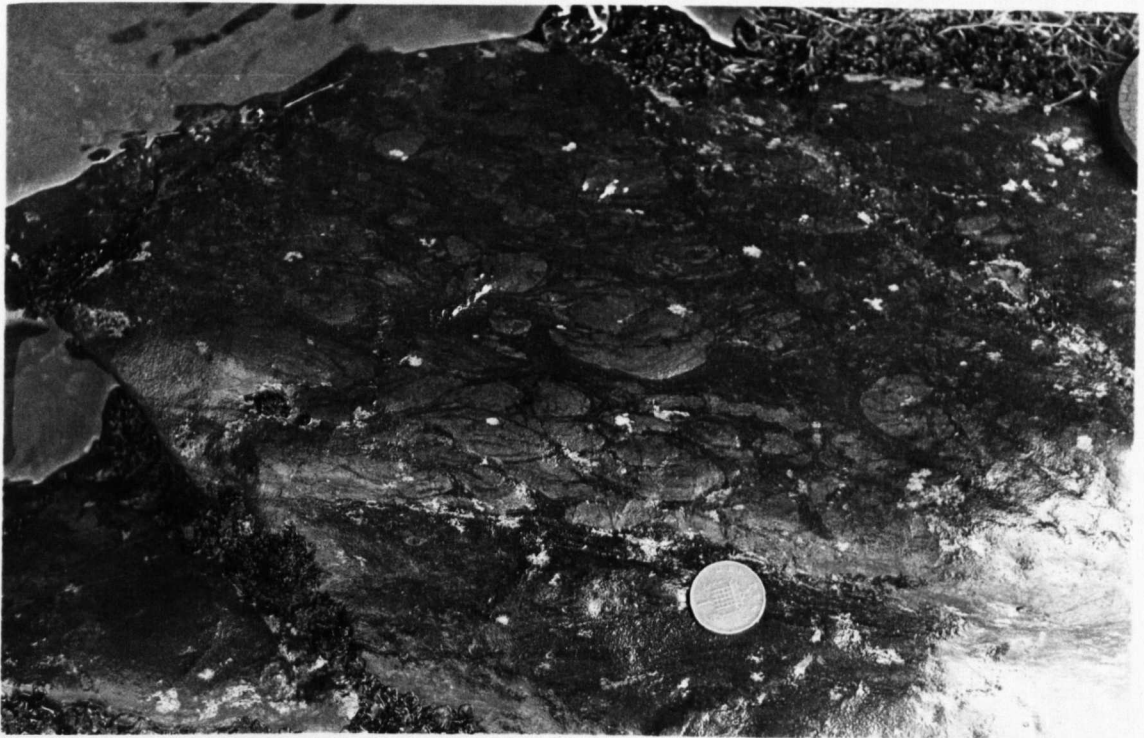


Plate 19: Ball-and-pillow structure in disrupted sandstone bed, Glencaple Formation. 1p coin for scale.

angular bedding fragments less than 4 cm in length and of variable shape. The lamination present in some fragments is sharply truncated at the contact with the surrounding mudstone. Bedding is vaguely discernible due to the parallel orientation of clasts. Folds are in lateral continuity with this subfacies and may thus be genetically related. It is suggested that fragmented bedding of this type resulted from downslope mass movement in the manner of a debris flow, with excess pore pressures in the matrix.

The second type of fragmentary bedding consists of closely packed ball-and-pillow structures concentrated in layers which represent vestiges of bedding. Pillows are well rounded and less than 4 cm in diameter (Plate 19). The shape of fragments depends on the amount of rotation bedding has undergone - this varies from being hook-like to ovate, the latter reflecting bedding rotation of approximately 180° . "Pseudo-nodules" are interpreted to form when a sand layer liquefies, the bed having such low strength and cohesion that the overlying sand sinks into the soft mud beneath (Kuenen 1958). These structures may also be current-induced.

Convolute lamination: differs from fold structures described above in exhibiting differential deformation between successive laminae of laminite sequences. These horizons

are of the order of a few centimetres thick. Convolute lamination indicates simultaneous deposition and deformation as fallout from turbulent suspension (Sanders 1965).

Walker & Mutti (1973) Facies F; Mutti & Ricci-Lucchi (1975) Facies F.

4.3 STRATIGRAPHICAL DISTRIBUTION OF FACIES

4.3.1 Mill Burn Block

Laminites are the most common rocks, although it is emphasised that the few exposures available may not accurately reflect the dominant lithology of the block as a whole. Disorganised conglomerates and graded sandstones (T_{ae} sequences) are subordinate to the laminites.

4.3.2 Crawfordjohn Block

Basal lithologies of the Crawfordjohn Block include cherts and siliceous mudstones of pelagic and hemipelagic origin; these facies form less than 5% of the total sequence. The rest of the thickness consists of graded sandstones (T_{ae} sequences) with subordinate laminites. Ungraded sandstones are rare. Bed thicknesses are comparable to the Abington Formation, although the thickness is greater in the latter (Fig. 15a).

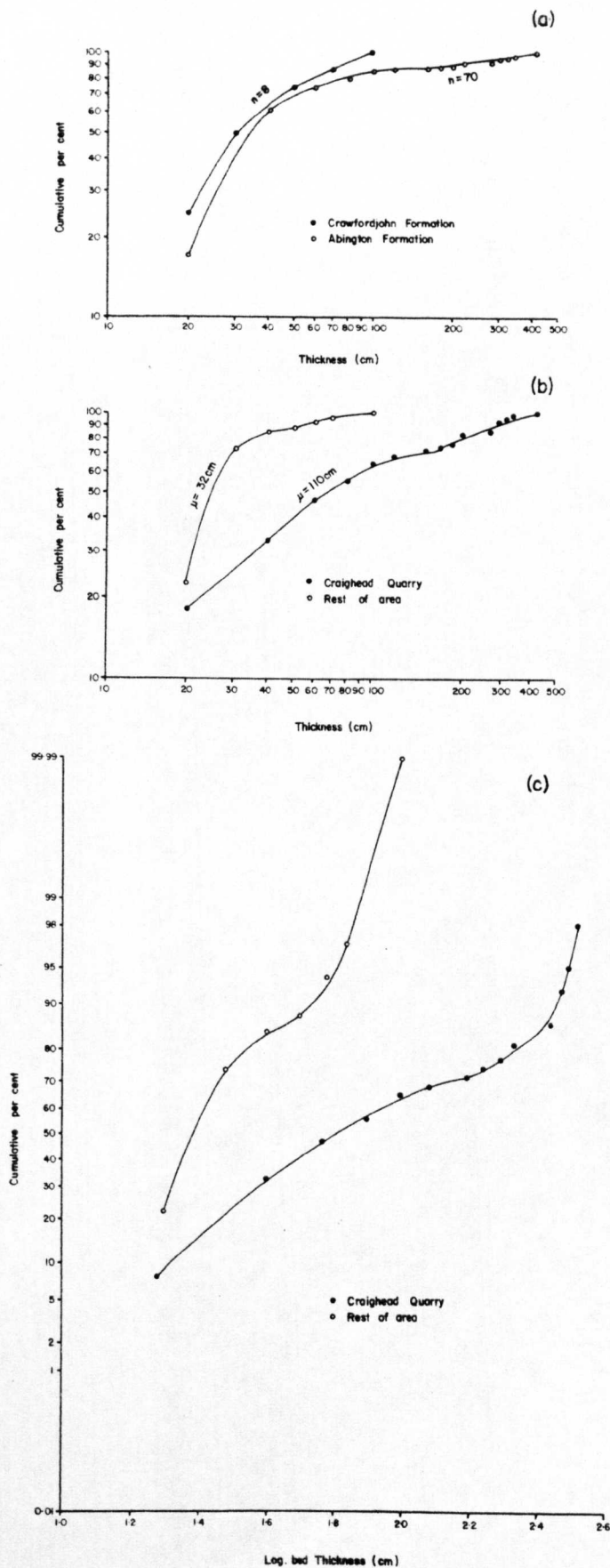


Fig. 15: (a) Bed thickness: Crawfordjohn and Abington Formations, log./log. plot.
 (b) Abington Formation: bed thickness data, log./log. plot.
 (c) Abington Formation: bed thickness plotted on arithmetic probability paper.

	A	B	C	D	E	F	G	H
Bed thickness (i) range	>60cm	mm-cm	20-100cm	15-120cm	0.2-4m	10-80cm	0.4-4m	5-120cm
(ii) mean	-	-	44cm	32cm	110cm	28cm	105cm	24cm
Lateral wedging	-	rare	no	no	rare	no	-	no
Amalgamation	-	no	rare	rare	yes	rare	yes	rare
Sharp tops ¹	-	yes	no	no	no	no	yes	no
Sharp bases ¹	yes	yes	yes	yes	yes	yes	yes	yes
Grain-size (i) typical	SP	silt	CS	CS	VCS	CS	VCS	MS
(ii) maximum	MP	FS	VCS	VCS	pebble	pebble	granule	CS
Graded ²	none	none	D	D	D, I	D	none	D
Bouma sequences	none	none	ae	ae	ae	a-e	none	ae
Mudst./sandst. clasts	yes	no	no	yes	<35cm	yes	<2cm	no
Soft sed. deformation	no	no	no	no	no	yes	rare	no
Associated facies ³	5	5	4, 6	2, 6, 7, 10	3, 4, 7	1, 3, 4, 6, 7, 10	3, 5, 6	4

Table 2: Summary of sedimentological characteristics of lithostratigraphical units.

A = Haggis Rock; B = Mill Burn Member; C = Crawfordjohn Fm.; D = Abington Fm. (thick-bedded facies); E = Abington Fm. (very thick-bedded facies); F = Glencaple Fm.; G = Elvan Fm.; H = basal Elvan Fm.
 Superscripted numbers 1. Describes sand layer only. 2. D = Distribution grading, I = inverse grading. 3. Associated facies 1 = cobbly siltstones; 2 = disorganised conglomerates; 3 = organised pebbly sandstones; 4 = ungraded ssts.; 5 = graded ssts.; 6 = 'base-missing' ssts.; 7 = laminites; 8 = mudstones; 9 = cherts; 10 = disturbed beds.

4.3.3 Abington Block

Chert and mudstone facies of the Raven Gill Formation, Kirkton beds and Moffat Shales are again restricted to the base of the block. Pelagic and hemipelagic sedimentation extended from Arenig to upper Caradoc.

The overlying Abington Formation is dominated by thick-bedded, graded sandstones (T_{ae} sequences); disorganised conglomerates, graded sandstones (T_{a-e} sequences), 'base-missing' sandstones, laminites and disturbed beds occur but are relatively rare, and show no regular distribution within the turbidite sequence.

At Craighead Quarry (91892378) near the top of the succession, a contrasting group of facies is coarser-grained, more thickly bedded (mean thickness = 110 cm) and shows more frequent amalgamation of bedding than the typical Abington lithology (Appendix 6; Fig. 15b). Cumulative curves of bed thickness plotted on probability paper (Fig. 15c) reveal that the distribution of bed thickness in Craighead Quarry is almost normal except for the incoming of a large number of very thick beds which causes the upturn in the curve above 2.4 log. thickness. This sudden change in sedimentation may relate to channel diversion. Although graded sandstones (T_{ae} sequences) are seen, organised pebbly sandstones and ungraded sandstones are common. The sand:shale ratio for

this section is 11:1, which is probably the highest value the Abington Formation attains. Bedding is sometimes lenticular on the scale of tens of metres and a thinning- and fining-upward cycle has been recognised (Plate 20). This thick-bedded sequence extends for a minimum of 40 m across strike.

4.3.4 Elvanfoot Block

In contrast to the lithological diversity of the pre-turbidite succession in the Abington Block, the pelagic and hemipelagic facies of the Elvanfoot Block are restricted to the development of black cherts and mudstones, with sporadic laminite incursions.

The overlying clastic sediments of the Elvan and Glencaple Formations display a crude first order cyclicity of bed thickness (Ricci-Lucchi 1975a) (Fig. 16a). Above the Moffat Shale/Elvan Formation contact and extending 30 m across strike, turbidites are finer-grained and more thinly bedded than the typical Elvan lithology. Thereafter the Elvan Formation retains its very thick- to thick-bedded character stratigraphically upwards into the Glencaple Formation; the latter formation is medium-bedded and defines the upper part of the cycle. The cyclicity may also be recognised petrographically (see 3.3.4 and 3.3.5).

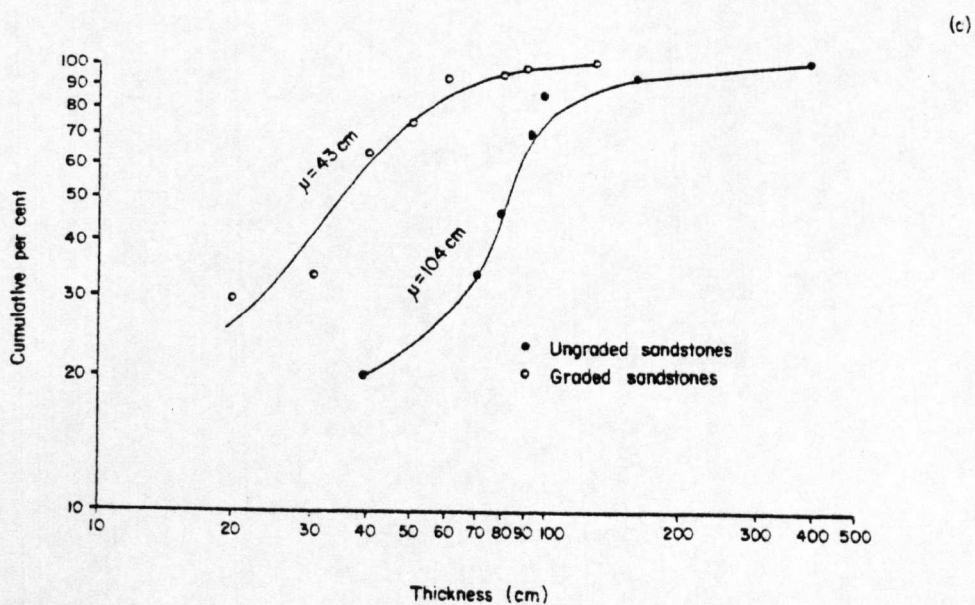
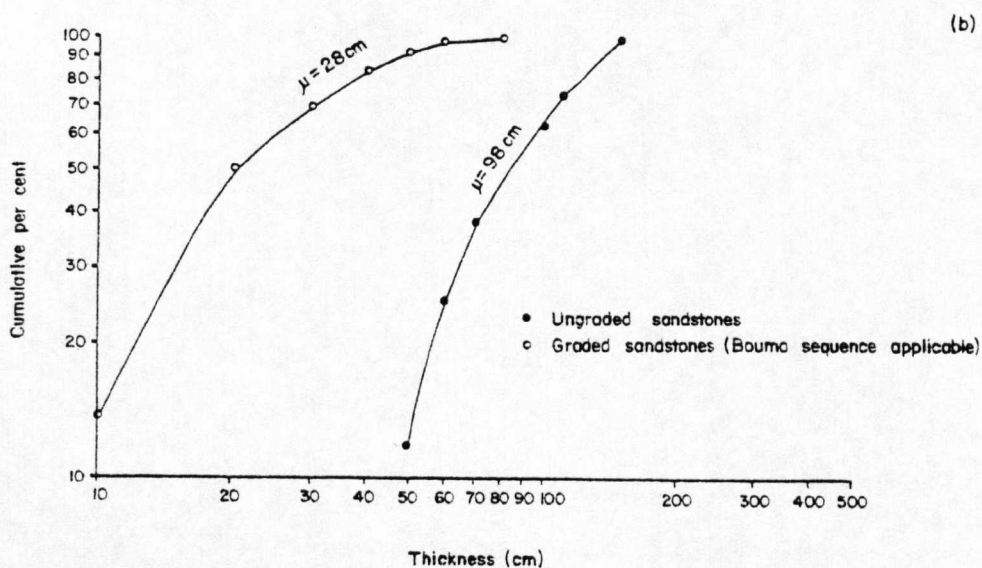
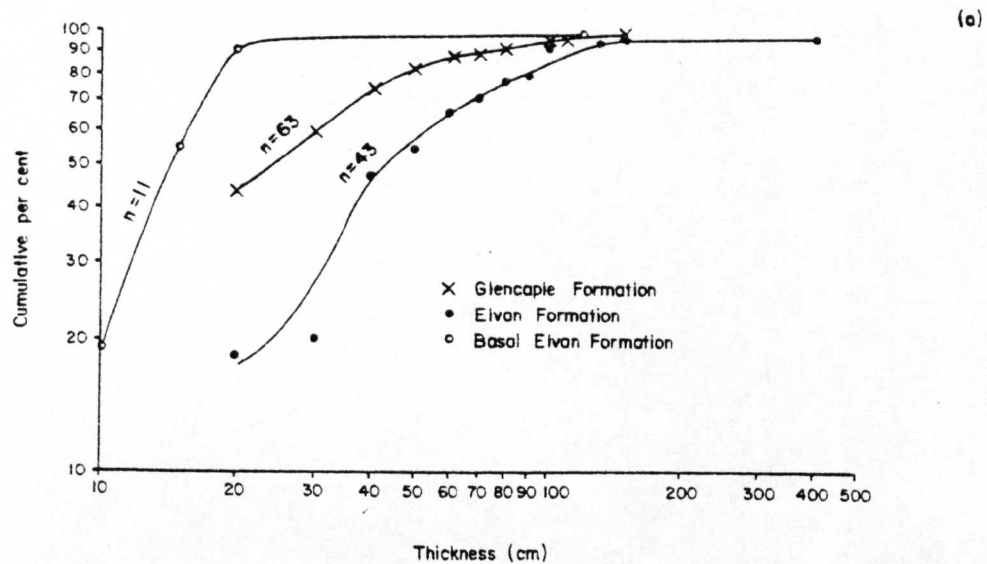


Fig. 16: (a) Bed thickness: Elvan and Glencaple Formations, log./log. plot.
 (b) Glencaple Formation: bed thickness data, log./log. plot.
 (c) Elvan Formation: bed thickness data, log./log. plot.



Plate 20: Thinning and fining upward sequence in Abington Formation, Craighead Quarry (younging right to left). Tae sandstones underlie laminite succession.

Basal lithologies of the Elvan Formation are dominated by graded sandstones and both T_{ae} and T_{a-e} subfacies occur. The remaining part of the Elvan Formation, by contrast, comprises organised pebbly sandstones and ungraded sandstones, in addition to graded sandstones (T_{ae} sequences). 'Base-missing' sandstones and laminites are less well developed, generally showing lenticularity at outcrop scale.

The range of facies shown by the Glencaple Formation is greater than that of any other lithostratigraphical unit. The frequent development of graded sandstones (T_{a-e} sequences) and 'base-missing' sandstones is restricted to this formation; cobbly siltstones occur at one locality in the area, namely, in Glencaple Burn (92461966). Disturbed bedding types include folds (produced by slumping and current-drag effects), fragmented bedding, pseudo-nodules and convolute lamination. Cobbly siltstones and disturbed beds occur in the upper Glencaple Formation. All facies types described from the Elvan Formation are intercalated with sediments of the Glencaple Formation. Ungraded sandstones in both formations are more thickly bedded than graded units (Figs. 16b and 16c).

4.4 PALAEOCURRENT ANALYSIS

In the absence of exposed sole markings from sandstones in the area, palaeocurrent observations are essentially

restricted to those obtained from cross-laminae. It is stressed that the current directions described pertain to the upper parts of sedimentary units, and not to the base of a bed; it is possible, if not probable, that direction varied throughout deposition. Also, reworking of the T_c division by later currents and current-ponding effects may have increased the spread of directions. Exposure of cross-lamination is usually seen in two dimensions, precluding direct measurement of the current azimuth.

A further complication arises from the variability of fold plunge through the area, which ranges from subhorizontal to vertical (Fig. 18). Unfolding techniques require accurate assessment of local fold plunge; this control is generally lacking, as is the coincidence of occurrence of both folds and current indicators. In view of all these factors, and the statistically poor frequency of development, directional indicators are subdivided into those which are approximately strike-parallel or transverse to strike (Table 3). All current directions are given from the source to the site of deposition. Data are inconclusive but may contribute to further wide-ranging studies.

PAGE

NUMBERING

AS ORIGINAL

Table 3: Current data

LITHOSTRATIGRAPHICAL UNIT	CURRENT DIRECTION ¹				
	STRIKE PARALLEL			TRANSVERSE	
	NE	SW	NE or SW ²	NW	SE
Haggis Rock	-	-	-	-	-
Mill Burn Mbr.	-	-	-	-	-
Crawfordjohn Fm.	1	-	-	-	-
Abington Fm.	3	4	2	-	1
Glencaple Fm.	9	3	1	3	-
Elvan Fm.	-	2	2	-	3

¹ Direction given from source to depositional site.

² Data from scours at base of turbidite beds.

CHAPTER 5: STRUCTURAL GEOLOGY

Deformation in the Abington area is attributed to three distinct phases, the first of which (D_1) is the most widely recognisable. Subsequent phases (D_{2-3}) are relatively minor in importance and are of local development. A wrench fault system may represent a fourth period of deformation.

All directional measurements of planar and linear structural elements are given as three-figure bearings corrected to true north. Data are portrayed stereographically using the lower hemisphere of the Lambert equal-area projection.

Use of facing terminology follows Shackleton (1958). Vergence is used in the sense of Roberts (1974), except when dealing with steeply plunging folds, in which case the terms dextral and sinistral are employed (when viewed down plunge).

5.1 PRIMARY DEFORMATION (D_1)

5.1.1 S_1 cleavage

Cleavage (S_1) is not readily identifiable throughout the area. It is developed most commonly in fine-grained lithologies (e.g. interturbidite silty mudstones and siliceous mudstones) and more rarely in sandstones. In thin section the fabric is

defined by the pre-existing (sedimentary) orientation of inequidimensional minerals and superimposed tectonic cleavage, both of which are typically subparallel. In the field, S_1 can be recognised with certainty only where an angular disparity exists between it and bedding. Three types of cleavage have been identified in thin section, which are described generally following the terminology of Powell (1979).

Domainal cleavage: Domainal cleavage is the most commonly occurring tectonic fabric in the Abington area, and is found in all structural blocks. It is essentially restricted in development to silty mudstones and very fine sandstones (T_d and T_e Bouma divisions) interbedded with uncleaved and thicker sandstone units. Within the silty mudstones the main mineral constituents are illite, chlorite, quartz and albite, with minor quantities of opaque ores. These minerals are arranged in a domainal fabric, with dark seams of phyllosilicates and opaques separated by light quartz-rich bands up to 40 μm in width (Plate 21). Although quartz is the dominant mineral of the light bands, minor amounts of albite, chlorite and illite are also present.

Individual phyllosilicate seams rarely persist laterally for more than 300 μm before anastomosing with other seams, and thereby enclose lenses (microlithons) of individual quartz

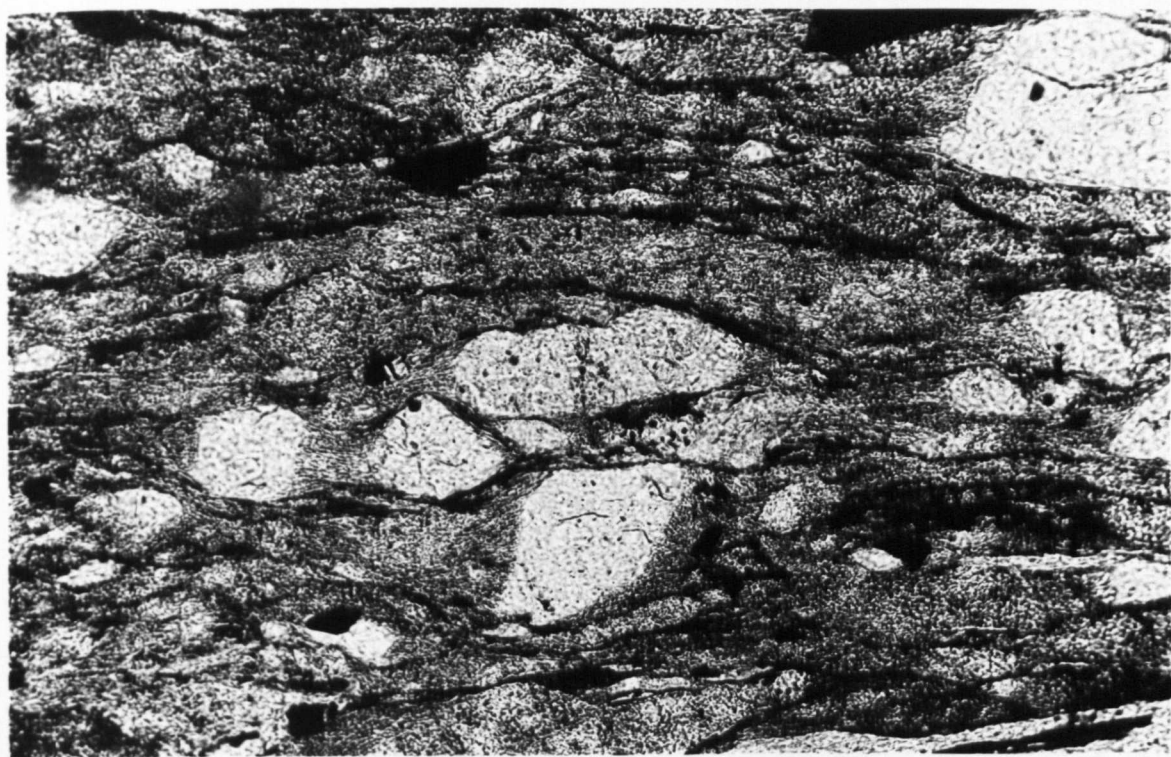


Plate 21: Strong S_1 cleavage in basal Elvan Formation sandstone. Mica-rich pressure shadows connect detrital quartz grains, x 25, PPL.

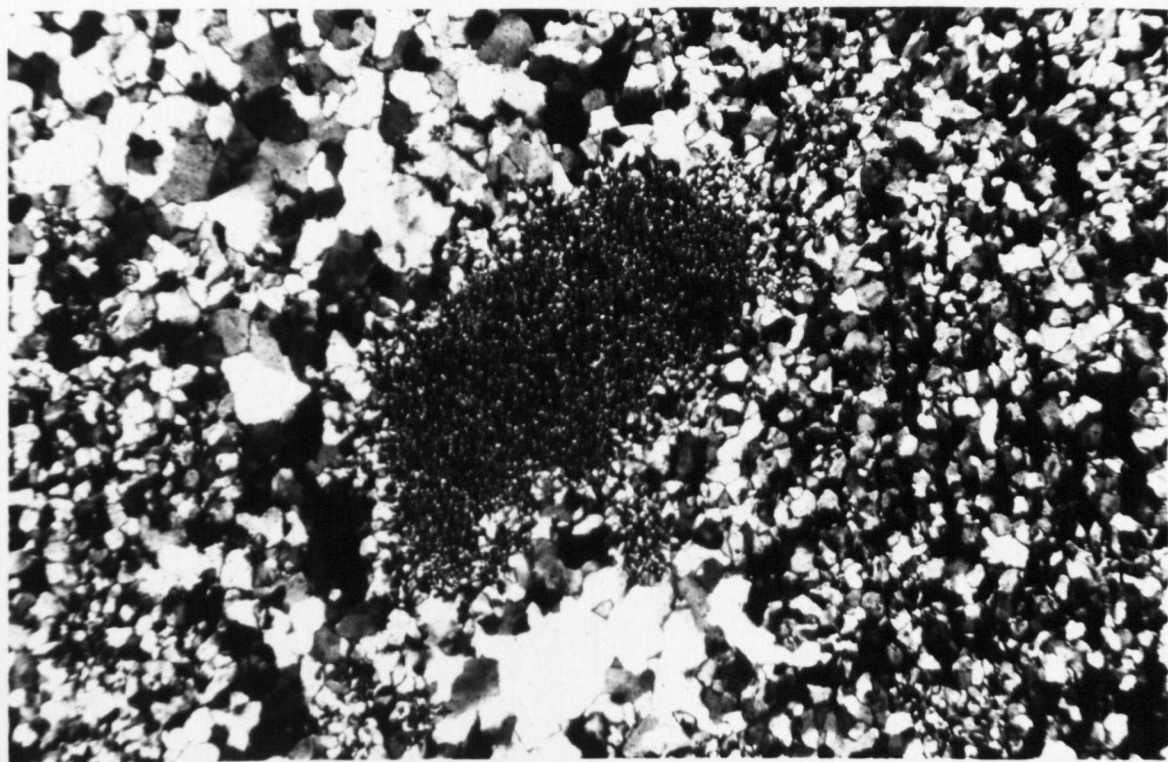


Plate 22: Grumous texture in chert in the vicinity of the Raven Gill Fault, x 25, CPL.

grains or thin siltstone beds. The original sedimentary alignment of inequidimensional minerals is preserved in the microlithons. In many examples detrital quartz grains are truncated on two sides by adjacent phyllosilicate seams, the shape of which is modified to produce a slight elongation parallel to cleavage. Where intensely developed, truncated grains show pressure shadows (Spry 1969) of quartz and illite, the fringes of which are parallel to cleavage and commonly connect adjacent quartz grains (Plate 21). In more weakly deformed lithologies, domainal fabrics are nonpenetrative (Turner & Weiss 1963) even at thin section scale and rough, spaced cleavage predominates.

Williams (1972) interpreted dark phyllosilicate seams to have been produced by the selective removal of quartz by pressure solution, further evidence of which is supported by the presence of truncated quartz grains.

S_1 cleavage within sandstones is an infrequently developed, irregularly spaced rough (Powell 1979) cleavage which is superimposed on a weakly orientated pre-existing planar anisotropy.

Continuous cleavage: Nondomainal cleavage is defined by micas (illite and chlorite) arranged in parallel orientation at an angle with bedding, with no evidence of dark pressure-solution seams. This fine, continuous cleavage (Powell 1979) has been

recorded only from a mica-rich siltstone at one locality (89521700) which shows S_1 at a low angle to bedding.

Bimodal cleavage: Siliceous mudstones with chert nodules found in the Leadhills Imbricate Zone display a domainal fabric consisting of recrystallised mica bundles with subcircular to ovate chert microlithons. Illite/chlorite bundles show a bimodal distribution, with two distinct orientation maxima (intersecting at 17°) which are bisected by the plane of bedding. Silica nodules generally lack the necessary layer silicates to produce this fabric and form the poorer cleaved domain of microlithons. Bimodality in siliceous mudstones is maintained even in the absence of chert nodules. Pressure-solution seams are superimposed on both sets of mica bundles.

Hobbs et al. (1976) suggested that bimodal fabrics formed due to effects of layer-parallel strain superimposed on an original bedding fabric, with passive rotation of micas into the XY plane of the strain ellipsoid. However, as cleavage and bedding are subparallel in the siliceous mudstones, this mechanism is not applicable as shortening occurred perpendicular to bedding. The origin of bimodal fabric in the Leadhills district is not known.

5.1.2 F₁ folds

Throughout most of the area, rocks have been deformed into an approximately vertical attitude, with a modal orientation of $059^{\circ}/83^{\circ}$ SE (Fig. 17). Bedding typically faces towards the NW, although reversals of younging direction (recognised on sedimentological criteria) occur in all structural blocks. A total of 69 folds were sufficiently well exposed in the Mill Burn, Abington and Elvanfoot Blocks to permit structural observations to be made.

As far as can be observed, bedding and fold orientations do not vary significantly between the Crawfordjohn, Abington and Elvanfoot Blocks (Figs. 17 and 18). In the absence of evidence to the contrary, these blocks are dealt with as one unit. Structures in Mill Burn differ sufficiently from the rest of the area as to warrant separate description (Fig. 19).

Crawfordjohn, Abington and Elvanfoot Blocks: Bedding orientation is relatively uniform throughout these blocks (Fig. 17a), being subvertical, and typically facing towards the NW (cf. steep belts of Craig & Walton 1959). Reversals of sedimentary younging generally provide the only direct evidence of folding in the sandstone formations. Fold closures are, however, seen most frequently in the Leadhills Imbricate Zone.

Folds are tight to isoclinal and mostly upright plunging, although a few inclined plunging and vertical folds occur.

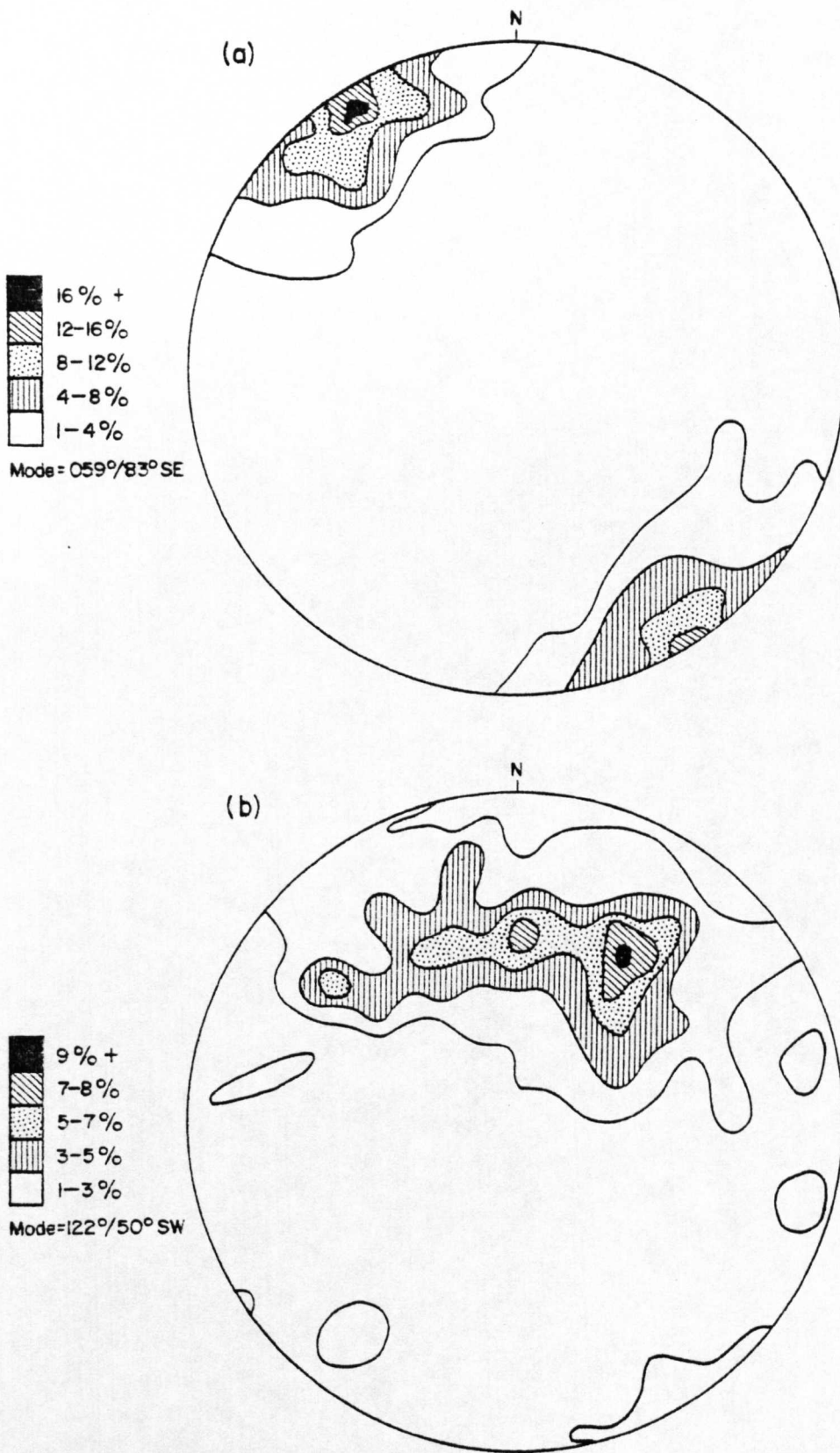
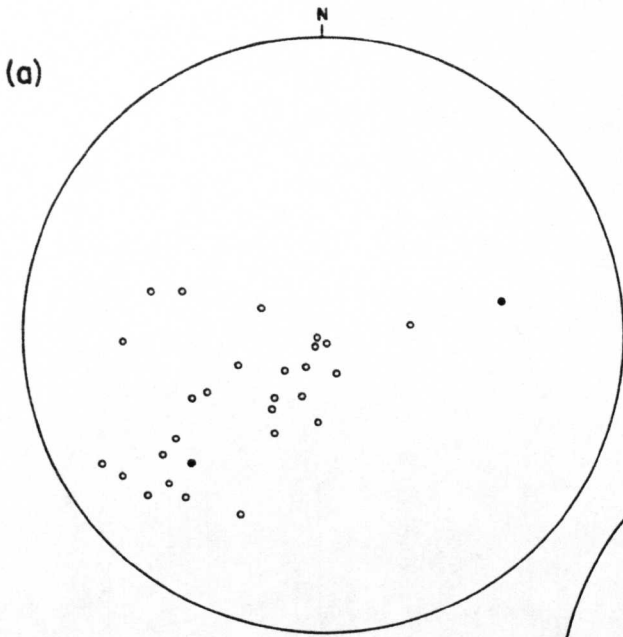


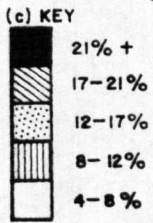
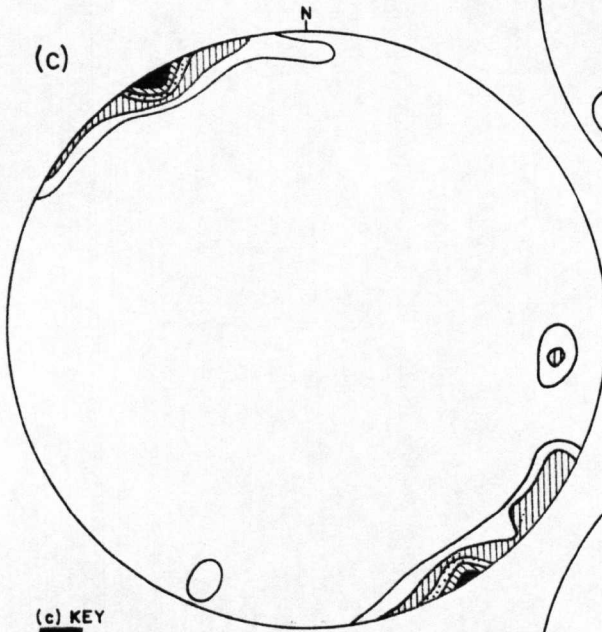
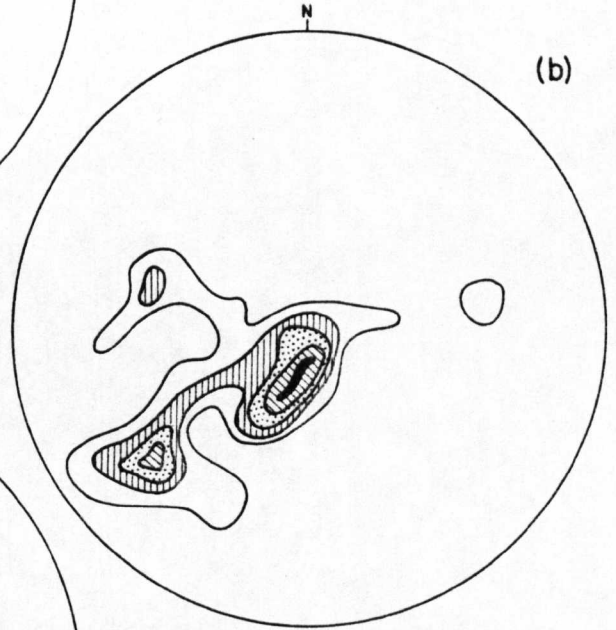
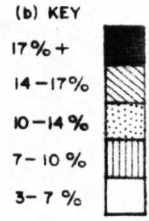
Fig. 17: (a) Stereonet of poles to bedding, Abington and Elvanfoot Blocks; $n = 100$.
 (b) Stereonet of poles to bedding, Mill Burn structural subarea; $n = 97$.

Fig. 18 (overleaf)

- (a) Stereogram of F_1 fold plunges, Abington Block; $n = 29$.
- (b) Stereogram of F_1 fold plunges (contoured), Abington Block; $n = 29$.
- (c) Stereogram of poles to F_1 axial surfaces, Abington Block; $n = 24$.
- (d) Stereogram of poles to F_1 axial surfaces, Elvanfoot Block; fold plunge (black square); $n=6$.



(a) KEY
VERGENCE
○ Unknown
● SE



(d) KEY
■ Fold hinge
○ Axial surface

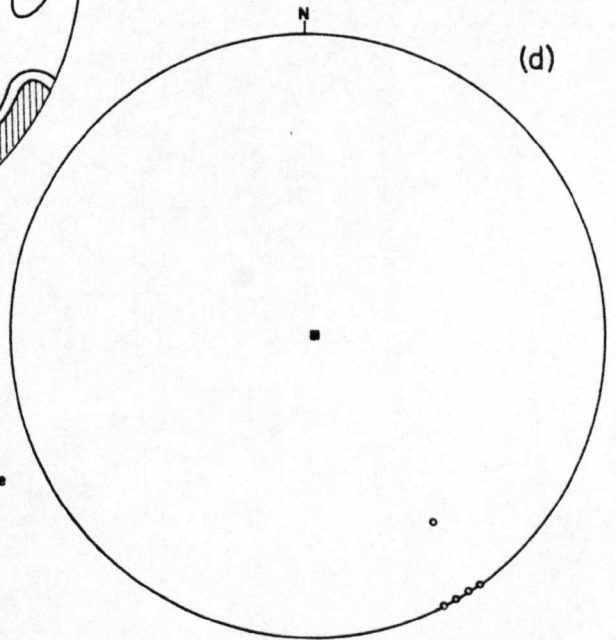
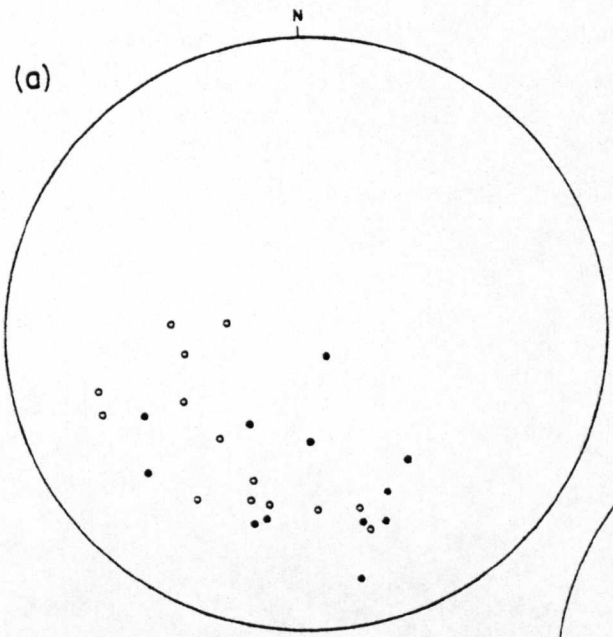
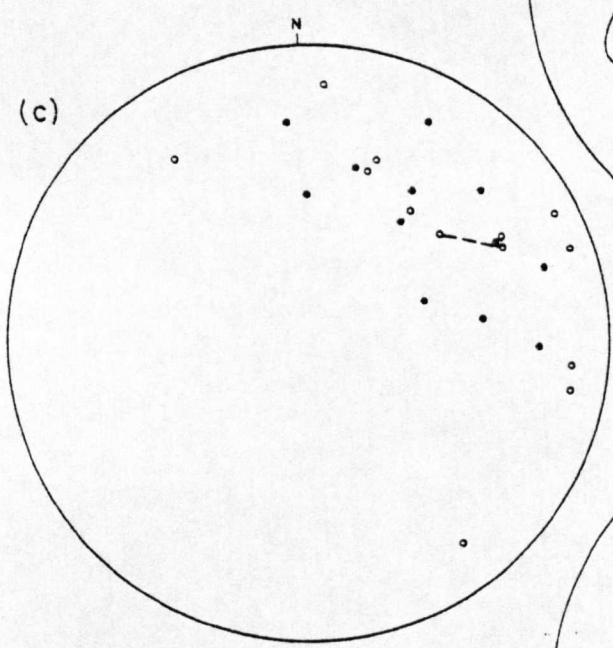
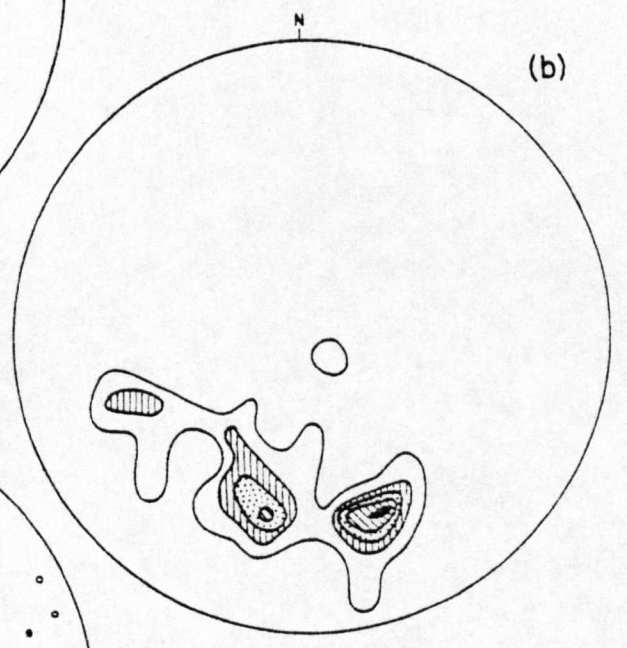
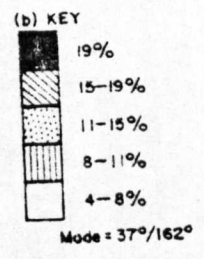


Fig. 19 (overleaf)

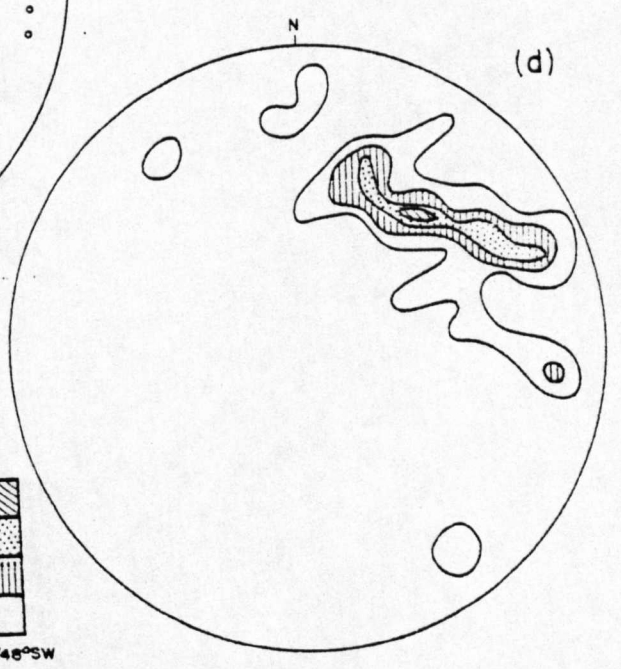
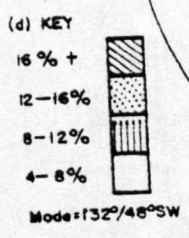
- (a) Stereogram of F_1 fold plunges, Mill Burn structural subarea; $n = 26$.
- (b) Stereogram of F_1 fold plunges (contoured), Mill Burn structural subarea; $n = 26$.
- (c) Stereogram of poles to axial surfaces of F_1 folds, Mill Burn structural subarea; dashed line, curved axial surface; $n = 2$.
- (d) Stereogram of poles to axial surfaces of F_1 folds (contoured), Mill Burn structural subarea; $n = 24$.



(a) KEY
 VERGENCE
 ○ Unknown
 ● Sinistral



(c) KEY
 FOLD VERGENCE
 ○ Unknown
 ● Sinistral



Fold plunge is consistently towards the SW, with two maxima at 78° towards 205° and $36^\circ/228^\circ$ (Fig. 18); axial surfaces are subvertical and closures are generally rounded. Single chert/mudstone contacts in a thin-bedded sequence folded about vertical fold axes (90021973) show broad, rounded closures (wavelength large, amplitude small) alternating with V-shaped closures (wavelength small, amplitude large) which 'point' towards the more viscous chert bed (cf. Ramsay 1967, p. 383).

The maximum amplitude of minor folds directly seen in the field is 1.5 m, with an axial-surface separation of 2 m. Two examples of south-easterly verging fold pairs have been recorded. All other folds show one closure, the other presumably displaced by faulting.

Outwith the Mill Burn subarea (see below), folds are only extensively developed in the Glencaple fold belt (92481974-92451941) immediately south of the Leadhills Imbricate Zone. This belt is 360 m wide across strike and consists of large-scale folds (inferred from reversals of younging direction) which have an average axial-surface separation of 17 m (Fig. 20); a 30 m succession of sandstones forms the thickest continuous SE-younging limb exposed in the area. Hinges of major F_1 folds are rarely seen in the field, possibly due to the presence of axial planar strike faults and the paucity of exposure.

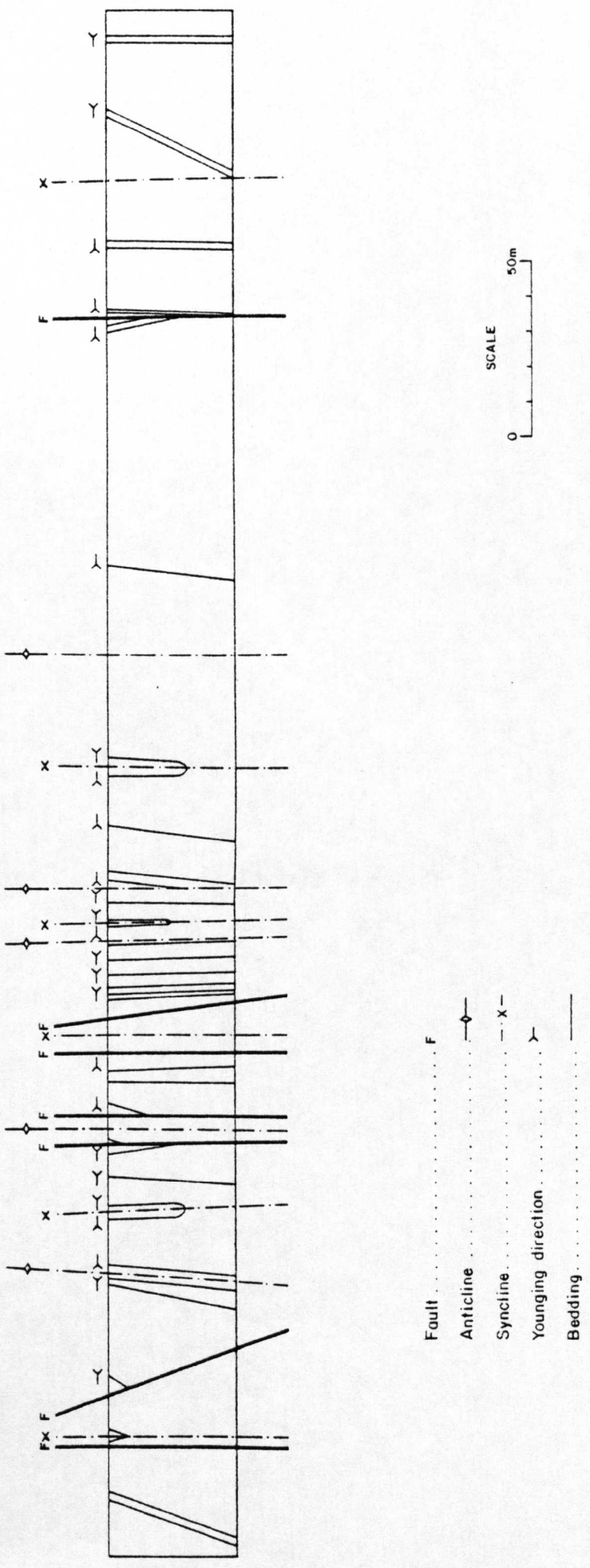


Fig. 20: Structural section in Glencaple Burn (true dips shown).

Folds occurring in Hershaw Burn (92981981 - 93161961) may represent the north-eastward extension of the Glencaple fold belt. To the SE, lack of exposure precludes establishment of lateral extent of the belt. This structure, though narrow, is comparable to the 'flat belts' of Craig & Walton (1959).

Reversals of bedding are relatively common in all fault blocks, but the width of SE-younging limbs rarely exceeds a few metres. SE-verging fold pairs are inferred from such reversals, assuming that structures are upward facing.

As in the Mill Burn subarea (see below), the determination of a deformational chronology is hindered by the variable and limited development of S_1 cleavage which is most frequently seen in mudstones and laminites interbedded with sandstone units. Cleavage has a modal orientation of $067^\circ/87^\circ$ SE with little variation. The clockwise rotation of S_1 with respect to fold hinges, typical of the Central and Southern Belts, has not been reported in the three structural blocks under consideration, although it is noted that the modal orientation of S_1 differs by some 8° (in a clockwise sense) from modal bedding and axial plane orientations (Fig. 21). The facing direction of bedding on S_1 is variable; NW-younging limbs typically show upward-facing relationships where S_1 is

Structural block	NW-younging limbs		SE-younging limbs	
	Upward facing	Downward facing	Upward facing	Downward facing
Mill Burn	-	1	-	-
Crawfordjohn	-	-	-	-
Abington	4	2	-	1
Elvanfoot	2	-	1	-

Table 4: Facing directions of bedding on cleavage for each structural block. Figures in table refer to number of localities from which facing data were obtained.

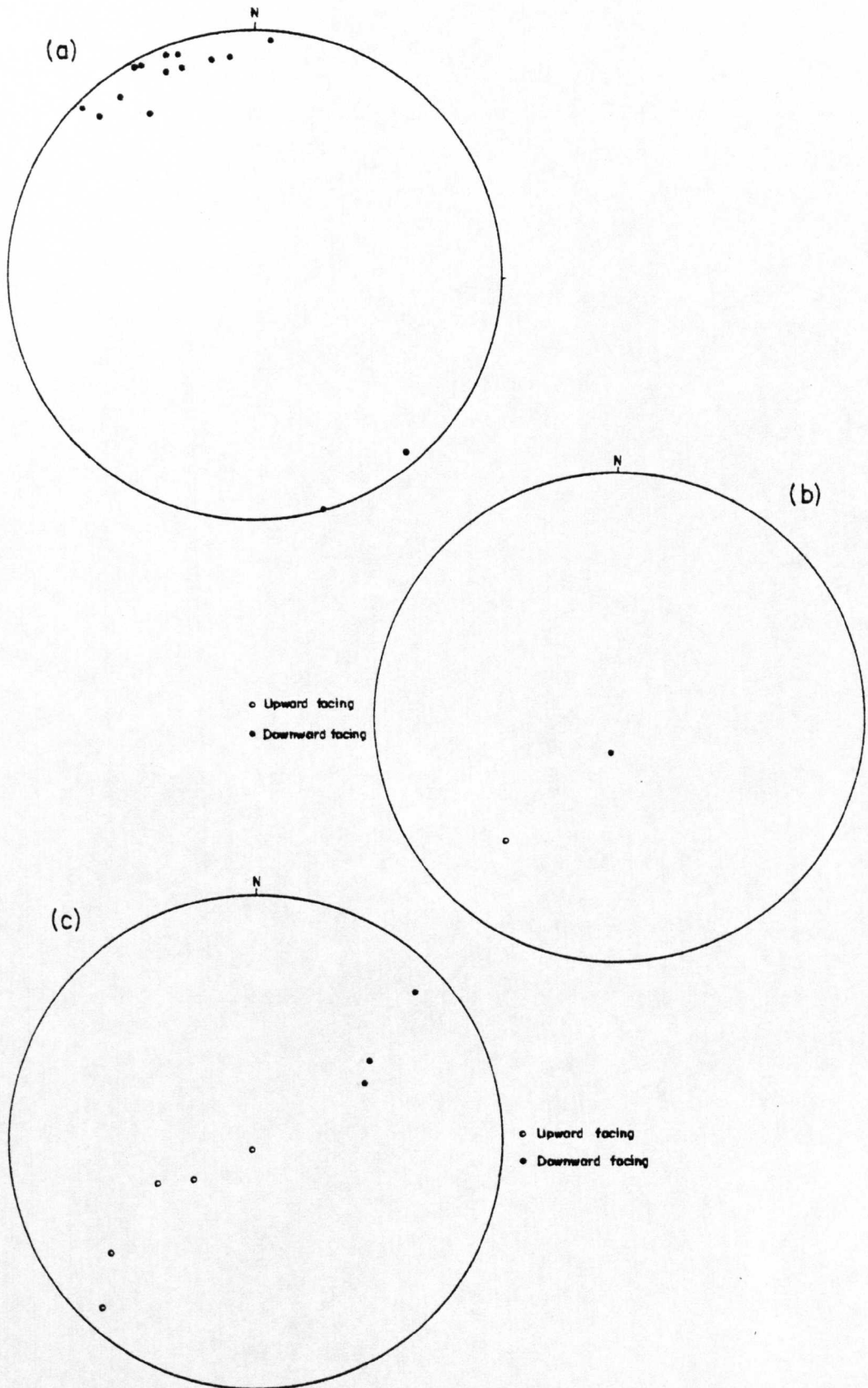


Fig. 21: (a) Stereonogram of poles to cleavage (S_1); $n = 15$.
 (b) Stereonogram of bedding/cleavage intersection lineation from SE-younging beds. L_1 stereographically derived.
 (c) Stereonogram of bedding/cleavage intersection lineation from NW-younging beds. L_1 stereographically derived.

developed. Other permutations are less common (Table 4).

Bedding/cleavage intersection lineations (L_1) have not been observed. However, these have been determined stereographically and all folds facing upward on S_1 show steep plunges towards the SW including a single observation from a SE-younging limb (Fig. 21). Downward-facing limbs, in contrast, generate plunges towards the NE. Cameron (1977) noted that L_1 on north- and south-younging limbs generally plunges at low angles towards the SW and NE respectively; sparseness of information in the Abington area precludes use of the data to ascertain the geometrical configuration of cleavage and bedding from L_1 plunge orientation alone.

Steep fold plunges observed in the three structural blocks under consideration may be explained by (a) rotation of bedding between dislocations, or (b) inhomogeneous strain (Stringer & Treagus 1980).

Mill Burn subarea: In Mill Burn, laminites of the Mill Burn Member form a system of inclined plunging (and rarer upright plunging) folds (Rickard 1971) (Plate 23). Profiles are tight to isoclinal, nonparallel and show rounded closures with some hinge thickening. Axial-surface separation is characteristically less than 30 cm; most dip towards the SW at angles of approximately 50° (Figs. 19c, 19d; Appendix 8)



Plate 23: F_1 fold, Mill Burn subarea, viewing up-plunge. Inclined plunging, sinistrally verging tight fold.

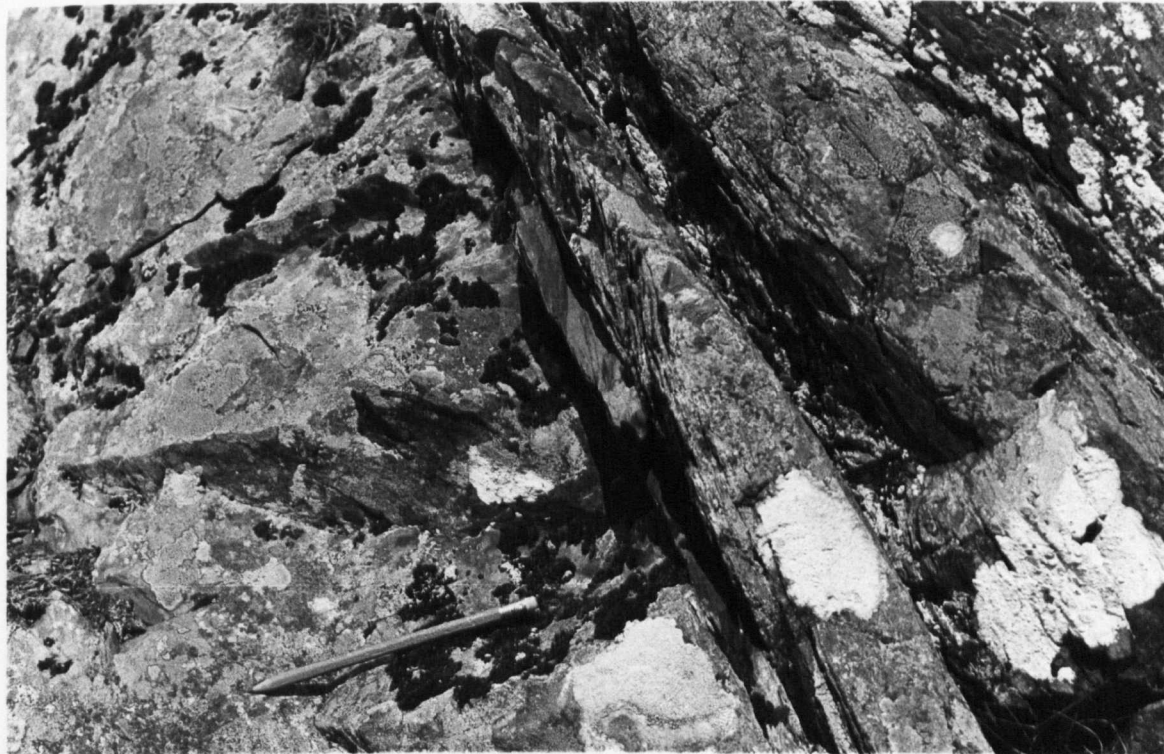


Plate 24: Downward facing bedding/cleavage relationships, Mill Burn subarea. Turbiditic sandstone bed (by pencil) youngs right to left (NW) and is inverted; cleavage developed in grey siltstone (centre) is approximately vertical.

which represents a marked divergence when compared to regional strike. Fold plunge has a modal orientation of $37^{\circ}/162^{\circ}$ (Fig. 19b), and axial surfaces and hinges show variability sufficient to scatter points on stereograms over an entire quadrant. Individual folds may show curved axial surfaces, vergence being typically sinistral (Fig. 19c).

Axial planar cleavage is poorly developed, and is seen to transect folds (cleavage rotated clockwise from axial planes, T. B. Anderson, pers. comm. 1980) as has been reported from elsewhere in the Southern Uplands and Longford-Down (Cameron 1977; Anderson & Cameron 1979; Phillips et al. 1979; Stringer & Treagus 1980). S_1 cleavage in inter-turbidite mudstones associated with overturned beds is sub-vertical ($046^{\circ}/80^{\circ}$ SE) and bedding faces down on cleavage (Plate 24).

Possible alternative explanations for the anomalous bedding and fold orientations in the Mill Burn subarea are:

- bedding planes nonorthogonal with respect to stress axes prior to D_1 deformation (Stringer & Treagus 1980),
- local deflection of D_1 stress axes,
- post- D_1 modification by F_2 folding or nearby wrench fault.

Comparisons with other studies of the Northern Belt to

the WSW of the Abington district (i.e. Rhinns of Galloway, (Kelling 1961); west Nithsdale, (Floyd 1975)) show that SW plunging folds are developed in all areas. The principal contrasts among the three areas are:

- fold hinges in west Nithsdale are more variable in the amount of plunge, and are broadly distributed around a great circle,
- the subvertical fold maximum is absent in the Rhinns of Galloway where hinges are subhorizontal or gently plunge towards the WSW,
- NE-plunging folds are absent from the Abington district,
- no equivalents to the fold orientations in the Mill Burn subarea have been observed elsewhere.

5.2 SECONDARY DEFORMATION (D_2)

Examples of F_2 folds occur in the Abington and Mill Burn Blocks, and are recognised by the folding of bedding-parallel S_1 fabrics. One locality (88101707) in the Leadhills Imbricate Zone shows F_2 folds with NNE-trending axial surfaces and SSW plunging hinges at $50-60^\circ$ (Fig. 22a). Length of the common limb of fold pairs is 15 cm. The folds are conjugate; vergence of antiformal/synformal pairs is towards the NW.

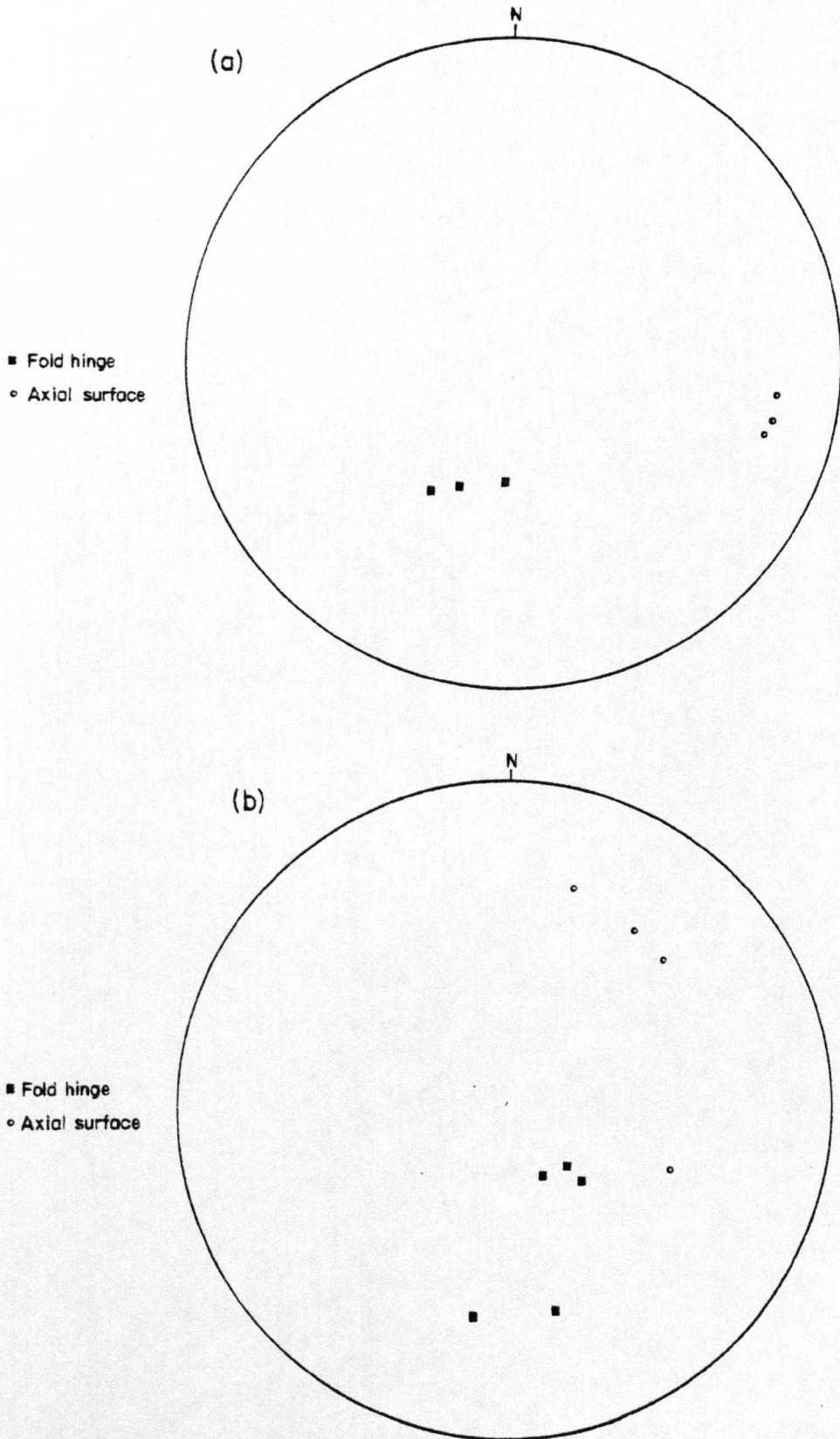


Fig. 22: (a) Stereonogram of F_2 folds, Abington Block. All folds show north-westerly vergence; $n = 3$.
 (b) Stereonogram of F_2 folds, Mill Burn structural subarea. All folds show dextral vergence; $n = 5$.

F_2 folds in Mill Burn show moderate southerly and steep south-easterly plunges with axial-surfaces dipping relatively steeply towards the SW (Fig. 22b). Fold style is variable and ranges from open to tight, the latter being disharmonic; wavelengths are less than 30 cm. In contrast to F_1 , dextral vergence typifies F_2 . No S_2 fabric has been recognised accompanying F_2 folds.

5.3 KINK-BANDS

Despite the widespread presence of suitable lithologies (mudstones and laminites) in which kink-bands could develop, they only occur at two localities in the Leadhills Imbricate Zone. A conjugate system at (91491962) shows sharply angular dextral and more rounded, open sinistral deflections of S_1 . Width of the kink-bands measured along the foliation (Anderson 1969) is 4-25 mm. Both kink pairs are subvertical - the dextral set strikes NE-SW, the sinistral set E-W (Fig. 23). Assuming that conjugate kink-bands are symmetrically disposed with respect to σ_1 as in Co. Down, the inferred σ_1 is aligned anticlockwise of bedding, sub-horizontally on an azimuth of $032^\circ/212^\circ$ (cf. Cameron 1977). The angle between σ_1 and bedding (28°) is greater than the corresponding value in Down (9°). The only other record of kink-bands from the Northern Belt is from west Nithsdale (Floyd 1975).

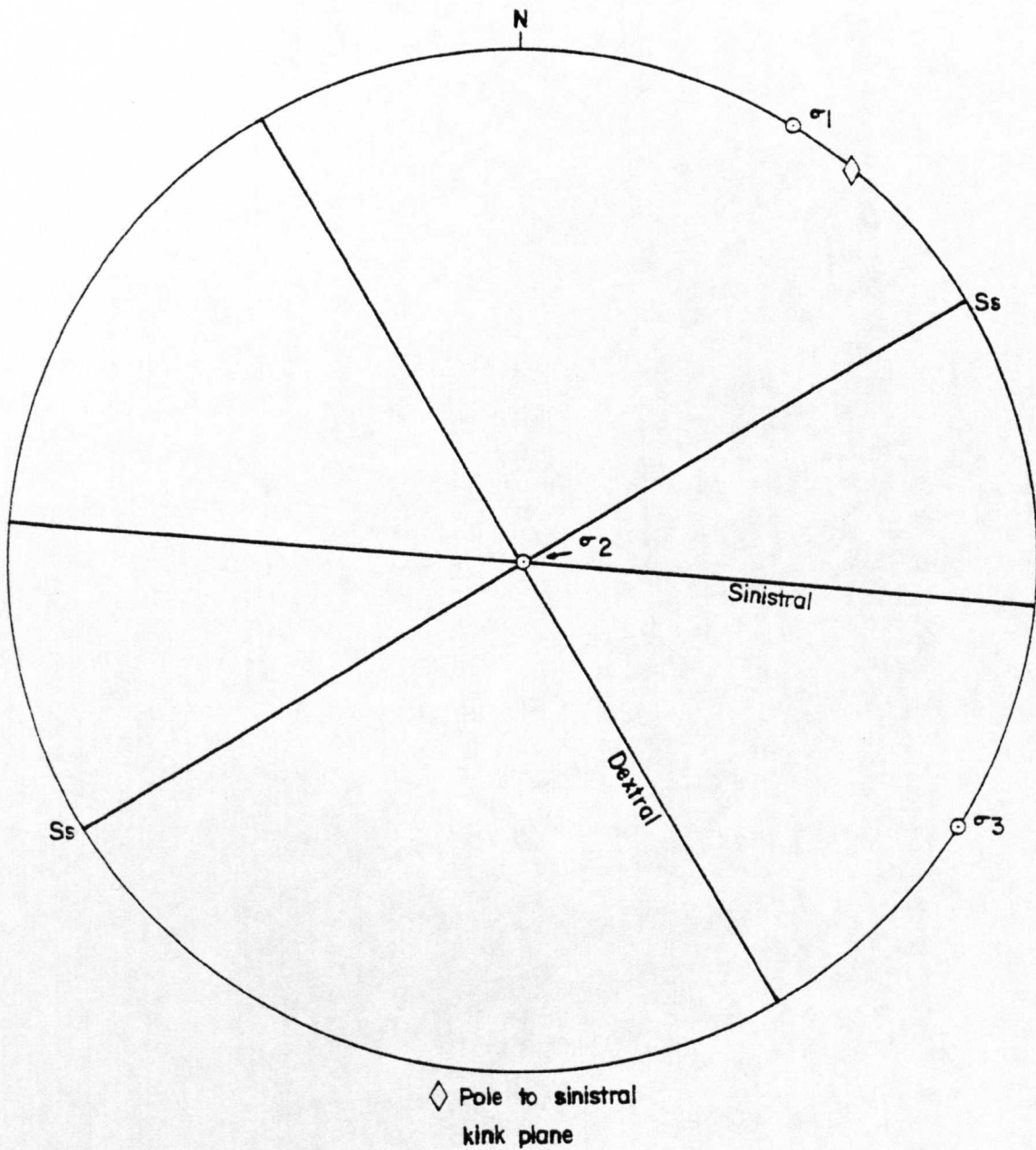


Fig. 23: Geometrical configuration of conjugate kink-band system; relationship to inferred principal stress axes and bedding shown.
 $\sigma_1 = 00^\circ/032^\circ$; $\sigma_2 = 90^\circ$; $\sigma_3 = 00^\circ/122^\circ$.
 Sinistral = $096^\circ/90^\circ$
 Dextral = $151^\circ/90^\circ$

5.4 FAULTING

Outcrop distribution in the Abington area is primarily controlled by large strike-parallel faults and fault zones, recognised on structural and palaeontological data, trending ENE-WSW and separating thick clastic sedimentary sequences. Lithologies above the faults are strongly imbricated into linear outcrop belts, surrounded to the NW and SE by younger sandstones, thereby defining inliers. Imbricate zones are consistently offset by wrench faults.

Four major faults - the Crawfordjohn, Shield Burn, Wellgrain Dod and Fardingmullach (Floyd 1975) Faults - subdivide the area into four structural blocks (Fig. 3). The Shield Burn, Wellgrain Dod and Fardingmullach Faults are overlain structurally to the NW by the Shield Burn, Leadhills (Leggett et al. 1979) and Fardingmullach Imbricate Zones (IZ) respectively; of these, only the Leadhills IZ is adequately enough exposed as to merit discussion in detail. Faults bounding inliers consistently show stratigraphical downthrow to the SE, a feature recognised by Craig & Walton (1959) and Kelling (1961), and upon which regional interpretation of the Southern Uplands is based (e.g. Mitchell & McKerrow 1975; Leggett et al. 1979).

The term imbricate zone (corresponding to the 'lines' of Floyd 1975, after Peach & Horne 1899) is used to

describe concentrations of strike-parallel faults effecting considerable repetition of strata.

5.4.1 Leadhills Imbricate Zone

The Leadhills Imbricate Zone is 1700 m wide across strike and consists of repetitions of the 180 m thick sequence of the Raven Gill Formation, Kirkton beds, Moffat Shales, plus slivers of the overlying Abington Formation (Fig. 24; Appendices 8-10). Faults which comprise the imbricate zone can be recognised from stratigraphical evidence. Vertical black Moffat Shales (D. clingani zone) of the Fardingmullach Imbricate Zone pass conformably north-westwards into sandstones of the Elvan and Glencaple Formations. These formations are succeeded to the NW by older black mudstones (C. peltifer). A fault (the Wellgrain Dod Fault) must therefore occur between the sandstones and the black mudstones (Fig. 25). Significantly, the fault separates quartz-rich sandstones (Abington Formation) to the NW from quartz-poor sandstones (Glencaple Formation) to the SE. The quartz-rich sandstones are 650 m thick. Similarly, a fault is required on the basis of stratigraphy to separate the Abington Formation (upper Caradoc) from the Raven Gill Formation (Arenig) to the NW (Raven Gill Fault, Fig. 25).

The Leadhills Imbricate Zone displays internal organisation of the fault slices at the base of the Abington Block.

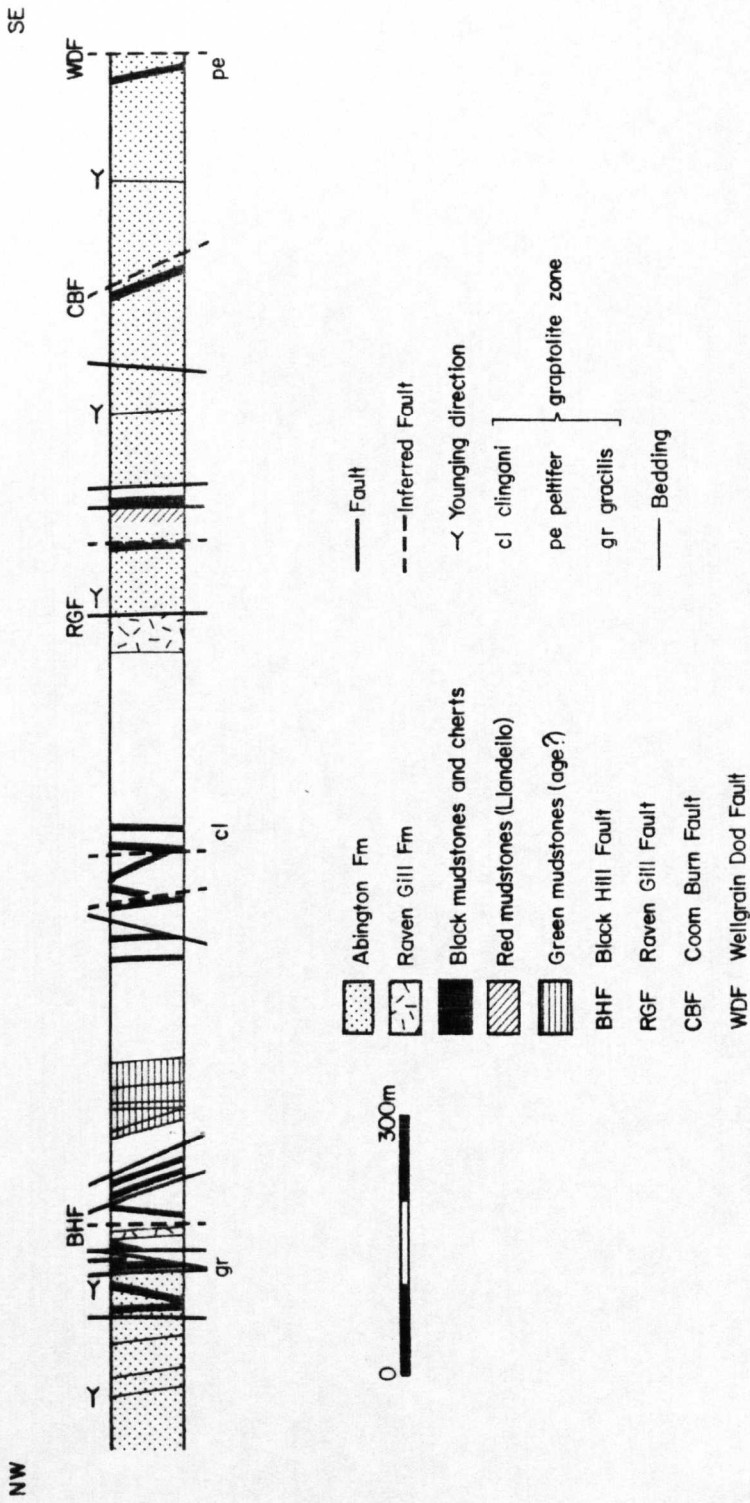


Fig. 25: Composite structural profile across the Leadhills Imbricate Zone

Older rocks crop out towards the centre of the inlier, in the sequence C. peltifer black mudstones, Llandeilo red mudstones and Arenig mudstones and cherts (Fig. 25). To the NW of the Arenig strata, strike faults of approximately equal displacement bring to the surface fault slices generally consisting of black mudstones, cherts and slices of turbiditic sandstones of the Abington Formation. Imbrication is intense: in a transect of 700 m across strike in poorly exposed terrain, a minimum of 11 fault slices have been identified on stratigraphical grounds. This number could easily be doubled if faults contained within an individual lithology were taken as defining further slices. Metamorphic recrystallisation of siliceous mudstones, cherts and sandstones is seen in the immediate vicinity of the fault zones (Sections 6.1.1, 6.1.2). Towards the NW margin of the inlier the imbricate wedges die out, and black mudstones are inferred to pass up into sandstones of the Abington Formation.

Certain lithological units show a relatively consistent outcrop distribution with respect to their structural position within the imbricate zone, for example:

- The Arenig to upper Caradoc pelagic sediments and associated igneous rocks are concentrated in the central and northern parts of the imbricate zone, forming a unit generally less than 850 m wide.

- Abington Formation sandstones occur both to the NW and SE of this outcrop belt. To the SE, at least two slices of the Abington Formation are consistently developed, although the combined thickness of both units changes markedly along strike, from 200 m in Bellgill Burn to over 650 m in Laggen Gill.
- Thick sequences of dark grey, flaggy mudstones (Moffat Shales) which infrequently contain graptolites, tend to occupy the SE area of the 'pelagic outcrop belt'.
- The Raven Gill Formation occurs at three structural levels at least within the imbricate zone, namely near the base (e.g. in Raven Gill), in the centre (e.g. Craig Dod, 92022038) and towards the NW margin (e.g. Glencaple Burn, 92262147 and Cleuch Burn, 90031963).

The nature of most outcrop-controlling faults remains conjectural in the absence of suitable exposure. However, the fault juxtaposing Caradoc Abington Formation sandstones against the Arenig Raven Gill Formation to the NW is traceable to a distance of 135 m along strike in the southern scarp of Raven Gill (92021983). The outcrop of the Raven Gill Fault remains essentially straight despite the 76 m drop in height along the length of the scarp.

suggesting the fault plane is vertical. Usually uncleaved, sandstones to the south of the fault show a fabric of discrete, closely spaced planes (orientation $058^{\circ}/86^{\circ}\text{SE}$ which possibly represent a shear zone involving volume reduction (cf. Ramsay 1980). Minor quartz veining also occurs.

Other major faults are normally not exposed, or, more rarely, are seen only on subhorizontal erosion surfaces. Shear fabrics similar to those in Raven Gill are developed in Llandeilo green siliceous mudstones in Glencaple Burn (92481983); elongated mineral fibres in the plane of the fabric plunge to the SW at angles in excess of 35° , implying transport along that azimuth (W.E.A. Phillips, pers. comm., 1980).

Black mudstones of the Moffat Shales display minor brittle fractures but exposures frequently do not display any bedding, or preserve only wispy remnants. Instead, thorough shearing generates massive lithologies locally containing planar or curved surfaces on which a thin veneer of material with a lead-grey sheen (?deformed graptolites) preserves fine slickencrysts. Such structures impart a crude planar element to the outcrop, subparallel to regional strike. These fault zones are inferred to be a result of relatively penetrative deformation. Deformation of incompetent lithologies may be aided in addition by thermal softening

produced by strain heating in the immediate vicinity of the fault zone (Brun & Cobbold 1980).

Later brittle deformation is recorded by faults and associated vein systems, which occur at both low and high angles to bedding azimuth. Zones of relatively ductile deformation within black mudstones are accompanied by strike-parallel, brittle faults of listric geometry, with subvertical axes of curvature. The difference in ductility between the fault sets recorded by the mudstones implies two discrete faulting events, rather than the mutual merging or intersection of shear zones propagating in opposite directions.

Although the imbricate zone is mappable throughout the area, component faults are not generally traceable between stream sections due to lack of exposure, probably lateral mergence of faults and consistent offset of outcrop by wrench faults (see Section 5.4.5). The thickness variation of two packets of the Abington Formation at the base of the imbricate zone is interpreted as being produced by the lateral merging of faults.

In the absence of internal stratigraphical control, the presence of major strike faults is not demonstrable within the sandstone formations overlying the Leadhills IZ.

5.4.2 Shield Burn Imbricate Zone

Comprising repetitions of 'dolerites', green siliceous

mudstones, lithic tuffs, black cherts and sandstones of the Crawfordjohn Formation, the succession preserved in the Shield Burn IZ is inferred to range from Arenig through to Upper Llandeilo or lower Caradoc. The zone has a minimum thickness of 430 m. As in the Leadhills IZ, the oldest lithologies (Arenig 'dolerites') are found not at the base, but some distance (320 m) above it. Evidence of faulting is seen at most exposures.

Stratigraphical evidence for recognition of this inlier as a major outcrop-controlling structure is available; the upper Caradoc Abington Formation youngs predominantly north-westwards towards the inlier, and a fault must therefore separate the two structural units.

5.4.3 Fardingmullach Imbricate Zone

In the Abington area, the Fardingmullach IZ has an outcrop width of less than 200 m and comprises Moffat Shales with thin sandstone interbeds; the pre-Moffat Shale pelagic sequences of the Leadhills IZ are noticeably absent. Faults and sheared beds are abundant, particularly in black mudstones.

Stratigraphical evidence that the Fardingmullach IZ is an outcrop-controlling feature is not forthcoming from the present area, as the area to the south has not been mapped. Furthermore, the age of sediments south of the zone in

west Nithsdale (Shinnel Formation, Floyd 1975) is equivocal (see Section 2.6.2). Following Floyd (op. cit.) the Fardingmullach IZ is suggested to be a complex fault zone, comparable in style with the Leadhills IZ and occurring south-eastwards from volcanigenic sandstones.

5.4.4 Lateral continuation of imbricate zones

The persistence of major stratigraphical and petrographical units along strike enables the Leadhills and Fardingmullach Imbricate Zones to be traced a distance of 95 km through west Nithsdale into the Rhinns of Galloway, where they are exposed at Killintringan and Morroch Bay respectively (Floyd 1975; Weir 1979). In west Nithsdale, poor exposure does not allow the structure of the two imbricate zones to be described in detail; better coastal exposure in the Rhinns provides more information, in particular on the nature of the Fardingmullach IZ.

Fardingmullach Imbricate Zone: At Morroch Bay the Fardingmullach IZ is significantly thicker than in the Abington district (700 m compared to 200 m), and is tectonically more complex (Kelling 1961, Fig. 2); the structural style is closely comparable with the Leadhills IZ, with which the following characteristics are shared:

- substantial thicknesses of pre-gracilis

- cherts, tuffs and mudstones are exposed,
- pelagic sequences are concentrated in the northern part of the imbricate zone,
- outcrops of sandstones (Portpatrick Acid-clast Division) are found both NW and SE from the 'pelagic zone', the south-eastern segment forming a 230 m thick detached slab, which youngs north-westwards into Llandeilo sediments at Morroch,
- the Llandeilo lithologies, which are the oldest strata exposed, are repeated at three structural levels within the fault zone.

As is the case with the Fardingmullach IZ in the Abington district, sandstones of the Portpatrick Acid-clast Division immediately overlying Moffat Shales at Morroch Bay are noticeably richer in quartz, and poorer in feldspar, basic igneous fragments and ferromagnesian minerals than the overlying Portpatrick Basic-clast Division (Kelling 1961).

Leadhills Imbricate Zone: On stratigraphical and structural criteria, Kelling (1961) argued for a faulted contact between the quartz-rich Kirkcolm Group and the Portpatrick (Basic-clast) sandstones. It is suggested that the Leadhills IZ occupies the area extending north-westwards for 2400 m to Cave Ochtree Point (Kelling 1961, Fig. 3). Within this

zone, frequent shearing of Moffat Shale lithologies is described by Kelling, as is the repetition of fault packets containing quartz-rich sandstones which young consistently towards the NW. Kelling (op. cit.) concluded that repetition is a result of faulting, not folding.

Again, a thick belt of sandstones (1200 m) separates the southernmost fault of the inlier, the Killantringan thrust-zone, from the main outcrop development of Moffat Shales. Exposure in the inlier extends down to black cherts underlying N. gracilis black shales.

Shield Burn Imbricate Zone: In the Bail Hill area, McMurtry (1980a) described four structural sequences north of the Leadhills IZ, in contrast to three in the Abington area; the Crawick Block, bounded to the NW and SE by the Howcon and Eller Faults respectively, was interpreted as resulting from a fault splay from the Shield Burn IZ (Hepworth et al. 1981). A similar origin was proposed to explain the apparent bifurcation of the Abington Block south-westwards. In west Nithsdale and the Rhinns, the suggested lateral equivalents of the Shield Burn IZ are the Langlee Fault (Floyd 1975) and the Galdenoch Fault (Kelling 1961) respectively.

5.4.5 Wrench faults

Outcrop traces of the Leadhills, Fardingmullach and

Shield Burn Imbricate Zones are commonly offset by faults at high angles to bedding azimuths. Such faults with known displacement sense have not been observed in the field, and when necessary, fault trend was inferred to be parallel to the prevalent stream direction in the area (assuming that erosion excavates along structural weaknesses). However, all imbricate zones show a consistent horizontal component of sinistral displacement when traced along strike (Fig. 3). A maximum strike separation of 700 m is inferred, but it is stressed that this amount may well be taken up by movement along more than one plane. Maps produced by the Geological Survey of Scotland (Sheet 15, 3rd edition) and Mackay (1958) show a concentration of conjugate faults between Wool Law (89111683) and Wanlockhead. Although coincident with the Leadhills-Wanlockhead mining district which introduces a sampling bias, the base of the Leadhills IZ has a strike separation of 1300 m within this zone, suggesting that the concentration of wrench faults is a real phenomenon. The orientation of σ_1 inferred for the conjugate wrench system ($145^\circ/325^\circ$) is compatible with Caledonoid deformation. Eales (1979) suggested that early, more plastic fold and strike fault phases were followed by brittle deformation which produced the wrench system.

5.4.6 Minor faults

These are recognised by:

- small-scale displacements of planar elements,
- brecciation zones,
- planar veins with slickencrysts.

Relative displacements on faults are often difficult to determine, and use has been made of slickenside-striae to infer the azimuth of fault movement. All fibres observed in the field are straight, and only a few faults carry sets of slickensides at an angle to one another. This implies that reactivation of minor faults is uncommon (Bates 1974). Most striae are developed in thin quartz veins, or more rarely on uncoated sandstone.

A stereographic plot of fault planes recorded from all blocks shows most faults to be subvertical, with the grouping of data into five principal clusters (orientations given on Fig. 26); two of these are subparallel to regional strike (clusters D and E). Slickencrysts on strike-parallel faults indicate oblique movement at relatively shallow angles (less than 40°) on an east-west and NE-SW azimuth (Fig. 27a).

Three groups of fault planes are at relatively high angles to bedding (clusters A, B and C). Data are insufficient to establish possible movement sense in cluster A. However, cluster B - geometrically related to joints - exhibits slickenside lineations which range from vertical to steeply

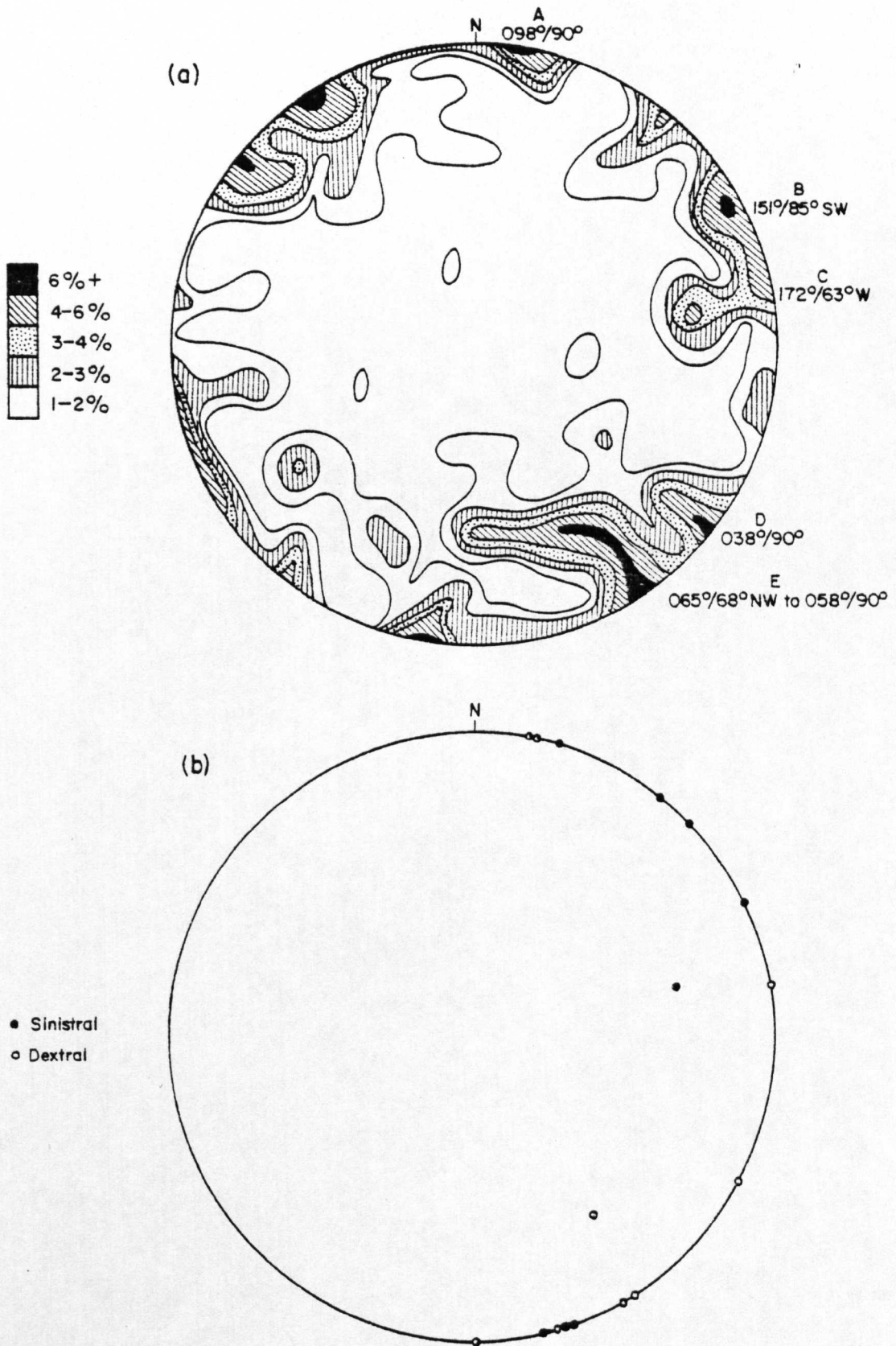
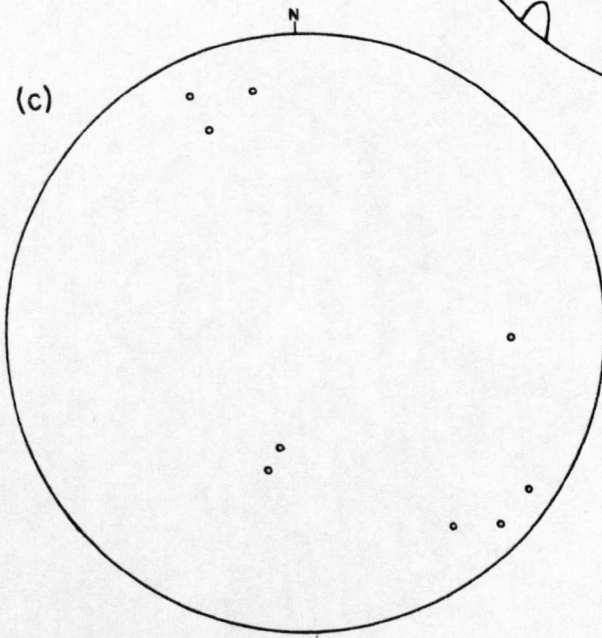
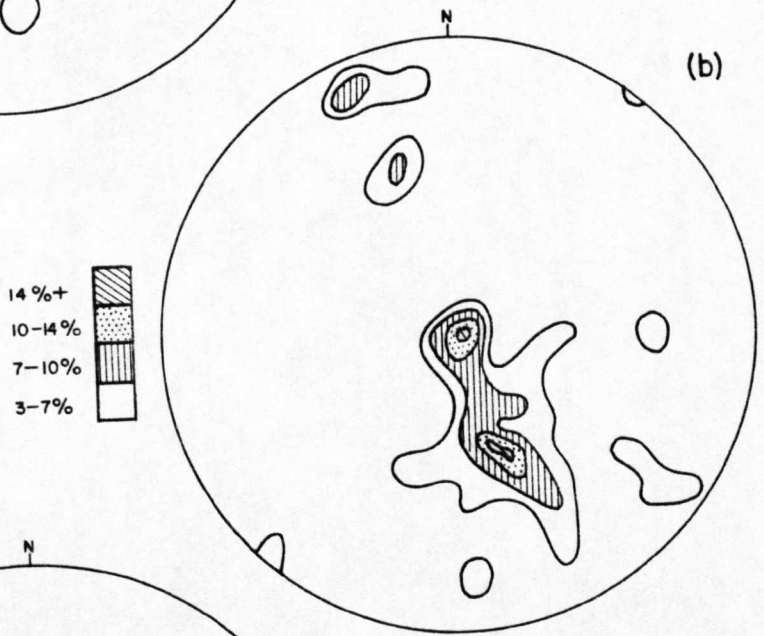
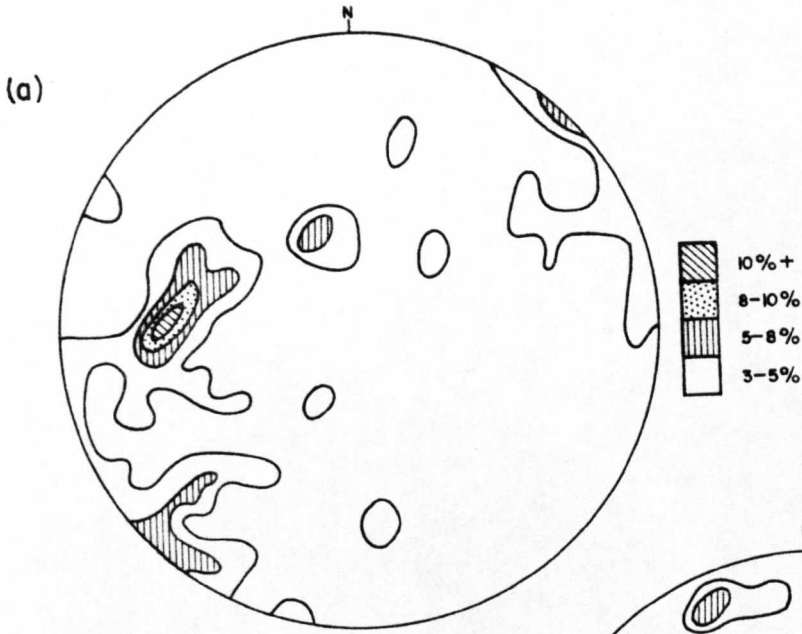


Fig. 26: (a) Stereogram of poles to fault planes, entire area; n = 116.
 (b) Stereogram of fault planes with known sense of displacement; n = 17.

Fig. 27 (overleaf)

- (a) Stereogram of slickenlines on strike-parallel faults, entire area; n = 38.
- (b) Stereogram of slickenside lineations on joint-parallel fault planes, entire area; n = 29.
- (c) Stereogram of slickenline lineation on fault planes at high angles to bedding (i.e. group C, Fig. 26a), entire area; n = 9.



plunging towards the south (Fig. 27b).

Cluster C consists of subvertical faults upon which striae generally plunge at low angles towards the NNW or SE suggesting these are wrench faults (Fig. 27c). The intermediate principal stress axis (σ_2) derived stereographically following the method of Williams (1958) is subvertical. In view of the consistent offset of outcrop patterns along imbricate zones, this group probably represents a more important fault system than the limited data imply. All authors who have studied structure in the Southern Uplands have described a conjugate wrench system, with north-south trending sinistral- and NW-SE trending dextral faults (see Floyd 1975, Fig. 92; Cameron 1977), though, as explained above, this evidence is not directly available from the present area (Fig. 26b). Cluster C is most reasonably equated with sinistral displacement.

Faults have been plotted according to structural subareas; namely, the Abington Block (north of the Leadhills IZ), the Leadhills IZ and the Elvanfoot Block (north of the Fardingmullach IZ) (Fig. 28). Strike-parallel faults are the dominant element of all three areas, although fault planes vary in the amount of dip, from steeply towards the SE in the Abington Block, vertical in the Leadhills IZ and steeply NW in the Elvanfoot Block. The presence of faults

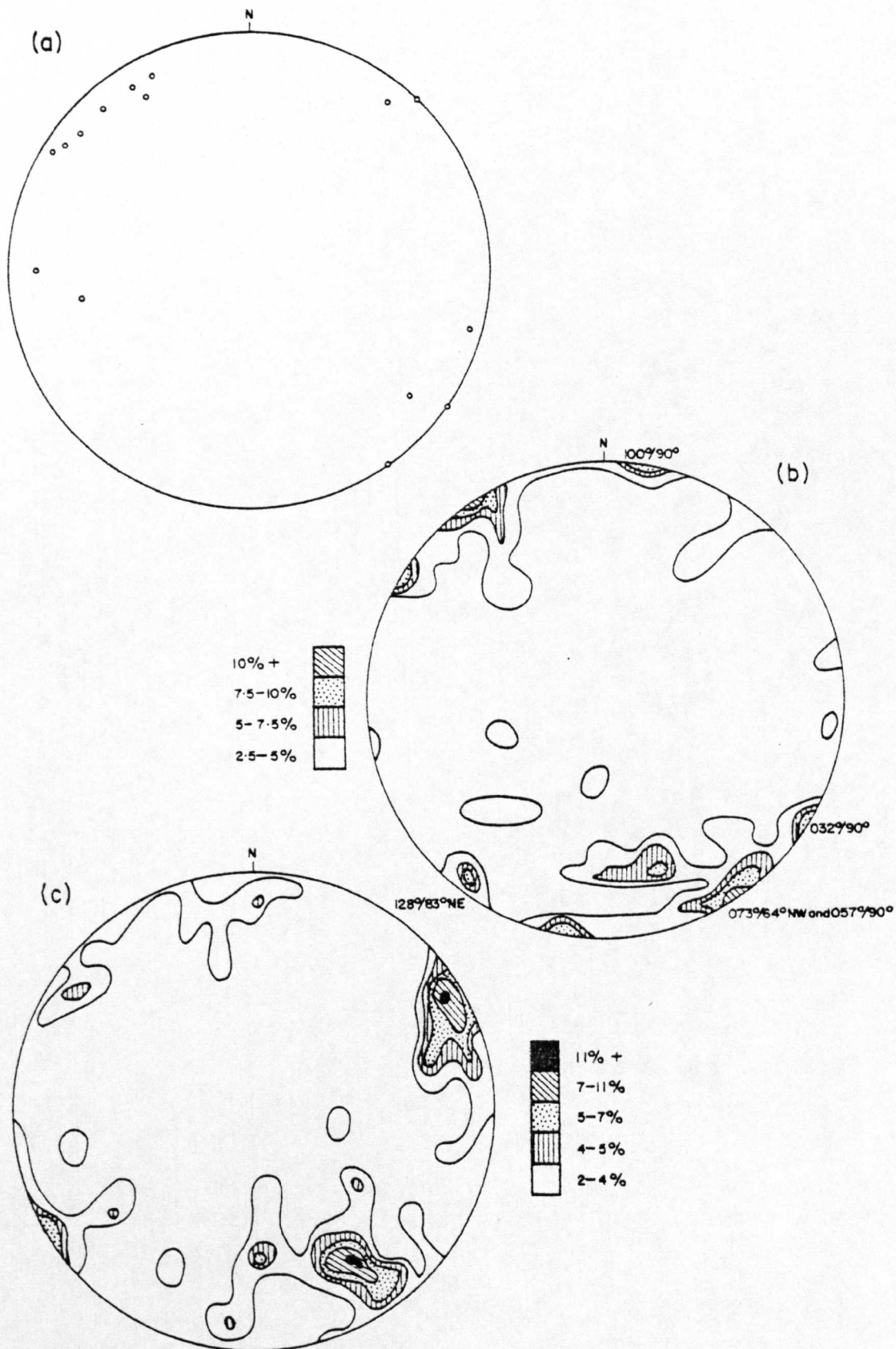


Fig. 28: (a) Stereogram of poles to fault planes, Abington Block (excluding Leadhills IZ); $n = 15$.
 (b) Stereogram of poles to fault planes, Leadhills Imbricate Zone; $n = 40$.
 (c) Stereogram of poles to fault planes, Elvanfoot Block (excluding Fardingmullach IZ); $n = 55$.

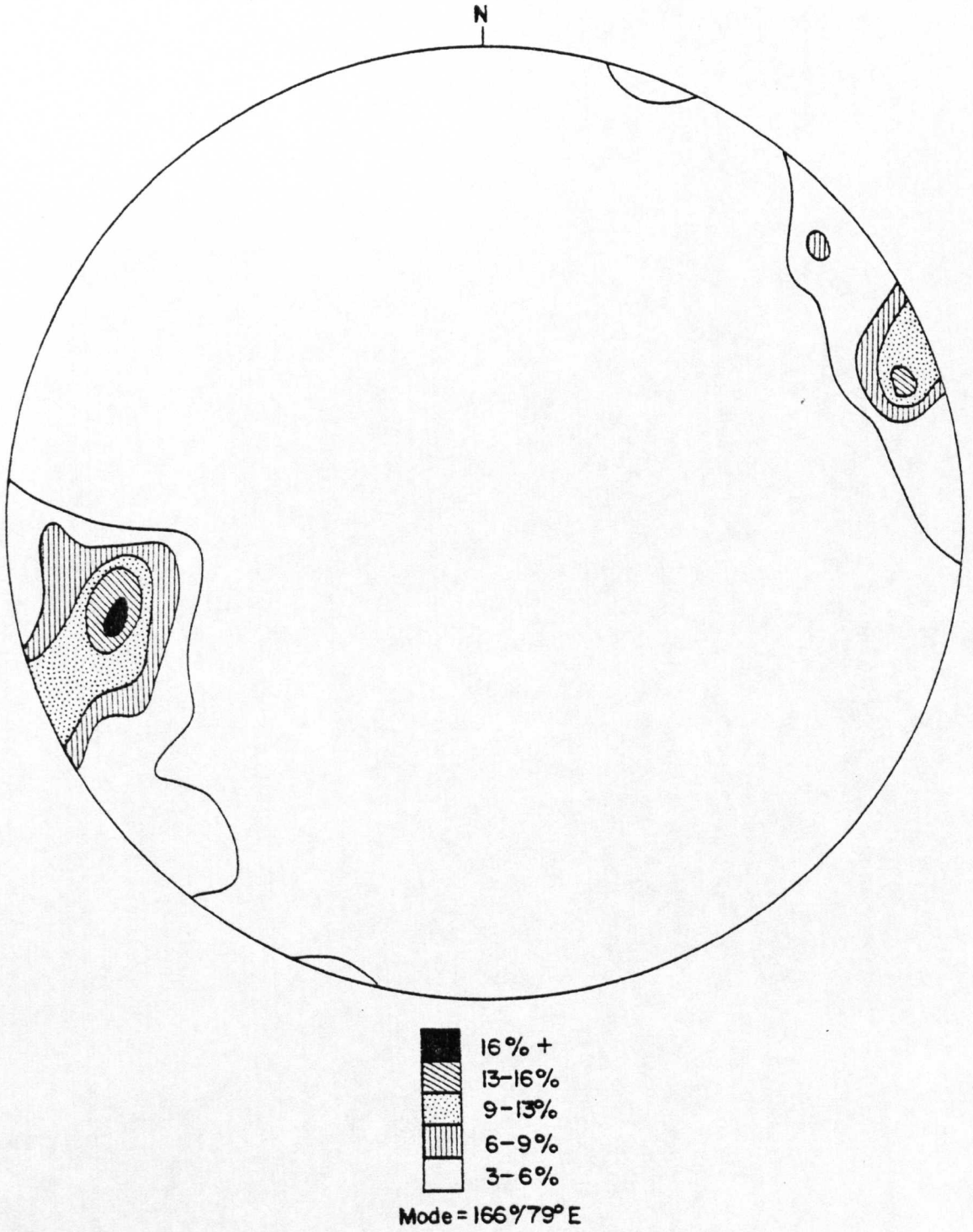


Fig. 29: Stereogram of poles to joint planes, entire area; n = 134.

subparallel to the modal joint orientation shows strong lithological control, being restricted essentially to very thick-bedded sandstones of the Elvan Formation.

5.4.7 Joints

Joints are systematic (planar and subparallel), forming sets (Price 1966) in all lithologies, but are best developed in massive sandstones of the Elvan Formation. Surfaces are planar, remarkably continuous and cross-cut major discontinuities including strike-parallel shear zones. Primary joints have a modal orientation $166^{\circ}/79^{\circ}\text{E}$ (Fig. 29) which is consistent throughout the area, and are classified as ac-joints; secondary (bc-) joints are best developed in massive sandstones. Master joints attain a maximum length of 25 m. Veins of quartz, calcite, chlorite and white mica occupy extension joints.

5.5 STRUCTURAL INTERPRETATION OF MOFFAT SHALE INLIERS

Lapworth (1889) regarded the narrow Moffat Shale inliers as forming the core of a large-scale anticlinorium (see Section 1.2), a view unchallenged until Craig & Walton (1959) concluded that the axis of the corresponding synclinorium to the south, the Hawick Line, was a strike fault effecting downthrow to the south. These reverse faults, or thrusts,

separated compound, NW-facing monoclines with tightly folded southern limbs. Similar faults were described from the Rhinns of Galloway (Kelling 1961). However, it is clear from sections in publication (cf. Kelling op. cit. Fig. 8) that outcrop of Moffat Shales is primarily controlled by regional folding in a manner comparable to that proposed by Peach & Horne (1899).

Working in the Central Belt, Toghill (1970) demonstrated that repetition of Moffat Shales was produced by displacement along reverse faults concentrated in zones, thereby producing imbricate structures. Duplication across strike of the basal fault of the imbricate zone (in this instance that of the Ettrick Valley Fault) was attributed to normal faulting. Showing translation towards the SE, this fault, which bounds the SE limit of the inlier, was extrapolated across the length of the Southern Uplands.

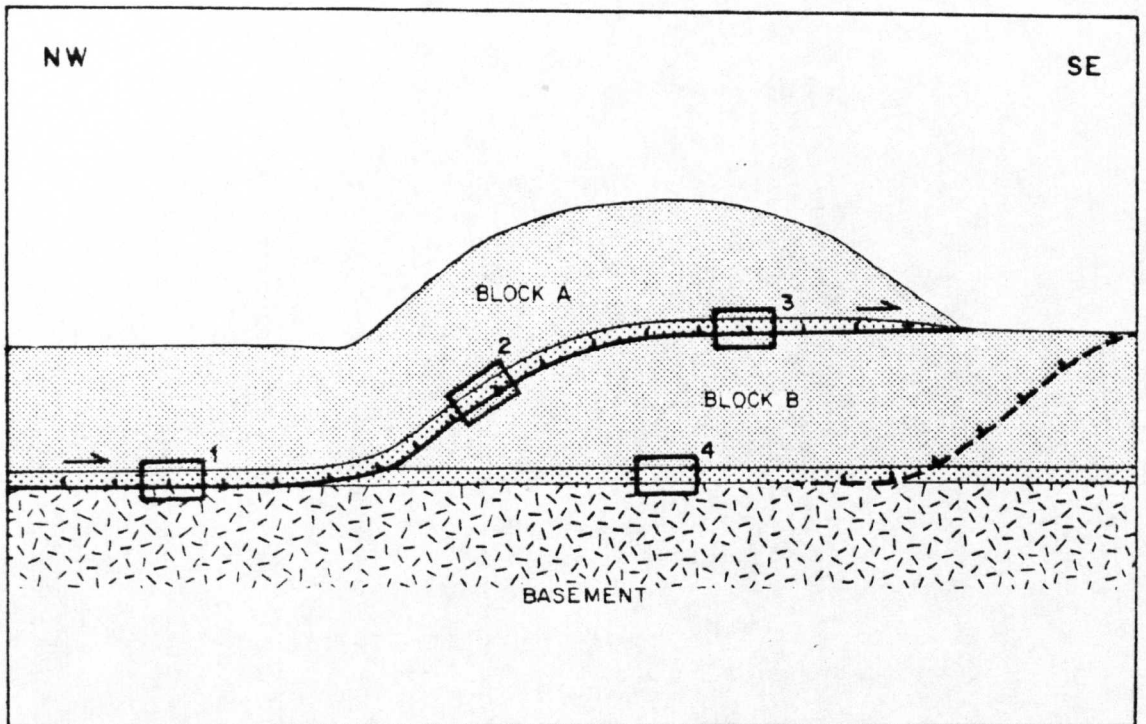
Developing the model, Weir (1974a) suggested that width of imbricate zones could be directly related to the dip of the basal reverse fault, or thrust, steep faults showing narrower bands of outcrop than more gently dipping structures. A décollement surface was proposed to occur at the base of the incompetent Moffat Shale sequence.

Dislocation zones of listric geometry were considered to arise in succession from the décollement (Weir 1979). The width of the Leadhills IZ was attributed to a plunge

culmination produced by a concealed granitic pluton centred on the Leadhills orefield. Late modification was invoked to explain the subvertical orientation of faults within the Leadhills and Fardingmullach Imbricate Zones. However, in view of significant amounts of NW bedding overturn, associated with cleavage showing no evidence of reorientation (e.g. in Mill Burn Block, Plate 24; Section 5.1.2), it is suggested that rotation of bedding and strike faults into, and sometimes through, the vertical developed either pre- or syn-D₁.

McKerrow et al. (1977) considered that movement on major strike faults occurred along low-angle thrusts, with displacements of the order of tens of km before rotation into verticality. Following this interpretation, strike faults in the Southern Uplands correspond to the definition of thrusts given in Dennis et al. (1981), that thrusts are map scale contraction faults, with no dip values or amounts of slip inherent in the term thrust (a 'contraction' fault being one which shortens an arbitrary datum plane, normally bedding). Thus fault blocks equate directly with the term thrust nappe (i.e. an allochthonous tectonic sheet which has moved along a thrust fault) (Dennis et al. op. cit.). Imbricate zones are envisaged as laterally extensive fault complexes which underlie largely coherent tectonic sheets up to 3.2 km thick.

The geometry of fault surfaces which facilitates development of fault blocks is speculative. The alternatives



- Active thrust with movement sense.....
- Location of future ramp.....
- Pelagic succession.....
- Sandstone sequence.....

Fig. 30: Schematic diagram illustrating possible structural locations at which imbricate zones could form. 1, in flat at base of thrust nappe detached from basement; 2, in ramp section; 3, in flat overriding lower thrust nappe (a late-stage structure); 4, at the base of a structural unit still attached to basement, resulting from shear failure within the pelagic succession associated with loading of Block A over Block B.

are step-like faulting, leading to the formation of ramps and flats, or straight low-angle faulting. The former is preferred, given the apparent parallelism of bedding on either side of individual faults and imbricate zones (Fig. 30). There are no structural criteria available to distinguish between overthrusting and underthrusting mechanisms responsible for the formation of structural blocks. Present-day exposure of the imbricate zones is essentially two-dimensional and normal to strike, leading to problems in ascertaining temporal and structural relationships between basal décollement and imbricate zone. Thus it is not known whether imbricate zones developed in front of the propagating décollement, or formed early in the thrust sequence and were themselves transported tens of km as part of the thrust nappe overlying the décollement (Fig. 30).

Summarising, it is envisaged that movement initially occurred along low-angle thrusts cutting up-section, thereby juxtaposing lithologies originally deposited tens of km apart. Imbricate zones formed laterally extensive fault zones underlying largely coherent thrust nappes several km in thickness. Innumerable brittle fractures, faults and shear zones effected displacement either by south-easterly overthrusting or north-westerly underthrusting. Rotation of bedding and thrusts occurred pre- or syn-D₁.

5.6 DEFORMATIONAL HISTORY

As with other areas of inland exposure in the Northern Belt, there is little direct evidence available for reconstruction of the deformational history. Following an early phase of soft sediment deformation, three deformational events have been recognised, of which only the first may be firmly assigned to regional Caledonian deformation (Table 5). A few F_2 folds have a Caledonoid orientation, but correlation of F_3 kink-bands into this scheme remains speculative at best.

Correlation of fold and fault phases is also problematical. Various authors (e.g. Anderson 1962; Floyd 1975; Cameron 1977; Eales 1979; Weir 1979) have equated the major strike faults with D_1 . As in Lecale, these faults locally separate zones of contrasting F_1 structure (cf. Section 5.1.2, Glencaple fold belt) and dislocate fold hinges; Cameron (1977) suggested that late movement on faults postdates the propagation of F_1 folds in the adjacent fault block. Eales (1979) inferred a similar sequence, with the addition of some strike faulting predating the main fold phase. However, in view of evidence from the Abington district which shows two discrete pulses of strike faulting (Section 5.4.1), reactivation ($?D_2$) of such faults cannot be discounted. Also, it is difficult to envisage how strike faults, dominated by subhorizontal to only moderately plunging lineations developed during fault movement, could

DEFORMATION	FOLD PHASE	VERGENCE	CLEAVAGE	FAULTS
D ₁	F ₁	SE/sinistral*	S ₁	Major strike faults; inlier and thrust nappe formation
D ₂	F ₂	NW/dextral*		? Reactivation of strike faults
D ₃	F ₃ (kink-bands)			
? D ₄				Wrench faults

* Refers to structures in Mill Burn subarea

Table 5 : Summary of deformational history

effect the large horizontal separation required on the basis of stratigraphy, unless the subhorizontal movement was a late modification.

Strike faults are displaced by later wrench movements. Information is not available from the present area to ascertain the relationships between wrench faulting and F_2/F_3 fold phases. Evidence from Co. Down suggests that wrench faulting postdates kink-band formation (Anderson 1962).

Despite the lack of correlation between numbering systems used by authors in the Southern Uplands and the more pronounced and widespread post- D_1 deformational phase in the Central and Southern Belts (see Weir 1979), broad agreement exists as to the general order of structural events, to which the Abington area is no exception.

Kelling (1961) and McMurtry (1980a) recognised three fold phases on the basis of fold orientation. Floyd (1975), also using directional analysis, inferred four fold phases predating the kink-band set, followed by a period of wrench faulting; strike faults were equated with D_1 . It is not known how the fold scheme of west Nithsdale equates with the two phases recorded in the Abington area, otherwise the general deformation sequence is comparable.

Weir (1979) proposed a deformational chronology for the Northern Belt based on previous work, which differs in several details from the present scheme. In Weir's scheme:

- a thrust fault (dip of fault plane less than 45°) phase is recognised, controlling outcrop distribution,
- all strike and thrust faults postdate F_1 folds,
- late wrenches predate kink-bands.

Regarding the thrust fault phase, Mackay (1958) suggested that the complex zone of dislocation controlling mineralisation in the Leadhills-Wanlockhead mining district is probably a thrust plane dipping 30° - 40° to the NW. This outcrops some 700 m south of the Leadhills IZ in the vicinity of Wanlockhead. Subsequent authors (i.e. Kelling 1961; Floyd 1975) have incorporated this information into models on the nature of the imbricate zone. However, the present author has found no evidence of such a structure in the Abington district.

CHAPTER 6: METAMORPHISM

This chapter attempts to assess the metamorphic grade attained during Caledonian deformation within the study area. Three principal techniques have been used, namely,

- illite crystallinity,
- determination of calc-aluminium silicate assemblages,
- 'vitrinite' reflectance.

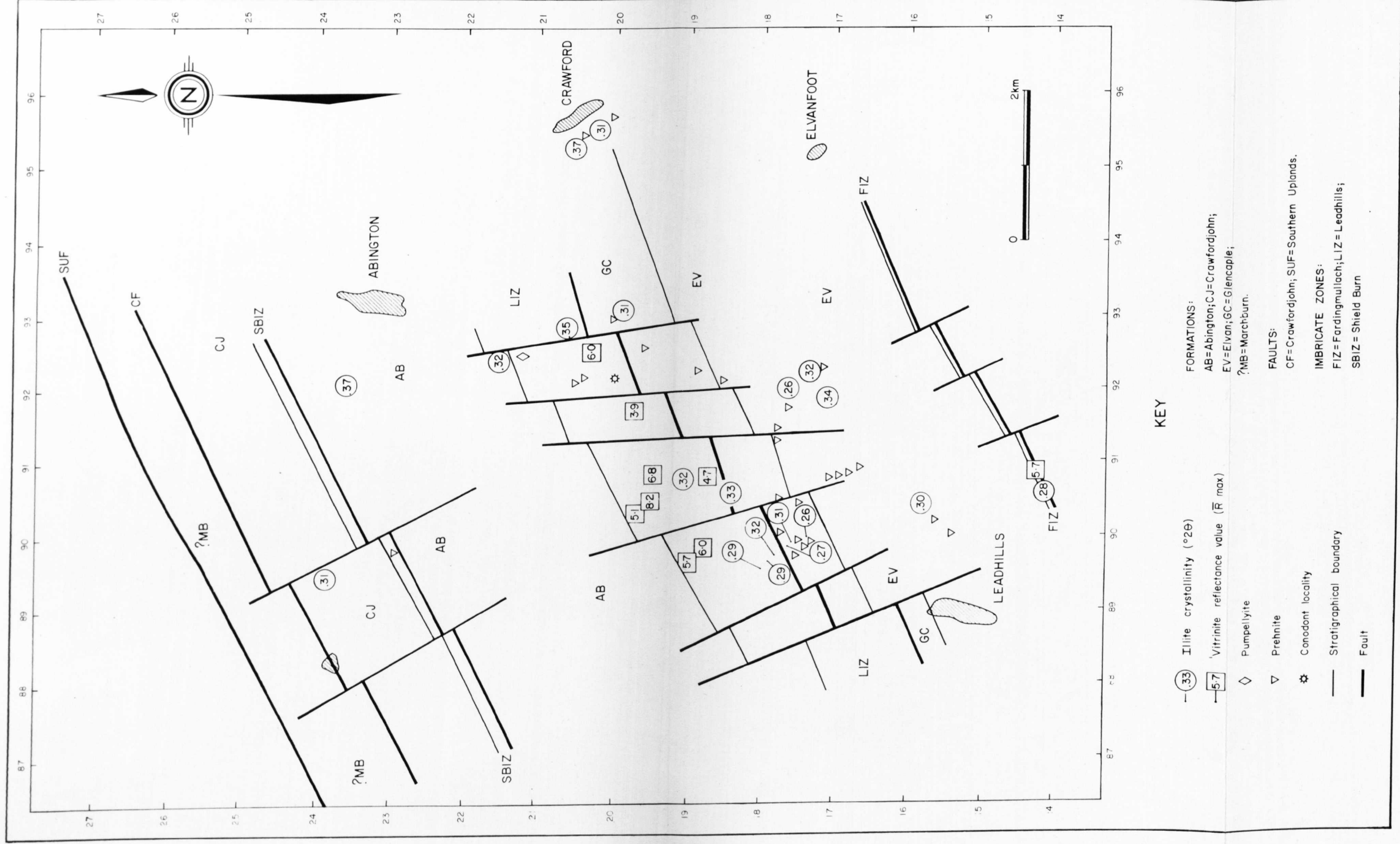
The distribution of values and results produced by these methods is shown on a metamorphic map (Fig. 31).

6.1 PETROGRAPHY

6.1.1 Sandstones

The effects of metamorphic recrystallisation in feldspar-rich sandstones are more complicated than in quartzose lithologies, due to the abundance of chemically reactive clastic minerals, rock fragments and matrix in the former.

Quartz-rich sandstones: No index minerals have been identified from quartz-rich sandstones. Cleavage is typically absent, and is not developed even where mudstone and siltstone clasts (showing evidence of soft sediment deformation) are present.



KEY

- (.33) Illite crystallinity ($^{\circ}2\theta$)
 - [5.7] Vitrinite reflectance value (\bar{R} max)
 - ◇ Pumpellyite
 - ▽ Prehnite
 - ☆ Conodont locality
 - Stratigraphical boundary
 - Fault
- FORMATIONS:
 AB=Abington; CJ=Crawfordjohn;
 EV=Elvan; GC=Glencaple;
 ?MB=Marchburn.
- FAULTS:
 CF=Crawfordjohn; SUF=Southern Uplands.
- IMBRICATE ZONES:
 FIZ=Fardingmullach; LIZ=Leadhills;
 SBIZ=Shield Burn

Fig. 31: Metamorphic map of the Abington district

Matrix content ranges from 11-52% (Appendix 4); corresponding values from modern deep-sea sands are consistently less than 12% which suggests that the quartz-rich sandstones of the Abington district have undergone metamorphic recrystallisation (Hubert 1964). The new mineral growth does not assume a strong preferred orientation. The groundmass of sandstones exhibiting higher matrix values is generally rich in carbonate. Minerals present in the matrix include illite, chlorite, carbonate and quartz.

Outwith imbricate zones, veins are not extensively developed. Wispy veins of probable metamorphic origin are irregular in thickness ($\sim 0.1-1.0$ mm) and consist of quartz with minor sericite, carbonate and plagioclase. These are cut by later veins which also are irregular in thickness ($\sim 0.5-2.0$ mm), have finer-grained margins and exhibit grain boundaries approximately perpendicular to the walls; at least two generations are recognisable based on cross-cutting relationships.

The nature and degree of alteration of feldspars is variable, not only in the study area, but also at the scale of thin section. Although turbid, relatively fresh albite may be found in most thin sections. Replacement of feldspar by carbonate or, more rarely, sericite, is generally selective along cleavage planes. However, more strongly altered feldspars may display pools of carbonate

or be completely pseudomorphed by the latter. Quartz-rich sandstones show the least amount of metamorphic alteration of all thin sections.

Quartz-poor sandstones: Sandstones of the Elvan and Glen-capple Formations are invariably more strongly altered than quartz-rich sediments of equivalent grain-size. Matrix content varies between 20-54% for both formations, with mean matrix values comparable to quartz-rich lithologies (~40%), although again there is little preferred orientation of new minerals. Cleavage is sometimes weakly developed in the sandstones. In the vicinity of major fault planes, an increase in the intensity of cleavage may be recognised by pronounced pressure solution seams, and micaceous 'pressure' shadows around detrital quartz grains (Plate 21).

Feldspar alteration is more enhanced in quartz-poor lithologies. Plagioclase is invariably turbid, with inclusions of carbonate, sericite or chlorite (rare), and grain boundaries are often diffuse. Irregular fractures in pyroxenes show no recognisable growth of new minerals; amphiboles are also relatively fresh.

Prehnite is frequently found in sandstones lacking a carbonate matrix. Two types of veins bear prehnite:

- (i) Wispy prehnite + quartz + chlorite (fibrous)

veins display diffuse margins with the surrounding host rock, vary in thickness laterally (0.1-2.0 mm), anastomose, and are seen to die out gradually at thin section scale. Where preferred orientation of prehnite is developed, this is usually subparallel to the walls of the vein.

Grain-size rarely exceeds 0.1 mm. Within the veins the presence of detrital quartz and feldspar remnants suggests gradual infusion rather than occupancy of pre-existing fractures by prehnite under metamorphic conditions. Prehnite also occurs infrequently in the groundmass of sandstones adjacent to these veins.

- (ii) Sharp-walled veins, laterally persistent for up to a few tens of centimetres, are 1-2 mm thick, exhibit prehnite + quartz + secondary carbonate assemblages and are irregularly shaped or straight. Prehnite is more coarsely grained (<0.3 mm) than in wispy veins, with crystal aggregates occurring as radiating sheaves (nucleated on the centre of the vein) or in "bow-tie" form. Where single prehnite

crystals are surrounded by quartz, both are subperpendicular to the wall. It thus appears that these veins fill pre-existing fractures. Following Norris & Henley (1976), Oliver & Leggett (1980) suggested that comparable veins elsewhere in the Northern Belt were formed due to thermal expansion of water (fluid) relative to rock, a process which initiated hydraulic fracturing and vein formation during burial metamorphism and uplift.

Wispy veins both cut, and are cut by, sharp-walled prehnite veins within a single thin section, suggesting at least three periods of prehnite formation; no offset is apparent along any vein. Both types are cut by later carbonate and quartz veins. Quartz + sericite veins also are found. Oliver & Leggett (1980) concluded that metamorphism and deformation occurred synchronously.

6.1.2 Fine-grained sediments

Descriptions of cleavage in silty mudstones, siliceous mudstones and fine sandstones are given in Section 5.1.1, descriptions of microvein systems in cherts in Section 4.2.9. X-ray diffraction studies suggest assemblages

consisting of quartz + feldspar + chlorite + illite for all lithologies (Section 6.2.1). Red cherts found a few metres above the Raven Gill Fault display a grumous texture (Spry 1969). The grumous texture displays circular to ellipsoidal aggregates of microcrystalline quartz, separated by more coarsely crystalline quartz grains up to 0.3 mm in diameter; although mostly anhedral, local patches of the coarse material show polygonal textures with straight boundaries and triple points (Plate 22). The coarsest grains are found in areas roughly equidistant between the centres of clots of cryptocrystalline quartz, the reverse of relationships normally described for contact metamorphosed rocks. It is suggested that the advance of a front of crystallisation developed from a nucleation point within the subspherical clots, but did not produce significant recrystallisation, possibly due to original chemical inhomogeneities. The clots may represent radiolarian remnants. Green cherts above the Coom Burn Fault (90561883) also show grumous textures, but differ from those in Raven Gill by being less strongly recrystallised (microcrystalline quartz is preserved), and having the coarsest-grained material within the more irregularly shaped clots. Mineral assemblages include quartz + minor chlorite, illite, ?vermiculite, iron oxide and carbonate. Recrystallisation is interpreted as having resulted from lattice

strain and heating accompanying fault movement. Sandstones above the basal fault of the Fardingmullach Imbricate Zone also show evidence of metamorphic (syntectonic) recrystallisation, with pronounced cleavage development (see p. 132).

6.1.3 Metadolerites, spilites and lithic tuffs

Petrographic details of these lithologies are given in Sections 2.3.1(i) and 2.4.1(i). No tectonic fabrics have been recognised. Despite mineralogical alteration, including the development of index minerals, original igneous textures persist.

Metadolerites: Raven Gill Formation metadolerites contain pumpellyite within veins and amygdales. Assemblages in veins of pumpellyite + chlorite + albite, and in amygdales of pumpellyite + albite, have been confirmed by electron microprobe analysis (Section 6.3). Pumpellyite is either brown or dark green, strongly pleochroic, and occurs as radial crystal aggregates (Plate 25). Prehnite is found in irregularly shaped veins up to 4 mm thick. Single crystals show strain extinction, suggesting that the prehnite was formed prior to tectonic deformation. Co-existing prehnite and pumpellyite within a thin section have not been recognised. Clinopyroxenes are altered to chlorite along cracks and grain margins; chlorite vesicles are common.

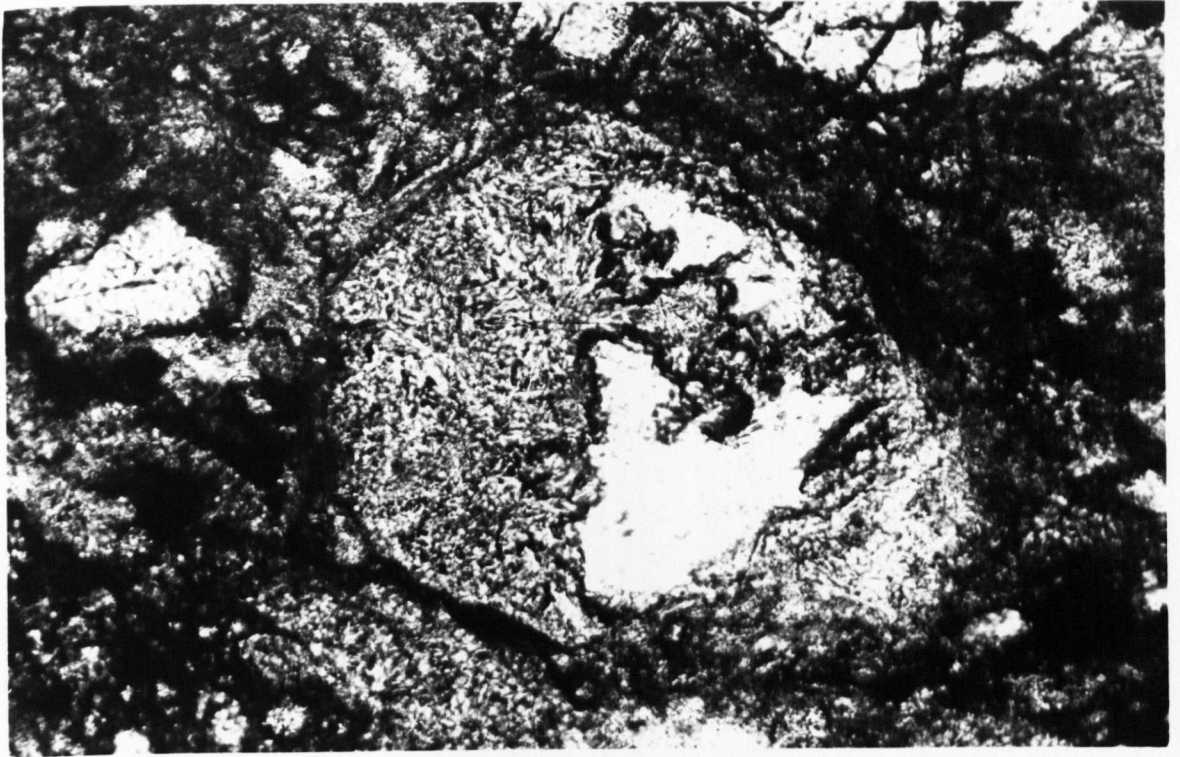


Plate 25: Amygdale in Raven Gill Formation metadolerite containing pumpellyite (strong relief) and albite (colourless), Glencaple Burn (923214). Scale bar represents 0.5 mm.

The groundmass is dominated by chlorite (recrystallised glass), although carbonate, sphene and iron oxide are frequently seen. Veining is extensive; monomineralic veins include carbonate, chlorite and albite. Albite + sericite veins are rare.

Feldspars in metadolerites of the Leadhills and Shield Burn Imbricate Zones are turbid, and show variable degrees of replacement by carbonate, chlorite and sericite; all feldspars analysed were found to be albitic in composition.

Spilites: Fine-grained lavas lacking pyroxene phases contain no recognisable prehnite or pumpellyite. Assemblages include albite + chlorite + sphene + carbonate + iron oxide + illite.

Lithic tuffs: Lithic tuffs from the Shield Burn Imbricate Zone contain plagioclase feldspars, determined optically to be oligoclase/andesine in composition. Biotite/phlogopite phenocrysts within volcanic clasts have lenses of prehnite which have grown along cleavage planes. Similar occurrences of prehnite, described from lithologies of the Bail Hill Volcanic Group, were believed to be inherited from the plutonic environment in which they crystallised (McMurtry 1980a).

6.2 X-RAY DIFFRACTION STUDIES OF SHEET SILICATES

6.2.1 Sheet silicate assemblages

Clay fractions were obtained from fresh mudstones, siltstones and sandstones following methods detailed in Appendix 11 and prepared as (i) dry, randomly orientated, (ii) glycolated and (iii) heated mounts. Instrumental conditions are specified in Appendix 12. Peak positions on diffraction charts were determined using quartz as an internal standard, and identified with the ASTM card index system (Berry *et al.* 1974).

The typical assemblage identified by X.R.D. consists of quartz + feldspar + 10\AA mica + chlorite (Fig. 32). The 10\AA mica is found in all lithological types examined, although certain sandstones contain only trace amounts. Pyrite occurs in black mudstones.

6.2.2 10\AA mica

Orientated, untreated samples show strong peaks at 10 and 5\AA , attributable to basal reflections (001) of white mica (Fig. 32). At both random and preferred orientations, the 10\AA peak is asymmetrical towards low angles, with the foot of the asymmetry situated at $\sim 10.91\text{\AA}$, indicative of a muscovite with some interlayer K^+ removed (i.e. illite, Fig. 33b). Saturation in ethylene glycol produces peak enhancement accompanied by a very slight increase in basal spacing, although not nearly enough to earn the classification

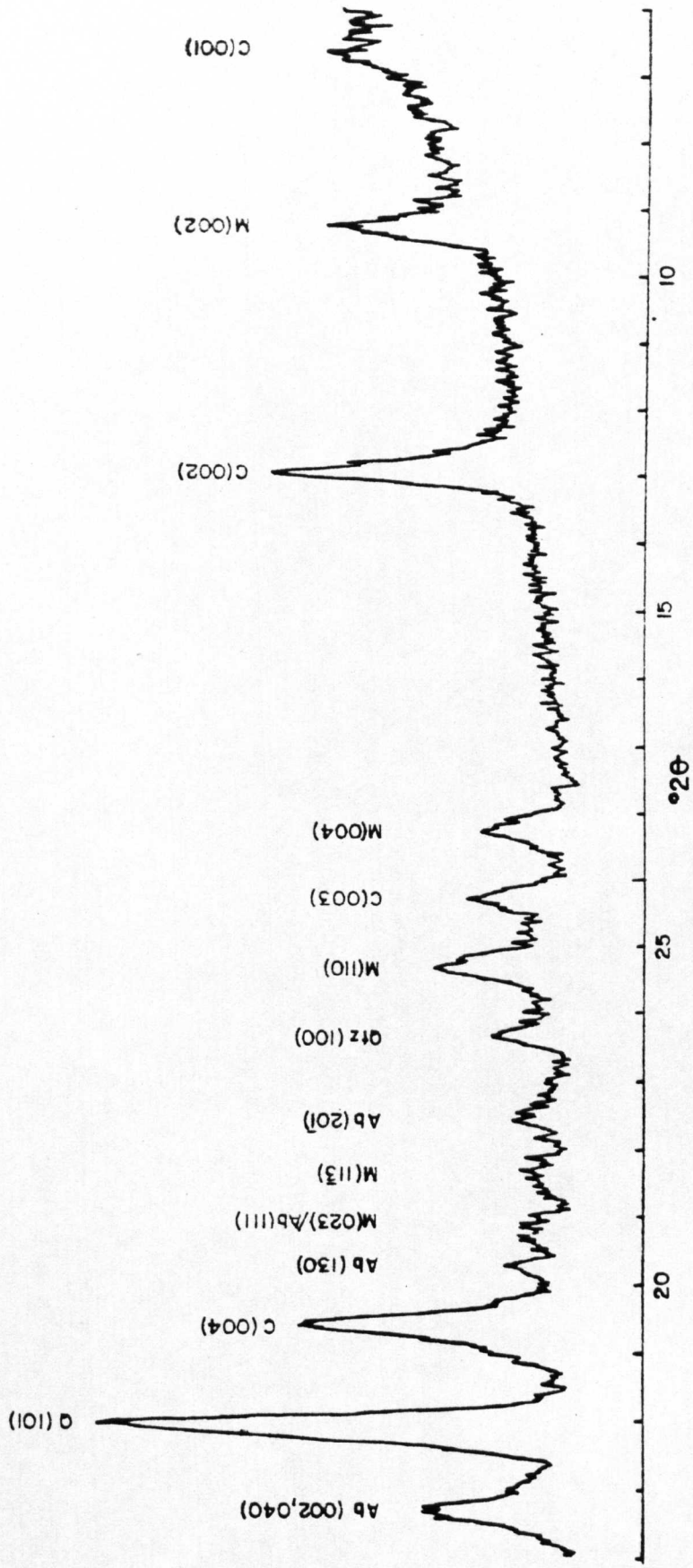


Fig. 32: X.R.D. scan of $-2\mu\text{m}$ fraction of mudstone (627); dry run, random orientation. 10\AA mica indexed as $2M_1$ muscovite.

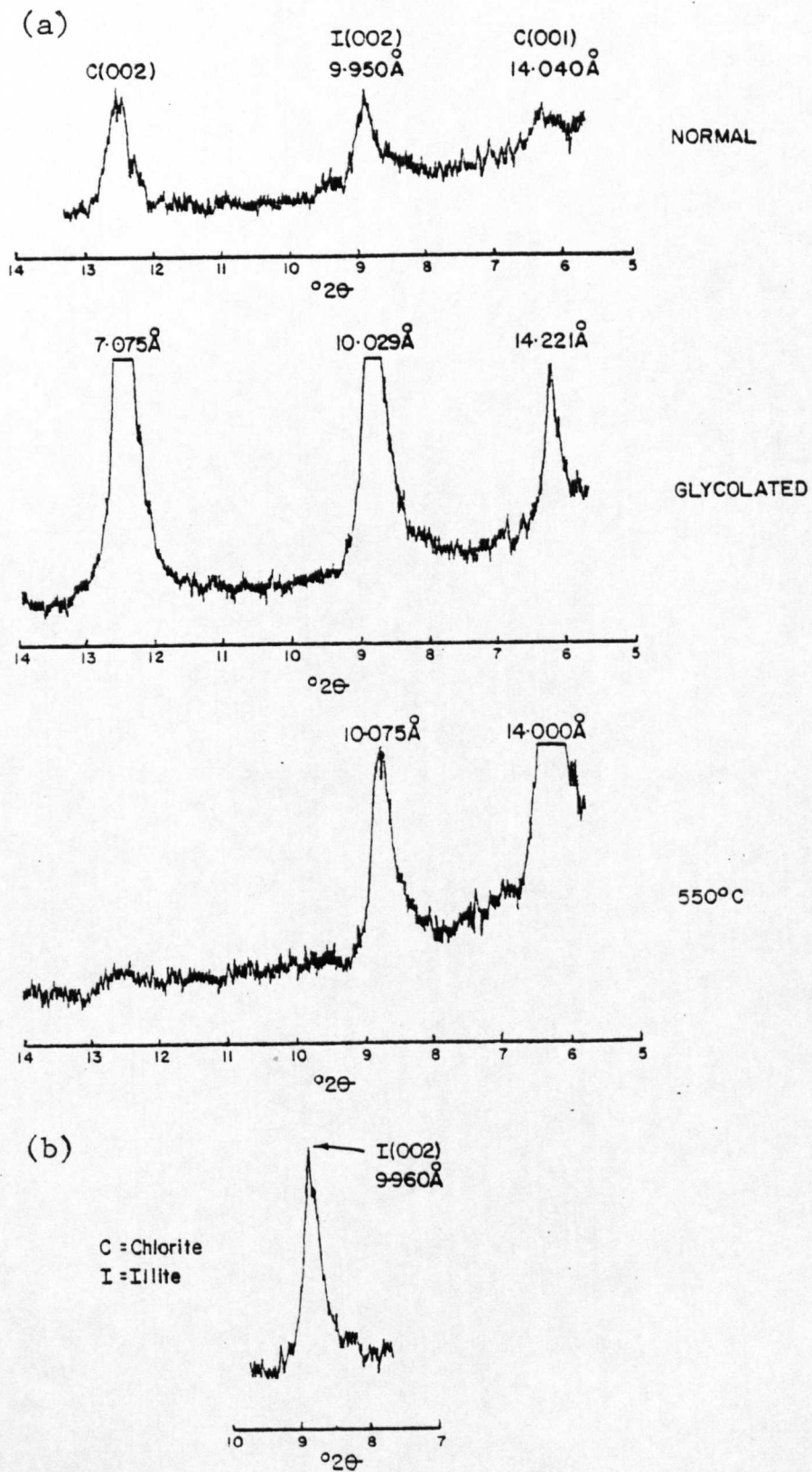


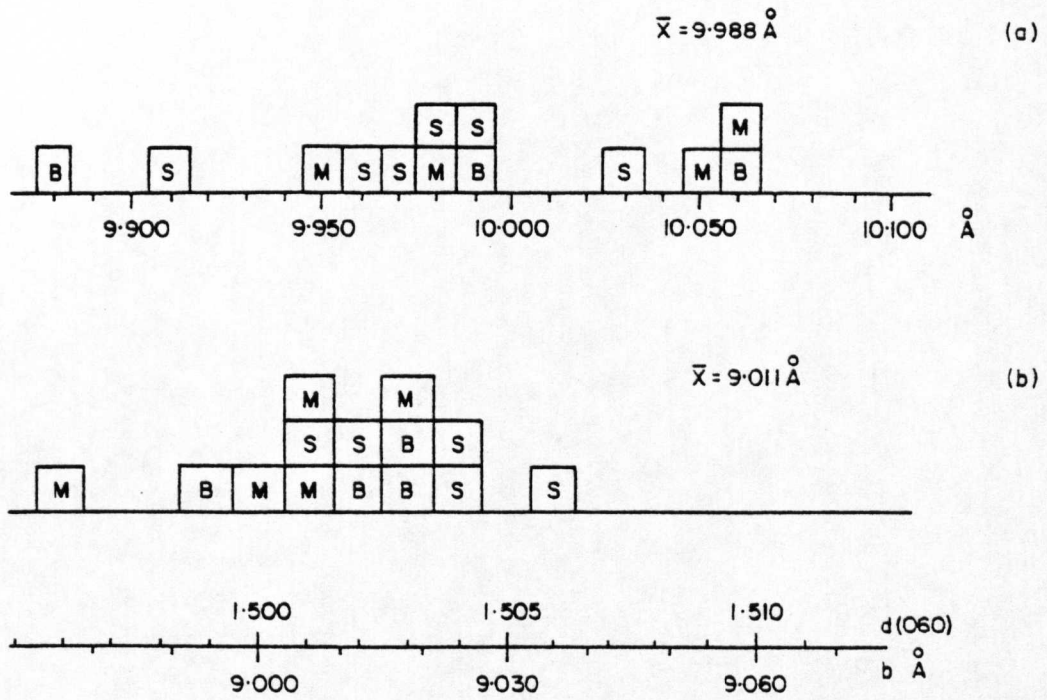
Fig. 33: (a) X.R.D. scans of mudstone 8/27, showing the effects of different treatments - normal, glycolated and heated to 550°C for 2 hours (b) Scan of well orientated mudstone (sample 193), showing illite (002) peak.

of smectite (Appendix 13). The presence of a small amount of expandable layers may account for the slight dilation of the crystal lattice. The persistence of the (002) reflection after heating confirms the mineral to be illite (Fig. 33a) (Thorez 1976).

A well ordered mica polymorph is implied by the presence of nonbasal reflections (Yoder & Eugster 1955). Comparison with other studies of low-grade metamorphism suggests that the illite of the prehnite-pumpellyite facies has the structure of the 2M polymorph (Dunoyer de Segonzac 1970).

$d(002)_{2M}$ spacing: Measurement of the 10\AA peak position gives the thickness of mica sheets, and ranges from $9.880\text{-}10.060\text{\AA}$ (Fig. 34a; Appendix 13). No lithological control is apparent. It has been suggested that limited substitution of Na for K in interfolial (X-) sites produces a reduction in the basal spacing (for which linear regression equations can be derived), without the appearance of paragonite as a separate phase (Yoder & Eugster 1954). Subsequent work has shown other factors (e.g. composition of the octahedral layer) to be important (Cipriani et al. 1968; Dunoyer & Hickel 1972). Liborio & Mottana (1970) noted that increasing metamorphic grade was accompanied by a diminution of basal spacing of micas ($9.982\text{-}9.917\text{\AA}$) and Dunoyer & Hickel (op. cit.) concluded that micas of the epimetamorphic zone ('epizone')

Fig. 34: (a) Histogram of $d(002)_{2M}$ spacing. B = black mudstone; m = mudstone; S = sandstone
 (b) Histogram of b parameter of illites.



show relatively consistent $d(002)$ values between different areas. The mean value from the study area ($d(002)=9.988\text{\AA}$) is significantly larger than previously reported epizone values ($\bar{X}=9.944\text{\AA}$, Alpes Piémontaises, Dunoyer & Hickel op. cit.), but smaller than probable low anchizone/diagenetic zone mudstones of Dob's Lin and Hartfell ($\bar{X}=10.01$ and 10.04\AA respectively; Watson 1976).

$d(060)$: The measured peak position is directly related to the \underline{b} parameter of the crystal lattice, $\underline{b} = d(010)$, which is itself dependent on the chemical composition of the octahedral layer. Values $d(060) \sim 1.50\text{\AA}$, $\underline{b} \sim 9.00\text{\AA}$ indicate dioctahedral micas (Fig. 34b; Appendix 13); trioctahedral micas ($d(060) \sim 1.54\text{\AA}$, $\underline{b} = 9.24\text{\AA}$) are not distinguishable in the present study as this peak position coincides with a strong quartz (211) reflection.

Parameter \underline{b} also permits distinction between muscovites and phengites. Substitution of Fe and Mg for Al in the octahedral sites expands the lattice, with \underline{b} greater in phengites than muscovites. Dominance of \underline{b} values less than 9.025\AA in the Abington area indicates muscovitic composition (Cipriani et al. 1968); only one sandstone shows phengitic micas (Fig. 34b). The \underline{b} parameter has also been used as an indicator of relative geobarometry accompanying metamorphism

(e.g. Fettes et al. 1976). However, the small sample size of the present study does not permit meaningful conclusions to be drawn.

6.2.3 Chlorite

Strong reflections at 14\AA (001), 7\AA (002), 4.7\AA (003) and 3.5\AA (004) reveal the presence of chlorite in all specimens examined. The d-spacings are not affected by treatment with ethylene glycol. Heat treatment enhances the (001) reflection and shifts the peak to a lower value (Fig. 33a); others (001) decrease in intensity or, more typically, are completely absent as the brucite layer is decomposed. Only one specimen shows a collapse subsequent to heating of $\sim 12\text{\AA}$ (specimen 407b, Appendix 14), probably indicating unstable interlayer spaces in the chlorite lattice (?Mg-vermiculite, Thorez 1976); all other chlorites are well crystallised.

The strength of even-order basal reflections and the weakness of (001) and (003) peaks suggests an iron-rich chlorite. Specimen 407b differs from others in showing a strong (001) peak and may represent a variety richer in Mg. Dioctahedral chlorites have (003) reflections typically more intense than the other reflections, and after heating at 500°C retain an (002) peak, the intensity

of which is similar to untreated material. The lack of these characteristics implies that it is the generally more common trioctahedral chlorite variety which is dominant in the Abington district.

Post & Plummer (1972) found a correlation between intensity ratios of the first five basal reflections and composition of chlorite species. As a first approximation, those in the Abington area are ripidolitic in composition (Appendix 15). The Mg-rich character of specimen 407b is further supported in that intensity ratios indicate a sheridanitic chlorite, the occurrence of which is apparently unique in the area.

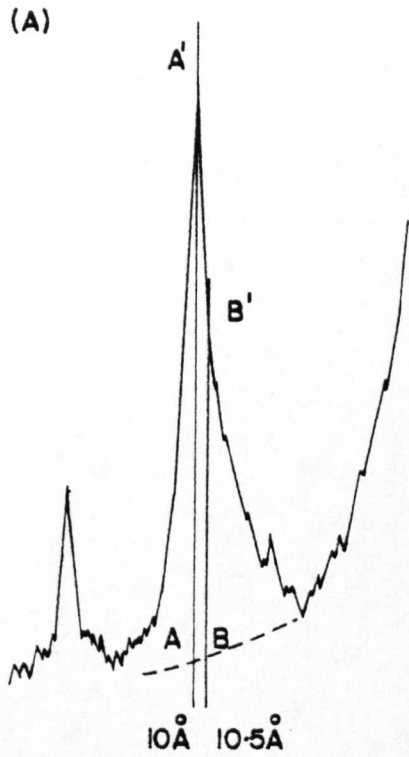
6.2.4 Illite crystallinity : methods

The application of the technique of illite crystallinity (IC) has been used extensively in Europe for over 15 years as a quantitative parameter to measure the degree of advancement of burial diagenesis and nascent regional metamorphism or anchimetamorphism (Harrassowitz 1926; Kübler 1967a; Dunoyer de Segonzac 1969; Frey 1970; Weber 1972a; Kisch 1980). With increasing incipient metamorphism, the crystallite size of illite increases concurrently with the progressive removal of expandable, mixed-layer clay minerals - X-ray diffraction peaks of the 10\AA mica (illite (001)) reflect this change by becoming narrower. This corresponds

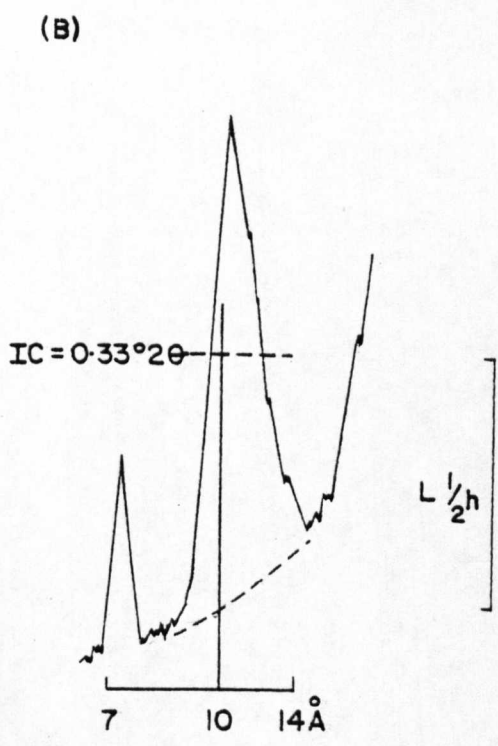
to the loss of interlayer water, the adsorption and fixing of potassium between the layers and the rearrangement of ions within the layers (Dunoyer de Segonzac 1970). In addition to temperature, the degree of crystallinity depends on other factors: initial chemical composition, hydrostatic pressure and the chemical composition of interstitial waters (Dunoyer de Segonzac 1969). The increase in peak sharpness has been quantified according to the following methods (Fig. 35), permitting definition of the fields of low-grade metamorphism (zone of diagenesis, anchizone and epizone; Fig. 36).

(a) Weaver index: This is defined as the ratio of the height of the mica (001) peak at 10\AA to that at 10.5\AA (Fig. 35a). This technique was not chosen as the ratios, although easily measurable at broad (high) values, become poorly defined at narrow (low) values (Dunoyer de Segonzac 1969).

(b) Kübler index: is the measurement of the width of the illite (001) peak at half peak height ($L_{\frac{1}{2}h}$) above background radiation (Fig. 35b) (Kübler 1964, 1968). In early studies, this was measured in mm. However, in order to assist inter-laboratory correlations, units of $^{\circ}\Delta 2\theta$ have recently been employed (Kisch 1978).



Sharpness ratio = $\frac{AA'}{BB'}$
 (after Weaver 1961)



Illite crystallinity = half peak width above background in mm or °2θ
 (after Kübler 1964;1968)

(C)

$$Hb_{rel} = \frac{Hb(001) \text{ Illite [mm]}}{Hb(100) \text{ Quartz [mm]}} \times 100$$

Hb_{rel} = 'Halbwertsbreite relativ'

(after Weber 1972b)

(D)

$$\text{Intensity ratio (IR)} = \frac{\text{intensity illite (002)mm}}{\text{intensity illite (001)mm}}$$

(after Esquevin 1969)

Fig. 35: Definition of parameters used in text with reference to illite

(c) Weber index: Weber (1972b) modified Kübler's method of IC determination by expressing the ratio of the half peak width of illite (001) to that of an external standard, namely, quartz (100). Despite the advantage of this method in not requiring an external polished slate standard to define the metamorphic field in which a particular specimen plots (anchizone, epizone, etc.), its use unfortunately has not been universally adopted (see below).

The measurement of IC unfortunately depends upon experimental conditions which include (B. Kübler, pers. comm. 1979; Appendix 16):

- X-ray tube focus,
- angular aperture in the focusing plane
(divergence slits),
- axial divergence (angular aperture of the
Soller assembly),
- width of receiving slit,
- positioning of the specimens on the goniometer
reference surface,
- rotation speed of goniometer,
- chart speed,
- time constant.

In addition, variations in preparation techniques and use of different grain-size fractions also affect IC (Appendix 16).

Specimens containing micas prepared to give strong parallel orientation produced the most internally consistent and reproducible data, and consequently all samples used in the determination of IC were prepared following the method given in Appendix 16. All samples were examined to assess the relationship (if any) between grain-size and IC; it was found that IC values were lowest (i.e. most strongly metamorphosed) for the coarsest fractions. Kisch (1980) recorded similar results and attributed this variation to admixtures of finer-grained authigenic illites with a clastic component of unweathered igneous and metamorphic micas. All subsequent work in this study used the 1-2 μm clay fraction.

In order to standardise data with other laboratories polished slate standards were procured from Kübler and measured at St. Andrews, using instrumental conditions essentially identical with Neuchâtel (Table 6). The standards are polished slate slabs, which consist predominantly of illite + chlorite + quartz crystals less than 20 μm thick, with IC values analagous to the epimetamorphic domain. Standards of poor crystallinity circulated by Kübler to other workers were found to be sensitive to humidity and also deteriorated with time. This problem was circumvented by the use of a further polished slab to which a metal pin is attached; when mounted in the specimen holder,

Standards	Mica ₀₀₂ 10Å		Quartz ₁₀₀ 4.25Å		Hb _{rel}	
	Intensity (CPS)	$L_{\frac{1}{2}}^{\circ 2\theta}$	Intensity (CPS)	$L_{\frac{1}{2}}^{\circ 2\theta}$		
31	Dec. 79- Jan. 80	2053±50	0.19±0.013 s = 0.010	-	0.20±0.016 s = 0.011	95
	Dec. 78	4812±56	0.21±0.01	374±14	0.19±0.01	111
	Feb. 75	7456±60	0.18±0.006	460	0.16	112
33	Dec. 79- Jan. 80	1222±76	0.39±0.017 s = 0.013	-	0.38±0.020	103
	Dec. 78	2352±24	0.39±0.005	112±4	0.40±0.02	97
	Feb. 75	3046±9	0.37±0.003	128	0.39	95

Registration conditions

40kV, 22mA; chart speed = 1200 mm./h; time constant = 2; Z = 3; scanning speed = 2°/min; discrimination : lower level 125 (235*), window 90 (140*); slits = 1°, 0.2, 1°.

* refers to St. Andrews

Table 6: Comparison between means of runs of Kübler standards (31,33) made at Neuchâtel (February 1975 and December 1978) and St. Andrews (December 1979 - January 1980). Standard deviations of results at St. Andrews also given.

the slab is incorrectly aligned with respect to incident X-rays, effecting a reduction in peak intensities and an increase in peak width (Appendix 17). Comparison of results between Neuchâtel and St. Andrews shows good agreement (Table 6).

A drawback of following Kübler's instrumental conditions meant that goniometer speeds of $2^{\circ}/\text{min.}$ were used, generating relatively narrow peaks. In particular, the quartz (100) peak ($\sim 0.19^{\circ}2\theta$) was difficult to measure precisely, with the result that Hb_{rel} values are not as accurate as could be produced using slower scanning speeds. Hb_{rel} values, however, are included for comparative purposes. Determination of IC for sample series was undertaken following the method outlined in Appendix 18. Anchizone boundaries follow those of Kübler (1967a, 1967b) (see Table 8).

6.2.5 Illite crystallinity : results

All IC determinations lie within the field of anchi-metamorphism on an Esquevin (1969) diagram, and most plot towards the higher grade boundary (Fig. 36, Table 7). Esquevin (op. cit.) related increasing intensity ratios (IR, see Fig. 35d) with increasing $\text{Al}/(\text{Mg}+\text{Fe})$ ratios in the octahedral site of dioctahedral micas. He concluded that only at ratios greater than 0.3 (i.e. aluminous illite, corresponding to phengite or muscovite phases) does peak width permit the

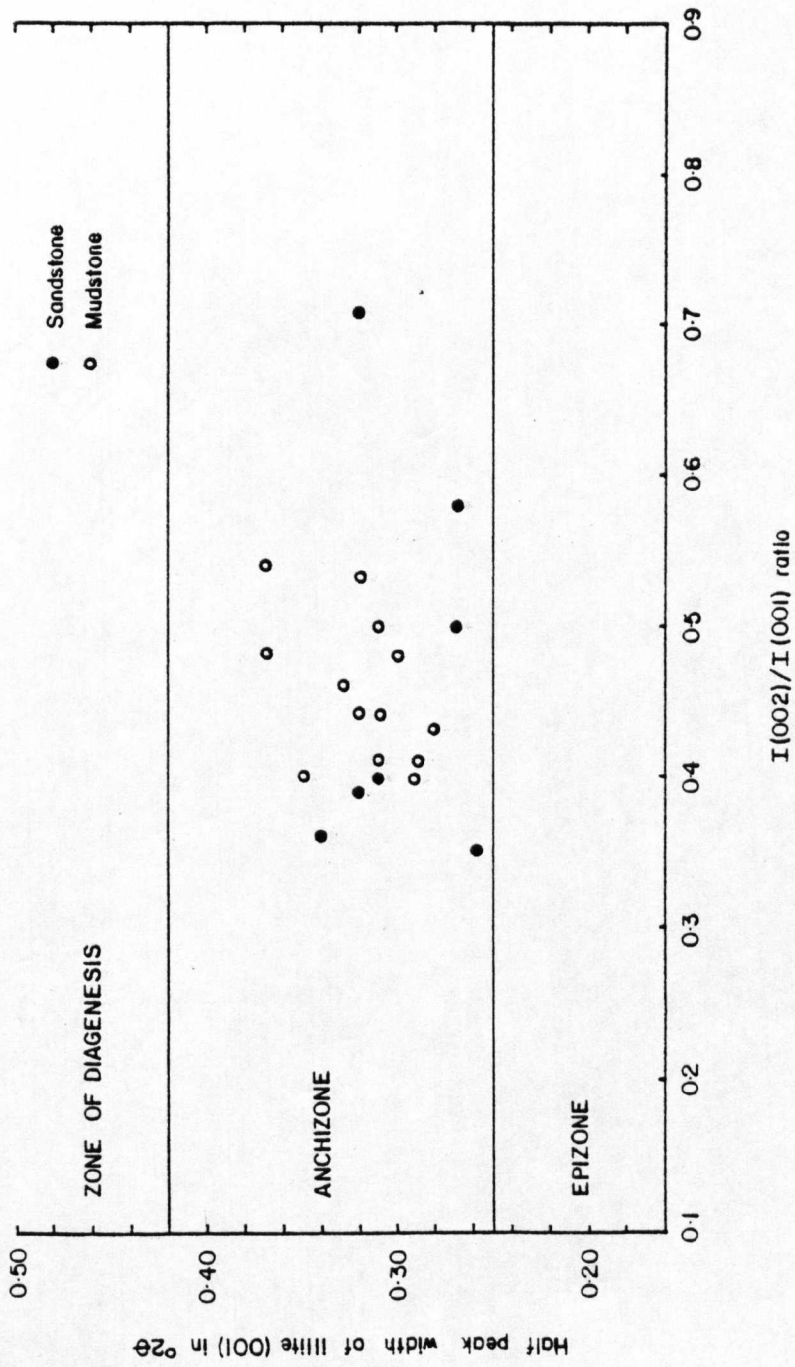


Fig. 36: Esquevin diagram showing illite crystallinity results. Fields of low-grade metamorphism after Kübler (1967a).

Specimen	Lithology	Illite crystallinity		Intensity ratio $\frac{I(002)}{I(001)}$
		$^{\circ}2\theta$	Hb _{rel.}	
172c	lam.	0.288	145	0.41
176	mst.	0.292	153	0.40
178	mst.	0.322	160	0.53
189	sandst.	0.266	135	0.58
191	mst.	0.310	163	0.44
261	mst.	0.318	169	0.39
272	lam.	0.346	184	0.40
293	sandst.	0.264	137	0.50
380	mst.	0.320	169	0.44
392	sandst.	0.325	169	0.71
407	bl. mst.	0.334	174	0.46
421	sandst.	0.260	137	0.35
482	sandst.	0.312	163	0.40
498	sandst.	0.342	170	0.36
627	lam.	0.312	163	0.50
667	mst.	0.374	185	0.48
688	mst.	0.374	185	0.54
702	mst.	0.313	155	0.41
827	mst.	0.298	149	0.48
837a	mst.	0.276	140	0.43

Lithologies: mst. = mudstone; bl. mst. = black mudstone;
lam. = laminite; sandst. = sandstone.

Table 7: Illite crystallinity results as measured using Kübler ($^{\circ}2\theta$) and Weber (Hb_{rel.}) indices.

Table 8: Correlation of anchizone limits defined by previous authors. Variations attributable principally to nonstandardisation of instrument conditions (see Kisch 1978, Table 1).

Author(s)	Low-grade anchizone boundary	High-grade anchizone boundary
Kübler (1967a, 1967b)	4.0 mm ($0.42^{\circ}2\theta$)	2.5 mm ($0.25^{\circ}2\theta$)
Kübler (1968), Frey (1970), Frey & Niggli (1971), Venturelli & Frey (1977)	7.5 mm	4.0 mm
Dunoyer (1969), Dunoyer & Heddebaut (1971), Saupé <u>et al.</u> (1977)	5.5 mm	3.5 mm
Sagon & Dunoyer (1972)	3.2 mm	2.7 mm
Weber (1972a, 1972b)	Hb _{rel} 150-155	Hb _{rel} 105-110
Ludwig (1972, 1973)	181	125
Dunoyer & Bernoulli (1976)	EA ¹ 275Å	EA ¹ 150Å
Ahrendt <u>et al.</u> (1978)	Hb _{rel} 350-500	Hb _{rel} 100-120
Kisch (1978, 1980)	$0.38^{\circ}2\theta$	$0.25^{\circ}2\theta$
Brazier <u>et al.</u> (1979)	$0.40^{\circ}2\theta$	$0.25^{\circ}2\theta$
Hepworth (this work)	$0.42^{\circ}2\theta$ (Hb _{rel} 220) ²	$0.25^{\circ}2\theta$ (Hb _{rel} 130) ²

¹EA = épaisseur 'apparente' - see Dunoyer & Bernoulli (1976), p. 1291.

²Hb_{rel} calculated from $^{\circ}2\theta$ values given.

reliable establishment of metamorphic grade preceding epizone conditions. These conditions are met in the Abington district.

Subsequent work is at variance as to whether IR equates directly with octahedral composition. Crystallochemical studies by Frey (1970) produced structural formulae of an illite and phengite in agreement with IRs. However, based on more analyses, Dunoyer & Heddebaut (1971) and Dunoyer & Hickel (1972) showed that the relationship between IR and $Al/(Mg+Fe)$ ratio is untenable in detail, a view which is followed in this study. The Esquevin diagram remains in current use (Saupé et al. 1977; Kisch 1980) and it is included for comparative purposes.

There is no association between IR and IC in the present area, irrespective of rock type. Lowest IC values are shown by three sandstone specimens, but whether this represents an increased admixture of higher grade detrital mica (cf. Section 6.2.4) or reflects a genuinely higher metamorphic grade cannot be established.

The areal distribution of IC values is shown in Fig. 31. Previous studies have demonstrated progressive decrease (i.e. peak narrowing) of IC values with depth of burial and concomitant temperature increase, a trend not distinguishable in either the Elvanfoot or Abington Blocks (Kübler 1967a;

Dunoyer de Segonzac 1970; Fig. 37). Indeed, values in the Glencaple Formation near the top of the Elvanfoot Block are less than those recorded from the Fardingmullach IZ. Significantly, sediments adjacent on both sides of the SE-boundary fault of the Leadhills IZ exhibit comparable crystallinities and are therefore considered to be of the same metamorphic grade.

The combination of poor exposure and deep weathering prohibits extensive sample collecting, a problem amplified in the Crawfordjohn and ?Marchburn Formations. A single determination from the Crawfordjohn Block suggests a grade similar to the blocks to the SE.

6.3 MINERAL CHEMISTRY

All analyses were carried out at the Grant Institute of Geology, University of Edinburgh using the energy-dispersive electron microprobe (Appendix 19). For the sake of completeness, data on the mineral chemistry of selected detrital phases obtained during the search for diagnostic calc-aluminium silicates are included in this section. A summary of microprobe analyses of metamorphic minerals is given in Table 9.

Pumpellyites: from Raven Gill Formation dolerites are of pumpellyite-(Fe) composition (Passaglia & Gottardi 1973), and

	PUMPELLYITE		PREHNITE		ALBITE		SPHENE		CHLORITE	
	Metadolerite	Sandstone	Spillite/metadolerite	Sandstone	Spillite/metadolerite	Sandstone	Spillite	Spillite/metadolerite	Sandstone	
SiO ₂	\bar{X} 36.54 s 0.23	\bar{X} 43.20 s 1.10	\bar{X} 67.34 s 0.89	\bar{X} 67.46 s 0.72	\bar{X} 29.73 s 33.66	\bar{X} 28.13 s 2.50	\bar{X} 24.85 s 0.81			
TiO ₂	-	-	-	-	-	-	-			
Al ₂ O ₃	22.32	23.28	19.03	19.12	3.57	16.77	19.82			
FeO	8.56	0.95*	0.48	0.06	1.95*	25.08	31.99			
MnO	0.05	-	-	-	-	0.37	0.47			
MgO	1.86	-	-	-	-	16.40	10.29			
CaO	22.47	26.58	0.27	0.39	26.89	-	-			
Na ₂ O	-	-	11.42	11.48	-	-	-			
K ₂ O	-	-	0.15	0.05	-	-	-			
TOTAL	91.80	94.01	98.69	98.56	95.80	86.75	87.42			
Si	16 cations	22 oxygens	32 oxygens	11.97	Si=4 ¹ 4.00	28 oxygens	5.64			
Ti	6.06	6.06	11.95	0.07	3.41	5.97	0.40			
Al	4.33	3.85	3.98	0.06	0.57	4.22	0.71			
Fe	1.18	0.11*	0.08	0.08	0.22*	4.48	0.75			
Mn	0.01	-	-	-	-	0.11	0.14			
Mg	0.46	-	-	-	-	5.17	0.93			
Ca	3.96	4.00	0.05	0.04	3.88	-	-			
Na	-	-	3.95	0.15	-	-	-			
K	-	-	0.03	0.05	-	-	-			
TOTAL	16.00	14.02	20.04	20.01	12.08	19.95	20.09			

¹ After Coombs et al. (1976a)

Table 9: Summary of microprobe analyses of metamorphic minerals. All iron as Fe²⁺ unless marked by asterisk (Fe³⁺).

are light brown or dark green and strongly pleochroic (Appendix 20, Fig. 38). Analyses are comparable with previous descriptions of pumpellyites from Northern Belt basalts (Oliver & Leggett 1980), with the exception of slightly lower SiO_2 , Al_2O_3 and more FeO in the specimens analysed for the present study. Compositional variation within a single thin section is marked, with a range sometimes exceeding that of entire compositional fields of other areas described in the literature (Fig. 39); complementary variation of Al and Fe is recognised (Oliver & Leggett 1980). Pumpellyite in the Raven Gill Formation overlaps compositionally with those described from the zeolite facies (e.g. Surdam 1969), prehnite-pumpellyite facies (Kuniyoshi & Liou 1976) and pumpellyite-actinolite facies (Coombs et al. 1976a; see Oliver & Leggett 1980).

Pumpellyite chemistry has been related to depth of burial, with increasing grade reflected by substitution of Al for Fe (Coombs et al. 1976a). However, this cannot account for the variability observed within a single specimen in the present results. Offler et al. (1981) concluded that bulk rock composition bears little relationship to pumpellyite composition, and the most important controls are the intensity of alteration and chemistry of fluids in contact with the solid phases upon which the pumpellyite nucleates; increasing

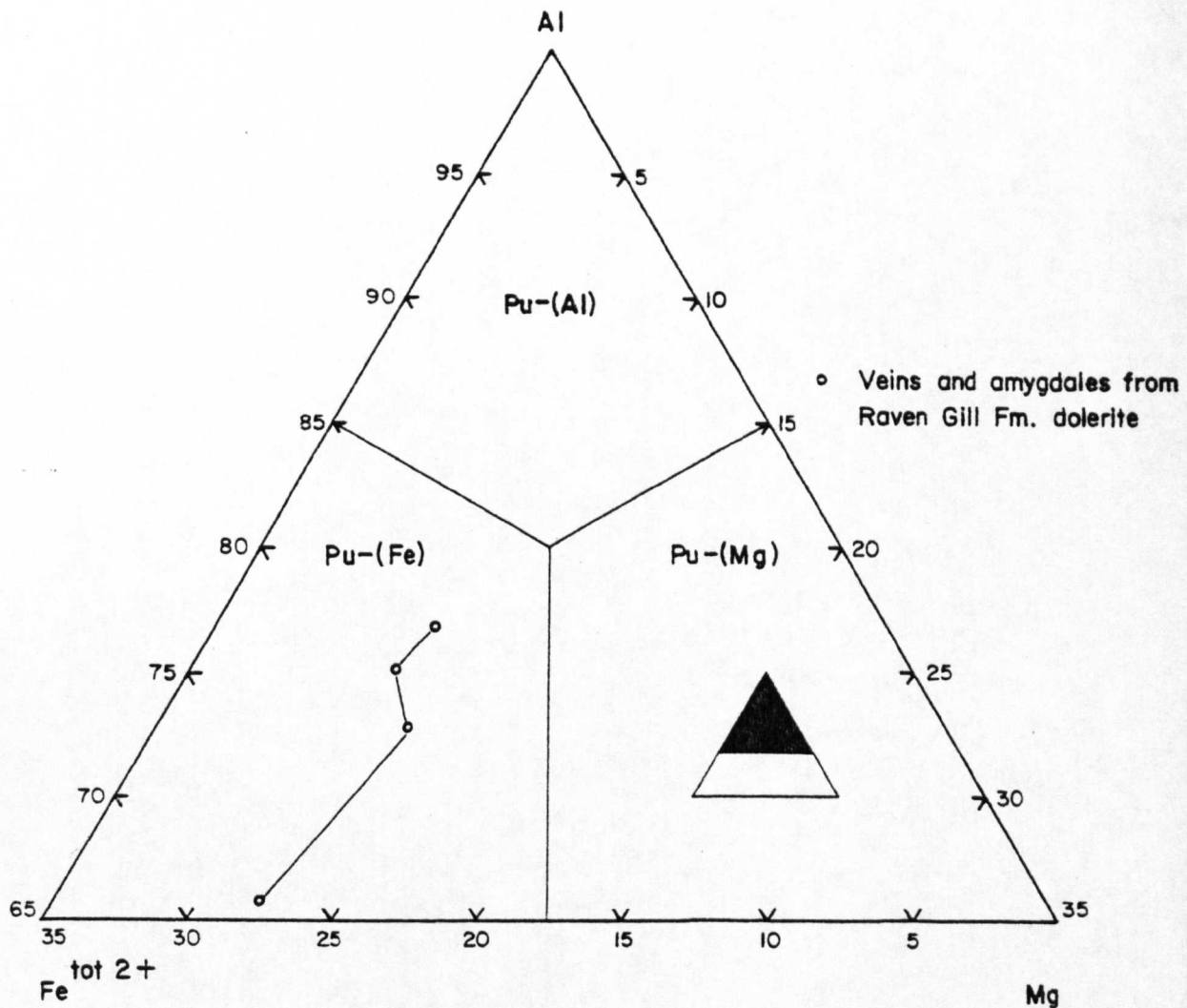


Fig. 38: Pumpellyite analyses: Al^{3+} , Mg^{2+} , $\text{Fe}^{\text{tot}2+}$ cation proportions. Compositional fields after Passaglia & Gottardi (1973).

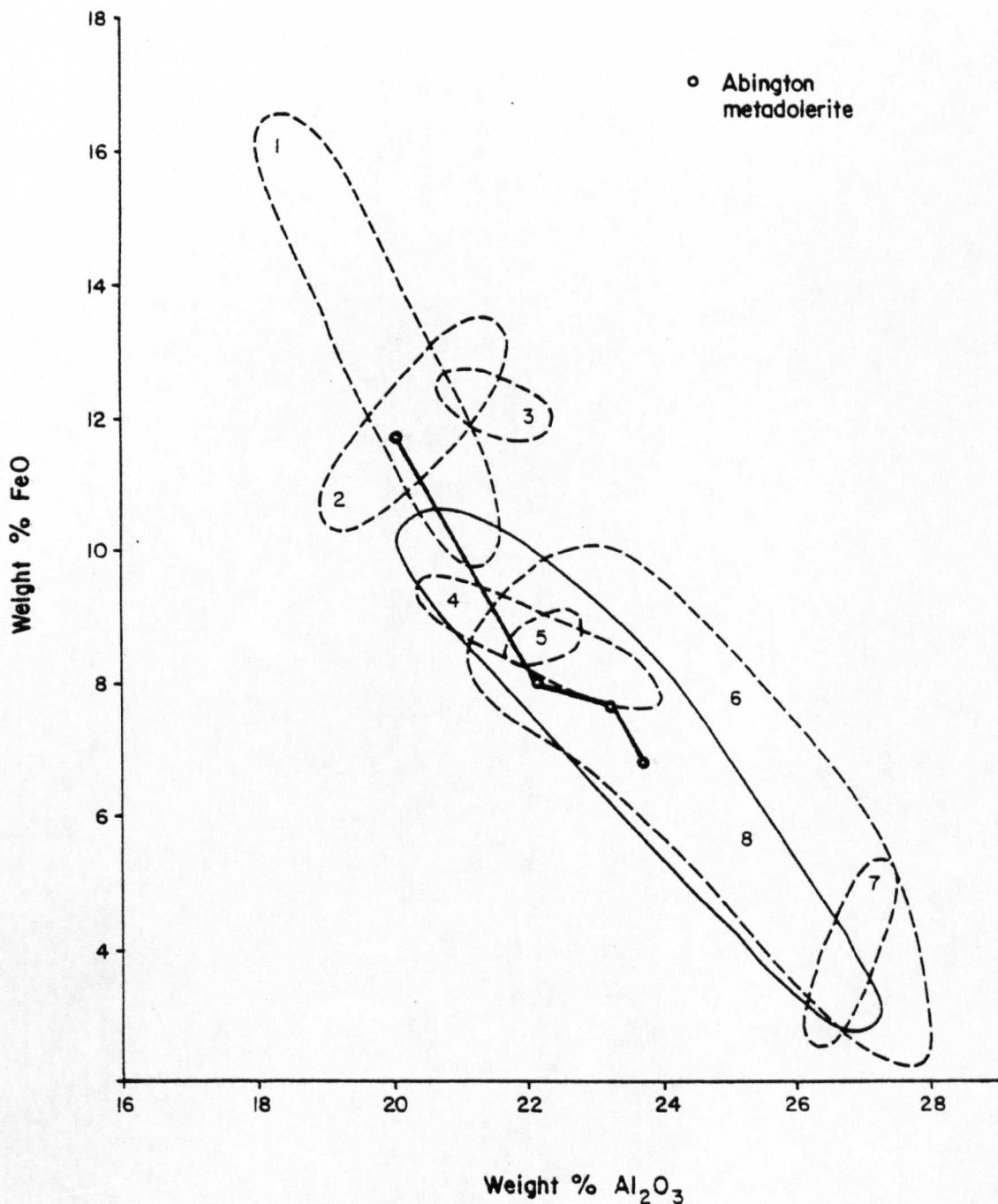


Fig. 39: Pumpellyite analyses; weight % FeO^{tot} against weight % Al₂O₃. Fields of composition: 1 Vancouver Is. (a) (Surdam 1969); 2 Murihuku Supergroup (Boles & Coombs 1977); 3 Upper Wakatipu Zones I & II (Kawachi 1975); 4 Upper Wakatipu Zone IIIa; 5 Vancouver Is. (b) (Kuniyoshi & Liou 1976); 6 Loèche (Coombs *et al.* 1976a); 7 Upper Wakatipu Zone IIIb; 8 Northern Belt (Oliver & Leggett 1980, solid line).

Fe content was attributed to higher $a_{\text{Fe}^{3+}}$ in the fluid phase produced by more extensive breakdown of magnetite and ilmenite. Variability within an individual specimen was attributed to local differences in the composition of the fluid phase, such differences possibly resulting from pumpellyite nucleation sites being near to Fe-bearing silicates and oxides - this requires a static fluid phase (Offler et al. op. cit.).

Prehnite: Analyses of vein prehnite in sandstones of the Elvan Formation are given in Appendix 21 and Fig. 40. There is little compositional variation, save minor substitutions of $\text{Fe}^{\text{tot}3+}$ and Al^{3+} . The analyses presented here are comparable to those of previous descriptions; prehnite from basalts shows greater $\text{Fe}^{\text{tot}3+}$ values than those from sandstones (McMurtry 1980a; Oliver & Leggett 1980).

Chlorite: Chlorites, analysed in spilites and sandstones show a compositional range from ripidolite through pycnochlorite/brunsvigite to diabantite (Appendix 22, Fig. 41). Such variations are also found in analyses of groundmass chlorite within a single polished thin section. Vein material, in contrast, is chemically more homogeneous, and plots within a relatively restricted field (Fig. 41). X.R.D. studies show

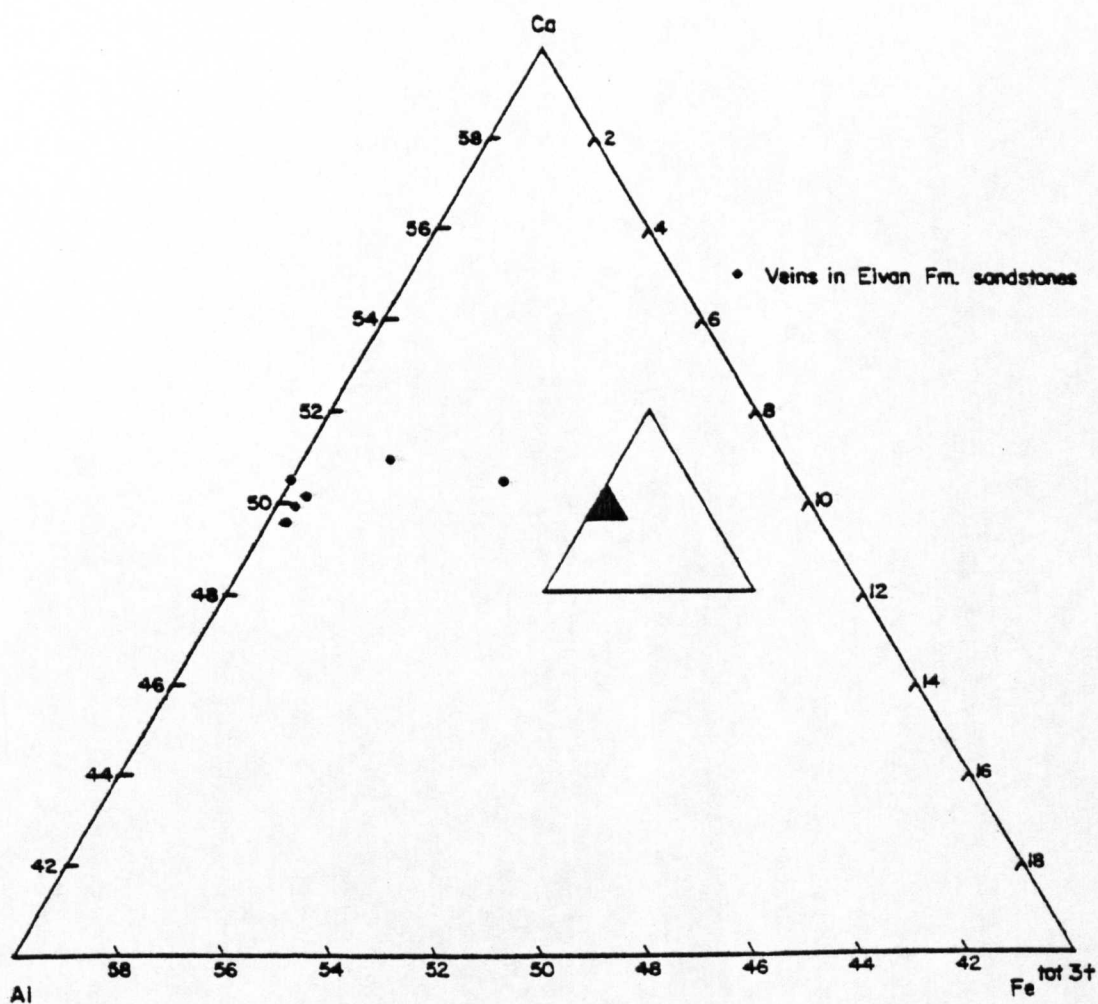


Fig. 40: Prehnite analyses; Al^{3+} , Ca^{2+} , $\text{Fe}^{\text{tot}3+}$ cation proportions

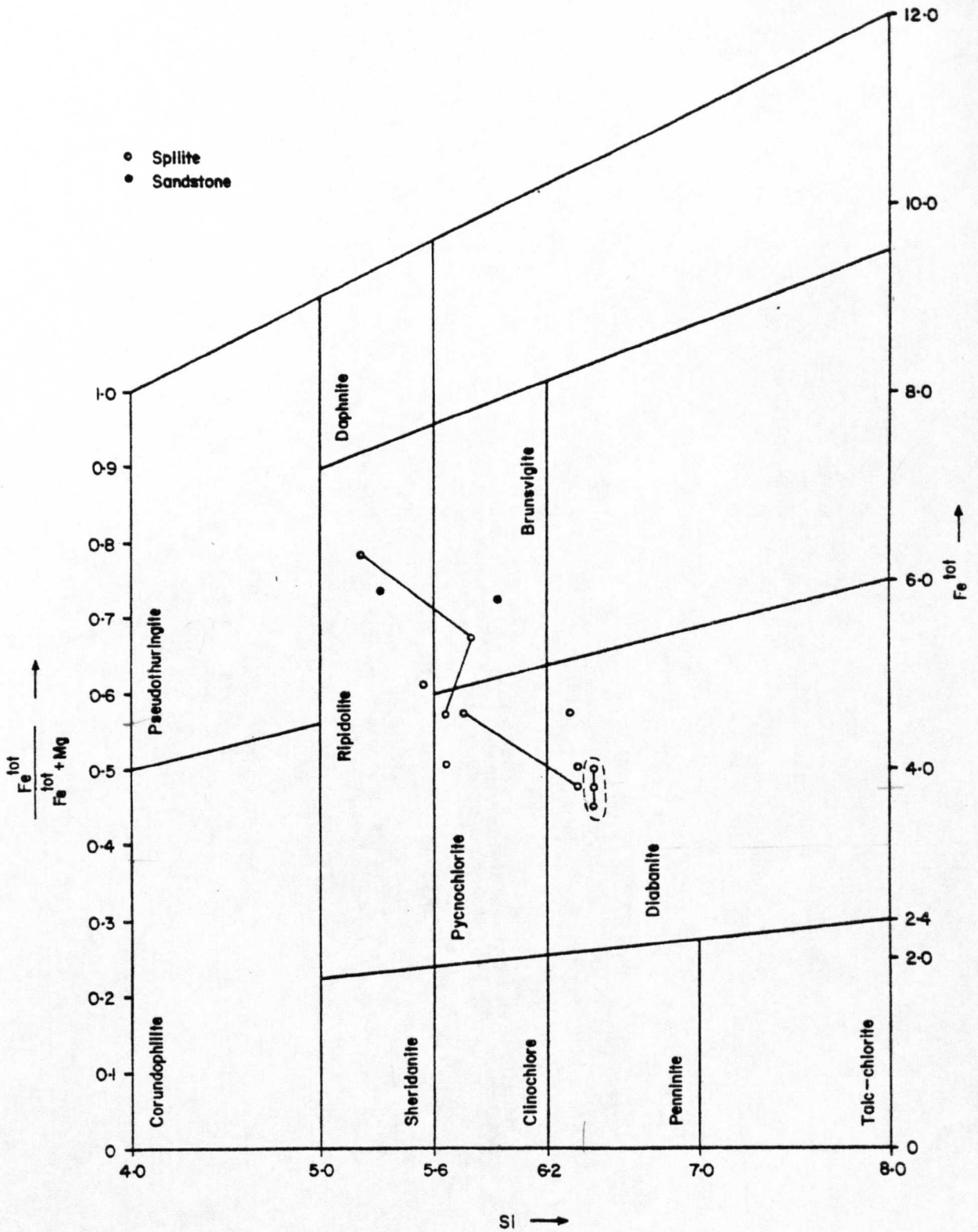


Fig. 41: Chlorite analyses; diagram after Hey (1954).
 Dotted compositional field of vein chlorite
 in single thin section. Other tie lines show
 compositional variation of groundmass chlorite
 in single thin section.

a limited compositional field for the $-2\mu\text{m}$ chlorite (Section 6.2.3).

Plagioclase: Probe analyses of plagioclase feldspars in spilites and sandstones from the Elvanfoot and Abington Blocks show albitic compositions ranging from Ab_{94} - Ab_{100} (Fig. 42). Although albite from sandstones and spilites plots within the same field, the latter are distinguished by their greater wt % FeO content (Appendix 23). Veins and amygdales in basic igneous rocks also contain albite. Lithic tuffs and dolerites in the Shield Burn IZ display feldspars, determined optically to be of andesine/oligoclase composition (see Section 2.3.1); comparable feldspars have been described from the Bail Hill Volcanic Group situated approximately along strike from this imbricate zone (McMurtry 1980a).

Sphene: A single sphene analysis from a Raven Gill Formation spilite shows a TiO_2 value less than any given in Deer et al. (1962), and less SiO_2 than those in Coombs et al. (1976a) (Table 9). Sphene from elsewhere in the Northern Belt is enriched in $\text{Fe}_2\text{O}_3^{\text{tot}}$ in contrast to the analysis presented here (Oliver & Leggett 1980). The Raven Gill Formation sphene falls within the field of sphenes from pumpellyite-actinolite bearing sandstones outlined by Coombs et al. (1976a), when plotted in terms of cation proportions of

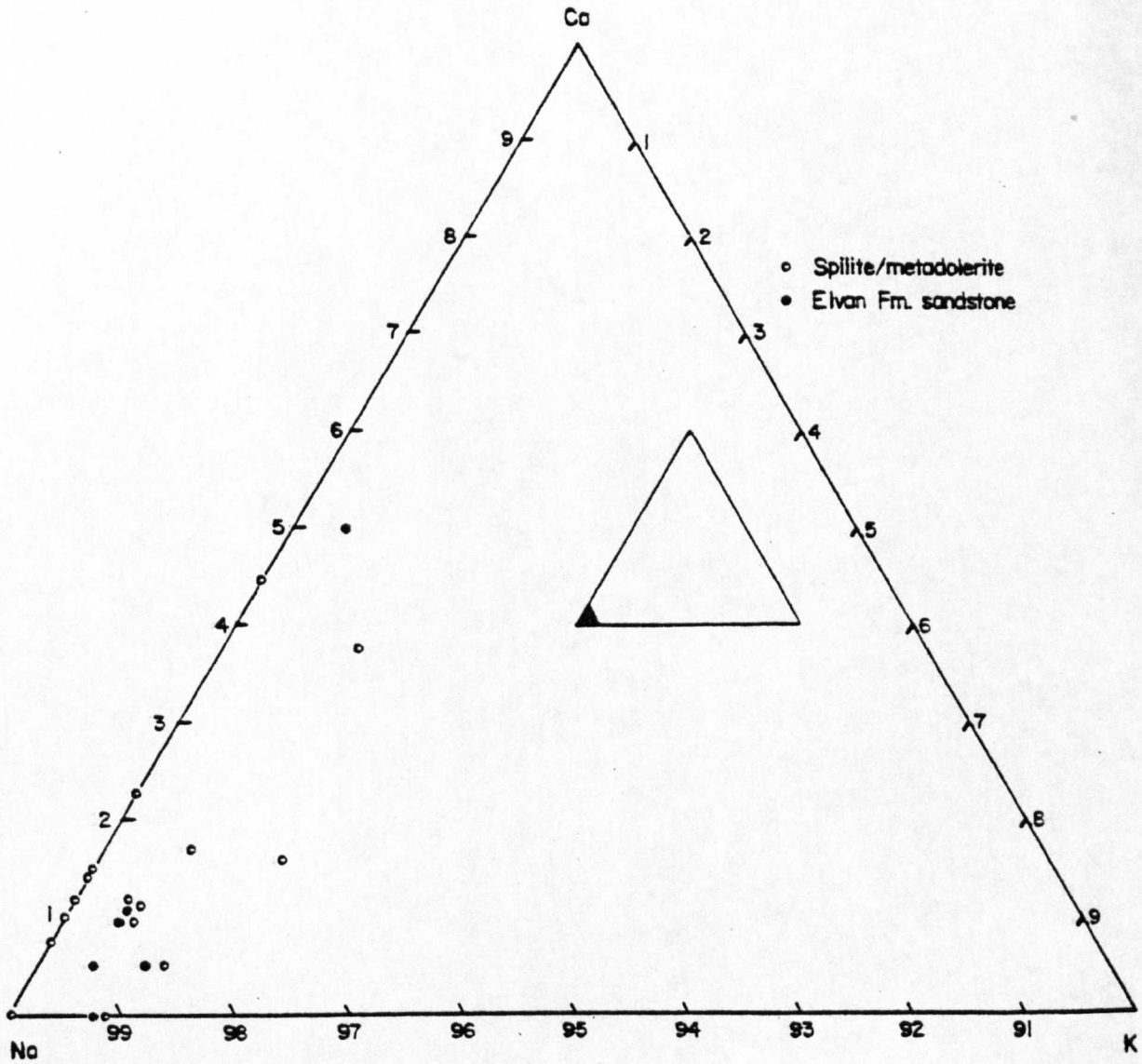


Fig. 42: Plagioclase analyses: Na^+ , Ca^{2+} , K^+ cation proportions

Al^{3+} , Ti^{2+} and $\text{Fe}^{\text{tot}3+}$ ($\text{Al}^{3+} = 14\%$; $\text{Ti}^{2+} = 81\%$; $\text{Fe}^{\text{tot}3+} = 5\%$).

Pyroxenes: have been analysed from dolerites of the Raven Gill Formation, and also from Elvan Formation sandstones (all the latter being detrital in origin). Results are given in Appendix 24 and Fig. 43. Dolerites contain pyroxenes of relatively restricted composition, which vary from salite to calcic augite within a single thin section. Two analyses from sandstones show calcic augite, similar in nature to those in the dolerites. Most pyroxenes contain > 0.1 wt % Cr_2O_3 and are high-aluminium salites and augites with between 5-8 wt % Al_2O_3 (analyses 3 and 11, Appendix 24).

Of the pyroxene analyses given by McMurtry (1980a, Table 3), pyroxenes from basalts of the Cat Cleuch Formation are most directly comparable with those presented here, although Abington pyroxenes contain slightly less Al_2O_3 and CaO , and more Cr_2O_3 , FeO^{tot} and MnO (Fig. 43). The absence of detectable Na_2O (< 0.5 wt %) is a feature of both areas. Xenoliths from Bail Hill contain diopside, and augite compositions are rare.

Salites and Ca-rich augites are particularly typical of hypabyssal rocks derived from alkali-olivine basalt magma, from which high-aluminium salites have also been recorded; chromian salite and Ca-rich augite from the olivine basalt-hawaiite-mugearite-trachyte series of the Hocheifel area,

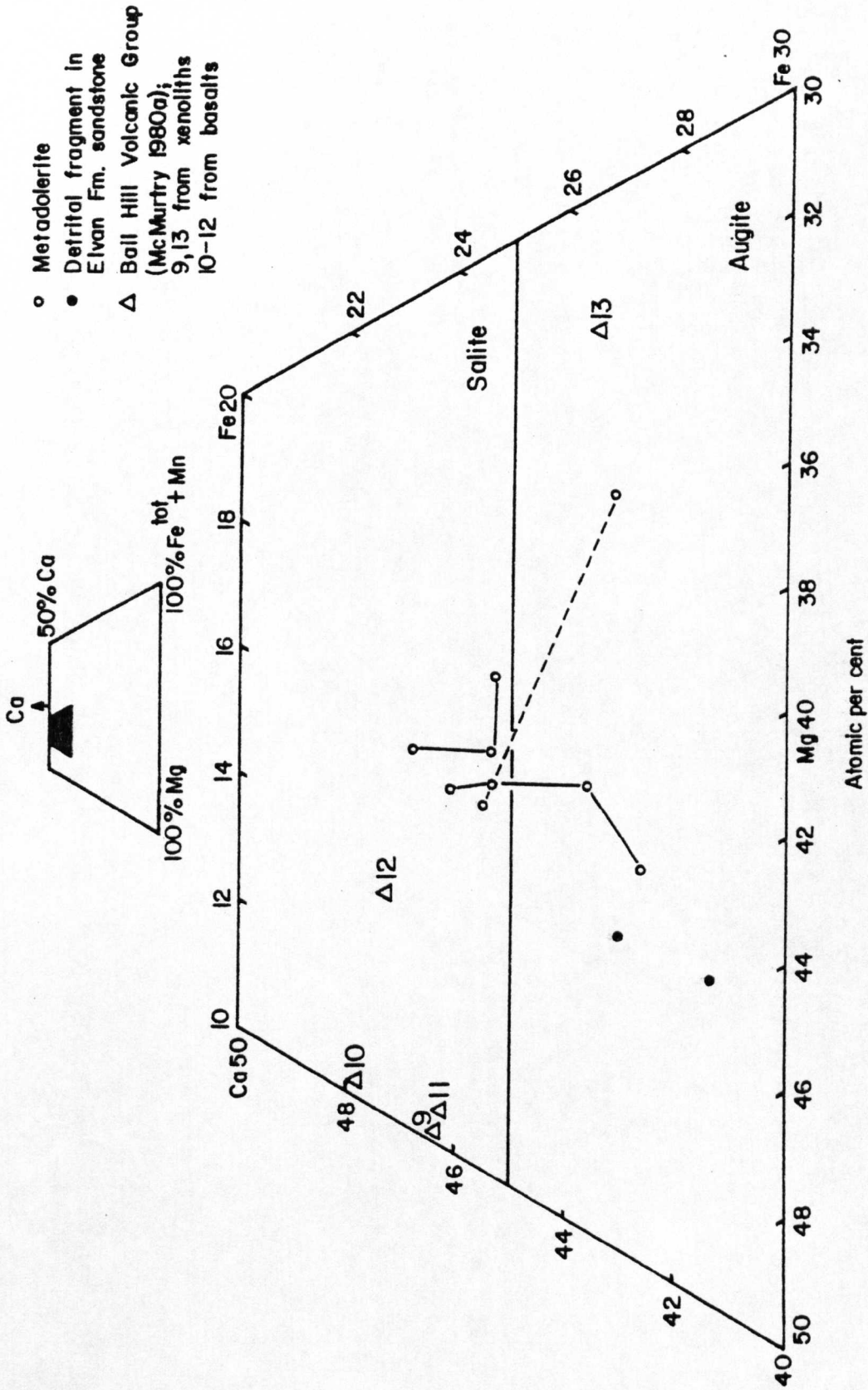
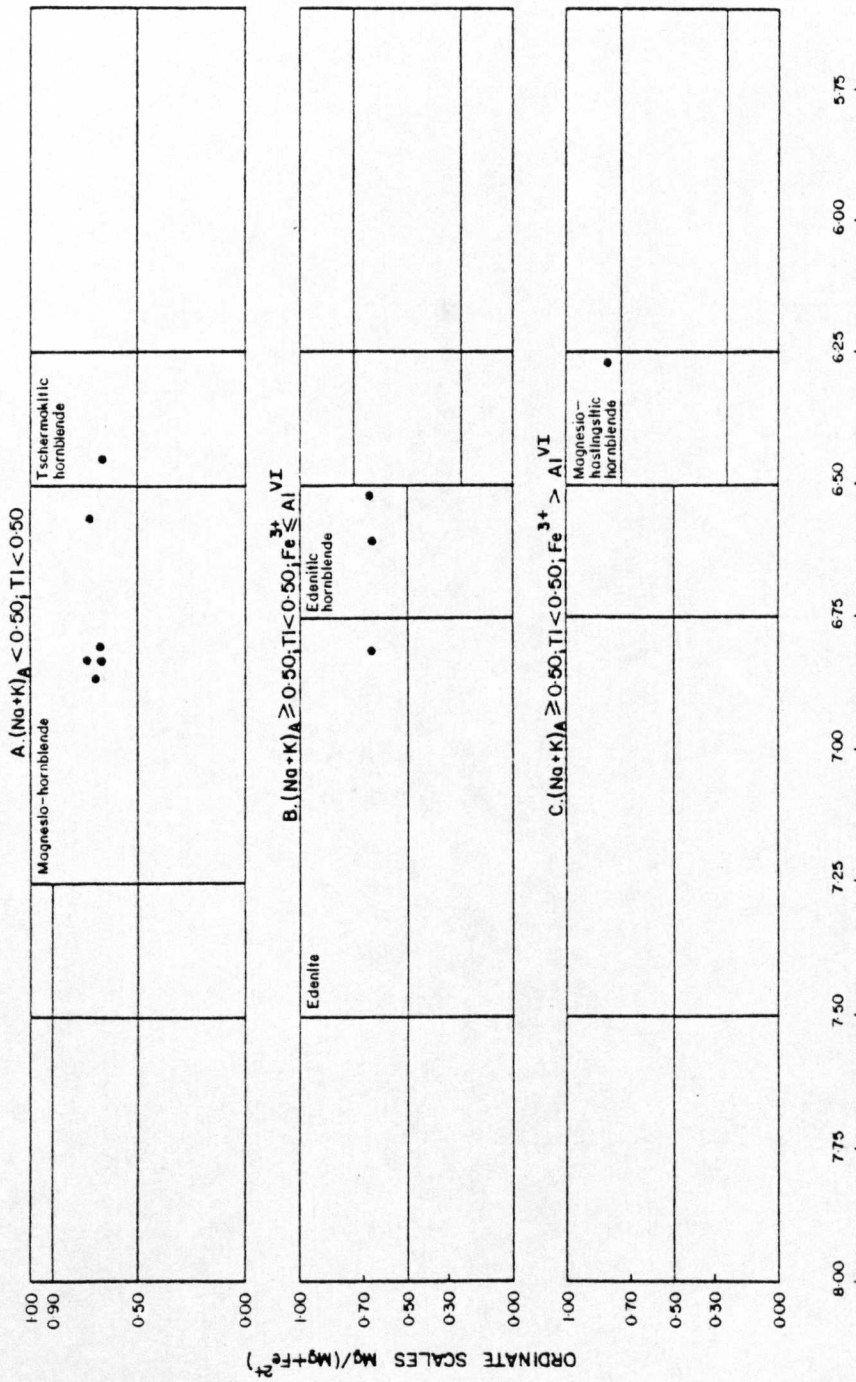


Fig. 43: Pyroxene analyses plotted on part of the pyroxene quadrilateral (inset). Compositionally similar analyses from the Bail Hill Volcanic Group also shown (from McMurtry 1980a, Table 3, using same numbering system).

W. Germany, are broadly comparable in composition with Abington pyroxenes (Deer et al. 1978). Ca-rich augites are also formed at early stages in the crystallisation history of basic magmas of tholeiitic affinity (e.g. the Bushveld Complex - Atkins 1969). Although data from the present area are limited, the evidence suggests that the metadolerites of the Abington area are subalkaline in character. This accords with conclusions of Lambert et al. (1981), based on analyses of immobile elements (Ti, Nb, Zr and Y) from the same localities as used in the present study.

Amphiboles: found in sandstones of the Elvan Formation occur both as fragments of single crystals and as phenocrysts in volcanic rock fragments (Section 3.3.5; Appendix 25; Fig. 44). Mineral species identified by microprobe analysis include tschermakitic hornblende, edenitic hornblende, edenite, magnesio-hornblende and magnesio-hastingsitic hornblende (classified after Leake 1978). Whilst primary magmatic amphiboles from the Bail Hill Volcanic Group are calcic, most are pargasites or ferroan pargasites; edenite and magnesio-hornblende have only been found as alteration products of pyroxene or rimming chlorite clusters (McMurtry 1980a). Compared with Bail Hill material, edenites in Elvan Formation sandstones are poorer in MgO and CaO, and richer in Na₂O and

CALCIC AMPHIBOLES: $(Co + Na)_B \geq 1.34$; $Na_B < 0.67$



ABCISSA SCALE SI

Fig. 44: Classification of amphiboles in Elvan Formation sandstones (after Leake 1978).

and FeO^{tot} ; Abington magnesio-hornblendes are poorer in MgO and richer in Al_2O_3 and FeO^{tot} . Spray & Williams (1980) describe the common presence of magnesio-hornblende and also tschermakitic hornblende from amphibolites in the Ballantrae Igneous complex. These show octahedral Al content consistently between 0.4 and 0.8 per unit cell, contrasting with values less than 0.4 in all but one of the amphiboles examined from the Abington district. No obvious source for the amphiboles is immediately apparent.

Phengites: Detrital white micas in Elvan Formation sandstones are phengites, with tetrahedral Si:Al ratios greater than 4:1 (Appendix 26). No muscovites have been recognised, contrasting with those micas which comprise the $-2\mu\text{m}$ fraction (Section 6.2.2) - this suggests a disequilibrium assemblage.

6.4 GRAPTOLITE REFLECTANCE

6.4.1 Introduction

Measurement of the reflectance of polished, microscopic organic debris or graptolite fragments has been used as a parameter of low-grade metamorphism (e.g. Marshall 1936; Watson 1976). It has long been known that with increasing temperature, the physical, chemical and optical properties of coals change; reflectance values in particular improve.

Watson (op. cit.) demonstrated increasing reflectance of graptolite fragments towards dykes, suggesting that temperature is the primary control on reflectance. Time and pressure are also important, the influence of the latter being unpredictable on the maximum reflectance and the degree of anisotropy (e.g. Chandra 1965; Paproth & Wolf 1973). In view of differences of chemical composition between graptolites and coals, no attempt is made to equate graptolite ('vitrinite') reflectance directly with coal rank scales.

Experimental methods (outlined in Appendix 27) follow those of Watson (1976, Appendix 4). The susceptibility of reflectance to variations in instrumental conditions, plus details of variability within individual graptolite fragments and total samples are well detailed in Watson (op. cit.).

Maximum reflectance ($R_o \text{ max}$) and mean maximum reflectance ($\bar{R}_o \text{ max}$) are given in percentage terms; bireflectance is the difference between minimum and maximum reflectance values. The bireflectance ratio is defined as:-

$$\text{Bireflectance ratio} = \frac{R_o(\text{max}) - R_o(\text{min})}{R_o(\text{max})}$$

where $R_o \text{ max}$ is the maximum reflectance in oil at a fixed wavelength, and $R_o \text{ min}$ is the minimum reflectance in oil at

the same wavelength. This ratio is an estimate of the degree of molecular ordering in the graptolite fragments; complete disorder is indicated by zero values.

6.4.2 Results

When examined in reflected light, graptolites exhibit concentric dark and light bands which probably represent the original layered periderm (Towe & Urbanek 1972). Granular and vesicular textures have not been observed.

Chart recordings of single graptolite fragments rotated through 360° show peaks and troughs alternating every 90° (Fig. 45). Similar measurements on a resin block containing two sections of a single graptolite orientated perpendicular and parallel to bedding respectively are shown in Fig. 46). The section parallel to bedding exhibits greater R_o max values and lower bireflectance. The bireflectance indicatrix for coals is usually uniaxial negative, with axes (three in number, orthogonal, with lengths proportional to reflectance values) in the plane of bedding of equal length, and both longer than the single vertical axis (see Watson op. cit., Fig. 123). All sections cut at different angles through coals should therefore show the true R_o max and the minimum reflectance (and consequently maximum bireflectance) should be recorded from sections perpendicular to bedding. Although

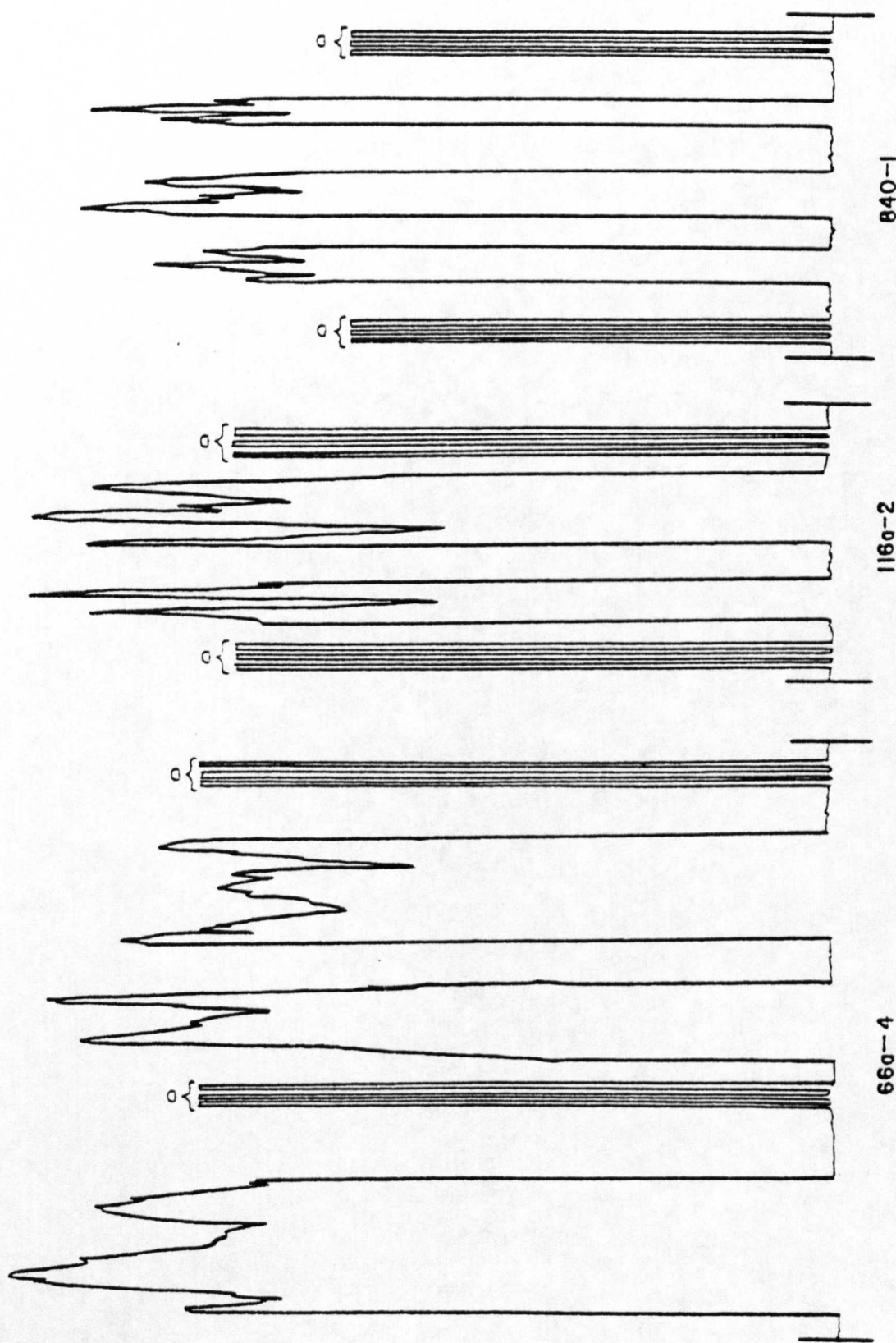


Fig. 45: Representative chart recordings of graptolite reflectance measurements from three localities; each run rotated through 360° . Fragments randomly orientated. D = diamond standard ($R = 5.23$).

(a)

R max = 2.23
R min = 0.77
Bireflectance = 1.46
Bireflectance ratio = 0.65

(b)

R max = 7.25
R min = 6.47
Bireflectance = 0.78
Bireflectance ratio = 0.11

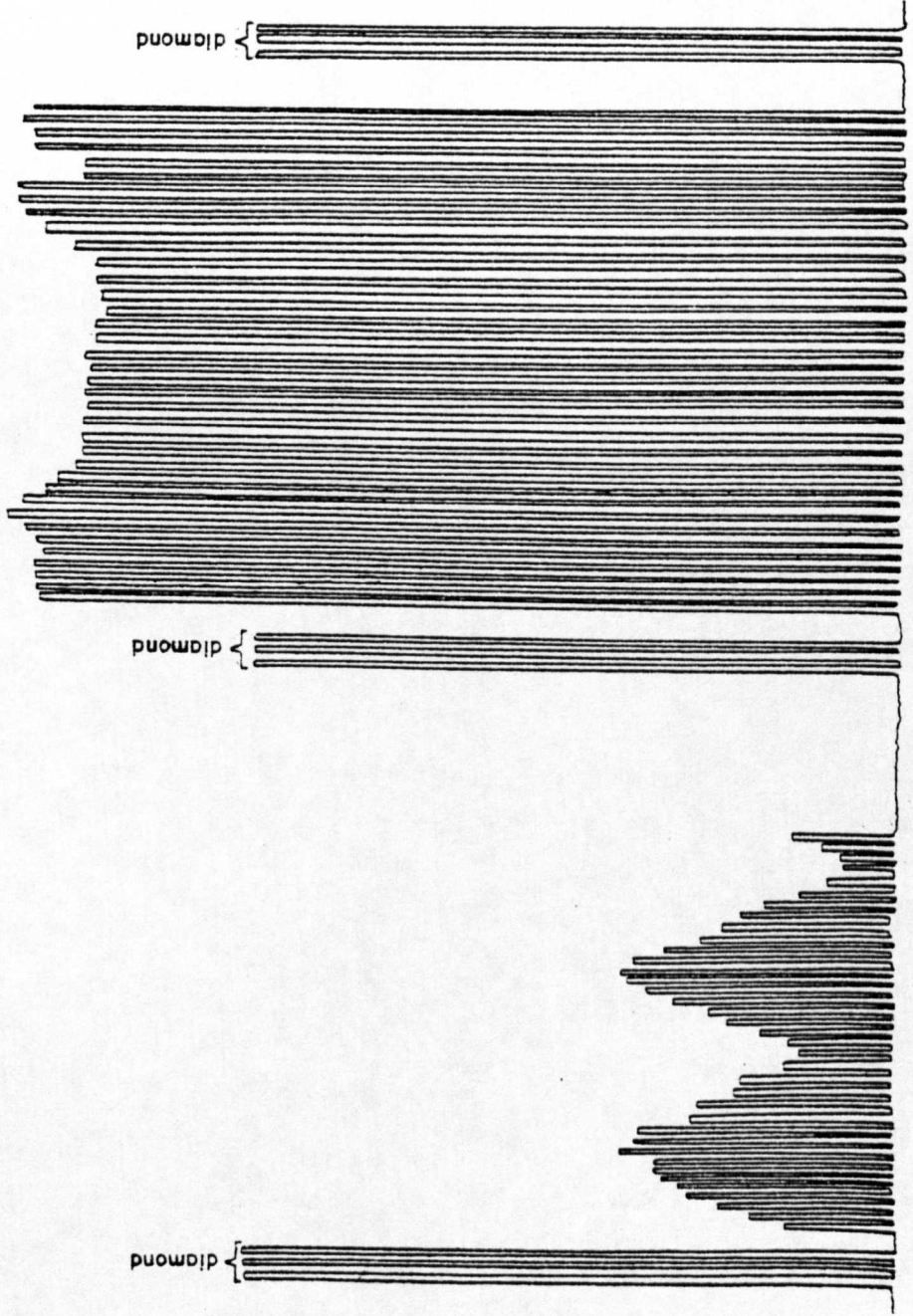


Fig. 46: Chart recording of reflectance measurements on graptolite (840-1) rotated through 360°; (a) section of graptolite perpendicular to bedding, (b) section parallel to bedding.

the graptolite section perpendicular to bedding displays the greatest bireflectance, $R_o \max$ is significantly less than the true $R_o \max$; also, the bedding-parallel section is bireflectant, and thus the isotropic section does not lie within bedding as occurs with coals. Attempts by Watson (op. cit.) to locate the position of the isotropic section were not successful, and he tentatively suggested that graptolites in the Moffat Shales behave as biaxial material. He attributed bireflectance in bedding-parallel sections as resulting from original morphological anisotropy and/or new growth of structural elements in a triaxial stress regime.

Variable statistics of reflectance measurements made over the greater part of a single graptolite are presented in Table 10: standard deviations are less than 0.64. Statistics for the total sample from the same locality are also given.

$\bar{R}_o \max$ values from the Leadhills Imbricate Zone range from 3.91 to 8.22 (Table 11). No trends have been discerned from the areal distribution of reflectance, although it is noted that the highest values ($\bar{R}_o \max = 8.22$) were recorded from a fault slice occupying a relatively high structural position in the imbricate zone (Fig. 31). Graptolites from a single locality from the Fardingmullach Imbricate Zone show

Table 10: Variable statistics for maximum reflectance values for samples 29a, b, d-2 and d-3

	Single Fragment ¹	Total Sample
Mean	7.90	7.64
Modal class	8.40 - 8.50	8.40 - 8.50
Standard deviation	0.64	0.95
Maximum R max	8.70	8.78
Minimum R max	6.21	6.03

¹ Sample 29b-1

Specimen	Grid Reference	R _o max	\bar{R}_o max	n ¹	s
21	90021973	5.75	5.14	3	0.53
29a	90041967	8.78	8.22	5	0.72
29b-1	"	8.70	7.90	21*	0.64
29d-2	"	7.43	6.25	5	0.77
29d-3	"	6.03	-	1	-
66	90661959	4.75	-	1	-
66a-1	"	6.84	5.80	4	0.98
66a-4	"	8.14	6.80	26*	0.52
116a	89331885	7.10	5.75	8	0.96
123	89381875	6.54	6.03	8	0.50
407b	90341828	4.77	4.68	2	0.13
594	91421967	4.97	3.91	13	0.90
834 ²	90231389	7.36	5.75	5	1.29
840-1	92472026	7.48	6.05	55*	0.61
840-3	"	5.32	4.27	9	0.80
840-5	"	5.99	5.81	3*	0.24

¹ Number of determinations on graptolite fragments on single polished slab.

² Locality in Fardingmullach Imbricate Zone.

* Determinations on single graptolite parallel to bedding.

Table 11: Graptolite reflectance values from Moffat Shales in the Leadhills Imbricate Zone

\bar{R}_o max = 5.75, a value which falls well within the range of results from the Leadhills IZ. It is therefore suggested that lithologies in both imbricate zones attained a comparable metamorphic grade.

Bireflectance ratios for a single graptolite (specimen 840-1) of 0.39 and 0.65 indicate good molecular ordering. This variable also is temperature dependent; Watson (op. cit.) records a general increase in this ratio towards a porphyrite dyke, quoting a maximum figure of 0.75 within 2 m of the contact.

6.5 DISCUSSION

6.5.1 Correlation of techniques used for establishing metamorphic grade

Kisch (1974, Fig. 1) regarded the anchizone, prehnite-pumpellyite facies and anthracite coal ranks as broadly equivalent. Assuming the anthracite/meta-anthracite boundary to be placed at 4% volatile matter (VM) content, which is equivalent to a reflectance of 4% (Patteisky & Teichmüller 1960), all graptolite \bar{R}_o max values in the Abington area with one exception correspond to meta-anthracite coal rank. Such discrepancies have also been noted by Saupé et al. (1977); illite crystallinity values from the province of Cuidad Real, Spain, indicate deep diagenetic and upper

anchizone conditions, whilst organic material (graptolites, chitinozoans and graphite) suggest lower anchizone conditions (Ro max 3.7 to 12.4%). It appears probable that either initial compositional differences between phytoclasts and chitinous material control reflectance, or the latter increases in reflectance more readily when subject to an elevation in temperature.

Kisch (1980) reports Ro max 'vitrinite' values from the mid-anchizone of western Sweden ranging from 3.7 to 4.3% (corresponding to high-rank anthracite).

6.5.2 Physiochemical conditions of metamorphism

Experimental work on the prehnite-pumpellyite facies indicates a stability field with pressures and temperatures exceeding 2 kb and 250°C respectively (Nitsch 1971; Liou 1971a). The upper limit of the facies, determined by the reaction prehnite + chlorite → pumpellyite + actinolite + quartz shows a negatively sloped equilibrium curve on a P-T diagram, with the latter assemblage stable above 320°C/2.5 kb to 250°C/9.5 kb (Nitsch 1971). The absence of lawsonite suggests that pressure did not exceed 4 kb (Oliver & Leggett 1980). Studies on clay mineral variation with depth show the persistence of kaolinite in the diagenetic zone down to at least 175°C/1.25 kb (Fig. 37); these are regarded as the minimum values for the low-grade anchizone

boundary. Frey (1970) suggested the broad equivalence of the occurrence of pyrophyllite with the anchizone.

Experimental work on the reaction:



indicated equilibrium temperatures in excess of 300°C at pressures of 1-2 kb (Velde & Kornprobst 1969; Thompson 1970). Thermodynamic considerations suggest this reaction can occur at 220°C and P_{total} of 1-2 kb with a water activity level $a_{\text{H}_2\text{O}} = 0.1-0.2$ (Frey 1977). Homogenisation temperatures of the order of 220°C were obtained from fluid inclusions in fissure minerals from anchizone sediments of the Glarus Alps (Stalder & Touray 1970; Frey op. cit.).

Definition of the anchizone/epizone transition in terms of P-T is complicated by discrepancies in illite crystallinity measurements from the pumpellyite-actinolite and greenschist facies (respective equivalents of very low- and low-grade divisions of Winkler 1974). The epizone has been equated with the greenschist facies (e.g. Kisch 1974). However, Coombs et al. (1976a) report the occurrence of pumpellyite + actinolite-bearing assemblages from epizonal sediments of the Taveyanne Formation (Valais, Switzerland) (Frey 1974; Kübler et al. 1974). It therefore appears that the higher temperature

limits of the anchizone and prehnite-pumpellyite facies are broadly equivalent. Little is known about the effects of pressure on illite crystallinity.

Although not separated from the host rock and mostly coated by a thin film of ?sulphurous material, conodonts from Raven Gill Formation mudstones show a colour alteration index (CAI) less than 5, suggesting temperatures below 300°C (Epstein et al. 1977).

As reported from metabasalts and dolerites in the Leadhills Imbricate Zone (Oliver & Leggett 1980), it is noted that the presence of carbonate in veins and the ground-mass of Glencaple and Elvan Formation sandstones suppresses the development of prehnite-quartz veins. This is indicative of a CO₂ content in the fluid phase above a critical value; conversely, parageneses including Ca-Al minerals proves that the fluid consisted predominantly of H₂O (Winkler 1974; pp. 191-2). Spinel in metabasalts and dolerites implies P_{CO₂} less than 50 bars (Schuiling & Vink 1967; Oliver & Leggett op. cit.).

In conclusion, it is considered that metamorphism in the Abington area occurred at temperatures and pressures between 250-320°C and 2-3 kb respectively.

6.5.3 Comparison with other areas

Until recently, the Southern Uplands have received only

scant attention in terms of regional metamorphic studies. Rust (1965) described quartz + illite + chlorite + kaolinite assemblages from argillites in the Silurian rocks around Whithorn. Replacement of feldspars, basic igneous fragments, argillaceous fragments and matrix by carbonate was attributed to diagenesis, whereas chlorites showing preferred orientation parallel to axial planar cleavage in the matrix were believed to be metamorphic. Further east near Gatehouse, Weir (1974b) concluded that quartz + feldspar + illite + chlorite + carbonate assemblages from sediments represented lowest-grade greenschist facies. It is now known that such assemblages remain stable from the zeolite through to greenschist facies and are nondiagnostic.

Working in the Moffat Shale inliers of the Central Belt, Watson (1976) deduced lower greenschist facies metamorphism, again on nondiagnostic quartz + albite + sericite + chlorite assemblages. Reflectance work on graptolites from Luce Bay showed values ranging in general from 1.31 to 3.26% with only one sample in excess of 4.0 (mean \bar{R}_o max = 2.95, $s = 1.05$). A higher rank was suggested for the Moffat inliers, as the population ranges from 0.75 to 6.67, with mean \bar{R}_o max of 3.67% ($s = 1.22$). A mean \bar{R}_o max of 5.88% ($s = 1.21$) from the Abington district indicates an appreciable increase in metamorphic grade north-westwards from Moffat. In view of

the development of index minerals in the study area, the grade near Moffat is probably less than prehnite-pumpellyite facies, and may be low anchizone or even zeolite grade.

More abundant fossil localities in the Central Belt have allowed Watson (op. cit.) to demonstrate in Luce Bay that metamorphic rank decreases stratigraphically upwards above major strike faults. The Moffat inliers, in contrast, increase in rank north-westwards up through the succession, and it was concluded that metamorphism took place after folding and strike faulting.

Bentonites in Lecale, Co. Down, contain 10\AA mica (suggested to be a randomly interstratified mineral, possibly montmorillonite), chlorite, quartz and feldspar, whilst shales show quartz, feldspar, chlorite and mica (subsidiary) which are more typical Southern Uplands assemblages. If the geochemically distinctive bentonites can be used to infer metamorphic grade, the more weakly metamorphosed part of the anchizone is indicated (Cameron 1977; Cameron & Anderson 1980).

Basic lithologies of the Bail Hill Volcanic Group contain feldspars (albite-bytownite in composition) with no secondary albitisation (McMurtry 1980a). The presence of thomsonite, prehnite, pumpellyite, albite and carbonate in amygdales associated with analcite-carbonate veins in lavas, suggests zeolite facies metamorphism. This is confirmed by the presence of kaolinite from siltstones of the Stoodfold Member (McMurtry op. cit.; Hepworth et al. 1981).

Oliver & Leggett (1980) established prehnite-pumpellyite facies metamorphism for spilites and metadolerites in the Leadhills Imbricate Zone following recognition of comparable assemblages in Co. Cavan (Oliver 1978). The diagnostic mineral assemblage was also reported from basic-clast sandstones of the Central Belt and the Portpatrick Group. Pumpellyite has not been found in veins in the Elvan and Glencaple Formations, and although the mineral assemblages present do not define the metamorphic grade, a grade less than greenschist facies is indicated. The absence of zeolites coupled with illite crystallinity studies, however, suggest prehnite-pumpellyite facies conditions.

CHAPTER 7: DISCUSSION

7.1 PLATE TECTONIC FRAMEWORK

Since Wilson (1966) suggested the existence of a Lower Palaeozoic ocean separating the north-western and south-eastern forelands of the Caledonian-Appalachian orogen, plate tectonic models and reconstructions have proliferated up to the point where a total of six former subduction zones has been postulated (review given in Holland et al. 1979). Of these, the model presently most favoured calls for a north-westerly dipping subduction zone which migrated from the line of the present-day Southern Uplands Fault to the site of the Solway Firth during ?Caradoc to Wenlock times. By analogy with modern fore-arc regions, an accretionary complex NW of the subduction zone was formed by the scraping off of oceanic sediment from the downgoing plate (Mitchell 1974; McKerrow et al. 1977). Detachment of sediment from the underlying basement apparently takes place along regularly spaced fault planes, initiated as low-angle faults and progressively rotated towards verticality as subduction continues (e.g. Seely et al. 1974; Karig & Sharman 1975). This configuration is compatible with the general structure of the Southern Uplands, explaining the paradox of dominantly NW-younging sediments which display youngest graptolite zones on the

south-eastern flanks of the complex, by persistent down-throw on faults to the SE (Mitchell 1974; Mitchell & McKerrow 1975; Anderson & Cameron 1979).

7.2 PETROGRAPHIC COMPARISONS WITH MODERN AND ANCIENT FORE-ARC REGIONS

Recent advances in knowledge of the relationships between plate tectonic setting and the compositions of sands and sandstones provides a framework with which the Abington area can be compared. The volcanigenic, quartz-poor sandstones of the Elvan and Glencaple Formations are considered first.

These sediments were previously recognised as andesitic in derivation (e.g. Kelling 1961, 1962), and were considered to be related to an Ordovician volcanic chain produced on the Laurentian continent as an accompaniment to north-westerly subduction (Mitchell & McKerrow 1975). McMurtry (1980a, 1980b) has proposed an alternative explanation, namely, derivation from an intrabasinal, within-plate, volcanic source on the basis that analyses of clinopyroxenes and amphiboles in sandstones from the Longford-Down inlier in Ireland (Sanders & Morris 1978) are similar in composition and association to Bail Hill material. Igneous and detrital clinopyroxene compositions also are closely related in the Abington area, although no

obvious source has been recognised for amphiboles present in sandstones in the Elvan/Glencaple Formations. However, derivation from an intraplate source such as Bail Hill is considered unlikely due to the large volumetric contrast between the former seamount and the laterally extensive basic-clast formations of the Northern Belt. Pyroxenous sandstones of local occurrence (e.g. Blackcraig Formation, Floyd 1975) may owe their origin to small, intraplate alkalic seamounts as originally suggested (McMurtry 1980a).

Both the Elvan and Glencaple Formations show characteristics of dissected magmatic arc provenance, although it is noted that the compositional fields do not equate with volcanic fore-arc sources described from modern and ancient environments (Valloni & Maynard 1981; Dickinson & Suczec 1979; Fig. 47). The relatively large quartzo-feldspathic input and associated metamorphic rock fragments imply that Highland-type material was available, either by reworking of earlier accreted slices or by direct transport through a canyon system incised across the accretionary complex. The Elvan Formation is comparable in composition with recent sediments from back-arc and leading edge (i.e. strike-slip) terrains (Valloni & Maynard op. cit.). An alternative source possibly could be an area of nearly continuous volcanic cover in which intermittent unroofing of granodiorite plutons provided limited quartzo-feldspathic debris - this configuration

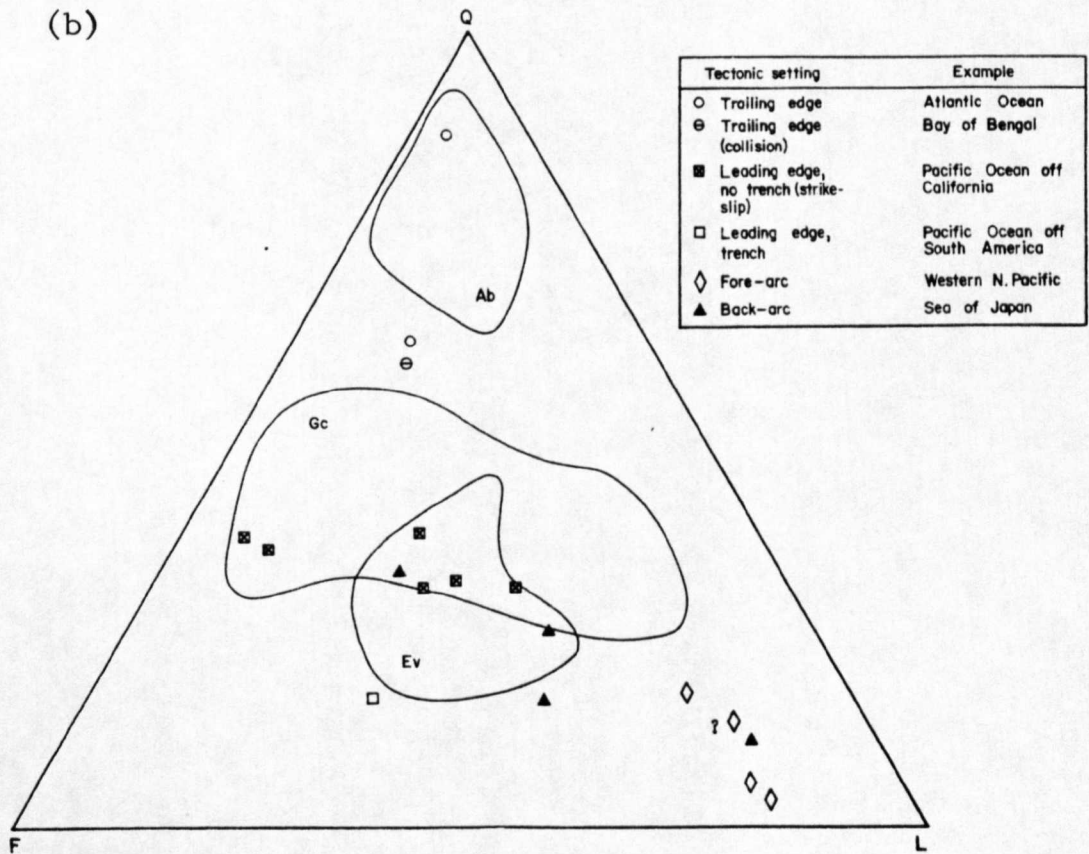
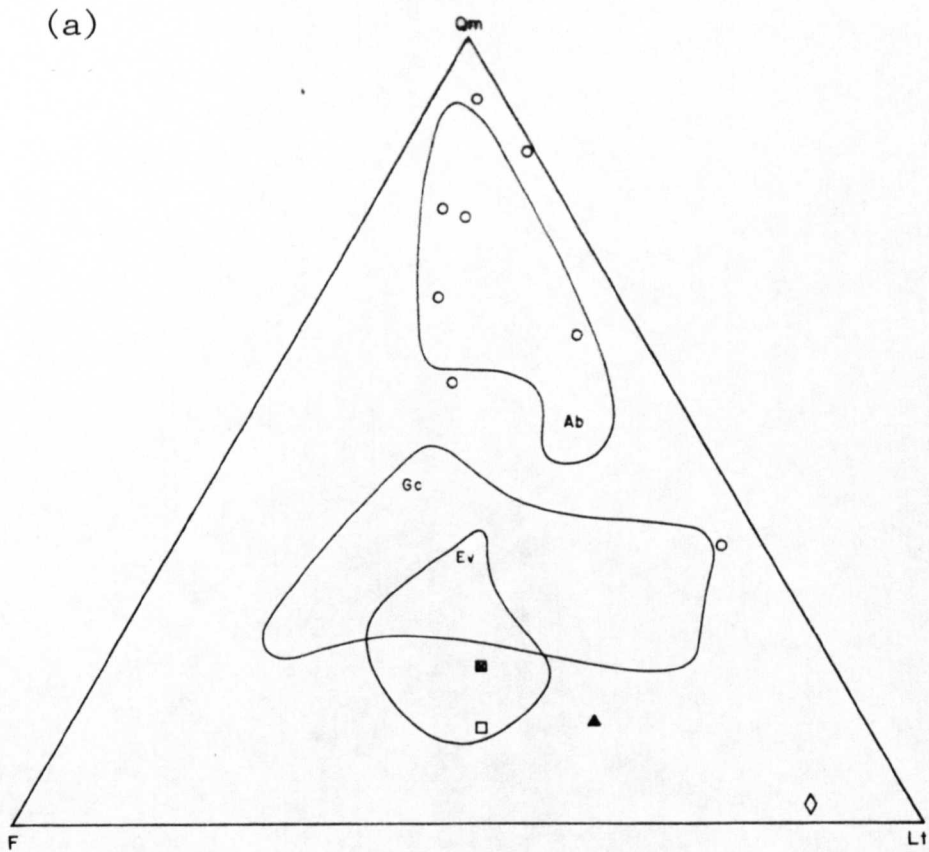


Fig. 47: Comparison of point count results with compositional means of modern deep-sea sands from known tectonic environments (data after Valloni & Maynard 1981). (a) Qm-F-Lt plot (b) Q-F-L plot. Formations: Ab Abington/Crawfordjohn; Gc Glencaple; Ev Elvan

is analogous to the modern Aleutian ridge (Scholl et al. 1975). Sanders & Morris (1978) suggested the volcanoclastic Red Island Formation (?Llandeilo) in the Longford-Down inlier to consist of reworked andesitic tuffs, individual crystals retaining crystal faces being interpreted as volcanic ejecta, and igneous clasts as lapilli.

The presence of glaucophane suggests derivation from a subduction-related blueschist terrain, probably Girvan (Floyd 1975); detrital prehnite was possibly eroded from the base of accreted thrust slices. Cherts and other fine-grained sediment in the Elvan and Glencaple Formations may have been acquired and incorporated into turbidity currents as arc-derived detritus was transported across the accretionary complex (see below). The change from pyroxene-rich to pyroxene-poor sandstones through the Elvanfoot Block probably relates to the primary igneous evolution of the magmatic arc.

Sandstones of the Crawfordjohn/Abington Formations, compared to modern sands, plot closer to the Q pole of the QFL diagram than even trailing-edge (a) Atlantic type ($Q_{66}F_{23}L_{12}$) and (b) collision (Indian Ocean, $Q_{58}F_{29}L_{14}$) settings (Valloni & Maynard 1981; Fig. 47). The formations are most closely related to recycled collision orogen provenances of ancient sandstones (Dickinson & Suczec 1979; Fig. 48). This is supported by the presence of sometimes polydeformed metamorphic clasts of diverse composition, and

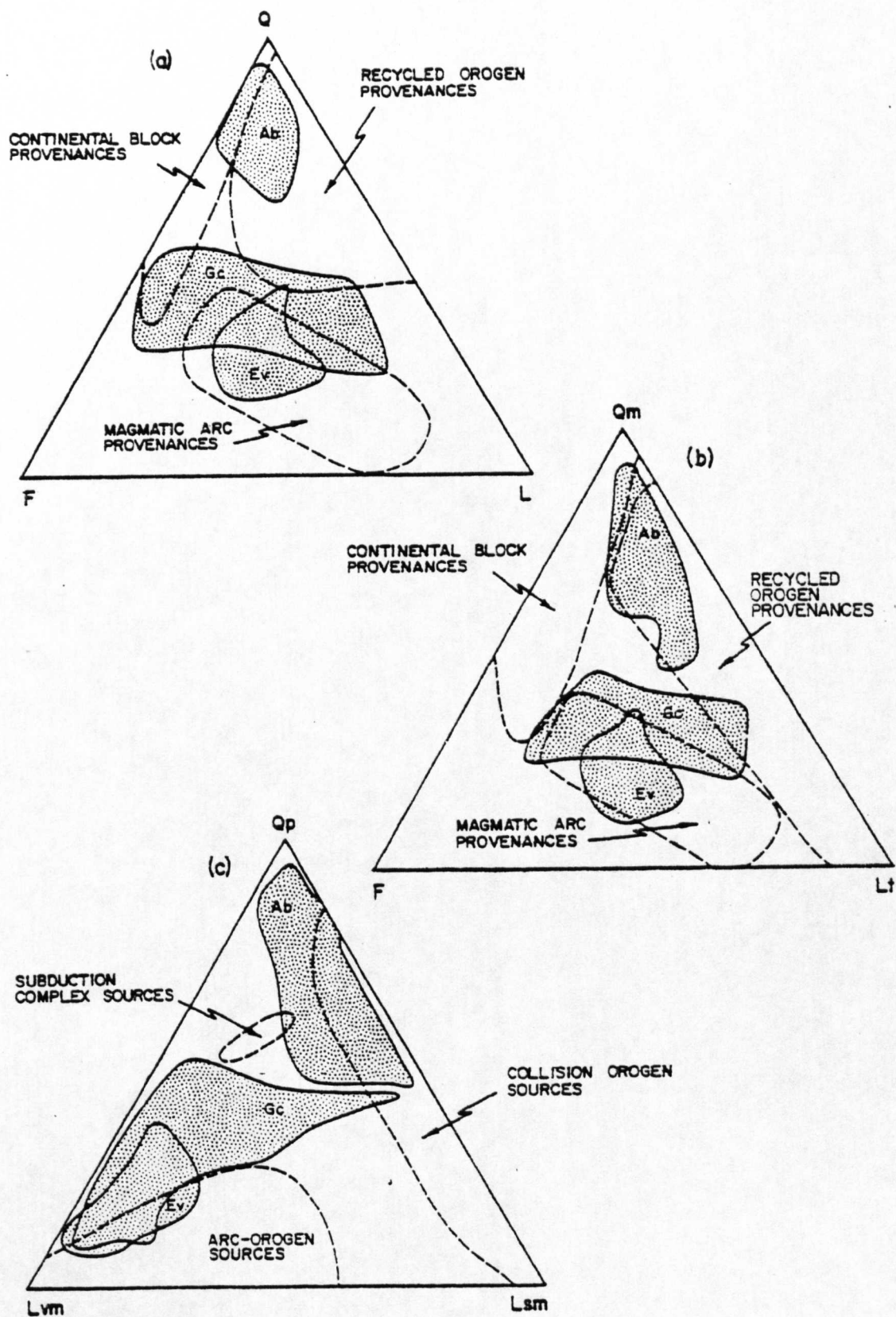


Fig. 48: Compositional plots for mean framework modes for sandstones from different tectonic environments (after Dickinson & Suczek 1979). Formations: Ab Abington/Crawfordjohn; Gc Glencaple; Ev Elvan.

minerals of Highland aspect. Acid igneous fragments indicate that the plutonic roots of the orogen were also exposed in Caradoc times. Using evidence from boulders in Lower Old Red Sandstone conglomerates, van Breemen & Bluck (1981) argued for a suite of subduction-related, Ordovician (~ 460 Ma) granites, inferentially located south of the Great Glen Fault. Such a source may account for the acidic fragments found in the Crawfordjohn/Abington Formations.

Cherts and black mudstones were derived either from sediment-starved, lower-slope basins/channel margins, or from previously accreted rocks to the NW of the present area - clasts showing evidence of soft sediment deformation indicate the former provided a significant contribution. Basic igneous clasts may also have been recycled from accreted thrust sheets.

A problem fundamental to the understanding of the tectonic setting of the Northern Belt concerns the juxtaposition of quartz-rich and basic-clast sandstones, a problem amplified by the apparent similarity in ages between the Abington and Elvan Formations. Possible explanations and tectonic settings to account for the petrographic provinces include (Fig. 49):

- (a) a marginal-basin environment with shedding of arc and continental material into the same basin,
- (b) a stable Atlantic margin with volcanoclastic

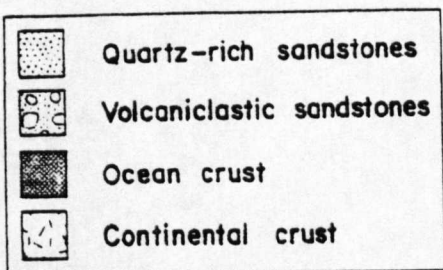
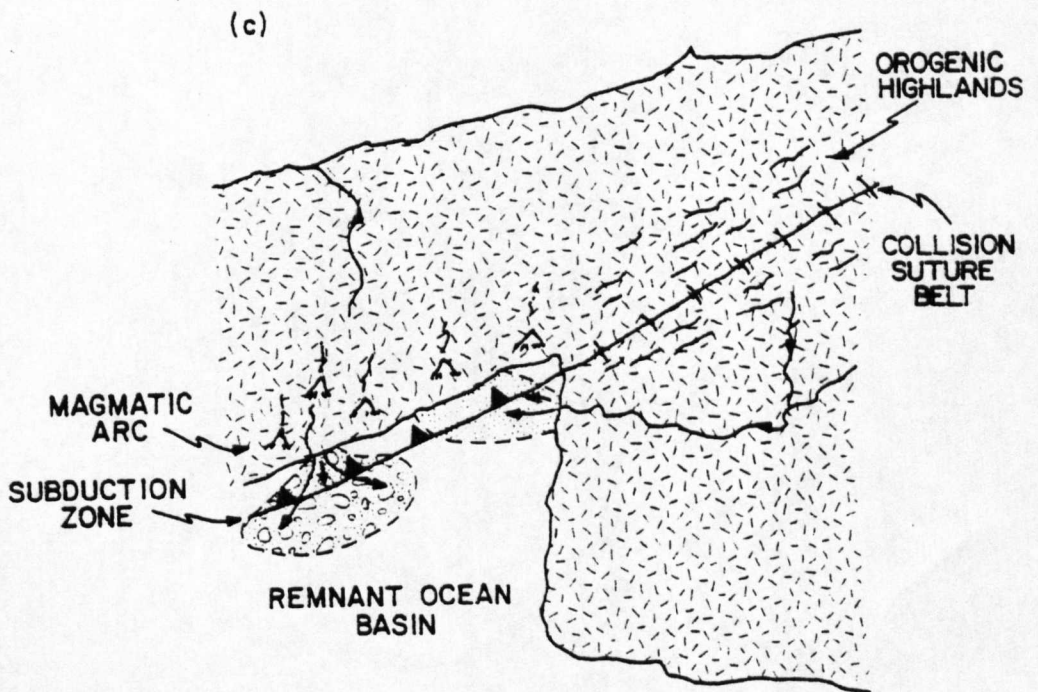
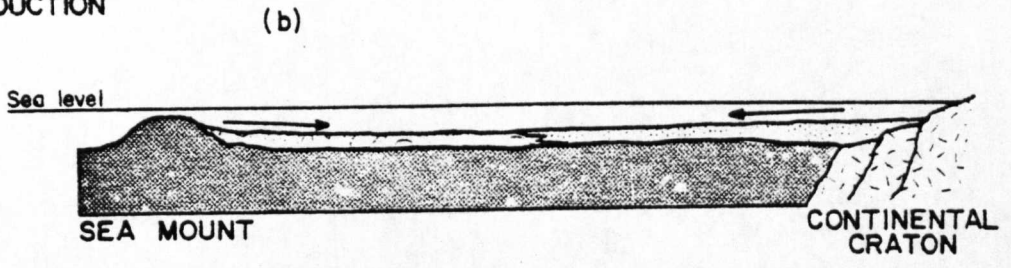
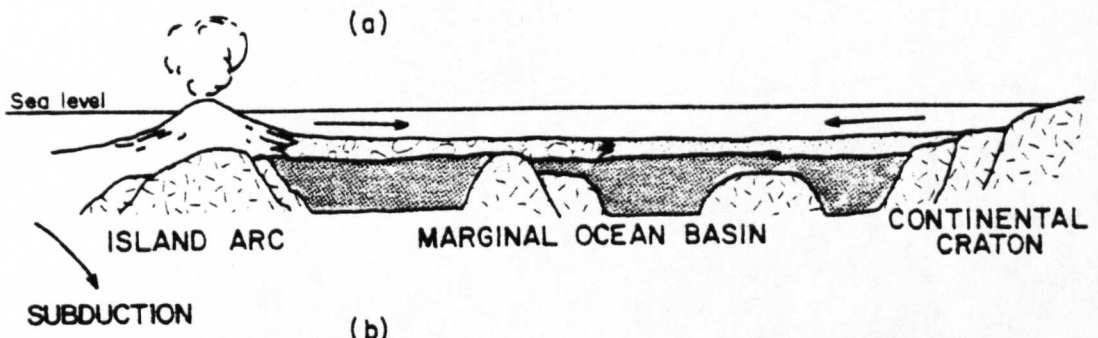


Fig. 49: Possible ocean/continent configurations to account for petrographic provinces (a) marginal ocean basin - after Winn & Dott 1978 (b) passive margin with sea-mount (c) remnant ocean basin - modified from Dickinson & Suczec 1979.

debris from a system of seamounts or intraplate volcanic islands (e.g. Principe, off Nigeria - Valloni & Maynard 1981),

- (c) a remnant ocean basin with collision suture belt and subduction zone in lateral continuity.

The author is not aware of any literature which indicates the presence of two distinct petrographic provinces within trenches of modern fore-arc systems, indeed, they tend to be uniformly volcanigenic with little input of quartz (e.g. Stewart 1978). The seamount hypothesis has already been discounted. To fit with observations in the Northern Belt, subsequent tectonic thrusting within the marginal basin normal to the trench axis is required for hypothesis (a), and strike-slip displacement of the order of ?hundreds of km for (c).

Unfortunately, petrographic studies of active accretionary complexes do not clarify matters. Mélange sandstones (representing accreted material) and overlying upper-slope basin sandstones are petrographically comparable to those from the Abington/Crawfordjohn Formations, plotting broadly within the recycled orogen field on a QFL diagram and showing low proportions of volcanigenic debris despite the close proximity to the Sumatran volcanic arc (Moore 1979). Exposure of a wide variety of nonvolcanic rocks forming the frontal arc off Sumatra and location of the major drainage-

divide between the volcanic chain and accretionary complex were invoked to explain the paradox. Similarly, in the Northern Belt, ponding of basic-clast debris behind a mountain chain or topographically high trench-slope break may have allowed quartzose sediment - derived axially from continental/orogenic highland sources (Fig. 49c) - to accumulate in the trench. The imposition or removal of such tectonic barriers possibly coincided with a renewed phase of underthrusting and accretion of a further structural block. This model, whilst explaining the development of quartz-rich sediments exclusive of volcanigenic debris, would not explain how axially derived quartzose sediments could be excluded from the volcanigenic suite once the barrier was removed.

Petrographic contrasts between *mélange* and slope sediments assist in recognition of the two tectonic environments on Nias Island (Moore 1979), although the petrographic clusters are not sufficiently distinct to fall in separate provenance fields defined by Dickinson and Suczec (1979). In contrast, structural and sedimentological observations would suggest the petrographically distinct Abington and Glencaple Formations occupy tectonic locations within the accretionary complex which are directly comparable to one another.

Dickinson (1971) described paired petrographic provinces from New Zealand, with volcanigenic sandstones of shelf aspect situated inboard of relatively quartz-rich, trench

sandstones - the latter, however, do not plot within either the continental block or recycled orogen fields as does the Abington Formation. Bypassing of the shelf through canyons permitted 'quartz-rich' sediments to be deposited in the trench; volcanoclastic material may have arisen by direct air-fall onto the shelf, with subsequent reworking by traction currents (Dickinson, op. cit.). More recent reconstructions derive the quartzo-feldspathic Alpine Assemblage from the oceanward side of the orogen (Coombs et al. 1976b). The Te Anau Assemblage - interpreted as an accretionary complex - contains volcanogenic sandstones with little quartz (Carter et al. 1978).

Leggett (1980) suggested that trench and ocean floor/abyssal plain turbidite accumulations in the Southern Uplands may be distinguished by their quartz-poor/volcanoclastic-rich and quartz-rich characteristics respectively. The modern examples demonstrating this unfortunately were not well chosen (Bartolini et al. 1975, in the Mediterranean; Stewart 1976, in the Aleutians). Whilst the Hellenic and Aleutian Trenches, rich in volcanoclastics, are situated landward of more quartz-rich, abyssal plain turbidites, this is simply due to both trenches being situated out of range of terrigenous (i.e. cratonic) sediment input. Bartolini et al. (op. cit., p. 223) write:

"...we can state that no intermixing of even

the finest grained sediment exists on either side of the Mediterranean Ridge between the Hellenic Trench...and the Western Nile Cone."

In view of the inferred absence of a continental source situated south-eastwards from the Southern Uplands in Caradoc times (see below), this distinction is considered untenable for the Elvan/Abington Formations.

7.3 TRENCH SEDIMENTATION

The clastic sediments have been interpreted as trench deposits principally because of the dominance of linear sediment dispersal patterns (NE-SW) and the general lack of a source to the SE (Dewey 1971; Piper 1972; Leggett 1980). Recent work, however, shows accretionary complexes to consist both of trench and slope-basin sediments (Moore et al. 1980) and Piper's (1972) conclusion must be reassessed with a view to distinguishing between deposits of these two environments.

Linear sediment dispersal patterns may not be a diagnostic feature of trench sedimentation. Moore et al. (1980, Fig. 4) show laterally persistent trench-slope basins, down which axial currents could flow given suitable gradients. Trench and slope-basin sediments have been distinguished principally by contrasts in lithology, deformational style and the presence of coarsening- and thickening-upward cycles

in the latter (G.F. Moore & Karig 1976; J.C. Moore & Karig 1976; G.F. Moore & Karig 1980). J.C. Moore & Karig (1976) also recognise coarsening-upward sequences as diagnostic of trench sedimentation. In the Northern Belt lithological contrasts occur, but are explained by sedimentation in pelagic and clastic environments. Evidence for large scale coarsening-upward cycles does exist (e.g. Kiln/Spothfore Formations, Crawick Block) but fining- and thinning-upward sequences also occur (e.g. Elvan/Glencaple Formations, Elvanfoot Block).

The slope-basin model implies that slope-basin sediments show progressively shallower dips and decrease in structural complexity towards higher stratigraphical and structural levels (G.F. Moore & Karig 1976, Fig. 5). In contrast, the Northern Belt shows no such variations, bedding orientation being approximately vertical and parallel in sections from low to high stratigraphical levels. Moore (1979) and Speed (in Underwood & Karig 1980) describe an unconformity between slope-basin strata (turbidites) and the underlying *mélange* (dominantly pelagic deposits) of the accretionary complex. The equivalent contact in the Northern Belt would be between the base of a sandstone formation and the top of the Moffat Shales of the underlying imbricate zone, but this is seen to be conformable.

Underwood & Karig (1980) proposed that these deposits can be separated on the basis of a sharp textural contrast between coarse-grained trench deposits and the overlying fine-grained, lower trench-slope sediments. No evidence is available to support the occurrence of the latter in the Abington district, and it would therefore seem that the clastic sediments represent trench accumulations as originally suggested by Piper (1972).

A review of literature on modern and ancient trench environments shows that an adequate framework does not exist at present with which the sedimentary facies and facies associations of the Abington district can be compared. However, comparison with rates of deposition calculated from modern trenches permits a crude estimate to be made of the age range of the sandstone formations. Assuming a moderate sedimentation rate for trench sediments of 1000 m/Ma (Piper et al. 1973) and a postdepositional compaction of 50% (cf. Moore et al. 1980), the clastic sediments in the Elvanfoot Block might have been deposited in less than 6.5 Ma. This figure is compatible with the time range of 6.5 Ma calculated by Carter et al. (1980) for the D. clingani zone. It is possible that the other, thinner turbidite formations were likewise deposited within the space of a single graptolite zone, although Leggett et al. (1979) described a Silurian turbidite sequence spanning six zones (M. convolutus to

M. griestoniensis). This situation may be explained by comparing the duration of Caradoc and Llandovery graptolite zones; N. gracilis spans 9 Ma, whilst the G. persculptus to M. turriculatus zones (eight in number) which form the bulk of the Llandovery only extend for the slightly longer duration of 9.5 Ma (Carter et al. 1980).

In the Northern Belt, axial transport and deposition was principally by turbidity currents (e.g. McMurtry 1980a). No evidence has yet been found to suggest that the deposition of the bulk of the sandstones was related directly to an axial channel, such as occurs in the Chile Trench (Scholl et al. 1970; Schweller & Kulm 1978) and the eastern Aleutian Trench (Piper et al. 1973; von Heune 1974). Indeed, three fans from the NW were described by Holroyd (1978).

Apart from the locally developed thick-bedded facies of the Abington Formation (which probably is related to a broadly channelised distributary system) the majority of the sediments were deposited by sheet flows. Retention of distinctive sedimentological characteristics over 20 km downbasin and parallel bounding surfaces to most sandstone units suggest individual flows of large volume occupying the whole width of the trench, and extending for considerable distances over the flat, featureless trench floor. Similar flows from narrow elongate basins have been described by Hesse (1974), Ricci-Lucchi (1975b) and Elmore et al. (1979).

However, the sequences of massive coarse sandstones in the Elvan Formation indicate that other mechanisms, such as high concentration sediment gravity flow, can produce thick sedimentary bodies. The clastic sediments show a spectrum of sediment transport mechanisms including debris flow, high concentration sediment gravity flow and high and low density turbidity current flow (Table 2).

The transition from lateral to axial flow in the trench is thought to have resulted from deflection of the turbidity currents by the outer slope (Piper 1972; Schweller & Kulm 1978). It is suggested that this transition was accomplished in the vicinity of the depositional site of the massive Elvan Formation. This is the coarsest-grained and thickest-bedded of the laterally persistent lithologies and is considered hydrodynamically to be transitional between laterally derived debris flows of the Haggis Rock Member and axially derived, high concentration, turbulent suspensions of the Abington Formation. The consistency of sedimentological characteristics which allows all the units to be mapped in the field as formations, suggests a single stable source for each of them, operational over a considerable length of time.

Nowhere in the area can a lateral transition be seen from proximal to distal facies as described from deep-sea fans and basins (Bennetts & Pilkey 1976; Stanley et al. 1978; Elmore et al. 1979) and turbidite models (Mutti & Ricci-Lucchi 1975),

but at separated localities different lithologies can be recognised which individually are comparable with components of the fan model. The fact that these can be identified and form thick sequences suggests that sediment supply originated from widely separated points, as in the Chile Trench, and not from a large number of closely spaced canyons which would produce a greater variety of lithologies. In the following section, the depositional environment of stratigraphical units is discussed with units arranged in terms of the inferred relative distance from source (Fig. 50).

Haggis Rock/Mill Burn Member: Disorganised conglomerates have been interpreted to have formed in slope channels and on inner fans (Walker & Mutti 1973). Conglomeratic units in the Northern Belt indicate transport towards the SE, and it is suggested that Haggis Rock is related to a canyon system incised across the lower slope of the accretionary complex (Holroyd 1978; McMurtry 1980a). Clasts showing evidence of soft-sediment deformation provide evidence for the nature of contemporaneous sedimentation on the lower-slope basins and canyon systems, which evidently was dominated by pelagic and ?hemipelagic lithologies in the present area (see section on preturbidite formations below).

Underlying (?enclosing) laminites of the Mill Burn Member are interpreted as overbank deposits associated with

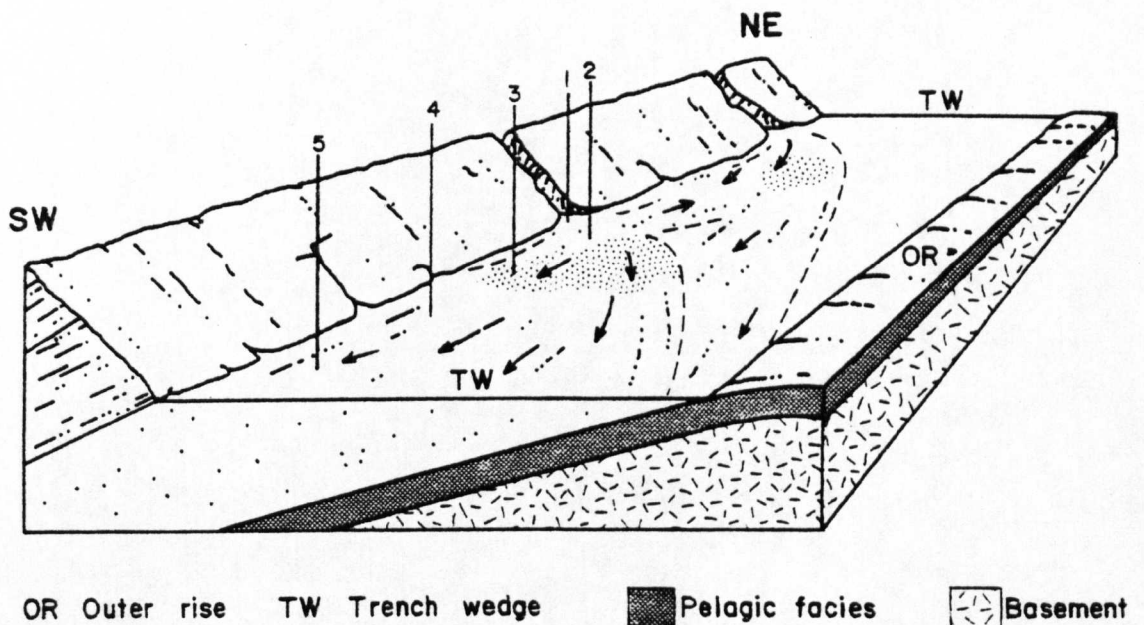


Fig. 50: Schematic diagram of the distribution of sedimentary facies within the Abington area (cf. Hepworth *et al.* 1981). No stratigraphical correlations are implicit unless stated in the text. 1 = Haggis Rock Member/Mill Burn Member; 2 = Elvan Formation; 3 = Abington Formation (very thick-bedded facies); 4 = Abington Formation (thick-bedded facies); 5 = Glencaple Formation.

the conglomerates and pebbly sandstones.

Location at the break of slope between the inner trench wall and the flat trench bottom is speculated for this facies association, forming a sedimentary body of positive relief (i.e. inner fan) above the trench floor.

Elvan Formation: Massive, thick- to very thick-bedded and ungraded sandstones characterise the Elvan Formation.

Environments from which this facies has been reported include channelised submarine fans seaward of deltas (Walker 1966), delta-front troughs (De Vries Klein et al. 1972), thinning-upward cycles in channel fills (Ricci-Lucchi 1975a), braided, canyon-mouth fans on an abyssal plain (Cleary et al. 1977) and canyon-fill sequences (Stanley et al. 1978). There is thus a general consensus that these deposits formed in proximal fan environments. The lack of associated canyon-wall deposits (slump facies, etc.), channelling and material coarser than granule size precludes deposition of the Elvan Formation in an inner fan (definition of Ricci-Lucchi 1975a), as does the widespread and thick development of the lithology. Deposition in the trench near a canyon mouth is considered likely (Fig. 50), but whether this facies represents a broadly channelised distributary system or nonchannelised sheet-flow accumulation is not known due to lack of knowledge of the geometry of the sand bodies.

Abington Formation (very thick-bedded facies): Thinning and fining-upward sequences have been recorded from this facies, a feature typical of mid-fan distributary channels (Walker & Mutti 1973). Thick-bedded, generally ungraded, very coarse sandstones are common, a lithology which is reminiscent of the Elvan facies. However, most beds are thinner than the Elvan lithologies and contrast by showing internal sedimentary structures, including distribution and inverse grading. It is suggested that this facies represents deposits from more 'mature' flows than the Elvan facies. Hence these deposits are inferred to occur downcurrent from massive sandstones (Fig. 50).

Abington/Crawfordjohn Formations (thick-bedded facies): T_{ae} sequences are generally considered typical of a 'proximal' environment (Walker 1976) or immature 'classical' turbidites (Ricci-Lucchi 1975a). Such sequences have been described as passing downcurrent and laterally into more complete Bouma sequences (Elmore et al. 1979). Haner (1971) describes T_{ae} deposits from braided channels 300-400 cm wide and 1.5-4.5 m deep distally, interpreted by Walker & Mutti (1973) as mid-fan (channelled) deposits. They have also been found in association with thinning-upward sequences (Gonzalez & Middleton 1976) from the mid-fan. The lack of conspicuous channels in this facies suggests deposition as sheet flows,

analogous to a mid-fan, nonchannelised area (Fig. 50).

Glencaple Formation: Complete vertical sequences of Bouma divisions have been described from mid-fan channels (Nelson & Kulm 1973), outer fan nonchannelised depositional lobes (Mutti & Ricci-Lucchi 1975) and sparsely channelled, mid-fan depositional lobes (Walker & Mutti 1973). Elmore et al. (1979) describe 'complete' sequences from the Hatteras Abyssal Plain, W. Atlantic Ocean. Medium-bedded turbidites showing relatively complete Bouma sequences have been documented to pass upcurrent both into ungraded, coarse-grained, thick-bedded channelised deposits (i.e. Walker 1966; Nelson & Kulm 1973; Walker & Mutti 1973; Stanley et al. 1978) and T_{ae} sequences (Elmore et al. 1979).

This facies of the Glencaple Formation is suggested to be the most distal of all the sandstone lithologies observed, and is thought to have formed from low concentration flows in the trench environment (Fig. 50). The presence of thick-bedded Elvan lithologies is interpreted as indicating sporadic incursions of high concentration flows, a result of local progradations of the channelised mid-fan in a down-fan direction (Walker & Mutti 1973). The transition from the Elvan Formation to the Glencaple Formation is attributed either to a lateral shift in the axis of deposition of the

coarse-grained, thick-bedded facies, or to a general decrease in the volume of turbidite flows into the trench. The former interpretation assigns the Glencaple Formation to 'overbank' deposition with respect to the Elvan Formation, the latter regards the Glencaple as a downcurrent equivalent.

Boulder siltstones in this formation imply the presence of slopes. This material may represent accumulations of turbiditic sands and silts, redistributed by slumping from either the inner-trench wall or areas of positive relief within the trench, the latter being produced by lateral thickness variations of the previously deposited sandstone (D. Ellis, pers. comm. 1981). The disturbed bedding facies may have a similar origin.

Pre-turbidite formations: Black mudstones and cherts have been regarded as oceanic in origin for many years (e.g. Hinde 1890), deposited outwith the realms of terrigenous sedimentation. This view is followed herein. More recently, these sediments have been ascribed to the pelagic plate facies (Schweller & Kulm 1978) in accordance with their stratigraphical position between the inferred oceanic (basaltic) basement and overlying trench sediments (e.g. Leggett 1980). The equivalent rocks to radiolarian oozes

and red and brown clays which form below the calcite compensation depth in modern ocean basins are all recognisable in the Arenig to Caradoc strata in the Leadhills Imbricate Zone viz. Raven Gill Formation and Kirkton beds. It is also noted that the inner slope and hilly areas of the Puerto Rico trench contain brown abyssal clays and oozes (Conolly & Ewing 1967). The presence of semi-lithified sandstones (McMurtry 1980a) and black shales in conglomerates provides evidence on the nature of lower slope/within canyon sequences; the latter, in particular, conforms with previous models which suggest low sedimentation rates on the inner trench wall due to bypass of coarser material through canyon systems (Underwood & Karig 1980).

7.4 FORE-ARC TECTONICS AND LOW-GRADE METAMORPHISM

The major structural features of the Abington district have all been recognised in modern and ancient accretionary complexes. However, fundamental differences exist between the Northern Belt and other regions described in the literature. In particular, most accretionary complexes are characterised by tectonic *mélange* terrains notably absent in the study area. From accounts of tectonic *mélange* (Cowan 1974, p. 1632; Connelly 1978) it is suggested that structurally *mélange* and imbricate zones are equivalent in that both facilitate displacement throughout a zone underlying thick

slabs of consolidated rock.

Folds and faults (thrusts) separating 'blocks' of contrasting lithostratigraphical units are typical of both modern and ancient accretionary complexes. DSDP Leg 31, site 298, cored an oceanward-verging, overturned anticline from the lowermost slope section of the Nankai Trough (J. C. Moore & Karig 1976). Cross sections of Cretaceous trench deposits on Shumagin Island, off Alaska, show thick homoclinal sections, dipping 45° landwards, flanked by a series of well developed folds which are separated from the former by high angle, strike-parallel reverse faults (J. C. Moore 1973). This configuration finds direct analogy with structures particularly common in the Southern and Central Belts (Craig & Walton 1959). F_1 fold vergence in the Southern Uplands/Longford-Down belt is characteristically south-eastwards, and, by inference, oceanward (Anderson & Cameron 1979).

Other areas consisting of discrete structural units, grossly sheetlike in geometry, and separated from one another by major faults, include Nias Island (G. F. Moore & Karig 1980), Kodiak Island (Connelly 1978) and the Franciscan Complex (e.g. Cowan 1974).

The incorporation of the Abington Formation as part of the underlying Leadhills Imbricate Zone differs from styles of tectonic mixing found in other complexes. On Kodiak

Island (Connelly 1978) the underthrust turbidite (Kodiak) sequence is transformed into a 1 km thick broken formation below the thrust contact, and contains fragments of the overlying *mélange* sequence (Uyak Complex). However, the landward and structurally higher *mélange* sequence compares with the Abington Formation within the Leadhills Imbricate Zone by containing kilometre-sized slivers of the Kodiak Formation 3 km structurally above the thrust contact. It is suggested that lithological contrasts and more intense deformation of Kodiak Island explain the differing structural styles.

In modern accretionary complexes, the concomitant rotation of bedding and thrusts gradually increases in amount upslope, from gently (landward) dipping near the base of the inner trench slope to over 70° at the trench-slope break (G. F. Moore & Karig 1980); thrusts at the trench-slope break on Nias Island also dip landward in excess of 45° . The initiation of faulting probably occurred along an inclined plane of high shear stress which extended up for some tens of kilometres through the trench-wedge sediments, possibly resulting from episodic subduction (Cowan 1974; Karig & Sharman 1975 and references therein).

A mechanism of oblique north-westerly subduction may account for discrepancies between inferred and observed

transport directions on faults within the area. Modern examples of accretionary complexes may be formed during oblique subduction and include the Taupo-Hikurangi subduction system, New Zealand (Cole & Lewis 1981) and the Sunda (Nias) arc system off Sumatra (G. F. Moore & Karig 1980; Karig 1980). Strike-slip faults absorb the component of subduction parallel to the arc, with displacements in excess of 100 km. They are preferentially sited towards the volcanic chain (Sumatra) or landward from the highest accretionary ridge (New Zealand). In the latter example, thrusting or reverse faulting with movement normal to the accretionary complex becomes less significant and strike-slip motion more important upslope from the trench towards the frontal arc* (Walcott 1978; Cole & Lewis 1981, Fig. 3). Thus in any one fault zone in the landward section of an ancient accretionary complex it may be predicted that fault-related lineations record only the later strike-slip component of movement. Such displacements may also assist in resolving the problem of the present configuration/juxtaposition of contrasting petrographic provinces (Section 7.2).

FOOTNOTE* : Terminology after Karig et al. 1979; equates with 'frontal ridge' of Cole & Lewis 1981.

F_1 deformation was possibly initiated in partially lithified sediments in response to oblique north-westerly subduction of the Iapetus Ocean plate. Thrust nappes and SE-verging folds were propagated within the inner trench wall of the accretionary complex. Folds of opposing vergence are inferred to have formed towards the end of subduction during ?continental collision (Cameron 1977).

The prehnite-pumpellyite metamorphic grade attained in the Abington area is similar to that found in native blocks in mélanges, the matrix of mélanges and sandstones of other subduction complexes: examples include Kodiak Island (Connelly 1978), the Franciscan Complex of California (Bailey et al. 1964; Cowan 1978) and the Te Anau Assemblage of New Zealand (Carter et al. 1978). Zeolite facies assemblages have been described from Cretaceous trench deposits of the Shumagin-Kodiak shelf (J. C. Moore 1973), and Eocene-Miocene volcanics of the Aleutian arc (Marlow et al. 1973).

Low-grade metamorphism of the Abington district most likely accompanied F_1 deformation. Essentially, each accreted wedge suffered first zeolite and then prehnite-pumpellyite facies metamorphism as it was thrust under, and incorporated into, the accretionary complex. The uniformity of illite crystallinity values across major

faults accords with the view that when bedding attained verticality, metamorphic gradients were eradicated between the bottom and top of each wedge; presumably, lower grades were represented at higher structural levels and subsequently removed by erosion (Oliver & Leggett 1980).

7.5 ABSTRACT

NE-SW faults in the Abington area of the Northern Belt of the Southern Uplands define blocks up to 3.2 km wide. The strata, folded and locally overturned, young predominantly to the NW but blocks to the SW contain younger sequences. Analogous configurations occur in modern accretionary margins. The oldest rocks, generally of pelagic and hemipelagic origin, are Arenig basalts, dolerites, cherts and brown mudstones underlying red mudstones, possibly Llanvirn, and black fossiliferous mudstones and cherts of Llandeilo and Caradoc age.

Trench sediments overlying pelagic sequences represent a range of depositional mechanisms. Rudites and associated fine-grained lithologies of lateral origin relate to a lower trench-slope canyon system, whilst axially transported sands, originating on the lower trench slope, were deposited by turbidity currents and related flows. Sandstone petrography varies markedly across strike, with quartz-rich compositions

suggesting a recycled orogen source, and ferromagnesian-rich compositions a dissected magmatic arc provenance.

Faults, initially low-angle thrusts, facilitated thrust nappe formation; faults and bedding were rotated through the vertical within the accretionary complex, predating or accompanying slaty cleavage development. Soft sediment deformation, two fold phases and a kink-band set are recognised. Imbricate fault zones, located in incompetent pelagic sequences, are equated with tectonic *mélange* of other accretionary complexes.

Index minerals, illite crystallinity and 'vitrinite' reflectance establish metamorphic grade as prehnite-pumpellyite facies.

ACKNOWLEDGEMENTS

I am particularly indebted to Dr. J. A. Weir for suggesting the project, and to both he and Professor E. K. Walton for advice, frequent stimulating discussions and encouragement throughout the project.

Parts of the manuscript were read by Dr. G. J. H. Oliver, Dr. C. H. Donaldson, Mr. D. Ellis (University of St. Andrews), Dr. D. J. Sanderson (Queen's University of Belfast) and Dr. D. S. Wood (Robertson Research International Ltd.). I am grateful to all of these for deflecting me from many errors.

I wish to thank Dr. S. H. Williams for graptolite identification. Graptolite reflectance work was undertaken at the Organic Geochemistry Unit of the University of Newcastle-upon-Tyne, with guidance from Professor D. G. Murchison and Dr. J. M. Jones; electron microprobe work was carried out at the Grant Institute of Geology, University of Edinburgh with much assistance from Dr. P. G. Hill and Mr. C. Begg.

Of the technical staff of the University of St. Andrews, I thank Mr. S. Bateman for general help, Messrs. A. Mackie and A. Barman for thin-section work, Mr. E. Cox for help with X-ray diffraction studies and Mr. J. Allan for photographic work. In addition, I gratefully acknowledge Robertson

Research International Ltd. for receipt of a grant to assist in completion of many text figures, drafted by Messrs. J. Baguley, D. C. Davies and R. Rees-Williams.

Special thanks are given to Jane Jukes for typing the manuscript and help with the thesis at all stages; and to Mr. P. W. Weston for proof reading the finalised draft.

Much of the land which I mapped is owned by the Hopetoun Estate, and to them I give thanks for access to the land even after the 12th of August, a period equally dangerous to both geologist and grouse alike; in particular, co-operation from the local gamekeeper, Mr. K. Wilson is acknowledged. During field mapping, I enjoyed home comforts provided by Mrs. E. Logan of Elvanfoot, and hospitality from Miss Ena Wilson, also of Elvanfoot. Lastly, but not least, I express thanks to the CZ motorcycle company for giving me much scope to develop my previously limited skills in motorcycle maintenance and repair.

Financial support for the study from the Natural Environment Research Council is gratefully acknowledged.

REFERENCES

- AHRENDT, H., HUNZIKER, J.C. & WEBER, K. 1978. Age and degree of metamorphism and time of nappe emplacement along the southern margin of the Damara orogen/Namibia (SW-Africa). Geol. Rdsch. 67, 719-42.
- ALLEN, J.R.L. 1963. The classification of cross-stratified units, with notes on their origin. Sedimentology, 2, 93-114.
- ANDERSON, T.B. 1962. The stratigraphy, sedimentology and structure of the Silurian rocks of the Ards peninsula, County Down. Unpublished Ph.D. thesis, University of Liverpool.
- ANDERSON, T.B. 1969. The geometry of a natural orthorhombic system of kink-bands. Pap. geol. Surv. Can. 68-52, 200-28.
- ANDERSON, T.B. & CAMERON, T.D.J. 1979. A structural profile of Caledonian deformation in Down. In: HARRIS, A.L., HOLLAND, C.H. & LEAKE, B.E. (eds). The Caledonides of the British Isles - reviewed. Spec. publ. geol. Soc. London, 8, 263-7.
- ATKINS, F.B. 1969. Pyroxenes of the Bushveld intrusion, South Africa. J. Petrol. 10, 222-49.
- BAGNOLD, R.A. 1941. The Physics of Blown Sands and Desert Dunes. Methuen, London, 265 pp.

- BAGNOLD, R.A. 1954. Experiments on a gravity-free dispersion of large solid spheres in a Newtonian fluid under shear. Proc. R. Soc. London, Ser. A, 225, 49-63.
- BAGNOLD, R.A. 1956. The flow of cohesionless grains in fluids. Philos. Trans. R. Soc. London, 249, 235-97.
- BAGNOLD, R.A. 1968. Deposition in the process of hydraulic transport. Sedimentology, 10, 45-56.
- BAILEY, E.H., IRWIN, W.P. & JONES, D.L. 1964. Franciscan and related rocks, and their significance in the geology of western California. Bull. Calif. Div. Mines Geol. 183, 89-112.
- BARTOLINI, C., MALESANI, P.G., MANETTI, P. & WEZEL, F.C. 1975. Sedimentology and petrology of Quaternary sediments from the Hellenic Trench, Mediterranean Ridge and the Nile Cone from D.S.D.P., Leg 13, cores. Sedimentology, 22, 205-36.
- BATES, D.E.B. 1974. The structure of the Lower Palaeozoic rocks of Anglesey, with special reference to faulting. Geol. J. 9, 39-60.
- BENNETTS, K.R.W. & PILKEY, O.H. 1976. Characteristics of three turbidites, Hispaniola-Caicos Basin. Bull. geol. Soc. Am. 87, 1291-300.
- BERGSTRÖM, S.M. 1971. Conodont biostratigraphy of the Middle and Upper Ordovician of Europe and eastern North America. In: SWEET, W.C. & BERGSTRÖM, S.M. (eds). Symposium on Conodont Biostratigraphy. Mem. geol. Soc. Am. 127, 83-162.

- BERRY, L.G., POST, B., WEISSMAN, S., McMURDIE, H.F. & McCLUNE, W.F. 1974. Selected Powder Diffraction Data for Minerals. First edition. Joint Committee on Powder Diffraction Standards, Swarthmore, Pennsylvania, 833 pp.
- BLATT, H., MIDDLETON, G.V. & MURRAY, R.C. 1972. Origin of Sedimentary Rocks. First edition. Prentice-Hall, New Jersey, 634 pp.
- BOLES, J.R. & COOMBS, D.S. 1977. Zeolite facies alteration of sandstones in the Southland Syncline, New Zealand. Am. J. Sci. 277, 982-1012.
- BOUMA, A.H. & HOLLISTER, C.D. 1973. Deep ocean basin sedimentation. In: MIDDLETON, G.V. & BOUMA, A.H. (eds). Turbidites and Deep Water Sedimentation. Soc. Econ. Paleontol. Mineral., Pacific Section, Short Course, 79-118.
- BRAMLETTE, M.N. 1946. The Monterey Formation of California and the origin of its siliceous rocks. Prof. Pap. U.S. geol. Surv. 212, 1-57.
- BRAZIER, S., ROBINSON, D. & MATTHEWS, S.C. 1979. Studies of illite crystallinity in southwest England. Some preliminary results and their geological setting. Neues Jahrb. Geol. Paläontol. Monatshefte, 11, 641-62.
- BRUN, J.P. & COBBOLD, P.R. 1980. Strain heating and thermal softening in continental shear zones: a review. J. struct. Geol. Oxford, 2, 149-58.

- BURST, J.F. 1959. Postdiagenetic clay-mineral environmental relationship in the Gulf Coast Eocene. Proc. natl. Conf. Clays, 6th - Natl. Acad. Sci. Res. Council, Publ. 1957, 327-41.
- BURST, J.F. 1969. Diagenesis of Gulf Coast clayey sediments and its possible relation to petroleum migration. Bull. Am. Assoc. Petrol. Geol. 53, 73-93.
- CAMERON, T.D.J. 1977. The stratigraphy, sedimentology, and structural geology of the Silurian rocks of East Lecale, Co. Down. Unpublished Ph.D. thesis, Queen's University, Belfast.
- CAMERON, T.D.J. & ANDERSON, T.B. 1980. Silurian meta-bentonites in County Down, Northern Ireland. Geol. J. 15, 59-75.
- CARTER, C., TREXLER, J.H., Jr. & CHURKIN, M., Jr. 1980. Dating of graptolite zones by sedimentation rates: Implications for rates of evolution. Lethaia, 13, 279-87.
- CARTER, R.M. 1975. A discussion and classification of subaqueous mass-transport with particular application to grain-flow, slurry-flow, and fluxoturbidites. Earth Sci. Rev. 11, 145-77.
- CARTER, R.M., HICKS, M.D., NORRIS, R.J. & TURNBULL, I.M. 1978. Sedimentation patterns in an ancient arc-trench-ocean basin complex: Carboniferous to Jurassic Rangitata Orogen, New Zealand. In: STANLEY, D.J. & KELLING, G. (eds).

Sedimentation in Submarine Canyons, Fans, and Trenches.

Dowden, Hutchinson & Ross, Stroudsburg, Pennsylvania,
340-61.

- CHANDRA, D. 1965. Reflectance of coals carbonized under pressure. Econ. Geol. 60, 621-30.
- CHURKIN, M., CARTER, C. & JOHNSON, B.R. 1977. Subdivision of Ordovician and Silurian time scale using accumulation rates of graptolitic shale. Geology, 5, 452-6.
- CIPRIANI, C., SASSI, F.P. & VITERBO BASSANI, C. 1968. La composizione delle miche chiare in rapporto con le costanti reticolari e col grado metamorfico. Rend. Soc. Ital. mineral. petrogr. 24, 153-87.
- CLEARY, W.J., PILKEY, O.H. & AYERS, M.W. 1977. Morphology and sediments of three ocean basin entry points, Hatteras Abyssal Plain. J. sediment. Petrol. 47, 1157-70.
- COLE, J.W. & LEWIS, K.B. 1981. Evolution of the Taupo-Hikurangi subduction system. Tectonophysics, 72, 1-21.
- CONNELLY, W. 1978. Uyak Complex, Kodiak Islands, Alaska: A Cretaceous subduction complex. Bull. geol. Soc. Am. 89, 755-69.
- CONOLLY, J.R. & EWING, M. 1967. Sedimentation in the Puerto Rico Trench. J. sediment. Petrol. 37, 44-59.
- COOMBS, D.S., ELLIS, A.J., FYFE, W.S. & TAYLOR, A.M. 1959. The zeolite facies, with comments on the interpretation of

- hydrothermal syntheses. Geochim. cosmochim. Acta, 17, 53-107.
- COOMBS, D.S., NAKAMURA, Y. & VUAGNAT, M. 1976a. Pumpellyite-actinolite facies schists of the Taveyanne Formation near Loèche, Valais, Switzerland. J. Petrol. 17, 440-71.
- COOMBS, D.S., LANDIS, C.A., NORRIS, R.J., SINTON, J.M., BORNS, D.J. & CRAW, D. 1976b. The Dun Mountain Ophiolite Belt, New Zealand : Its tectonic setting, constitution, and origin, with special reference to the southern portion. Am. J. Sci. 276, 561-603.
- COOK, D.R. 1976. The geology of the Cairnsmore of Fleet granite and its environs, southwest Scotland. Unpublished Ph.D. thesis, University of St. Andrews.
- COWAN, D.S. 1974. Deformation and metamorphism of the Franciscan subduction zone complex northwest of Pacheco Pass, California. Bull. geol. Soc. Am. 85, 1623-34.
- COWAN, D.S. 1978. Origin of blueschist-bearing chaotic rocks in the Franciscan Complex, San Simeon, California. Bull. geol. Soc. Am. 89, 1415-23.
- CRAIG, G.Y. & WALTON, E.K. 1959. Sequence and structure in the Silurian rocks of Kirkcudbrightshire. Geol. Mag. 96, 209-20.
- CROOK, K.A.W. 1974. Lithogenesis and tectonics : the significance of compositional variations in flysch arenites

- (graywackes). In: DOTT, R.H., Jr. & SHAVER, R.H. (eds).
Modern and Ancient Geosynclinal Sedimentation. Spec. Publ.
Soc. econ. Paleontol. Mineral. Tulsa, 19, 304-10.
- CUMMINS, W.A. 1962. The greywacke problem. Liverpool
Manchester geol. J. 3, 51-72.
- CURRY, R.R. 1966. Observations of alpine mudflows in the
Tenmile Range, central Colorado. Bull. geol. Soc. Am. 77,
771-6.
- DAVIES, I.C. & WALKER, R.G. 1974. Transport and deposition
of resedimented conglomerates : the Cap Enrangé Formation,
Cambro-Ordovician, Gaspé, Quebec. J. sediment. Petrol. 44,
1200-16.
- DEER, W.A., HOWIE, R.A. & ZUSSMAN, J. 1962. Rock-Forming
Minerals. Vol. 1. First edition. Longman, London, 333 pp.
- DEER, W.A., HOWIE, R.A. & ZUSSMAN, J. 1978. Rock-Forming
Minerals. Vol. 2A. Second edition. Longman, London,
668 pp.
- DENNIS, J.G., PRICE, R.A., SALES, J.K., HATCHER, R., BALLY, A.W.,
PERRY, W.J., LAUBSCHER, H.P., WILLIAMS, R.E., ELLIOT, D.,
NORRIS, D.K., HUTTON, D.W. & EMMETT, T. 1981. What is a
thrust? What is a nappe? In: McCLAY, K.R. & PRICE, N.J.
(eds). Thrust and Nappe Tectonics. Spec. Publ. geol. Soc.
London, 9, 7-9.

DE VRIES KLEIN, G., DE MELO, U. & FAVERA, G.C.D. 1972.

Subaqueous gravity processes on the front of Cretaceous deltas, Recôncavo Basin, Brazil. Bull. geol. Soc. Am. 83, 1469-92.

DEWEY, J.F. 1969a. Structure and sequence in the para-tectonic Caledonides. In: KAY, M. (ed). North Atlantic: geology and continental drift. Mem. Am. Assoc. Petrol. Geol. 12, 309-35.

DEWEY, J.F. 1969b. Evolution of the Appalachian/Caledonian orogen. Nature. London, 222, 124-9.

DEWEY, J.F. 1971. A model for the Lower Palaeozoic evolution of the southern margin of the early Caledonides of Scotland and Ireland. Scott. J. Geol. 7, 219-40.

DICKINSON, W.R. 1970. Interpreting detrital modes of graywacke and arkose. J. sediment. Petrol. 40, 695-707.

DICKINSON, W.R. 1971. Detrital modes of New Zealand graywackes. Sediment. Geol. 5, 37-56.

DICKINSON, W.R., HELMOLD, K.P. & STEIN, J.A. 1979. Mesozoic sandstones in central Oregon. J. sediment. Petrol. 49, 501-16.

DICKINSON, W.R. & SUCZEK, C.A. 1979. Plate tectonics and sandstone compositions. Bull. Am. Assoc. Petrol. Geol. 63, 2164-82.

DOTT, R.H., Jr. 1964. Wacke, graywacke and matrix - What approach to immature sandstone classification? J. sediment. Petrol. 34, 625-32.

- DUNOYER DE SEGONZAC, G. 1969. Les minéraux argileux dans la diagenèse passage au métamorphisme. Mém. Serv. Carte géol. Alsace Lorraine, 29, 320 pp.
- DUNOYER DE SEGONZAC, G. 1970. The transformation of clay minerals during diagenesis and low-grade metamorphism : a review. Sedimentology, 15, 281-346.
- DUNOYER DE SEGONZAC, G. & HEDDEBAUT, C. 1971. Paléozoïque anchi-métamorphique à illite, chlorite, pyrophyllite, allevardite et paragonite dans les Pyrénées Basques. Bull. Serv. Carte géol. Alsace Lorraine, 24, 277-90.
- DUNOYER DE SEGONZAC, G. & HICKEL, D. 1972. Cristallochimie des phengites dans les quartzites micacés métamorphiques de Permo-Trias des Alpes Piémontaises. Bull. Sci. géol. Strasbourg, 25, 201-29.
- DUNOYER DE SEGONZAC, G. & BERNOULLI, D. 1976. Diagenèse et métamorphisme des argiles dans le Rhétien Sud-alpin et Austro-alpin (Lombardie et Grisons). Bull. Soc. géol. Fr. 18, 1283-93.
- EALLES, M.H. 1979. Structure of the Southern Uplands. In: HARRIS, A.L., HOLLAND, C.H. & LEAKE, B.E. (eds). The Caledonides of the British Isles - reviewed. Spec. Publ. geol. Soc. London, 8, 269-73.
- ELMORE, R.D., PILKEY, O.H., CLEARY, W.J. & CURRAN, H.A. 1979. Black Shell turbidite, Hatteras Abyssal Plain, western Atlantic Ocean. Bull. geol. Soc. Am. 90, 1165-76.

- ENOS, P. 1977. Flow regimes in debris flow. Sedimentology, 24, 133-42.
- EPSTEIN, A.G., EPSTEIN, J.B. & HARRIS, L.D. 1977. Conodont color alteration - an index to organic metamorphism. Prof. Pap. U.S. geol. Surv. 995, 27 pp.
- ESQUEVIN, J. 1969. Influence de la composition chimique des illites sur leur cristallinité. Bull. Cent. Rech. Pau, 3, 147-53.
- FETTES, D.J., GRAHAM, C.M., SASSI, F.P. & SCOLARI, A. 1976. The basal spacing of potassic white micas and facies series variations across the Caledonides. Scott. J. Geol. 12, 227-36.
- FISHER, R.V. 1971. Features of coarse-grained, high concentration fluids and their deposits. J. sediment. Petrol. 41, 916-27.
- FLOYD, J.D. 1975. The Ordovician rocks of West Nithsdale. Unpublished Ph.D. thesis, University of St. Andrews.
- FREY, M. 1970. The step from diagenesis to metamorphism in pelitic rocks during Alpine orogenesis. Sedimentology, 15, 261-79.
- FREY, M. 1974. Alpine metamorphism of pelitic and marly rocks of the Central Alps. Schweiz. mineral. petrogr. Mitt. 54, 489-506.

- FREY, M. 1977. Progressive low-grade metamorphism of a black shale formation, central Swiss Alps, with special reference to pyrophyllite and margarite bearing assemblages. J. Petrol. 19, 93-135.
- FREY, M. & NIGGLI, E. 1971. Illit-Kristallinität, Mineralfazien und Inkohlungsgrad. Schweiz. mineral. petrogr. Mitt. 51, 229-34.
- FYFE, T.B. & WEIR, J.A. 1976. The Ettrick Valley Thrust and the upper limit of the Moffat Shales in Craigmichan Scaurs (Dumfries and Galloway Region : Annandale and Eskdale District). Scott. J. Geol. 12, 93-102.
- GEIKIE, A. 1871. On the order of succession among the Silurian rocks of Scotland. Trans. geol. Soc. Glasgow, 3, 74-95.
- GONZALEZ-BONORINO, G. & MIDDLETON, G.V. 1976. A Devonian submarine fan in western Argentina. J. sediment. Petrol. 46, 56-69.
- GRAHAM, S.A., INGERSOLL, R.V. & DICKINSON, W.R. 1976. Common provenance for lithic grains in Carboniferous sandstone from Ouachita Mountains and Black Warrior basin. J. sediment. Petrol. 46, 620-32.
- HAMPTON, M.A. 1972. The role of subaqueous debris flow in generating turbidity currents. J. sediment. Petrol. 42, 775-93.

- HANER, B.E. 1971. Morphology and sediments of Redondo Submarine Fan, Southern California. Bull. geol. Soc. Am. 82, 2413-32.
- HARKNESS, R. 1851. On the Silurian rocks of Dumfriesshire and Kirkcudbright. Q.J. geol. Soc. London, 7, 46-58.
- HARKNESS, R. 1856. On the lowest sedimentary rocks of the south of Scotland. Q.J. geol. Soc. London, 12, 238.
- HARLAND, W.B. & GAYER, R.A. 1972. The Arctic Caledonides and earlier oceans. Geol. Mag. 109, 289-314.
- HARRASSOWITZ, H. 1926. Anchimetamorphose, das Gebiet zwischen Oberflächen - und Tiefenumwandlung der Erdinde. Ber. oberhess. Ges. Nat. -u. Heilk. 12, 9-15.
- HEPWORTH, B.C., OLIVER, G.J.H. & McMURTRY, M.J. 1981. Sedimentology, volcanism, structure and metamorphism of the northern margin of the Lower Palaeozoic accretionary complex; Bail Hill-Abington area of the Southern Uplands of Scotland. In: LEGGETT, J.K. (ed). Trench-Fore-arc Geology. Spec. Publ. geol. Soc. London, 10, 277-90.
- HESSE, R. 1974. Long-distance continuity of turbidites; possible evidence for an early Cretaceous trench-abyssal plain in the East Alps. Bull. geol. Soc. Am. 85, 859-70.
- HESSE, R. 1975. Turbiditic and non-turbiditic mudstone of Cretaceous flysch sections of the east Alps and other basins. Sedimentology, 22, 387-416.

- HEY, M.H. 1954. A new review of the chlorites. Mineralog. Mag. London, 30, 277-92.
- HINDE, G.J. 1890. Notes on radiolaria from the Lower Palaeozoic rocks (Llandeilo-Caradoc) of the South of Scotland. Ann. Mag. nat. Hist. London, 6, 40-59.
- HOBBS, B.E., MEANS, W.D. & WILLIAMS, P.F. 1976. An Outline of Structural Geology. John Wiley & Sons, New York, 571 pp.
- HOLLAND, C.H., AUDLEY-CHARLES, M.G., BASSETT, G., COWIE, J.W., CURRY, D., FITCH, F.J., HANCOCK, J.M., HOUSE, M.R., INGHAM, J.K., KENT, P.E., MORTON, N., RAMSBOTTOM, W.H.C., RAWSON, P.F., SMITH, D.B., STUBBLEFIELD, C.J., TORRENS, H.S., WALLACE, P. & WOODLAND, A.W. 1978. A guide to stratigraphical procedure. Spec. Rep. geol. Soc. London, 10, 18 pp.
- HOLLAND, C.H., KELLING, G. & WALTON, E.K. 1979. O.T. Jones and after : A multitude of models. In: HARRIS, A.L., HOLLAND, C.H. & LEAKE, B.E. (eds). The Caledonides of the British Isles - reviewed. Spec. Publ. geol. Soc. London, 8, 469-81.
- HOLROYD, J. 1978. The sedimentologic and geotectonic significance of Lower Palaeozoic flysch rudites. Unpublished Ph.D thesis, University of Wales.
- HOWER, J. ESLINGER, E.V., HOWER, M.E. & PERRY, E.A. 1976. Mechanism of burial metamorphism of argillaceous sediment:

1. Mineralogical and chemical evidence. Bull. geol. Soc. Am. 87, 725-37.
- HUBERT, J. 1964. Textural evidence for deposition of many western North Atlantic deep-sea sands and silts by ocean-bottom currents rather than turbidity currents. J. Geol. Chicago, 72, 757-85.
- JOHNSON, A.M. 1970. Physical Processes in Geology. Freeman, Cooper, San Francisco, 577 pp.
- KARIG, D.E. 1980. Material transport within accretionary prisms and the "knocker" problem. J. Geol. Chicago, 88, 27-39.
- KARIG, D.E. & SHARMAN, G.F. III. 1975. Subduction and accretion in trenches. Bull. geol. Soc. Am. 86, 377-89.
- KARIG, D.E., SUPARKA, S., MOORE, G.F. & HEHANUSSA, P.E. 1979. Cenozoic evolution of the Sunda Arc in the central Sumatra region. In: WATKINS, J. & MONTADERT, L. (eds). Geological and Geophysical Investigations of Continental Slopes and Rises. Mem. Am. Assoc. Petrol. Geol. 29, 223-37.
- KARIG, D.E., LAWRENCE, M.B., MOORE, G.F. & CURRAY, J.R. 1980. Structural framework of the fore-arc basin, NW Sumatra. J. geol. Soc. London, 137, 77-91.
- KAWACHI, Y. 1975. Pumpellyite-actinolite and contiguous facies metamorphism in part of upper Wakatipu district, South Island, New Zealand. N.Z.J. Geol. Geophys. 18, 401-41.

- KELLING, G. 1961. The stratigraphy and structure of the Ordovician rocks of the Rhinns of Galloway. Q.J. geol. Soc. London, 117, 37-75.
- KELLING, G. 1962. The petrology and sedimentation of Upper Ordovician rocks of the Rhinns of Galloway. Trans. R. Soc. Edinburgh, 65, 107-37.
- KELLING, G. & HOLROYD, J. 1978. Clast size, shape, and composition in some ancient and modern fan gravels. In: STANLEY, D.J. & KELLING, G. (eds). Sedimentation in Submarine Canyons, Fans, and Trenches. Dowden, Hutchinson & Ross, Stroudsburg, Pennsylvania, 138-59.
- KISCH, H.J. 1974. Anthracite and meta-anthracite coal ranks associated with 'anchimetamorphism' and 'very-low-stage' metamorphism, I, II, and III. Proc. Kon. Ned. Akad. Wet. Amsterdam, Ser. B, 77, 81-118.
- KISCH, H.J. 1978. Incipient metamorphism of Cambro-Silurian rocks from the "Eastern Complex" Caledonides of Jämtland, western Sweden : illite crystallinity and vitrinite reflectance. Rep. joint German Israeli Res. Proj. E12, 1-49.
- KISCH, H.J. 1980. Incipient metamorphism of Cambro-Silurian clastic rocks from the Jämtland Supergroup, Central Scandinavian Caledonides, western Sweden: illite crystallinity and 'vitrinite' reflectance. J. geol. Soc. London, 137, 271-88.

- KRAUSKOPF, K.B. 1959. The geochemistry of silica in sedimentary environments. In: IRELAND, H.A. (ed). Silica in Sediments. Spec. Publ. Soc. econ. Paleontol. Mineral. Tulsa, 7, 4-19.
- KÜBLER, B. 1964. Les argiles, indicateurs de métamorphisme. Rev. Inst. Fr. Pet. Paris, 19, 1093-113.
- KÜBLER, B. 1967a. La cristallinité de l'illite et les zones tout à fait supérieures du métamorphisme. In: Etages tectoniques. A la Baconnière, Neuchâtel (Suisse), 105-22.
- KÜBLER, B. 1967b. Anchimétamorphisme et schistosité. Bull. Centr. Rech. Pau, 1, 259-78.
- KÜBLER, B. 1968. Evaluation quantitative du métamorphisme par la cristallinité de l'illite. Bull. Centr. Rech. Pau, 2, 385-97.
- KÜBLER, B., MARTINI, J. & VUAGNAT, M. 1974. Very low grade metamorphism in the western Alps. Schweiz. mineral. petrogr. Mitt. 54, 461-9.
- KUENEN, Ph.H. 1958. Experiments in geology. Trans. geol. Soc. Glasgow, 23, 1-28.
- KUENEN, Ph.H. 1966. Matrix of turbidites : experimental approach. Sedimentology, 7, 267-97.
- KUNIYOSHI, S. & LIOU, J.G. 1976. Burial metamorphism of the Karmutsen volcanic rocks, northeastern Vancouver Island, British Columbia. Am. J. Sci. 276, 1096-119.

LAMBERT, R.St.J., HOLLAND J.G. & LEGGETT, J.K. 1981.

Petrology and tectonic setting of some Ordovician volcanic rocks from the Southern Uplands of Scotland. J. geol. Soc. London, 138, 421-36.

LAMONT, A. & LINDSTRÖM, M. 1957. Arenigian and Llandeilian cherts identified in the Southern Uplands of Scotland by means of conodonts, etc. Trans. geol. Soc. Edinburgh, 17, 60-70

LANCELOT, Y. 1973. Chert and silica diagenesis in sediments from the Central Pacific. Initial Rep. Deep Sea drill. Proj. 17, 377-405.

LAPWORTH, C. 1874. On the Silurian rocks of the south of Scotland. Trans. geol. Soc. Glasgow, 4, 164-74.

LAPWORTH, C. 1876. On Scottish Monograptidae. Geol. Mag. 3, 308-21, 350-60, 499-507, 544-52.

LAPWORTH, C. 1878. The Moffat Series. Q.J. geol. Soc. London, 34, 240-346.

LAPWORTH, C. 1889. On the Ballantrae rocks of the south of Scotland, and their place in the upland sequence. Geol. Mag. 6, 20-4, 59-69.

LEAKE, B.E. 1978. Nomenclature of amphiboles. Mineralog. Mag. London, 42, 533-63.

LEGGETT, J.K. 1980. The sedimentological evolution of a Lower Palaeozoic accretionary fore-arc in the Southern Uplands of Scotland. Sedimentology, 27, 401-17.

- LEGGETT, J.K., MCKERROW, W.S. & EALES, M.H. 1979. The Southern Uplands of Scotland: A Lower Palaeozoic accretionary prism. J. geol. Soc. London, 136, 755-70.
- LIBORIO, G. & MOTTANA, A. 1970. Variazioni delle proprietà roentgenografiche delle miche chiare degli scisti di Edolo lungo direttrici metamorfiche. Rend. Soc. Ital. mineral. petrogr. 26, 179-204.
- LIU, J.G. 1971a. Synthesis and stability relations of prehnite, $\text{Ca}_2\text{Al}_2\text{Si}_3\text{O}_{10}(\text{OH})_2$. Am. Mineral. 56, 507-31.
- LIU, J.G. 1971b. P-T stabilities of laumontite, wairakite, lawsonite, and related minerals in the system $\text{CaAl}_2\text{Si}_2\text{O}_8\text{-SiO}_2\text{-H}_2\text{O}$. J. Petrol. 12, 379-411.
- LONG, G., NEGLIA, S. & FAVRETTO, L. 1964. Geochemical contribution to research for the reconstruction of the paleogeography of a sedimentary basin. In: COLOMBO, U. & HOBSON, G.D. (eds). Advanced Organic Geochemistry. Pergamon Press, London, 239-59.
- LOWE, D.R. 1976. Grain flow and grain flow deposits. J. sediment. Petrol. 46, 188-99.
- LUDWIG, V. 1972. Die Paragenese Chlorit, Muscovit, Paragonit und Margarit im 'Griffelschiefer' des Ordoviziums in NE-Bayern (mit einem Beitrag zum Problem der Illit-Kristallinität). Neues Jahrb. Geol. Paläontol. Monatshefte, 9, 546-60.
- LUDWIG, V. 1973. Zum Übergang eines Tonschiefers in die Metamorphose: 'Griffelschiefer' im Ordovizium von NE-Bayern.

Neues Jahrb. Geol. Paläeontol. Abhandlungen, 144, 50-103.

MACKAY, R.A. 1958. The Leadhills Wanlockhead mining district.

In: The future of non-ferrous mining in Great Britain and Ireland. Instn. Ming. Metall. London, 49-64.

MARLOW, M.S., SCHOLL, D.W., BUFFINGTON, E.C. & ALPHA, T.R.

1973. Tectonic history of the central Aleutian arc. Bull. geol. Soc. Am. 84, 1555-74.

MARSHALL, C.E. 1936. Alteration of coal seams by the intrusion of some igneous dykes in Northumberland and Durham. Trans. Instn. Ming. Eng. 91, 235-60.

McKEE, E.D., REYNOLDS, M.A. & BAKER, C.H. 1962. Laboratory studies on deformation in unconsolidated sediment. Prof. Pap. U.S. geol. Surv. 450D, 151-5.

McKERROW, W.S., LEGGETT, J.K. & EALES, M.H. 1977. Imbricate thrust model of the Southern Uplands of Scotland. Nature. London, 267, 237-9.

McMURTRY, M.J. 1980a. The Ordovician rocks of the Bail Hill area, Sanquhar, South Scotland: Volcanism and sedimentation in the Iapetus Ocean. Unpublished Ph.D. thesis, University of St. Andrews.

McMURTRY, M.J. 1980b. Discussion of: Evidence for Caledonian subduction from greywacke detritus in the Longford-Down inlier. J. Earth Sci. R. Dublin Soc. 2, 209-12.

MIDDLETON, G.V. 1967. Experiments on density and turbidity currents. III Deposition of sediment. Can. J. Earth

Sci. 4, 475-505.

- MIDDLETON, G.V. 1970. Experimental studies related to problems of flysch sedimentation. In: LAJOIE, J. (ed). Flysch Sedimentology in North America. Spec. Pap. geol. Assoc. Can. 7, 253-73.
- MIDDLETON, G.V. & HAMPTON, M.A. 1973. Sediment gravity flows: mechanics of flow and deposition. In: MIDDLETON, G.V. & BOUMA, A.H. (eds). Turbidites and Deep Water Sedimentation. Pacif. Sec. Short Course, Soc. Econ. Paleontol. Mineral. Tulsa, 1-38.
- MIDDLETON, G.V. & HAMPTON, M.A. 1976. Subaqueous sediment transport and deposition by sediment gravity flows. In: STANLEY, D.J. & SWIFT, D.J.P. (eds). Marine Sediment Transport and Environmental Management. John Wiley, New York, 197-220.
- MITCHELL, A.H.G. 1974. Flysch-ophiolite sequences: polarity indicators in arc and collision-type orogens. Nature. London, 248, 747-9.
- MITCHELL, A.H.G. & MCKERROW, W.S. 1975. Analogous evolution of the Burma Orogen and the Scottish Caledonides. Bull. geol. Soc. Am. 86, 305-15.
- MOORE, G.F. 1979. Petrography of subduction zone sandstones from Nias Island, Indonesia. J. sediment. Petrol. 49, 71-84.

- MOORE, G.F. & KARIG, D.E. 1976. Development of sedimentary basins on the lower trench slope. Geology, 4, 693-7.
- MOORE, G.F., BILLMAN, H.G., HEHANUSSA, P.E. & KARIG, D.E. 1980. Sedimentology and palaeobathymetry of Neogene trench-slope deposits, Nias Island, Indonesia. J. Geol. Chicago, 88, 161-80.
- MOORE, G.F. & KARIG, D.E. 1980. Structural geology of Nias Island, Indonesia: Implications for subduction zone tectonics. Am. J. Sci. 280, 193-223.
- MOORE, J.C. 1973. Complex deformation of Cretaceous trench deposits, southwestern Alaska. Bull. geol. Soc. Am. 84, 2005-20.
- MOORE, J.C. & KARIG, D.E. 1976. Sedimentology, structural geology and tectonics of the Shikoku subduction zone, southwestern Japan. Bull. geol. Soc. Am. 87, 1259-68.
- MUFFLER, L.J.P. & WHITE, D.E. 1969. Active metamorphism of Upper Cenozoic sediments in the Salton Sea-geothermal field and the Salton trough, southeastern California. Bull. geol. Soc. Am. 80, 157-82.
- MURCHISON, R.I. 1851. On the Silurian rocks of the South of Scotland. Q.J. geol. Soc. London, 7, 139-69.
- MUTTI, E. & RICCI-LUCCHI, F. 1975. Turbidite facies and facies associations. In: MUTTI, E., PAREA, G.C., RICCI-LUCCHI, F., SAGRI, M., ZANZUCCHI, G., GHIBAUDO, G. &

- JACCARINO, S. Examples of Turbidite Facies and Facies Associations from Selected Formations of the Northern Apennines. IX Int. Congr. Sedim. (Nice), Field Trip A-II, 21-36.
- NELSON, C.H. & KULM, L.D. 1973. Submarine fans and deep-sea channels. In: MIDDLETON, G.V. & BOUMA, A.H. (eds). Turbidites and Deep Water Sedimentation. Pacif. Sec. Short Course, Soc. Econ. Paleontol. Mineral. Tulsa, 39-78.
- NICOL, J. 1848. On the geology of the Silurian rocks in the valley of the Tweed. Q.J. geol. Soc. London, 4, 195-209.
- NITSCH, K.H. 1971. Stabilitätsbeziehungen von Prehnit- und Pumpellyit-haltigen Paragenesen. Contrib. Mineral. Petrol. 30, 240-60.
- NORMARK, W.R. 1970. Growth patterns of deep-sea fans. Bull. Am. Assoc. Petrol. Geol. 54, 2170-95.
- NORRIS, R.J. & HENLEY, R.W. 1976. Dewatering of a metamorphic pile. Geology, 4, 333-6.
- OFFLER, R., BAKER, C.K. & GAMBLE, J. 1981. Pumpellyites in two low grade metamorphic terranes north of Newcastle, NSW Australia. Contrib. Mineral. Petrol. 76, 171-6.
- OLIVER, G.J.H. 1978. Prehnite-pumpellyite facies metamorphism in Co. Cavan, Ireland. Nature. London, 274, 242-3.
- OLIVER, G.J.H. & LEGGETT, J.K. 1980. Metamorphism in an accretionary prism: prehnite-pumpellyite facies metamorphism of the Southern Uplands of Scotland. Trans. R. Soc.

- Edinburgh, 71, 235-46.
- PAPIKE, J.J., CAMERON, K.I. & BALDWIN, K. 1974. Amphiboles and pyroxenes - characterisation of other than quadrilateral components and estimates of ferric iron from microprobe data. Abstr. Prog. geol. Soc. Am. 6, 1053-4.
- PAPROTH, E. & WOLF, M. 1973. Some palaeogeographic interpretations of the carbonification in the Devonian and Carboniferous of the northern Rhenish Schiefergebirge. Geol. Palaeontol. 8, 469-93.
- PASSAGLIA, E. & GOTTARDI, G. 1973. Crystal chemistry and nomenclature of pumpellyites and julgoldites. Can. Mineral. 12, 219-23.
- PATTEISKY, K. & TEICHMÜLLER, M. 1960. Inkohlungs-Verlauf, Inkohlungs-Maßstäbe und Klassifikation der Kohlen auf Grund von Vitrit-Analysen. Brenst.-Chem. 41, 79-97.
- PEACH, B.N. & HORNE, J. 1899. The Silurian rocks of Britain, 1, Scotland. Mem. geol. Surv. Scotland, 749 pp.
- PETTIJOHN, F.J. 1950. Turbidity currents and graywackes - a discussion. J. Geol. Chicago, 58, 169-71.
- PETTIJOHN, F.J. 1957. Sedimentary Rocks. First edition. Harper & Row, New York, 718 pp.
- PETTIJOHN, F.J. 1975. Sedimentary Rocks. Third edition. Harper & Row, New York, 628 pp.
- PETTIJOHN, F.J., POTTER, P.E. & SIEVER, R. 1972. Sand and Sandstone. Springer-Verlag, New York, 618 pp.

- PHILLIPS, W.E.A., STILLMAN, C.J. & MURPHY, T. 1976. A Caledonian plate tectonic model. J. geol. Soc. London, 132, 579-609.
- PHILLIPS, W.E.A., FLEGG, A.M. & ANDERSON, T.B. 1979. Strain adjacent to the Iapetus suture in Ireland. In: HARRIS, A.L., HOLLAND, C.H. & LEAKE, B.E. (eds). The Caledonides of the British Isles - reviewed. Spec. Publ. geol. Soc. London, 8, 257-62.
- PIERSON, T.C. 1981. Dominant particle support mechanisms in debris flows at Mt Thomas, New Zealand, and implications for flow mobility. Sedimentology, 28, 49-60.
- PIPER, D.J.W. 1972. Trench sedimentation in the Lower Palaeozoic of the Southern Uplands. Scott. J. Geol. 8, 289-91.
- PIPER, D.J.W., VON HUENE, R. & DUNCAN, J.R. 1973. Late Quaternary sedimentation in the active eastern Aleutian Trench. Geology, 1, 19-22.
- POST, J.L. & PLUMMER, C.C. 1972. The chlorite series of Flagstaff Hill area, California: a preliminary investigation. Clays Clay Miner. 20, 271-83.
- POWELL, C.Mc.A. 1979. A morphological classification of rock cleavage. Tectonophysics, 58, 21-34.
- POWERS, M.C. 1953. A new roundness scale for sedimentary particles. J. sediment. Petrol. 23, 117-9.

- POWERS, M.C. 1959. Adjustment of clays to chemical change and the concept of equivalence level. Proc. natl. Conf. Clays, 6th - Natl. Acad. Sci. Res. Council, Publ. 1957, 309-26.
- PRICE, N.J. 1966. Fault and Joint Development in Brittle and Semi-brittle Rock. Pergamon Press, Oxford, 176 pp.
- RAMSAY, J.G. 1967. Folding and Fracturing of Rocks. McGraw-Hill, New York, 568 pp.
- RAMSAY, J.G. 1980. Shear zone geometry: a review. J. struct. Geol. Oxford, 2, 83-99.
- REINECK, H.E. & SINGH, I.B. 1975. Depositional Sedimentary Environments. Springer-Verlag, Berlin, 439 pp.
- RICCI-LUCCHI, F. 1975a. Depositional cycles in two turbidite formations of northern Apennines (Italy). J. sediment. Petrol. 45, 3-43.
- RICCI-LUCCHI, F. 1975b. Sediment dispersal in turbidite basins: examples from the Miocene of the Northern Apennines. Proc. IXth Int. Congr. Sedim. (Nice), Thème 5, 347-52.
- RICKARD, M.J. 1971. A classification diagram for fold orientations. Geol. Mag. 98, 324-32.
- RITCHIE, M. & ECKFORD, R.J.A. 1935. The Haggis Rock of the Southern Uplands. Trans. geol. Soc. Edinburgh, 13, 371-7.
- ROBERTS, J.L. 1974. The structure of the Dalradian rocks in the S.W. Highlands of Scotland. J. geol. Soc. London, 130, 93-124.

- ROCHELEAU, M. & LAJOIE, J. 1974. Sedimentary structures in resedimented conglomerate of the Cambrian flysch, L'Islet, Quebec Appalachians. J. sediment. Petrol. 44, 826-36.
- RODINE, J.D. & JOHNSON, A.M. 1976. The ability of debris, heavily freighted with coarse clastic materials, to flow on gentle slopes. Sedimentology, 23, 213-34.
- RUST, B.R. 1963. The geology of the area around Whithorn, Wigtownshire. Unpublished Ph.D. thesis, University of Edinburgh.
- RUST, B.R. 1965. The sedimentology and diagenesis of Silurian turbidites in South-east Wigtownshire, Scotland. Scott. J. Geol. 1, 231-46.
- SAGON, J-P. & DUNOYER DE SEGONZAC, G. 1972. La cristallinité des micas dans les schistes paléozoïques et briovériens du Bassin de Châteaulin (Massif armoricain). C.r. Séances Acad. Sci. Paris, Sér. D, 275, 1023-6.
- SANDERS, I.S. & MORRIS, J.H. 1978. Evidence for Caledonian subduction from greywacke detritus in the Longford-Down inlier. J. Earth Sci. R. Dublin Soc. 1, 53-62.
- SANDERS, J.E. 1965. Primary sedimentary structures formed by turbidity currents and related resedimentation mechanisms. In: MIDDLETON, G.V. (ed). Primary Sedimentary Structures and their Hydrodynamic Interpretation. Spec. Publ. Soc. econ. Paleontol. Mineral. Tulsa, 12, 192-219.

- SAUPÉ, F., DUNOYER DE SEGONZAC, G. & TEICHMÜLLER, M. 1977. Étude du métamorphisme régional dans la zone d'Almadén (Province de Ciudad Real, Espagne) par la cristallinité de l'illite et par le pouvoir réflecteur de la matière organique. Sci. Terr. Nancy, 21, 251-69.
- SCHOLL, D.W., CHRISTENSEN, M.N., VON HEUNE, R. & MARLOW, M.S. 1970. Peru-Chile trench sediments and sea-floor spreading. Bull. geol. Soc. Am. 81, 1339-60.
- SCHOLL, D.W., MARLOW, M.S. & BUFFINGTON, E.C. 1975. Summit basins of Aleutian Ridge, North Pacific. Bull. Am. Assoc. Petrol. Geol. 59, 799-816.
- SCHUILING, R.D. & VINK, B.W. 1967. Stability relations of some titanium-minerals (sphene, perovskite, rutile, anatase). Geochim. cosmochim. Acta, 31, 2399-411.
- SCHWELLER, W.J. & KULM, L.D. 1978. Depositional patterns and channelized sedimentation in active eastern Pacific trenches. In: STANLEY, D.J. & KELLING, G. (eds). Sedimentation in Submarine Canyons, Fans, and Trenches. Dowden, Hutchinson & Ross, Stroudsburg, Pennsylvania, 311-24.
- SEDGWICK, A. 1850. On the geological structure and relations of the frontier chain of Scotland. Edinburgh New Phil. Journal, 51, 250-8.
- SEELY, D.R., VAIL, P.R. & WALTON, G.G. 1974. Trench slope model. In: BURK, C.A. & DRAKE, C.L. (eds). The Geology of

- Continental Margins. Springer-Verlag, New York, 249-60.
- SHACKLETON, R.M. 1958. Downward facing structures of the Highland Border. Q.J. geol. Soc. London, 113, 361-92.
- SHARP, R.P. & NOBLES, L.H. 1953. Mudflow of 1941 at Wrightwood, southern California. Bull. geol. Soc. Am. 64, 547-60.
- SIEVER, R. 1962. Silica solubility, 0°-200°C., and the diagenesis of siliceous sediments. J. Geol. Chicago, 70, 127-50.
- SKEVINGTON, D. 1969. The classification of the Ordovician System in Wales. In: WOOD, A. (ed). The Precambrian and Lower Palaeozoic rocks of Wales. University of Wales Press, Cardiff, 161-79.
- SMITH, N.D. 1972. Flume experiments on the durability of mud clasts. J. sediment. Petrol. 42, 378-83.
- SPEARS, D.A. 1980. Towards a classification of shales. J. geol. Soc. London, 137, 125-9.
- SPRAY, J.G. & WILLIAMS, G.D. 1980. The sub-ophiolite metamorphic rocks of the Ballantrae Igneous Complex, SW Scotland. J. geol. Soc. London, 137, 359-68.
- SPRY, A. 1969. Metamorphic textures. Pergamon Press Ltd., Oxford, 350 pp.
- STALDER, H.A. & TOURAY, J.C. 1970. Fensterquarze mit Methan-Einschlüssen aus dem westlichen Teil der Schweizerischen

Kalkalpen. Schweiz. mineral. petrogr. Mitt. 50, 109-30.

STANLEY, D.J., PALMER, H.D. & DILL, R.F. 1978. Coarse sediment transport by mass flow and turbidity current processes and downslope transformations in Annot Sandstone canyon-fan valley systems. In: STANLEY, D.J. & KELLING, G. (eds). Sedimentation in Submarine Canyons, Fans, and Trenches. Dowden, Hutchinson & Ross, Stroudsburg, Pennsylvania, 85-115.

STAUFFER, P.H. 1967. Grain-flow deposits and their implications, Santa Ynez Mountains, California. J. sediment. Petrol. 37, 487-508.

STEWART, J.H. 1961. Origin of cross-strata in fluvial sandstone layers in the Chinle Formation (Upper Triassic) on the Colorado Plateau. Prof. Pap. U.S. geol. Surv. 424-B, 127-9.

STEWART, R.J. 1976. Turbidites of the Aleutian abyssal plain: Mineralogy, provenance, and constraints for Cenozoic motion of the Pacific plate. Bull. geol. Soc. Am. 87, 793-808.

STEWART, R.J. 1978. Neogene volcanoclastic sediments from Atka Basin, Aleutian Ridge. Bull. Am. Assoc. Petrol. Geol. 62, 87-97.

STRINGER, P. & TREAGUS, J.E. 1980. Non-axial planar S_1 cleavage in the Hawick Rocks of the Galloway area, Southern Uplands, Scotland. J. struct. Geol. Oxford, 2, 317-31.

- SURDAM, R.C. 1969. Electron microprobe study of prehnite and pumpellyite from the Karmutsen Group, Vancouver Island, British Columbia. Am. Mineral. 54, 256-66.
- THOMPSON, A.B. 1970. A note on the kaolinite-pyrophyllite equilibrium. Am. J. Sci. 268, 454-8.
- THOREZ, J. 1976. The Practical Identification of Clay Minerals. G. Lelotte, Dison, 90 pp.
- TOGHILL, P. 1970. The south-east limit of the Moffat Shales in the upper Ettrick Valley region, Selkirkshire. Scott. J. Geol. 6, 233-42.
- TOWE, K.M. & URBANEK, A. 1972. Collagen-like substances in Ordovician graptolite periderm. Nature. London, 237, 443-5.
- TURNER, F.J. & WEISS, L.E. 1963. Structural Analysis of Metamorphic Tectonites. McGraw-Hill, New York, 545 pp.
- TWENHOFEL, W.H. & TYLER, S.A. 1941. Methods of Study of Sediments. McGraw-Hill, New York, p. 54.
- UDDEN, J.A. 1898. Mechanical composition of wind deposits. Augustana Library Publ. 1, 69 pp.
- UNDERWOOD, M.B. & KARIG, D.E. 1980. Role of submarine canyons in trench and trench-slope sedimentation. Geology, 8, 432-6.
- VALLONI, R. & MAYNARD, J.B. 1981. Detrital modes of recent deep-sea sands and their relation to tectonic setting: a first approximation. Sedimentology, 28, 75-83.
- VAN BREEMEN, O. & BLUCK, B.J. 1981. Episodic granite plutonism in the Scottish Caledonides. Nature. London, 291, 113-7.

- VAN DER LINGEN, G.J. 1969. The turbidite problem. N.Z.J. Geol. Geophys. 12, 7-50.
- VELDE, B. & KORNPORST, J. 1969. Stabilité des silicates d'alumine hydratés. Contrib. Mineral. Petrol. 21, 63-74.
- VENTURELLI, G. & FREY, M. 1977. Anchizone metamorphism in sedimentary sequences of the northern Apennines. Rend. Soc. Ital. mineral. petrogr. 33, 109-23.
- VON HEUNE, R. 1974. Modern trench sediments. In: BURK, C.A. & DRAKE, C.L. (eds). The Geology of Continental Margins. Springer-Verlag, New York, 207-11.
- WALCOTT, R.I. 1978. Geodetic strains and large earthquakes in the axial tectonic belt of North Island, New Zealand. J. geophys. Res. 83, 4419-29.
- WALKER, R.G. 1966. Shale Grit and Grindslow Shales: transition from turbidite to shallow water sediments in the Upper Carboniferous of northern England. J. sediment. Petrol. 36, 90-114.
- WALKER, R.G. 1967. Turbidite sedimentary structures and their relationship to proximal and distal depositional environments. J. sediment. Petrol. 37, 25-43.
- WALKER, R.G. 1976. Facies Models 2. Turbidites and associated coarse clastic deposits. Geoscience Can. 3, 25-36.
- WALKER, R.G. & MUTTI, E. 1973. Turbidite facies and facies associations. In: MIDDLETON, G.V. & BOUMA, A.H. (eds).

- Turbidites and Deep Water Sedimentation. Pacif. Sec. Short Course, Soc. Econ. Paleontol. Mineral. Tulsa, 119-57.
- WALTON, E.K. 1955. Silurian greywackes in Peeblesshire. Proc. R. Soc. Edinburgh, B65, 327-57.
- WALTON, E.K. 1956. Two Ordovician conglomerates in south Ayrshire. Trans. geol. Soc. Glasgow, 22, 133-56.
- WALTON, E.K. 1961. Some aspects of the succession and structure in the Lower Palaeozoic rocks of the Southern Uplands of Scotland. Geol. Rdsch. 50, 63-77.
- WALTON, E.K. 1963. Sedimentation and structure in the Southern Uplands. In: JOHNSON, M.R.W & STEWART, F.H. (eds). The British Caledonides. Oliver and Boyd, Edinburgh, 71-97.
- WALTON, E.K. 1965. Lower Palaeozoic rocks: stratigraphy, palaeogeography and structure. In: CRAIG, G.Y. (ed). The Geology of Scotland. Oliver and Boyd, Edinburgh, 161-227.
- WALTON, E.K. 1967. The sequence of internal structures in turbidites. Scott. J. Geol. 3, 306-17.
- WARSHAW, C.M. & ROY, R. 1961. Classification and a scheme for the identification of layer silicates. Bull. geol. Soc. Am. 72, 1455-92.
- WATSON, S.W. 1976. The sedimentary geochemistry of the Moffat Shales: A carbonaceous sequence in the Southern Uplands. Unpublished Ph.D. thesis, University of St. Andrews.
- WEAVER, C.E. 1961. Clay minerals of the Ouachita structural belt and adjacent foreland. In: FLAWN, P.T., GOLDSTEIN, A.,

- Jr., KING, P.B. & WEAVER, C.E. (eds). The Ouachita Belt. Univ. Texas Publ. 6120, 147-60.
- WEBER, K. 1972a. Kristallinität des Illits in Tonschiefern und andere Kriterien schwacher Metamorphose im nordöstlichen Rheinischen Schiefergebirge. Neues Jahrb. Geol. Paläontol. Abhandlungen, 141, 333-63.
- WEBER, K. 1972b. Note on the determination of illite crystallinity. Neues Jahrb. Mineral. Monatshefte, 6, 267-76.
- WEIR, J.A. 1968. Structural history of the Silurian rocks of the coast west of Gatehouse, Kirkcudbrightshire. Scott. J. Geol. 4, 31-52.
- WEIR, J.A. 1974a. Tectonic style in Lower Palaeozoic rocks: the Clare-south Galway area and the Scottish Southern Uplands contrasted. Sci. Proc. R. Dublin Soc. Ser. A, 5, 107-12.
- WEIR, J.A. 1974b. The sedimentology and diagenesis of the Silurian rocks on the coast west of Gatehouse, Kirkcudbrightshire. Scott. J. Geol. 10, 165-86.
- WEIR, J.A. 1979. Tectonic contrasts in the Southern Uplands. Scott. J. Geol. 15, 169-86.
- WELSH, W. 1964. The Ordovician rocks of North-West Wigtownshire. Unpublished Ph.D. thesis, University of Edinburgh.
- WELSH, W. 1967. The value of point-count modal analysis of greywackes. Scott. J. Geol. 3, 318-28.

- WENTWORTH, C.K. 1922. A scale of grade and class terms for clastic sediments. J. Geol. Chicago, 30, 377-92.
- WILLIAMS, A. 1958. Oblique-slip faults and rotated stress systems. Geol. Mag. 95, 207-18.
- WILLIAMS, A., STRACHAN, I., BASSETT, D.A., DEAN, W.T., INGHAM, J.K., WRIGHT, A.D. & WHITTINGTON, H.B. 1976. A correlation of Ordovician rocks in the British Isles. Spec. Rep. geol. Soc. London, 3, 74 pp.
- WILLIAMS, P.F. 1972. Development of metamorphic layering and cleavage in low-grade metamorphic rocks at Bermagui, Australia. Am. J. Sci. 272, 1-47.
- WILSON, J.T. 1966. Did the Atlantic close and then re-open? Nature. London, 211, 676-81.
- WINKLER, H.G.F. 1974. Petrogenesis of Metamorphic Rocks. Third edition. Springer-Verlag, Berlin, 320 pp.
- WINN, R.D., Jr. & DOTT, R.H., Jr. 1978. Submarine-fan turbidites and resedimented conglomerates in a Mesozoic arc-rear marginal basin in southern South America. In: STANLEY, D.J. & KELLING, G. (eds). Sedimentation in Submarine Canyons, Fans, and Trenches. Dowden, Hutchinson & Ross, Stroudsburg, Pennsylvania, 362-73.
- WISE, S.W., Jr. & WEAVER, F.M. 1974. Chertification of oceanic sediments. In: HSÜ, K.J. & JENKYN, H.C. (eds). Pelagic Sediments: on Land and under the Sea. Spec. Publ. Int.

Assoc. Sedimentol. 1, 301-26.

YODER, H.S. & EUGSTER, H.P. 1954. Syntheses and stability of the muscovites. Am. Mineral. 39, 350-1.

YODER, H.S. & EUGSTER, H.P. 1955. Synthetic and natural muscovites. Geochim. cosmochim. Acta, 8, 225-80.

ZINGG, Th. 1935. Beiträge zur Schotteranalyse. Schweiz. mineral. petrogr. Mitt. 15, 39-140.

Appendix 1: List of graptolite specimens and zone
identification

All specimens were first described and identified by the author and subsequently re-assessed by S. H. Williams, who also interpreted the assemblages in terms of graptolite zones. Graptolite names are in accordance with Strachan (1971). The specimens are stored in the Department of Geology, St. Andrews University.

CAPLE GILL (NS89331885)

Climacograptus sp.

Climacograptus bicornis bicornis (Hall)

Dicellograptus sp.

Dicellograptus sextans sextans (Hall)

Dicranograptus cf. cyathiformis (Elles & Wood)

Dicranograptus rectus (Hopkinson)

Diplograptus multidentis diminutus (Elles & Wood)

?Glyptograptus sp.

Lasiograptus sp.

Orthograptus whitfieldi (Hall)

Specimen nos. 116a₁₋₁₅; 116b₁₋₆

Probably Diplograptus multidentis zone.

CLEUCH BURN (NS90041967)

Climacograptus antiquus antiquus (Lapworth)

Climacograptus bicornis bicornis (Hall)

Climacograptus bicornis tridentatus (Lapworth)

Dicranograptus ziczac (Lapworth)

Diplograptus sp.

Glyptograptus teretiusculus siccatus (Elles & Wood)

Lasiograptus costatus (Lapworth)

Orthograptus sp.

Specimen nos. 29a₁₋₃; 29b₁₋₇

Nemagraptus gracilis zone

KIRK GILL TRIBUTARY (NS91421967)

Climacograptus brevis (Elles & Wood)

Specimen no. 594₁

?Nemagraptus gracilis zone

LAGGEN GILL (NS90661959)

Dicellograptus sextans exilis (Elles & Wood)

Dicranograptus ramosus spinifer (Lapworth)

Specimen nos. 66a₁₋₃

Graptolite zone indeterminate - probably from N. gracilis
or D. multidentis zones.

LAGGEN GILL (NS90341828)

Climacograptus ?bicornis bicornis (Hall)

Dicellograptus sp.

Dicellograptus forchammeri forchammeri (Geinitz)

Dicellograptus sextans exilis (Elles & Wood)

Dicranograptus nicholsoni nicholsoni (Hopkinson)

Dicranograptus rectus (Hopkinson)

Dicranograptus cf. rectus (Hopkinson)

Orthograptus sp.

Orthograptus rugosus apiculatus (Elles & Wood)

Orthograptus truncatus truncatus (Lapworth)

Specimen nos. 407b₁₋₇; 407c₁₋₁₂

Climacograptus peltifer zone

OVERCLEUCH (NS92472026)

Climacograptus sp.

Dicellograptus sp.

Dicranograptus ramosus ramosus (Hall)

Diplograptus sp.

Orthograptus sp.

Orthograptus pageanus micracanthus (Elles & Wood)

Orthograptus quadrimucronatus quadrimucronatus (Hall)

Specimen nos. 840₁₋₈

Dicranograptus clingani zone

OVERCLEUCH (NS92202023)

Climacograptus brevis (Elles & Wood)

Glyptograptus sp.

Orthograptus calcaratus calcaratus (Lapworth)

Orthograptus calcaratus ?rugosus (Lapworth)

Specimen nos. 841₁₋₆

Dicranograptus clingani zone

WINDGATE BURN TRIBUTARY (NS90231389)

Corynoides sp.

Orthograptus calcaratus basilicus (Elles & Wood)

Orthograptus truncatus truncatus (Lapworth)

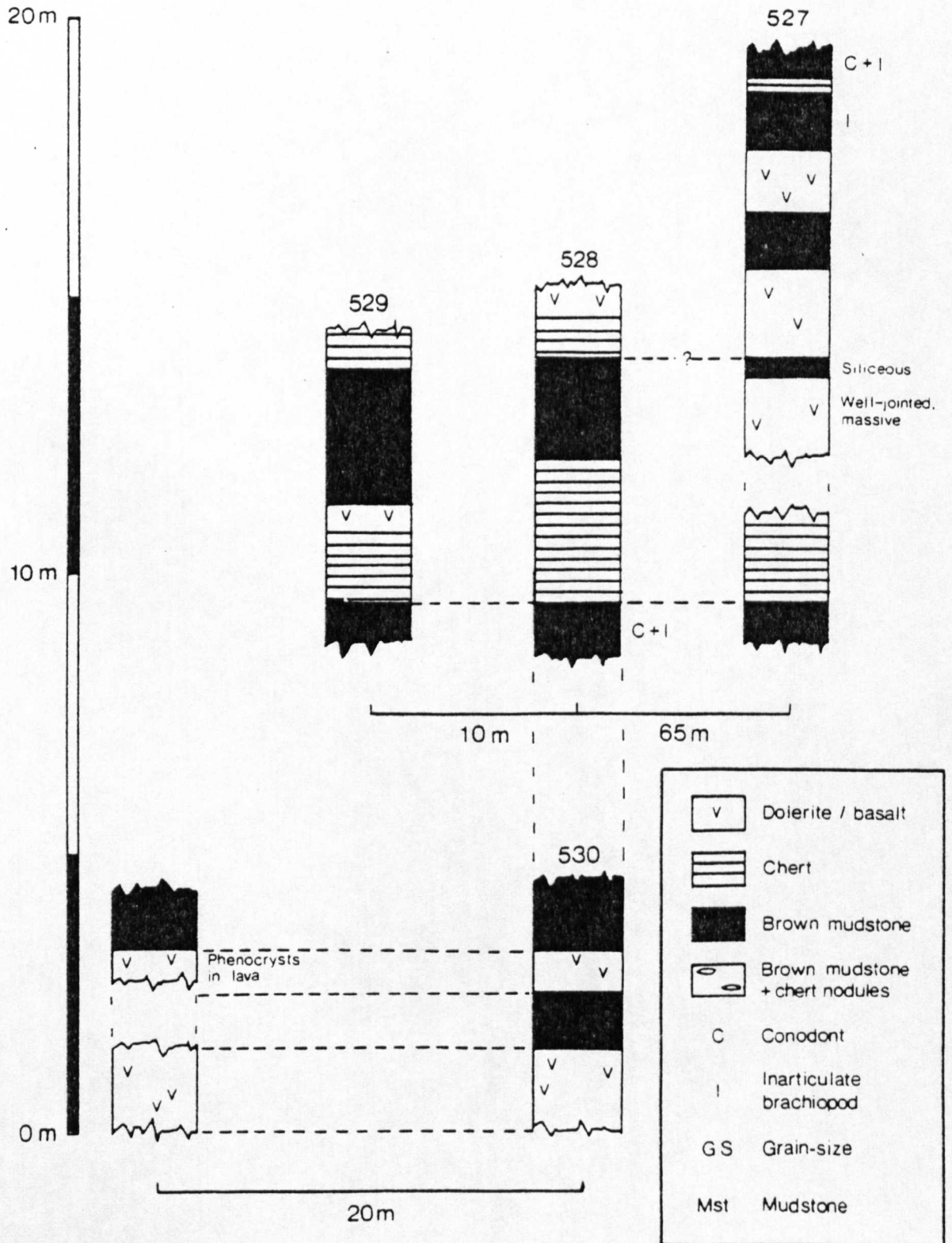
Orthograptus truncatus intermedius (Elles & Wood)

?Leptograptus sp.

Specimen nos. 834₁₋₁₁

?Dicranograptus clingani zone

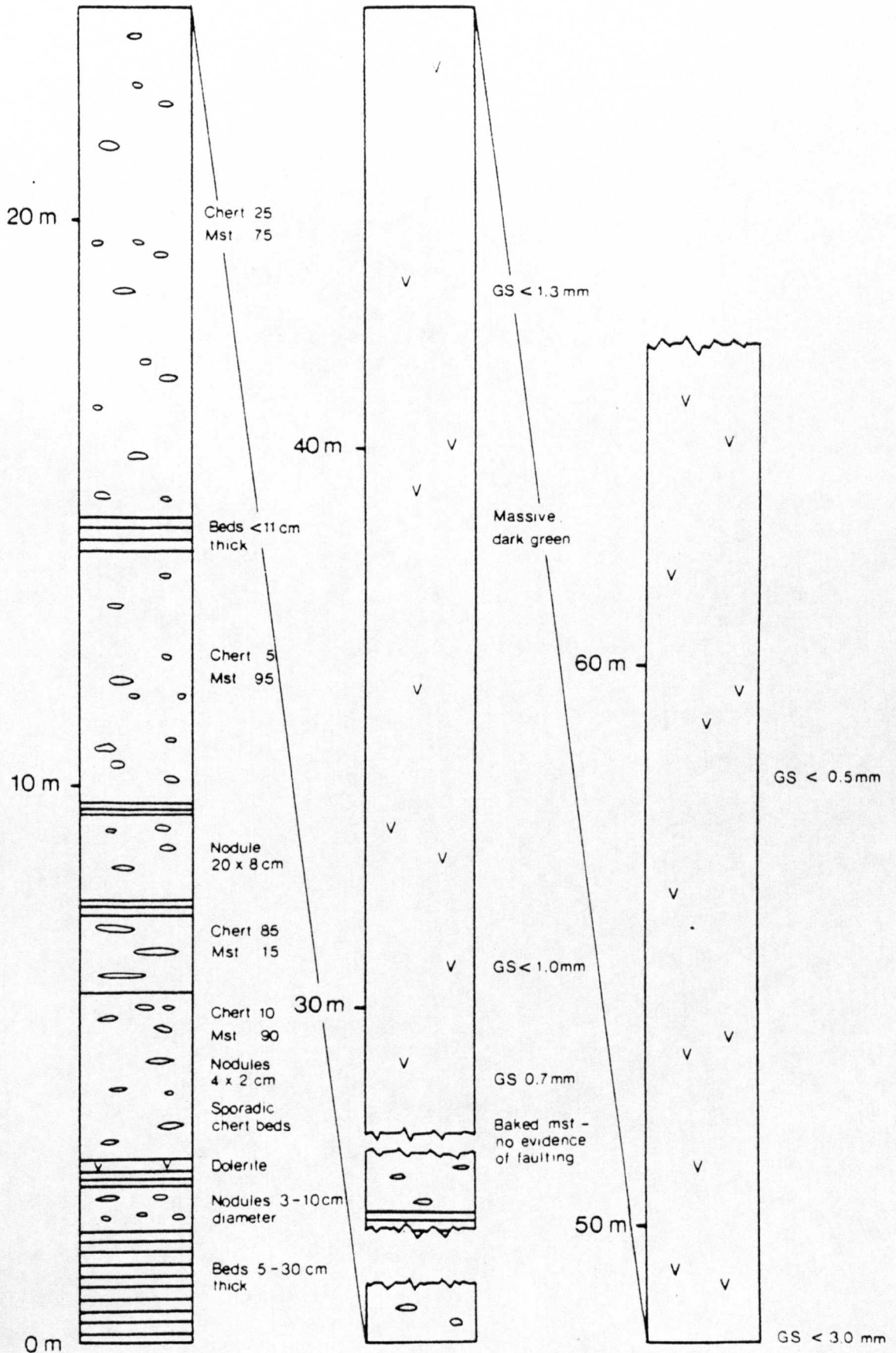
Appendix 2: Four stratigraphical sections through the Raven Gill Formation in the north scarp of Raven Gill (type section)



Appendix 3: Stratigraphical log of the Raven Gill

Formation in Glencaple Burn Chert/mudstone

ratios given; for key, see Appendix 2.



HAGGIS ROCK

Specimen	Q	F	Mi	Fm	B	A	Mm	S	Mx	Qp'	Fa	Ch	Grid Ref.
1 806b	436	62	104	0	30	141	12	17	198	141	0	9	916 263

CRAWFORDJOHN FORMATION

Specimen	Q	F	Mi	Fm	B	A	Mm	S	Mx	Qp'	Fa	Ch	Grid Ref.
1 623	373	65	97	0	38	71	25	41	290	67	4	4	8800 2208
2 624	335	65	96	0	15	49	16	26	398	31	18	7	8799 2212
3 749	517	66	76	0	0	63	66	7	205	63	0	4	8681 2219
Mean	408	65	90	0	18	61	36	25	298	54	7	5	

Q = Quartz (monocrystalline); F = Feldspar; Mi = Mica;
 Fm = Ferromagnesian minerals; B = Basic and intermediate igneous fragments;
 A = Acid igneous fragments; Mm = Metamorphic rock fragments;
 S = Sedimentary rock fragments; Mx = Matrix. Columns Q to Mx sum to 1000.
 Qp' = Quartz (polycrystalline); Fa = Fine acid igneous fragments;
 Ch = Chert fragments.

Appendix 4: Sandstone point count data

ABINGTON FORMATION

	Specimen	Q	F	Mi	Fm	B	A	Mm	S	Mx	Qp'	Fa	Ch	Grid Ref.
1	12b	371	77	26	0	7	64	7	70	378	56	8	0	8998 1983
2	22	412	155	37	0	26	92	31	19	268	92	0	12	9003 1972
3	24	388	78	20	0	0	212	54	59	189	212	0	15	9003 1971
4	64	494	38	44	0	1	13	2	0	408	13	3	0	9068 2012
5	78	353	115	17	0	37	81	15	13	369	81	0	0	8991 1873
6	110	439	88	15	0	2	61	11	0	384	55	6	0	8965 1814
7	125	374	60	6	0	3	29	27	0	501	24	5	0	8938 1876
8	178b	376	153	3	0	3	99	14	5	347	95	4	3	8940 1773
9	183b	491	62	30	0	0	73	18	0	326	61	12	0	8944 1769
10	185	520	48	21	0	8	58	13	2	330	53	5	0	8947 1768
11	188	443	73	13	0	5	47	4	1	414	36	11	0	8951 1763
12	262T	415	106	6	0	5	83	26	4	355	55	28	4	9224 2148
13	274c	421	138	6	1	21	82	16	26	289	72	10	9	9262 2062
14	278i	454	68	4	0	0	48	29	0	397	38	10	0	9270 2029
15	278ii	397	79	6	0	4	71	23	3	417	48	23	0	9270 2029
16	281b	440	89	38	0	23	168	8	6	228	130	38	1	9268 2026
17	346c	369	131	0	0	10	256	6	20	208	225	31	3	9140 2104
18	353c	478	46	31	0	23	125	7	2	288	84	41	1	9149 2067
19	463	257	70	34	0	8	480	24	14	113	470	10	4	9270 2023
20	606a	373	54	62	0	0	24	0	0	487	24	0	0	898 202
21	612	335	63	54	0	7	111	16	8	406	104	7	0	8911 2072
22	618b	417	35	66	0	12	63	9	31	366	60	3	2	8853 2163
23	650	497	64	52	0	7	79	4	24	272	79	0	0	8973 2225
24	655	364	10	94	0	0	6	3	0	523	6	0	0	9111 2288
25	661	368	61	99	0	5	86	11	53	317	76	10	0	9119 2286

cont.

ABINGTON FORMATION (cont.)

Specimen	Q	F	Mi	Fm	B	A	Mm	S	Mx	Qp'	Fa	Ch	Grid Ref.
26	467	41	50	0	23	39	10	33	337	37	2	2	9190 2377
27	466	49	53	0	12	60	4	41	316	45	15	6	9190 2376
28	427	54	72	0	27	57	14	39	310	51	6	0	9129 2358
29	388	43	94	0	31	104	28	21	291	94	10	0	9301 2431
30	384	46	70	0	20	101	31	32	316	91	10	0	9294 2441
Mean	413	72	38	0	11	96	15	17	338	86	10	2	

GLENCAPLE FORMATION

Specimen	Q	F	Mi	Fm	B	A	Mm	S	Mx	Qp'	Fa	Ch	Grid Ref.
1	221	160	10	1	65	66	3	13	461	24	42	1	8864 1656
2	208	329	2	13	24	30	46	38	310	20	10	17	8960 1746
3	151	170	24	75	128	58	7	11	376	45	13	0	8968 1728
4	188	121	37	2	123	49	7	21	452	20	29	0	9255 1958
5	153	247	36	20	153	46	0	24	321	28	18	0	9244 1949
6	125	329	37	12	52	40	6	0	399	25	15	0	9244 1949
7	170	198	36	7	89	45	0	1	454	26	19	0	9243 1956
8	150	150	19	15	94	36	6	4	526	29	7	0	9222 1906
9	307	215	4	0	42	51	43	2	336	33	18	1	9218 1896
10	174	212	12	0	104	93	5	28	372	26	67	18	9219 1878
11	177	188	6	0	153	81	22	73	300	54	27	23	9219 1878
12	182	228	26	0	84	39	0	5	436	22	17	0	9208 1862
13	147	125	61	2	388	42	16	2	217	36	6	0	9286 2008
14	252	89	53	0	155	131	15	77	228	124	7	0	9295 1988
15	115	93	34	38	247	35	2	17	421	35	0	0	9317 1964

cont.

GLENCAPLE FORMATION (cont.)

Specimen	Q	F	Mi	Fm	B	A	Mm	S	Mx	Qp'	Fa	Ch	Grid Ref.
16	159	234	42	0	105	23	2	0	435	23	0	0	957 203
17	124	162	35	4	189	24	12	49	401	24	0	0	957 203
Mean	177	191	28	11	129	52	11	21	379	35	17	3	

ELVAN FORMATION

Specimen	Q	F	Mi	Fm	B	A	Mm	S	Mx	Qp'	Fa	Ch	Grid Ref.
1	97	278	3	75	154	16	4	21	352	3	13	0	8910 1644
2	94	426	9	96	34	42	9	33	257	35	7	0	8961 1513
3	69	258	1	65	140	35	0	61	371	20	15	44	9007 1546
4	119	210	3	78	234	63	8	84	201	53	10	0	9074 1661
5	133	203	61	80	87	27	5	10	394	27	0	0	9069 1668
6	93	213	1	65	123	33	12	40	420	8	25	10	9191 1838
7	113	97	38	85	90	25	2	10	540	25	0	4	9203 1726
8	167	151	36	115	123	14	4	14	376	11	3	0	9202 1733
9	121	195	20	76	127	6	12	8	435	6	0	2	9191 1744
10	103	160	27	116	163	16	7	0	408	16	0	0	958 200
11	127	205	26	106	103	12	4	2	415	12	0	2	9013 1460
Mean	112	218	20	87	125	26	6	26	379	20	7	6	

BASAL ELVAN FORMATION

Specimen	Q	F	Mi	Fm	B	A	Mm	S	Mx	Qp'	Fa	Ch	Grid Ref.
1 731c	118	142	77	7	67	23	13	6	547	23	0	6	9197 1512
2 831	186	93	26	0	55	19	44	43	534	19	0	13	9010 1399
3 839	144	195	103	0	53	14	8	3	480	11	3	0	9034 1397
Mean	149	143	69	2	58	19	22	17	520	18	1	6	

Appendix 5: Petrography and stratigraphical distribution
of sandstone clasts

Polycrystalline quartz: Ubiquitous in all thin sections examined, polycrystalline quartz represents granitic fragments and fragmented vein material. Quartz, with inclusions of vermicular chlorite, occurs in all formations.

Microgranite: Microgranite clasts are equigranular and consist of subhedral to anhedral quartz and orthoclase + plagioclase + microcline + epidote + muscovite. Ferromagnesian minerals are typically absent. Feldspars are often strongly sericitised. HAGGIS ROCK; CRAWFORDJOHN FM.; ABINGTON FM.; GLENCAPLE FM.; ELVAN FM.

Granophyre: Rare clasts of aphyric granophyre, consisting of micrographically intergrown quartz and feldspar have been observed in some coarse-grained lithologies. HAGGIS ROCK; GLENCAPLE FM; ELVAN FM.

Rhyolite: Commonly represented in the acid clast component, rhyolites are generally porphyritic, with subhedral to anhedral phenocrysts of quartz ± orthoclase and, more rarely, plagioclase and muscovite. Internal relief is seen between feldspar and quartz grains (cf. Dickinson et al. 1979). The groundmass consists of a granular, microcrystalline aggregate of quartz and feldspar. HAGGIS ROCK; CRAWFORDJOHN FM.; ABINGTON FM.; GLENCAPLE FM.; ELVAN FM.

Quartz porphyry fragments are monomineralic, with rounded phenocrysts of anhedral quartz set in a cryptocrystalline groundmass. ABINGTON FM.; GLENCAPLE FM.; ELVAN FM.

Keratophyre: Keratophyres are rare, and are formed from equigranular, subhedral plagioclase and K- feldspars. Plagioclase laths occasionally define a trachytic texture. The presence of anhedral quartz identifies these as quartz-keratophyres. HAGGIS ROCK; ABINGTON FM.; ELVAN FM.

'Intermediate' lavas: These are characterised by the absence of ferromagnesian minerals and the presence of microlitic plagioclase feldspar which occurs both as a phenocryst and a groundmass phase. Trachytic textures are typically developed, defined by the parallel orientation of plagioclase laths. HAGGIS ROCK; CRAWFORDJOHN FM.; ABINGTON FM.; GLENCAPLE FM.; ELVAN FM.

Dolerite/diorite: Albitisation of the plagioclase with the accompanying formation of carbonate precludes the distinction between dolerite and diorite. Numerically subordinate to 'basalts', these lithic fragments are composed of plagioclase, clin amphibole, clinopyroxene and minor amounts of pseudomorphs after olivine. The green and brown pleochroic amphibole ($c^{\wedge} Z = -15^{\circ}$) poikilitically encloses the olivine pseudomorphs, subhedral, colourless to green pyroxene and plagioclase feldspar. ABINGTON FM.; ELVAN FM.

Basalt/andesite: The 'basalts' are typically porphyritic, with a phenocryst assemblage dominated by laths of plagioclase, although euhedral, colourless clinopyroxene and green/brown clinoamphibole frequently occur. Plagioclase is the main component of the groundmass, which is micro- or cryptocrystalline. The feldspar laths in both matrix and phenocryst assemblages frequently define a trachytic texture. GLENCAPLE FM.; ELVAN FM.

Spilite: Thin sections show euhedral plagioclase (albite) phenocrysts in a cryptocrystalline groundmass of light brown ferruginous or green chloritic aggregates with anomalous first order blue polarisation colours. Opaque minerals are ubiquitous, finely disseminated throughout the groundmass. The feldspar is usually severely altered, with compositional twinning destroyed and only the outline of the laths preserved. Trachytic textures are observed infrequently. HAGGIS ROCK; CRAWFORDJOHN FM.; ABINGTON FM.; GLENCAPLE FM.; ELVAN FM.

Metaquartzite: Metaquartzites are recognised by the presence of strained and elongated quartz crystals interlocked in a mosaic by highly sutured grain boundaries. Mineral assemblages include quartz + plagioclase + orthoclase + muscovite + chlorite. HAGGIS ROCK; CRAWFORDJOHN FM.; ABINGTON FM.; GLENCAPLE FM.; ELVAN FM.

Schist: Fragments showing a single penetrative fabric are predominantly muscovitic in composition, but quartz + muscovite, quartz + muscovite + chlorite and quartz + biotite + muscovite assemblages also occur. Crenulated muscovite schists are less common. HAGGIS ROCK; CRAWFORD-JOHN FM.; ABINGTON FM.; GLENCAPLE FM.; ELVAN FM.

Black mudstones consist of isolated quartz grains and mica flakes of coarse silt-grade and less set in a black carbonaceous matrix. The sediment is massive, apart from the sporadic occurrence of circular polycrystalline quartz- and mica-filled cavities, presumed to be remnants of radiolaria. HAGGIS ROCK; ABINGTON FM.; ELVAN FM.

Chert: Grey and black varieties are represented, comprising isolated ghosts of radiolarian tests set in a cryptocrystalline matrix of quartz with a little muscovite and chlorite. The rock is characteristically cut by quartz/chalcedony veins. Black cherts, rich in carbonaceous material, have been observed to contain flattened radiolaria. All cherts contain minor amounts of argillaceous impurities. HAGGIS ROCK; CRAWFORD-JOHN FM.; ABINGTON FM.; GLENCAPLE FM.; ELVAN FM.

Sandstone/siltstone: The most common sedimentary clast type, siltstones and fine sandstones form rafts which vary in size from less than a millimetre up to tens of centimetres in diameter; this material often penetrates between other grains, indicating that the clasts had not been lithified before transport. In the Elvan and Glencaple Formations, the clasts differ in composition from the enclosing sediments by containing an abundance of quartz and mica fragments.
HAGGIS ROCK; CRAWFORDJOHN FM.; ABINGTON FM.; GLENCAPLE FM.; ELVAN FM.

Carbonate occasionally forms the matrix of the greywackes and also occurs as replacement inclusions within feldspar.
HAGGIS ROCK; ABINGTON FM.; GLENCAPLE FM.; ELVAN FM.

Monomineralic fragments:

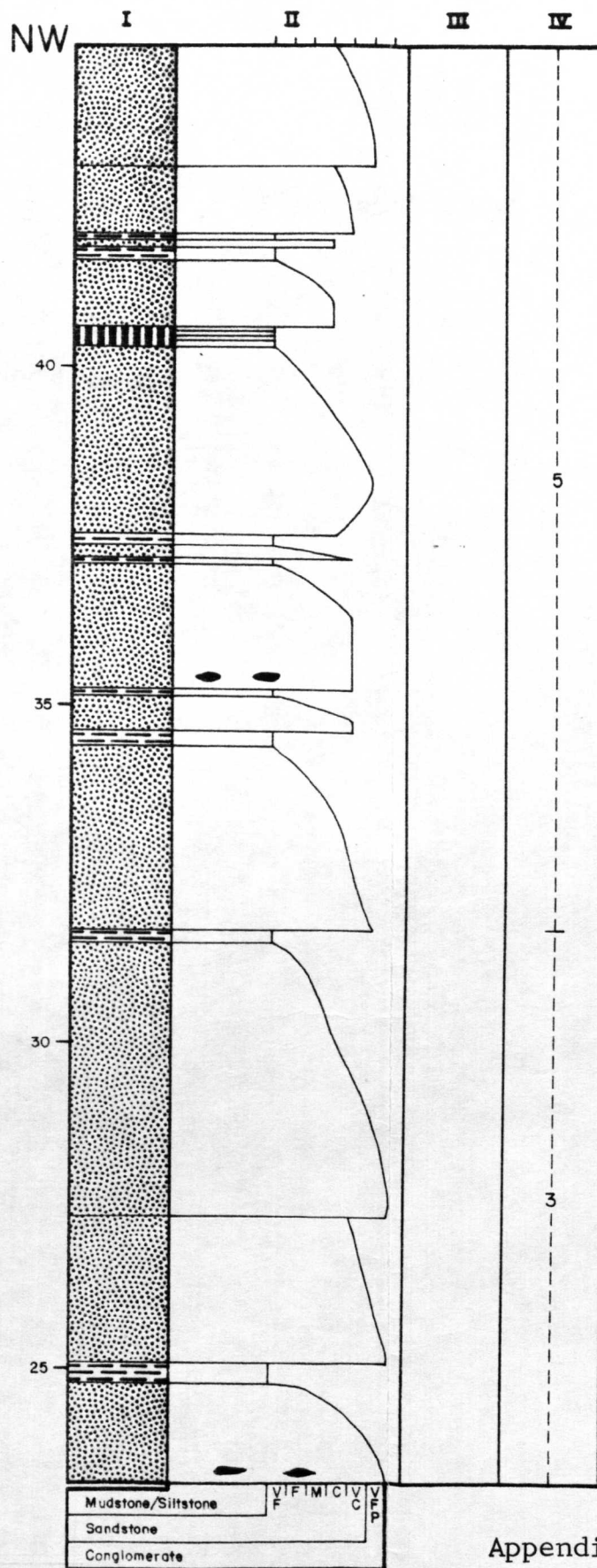
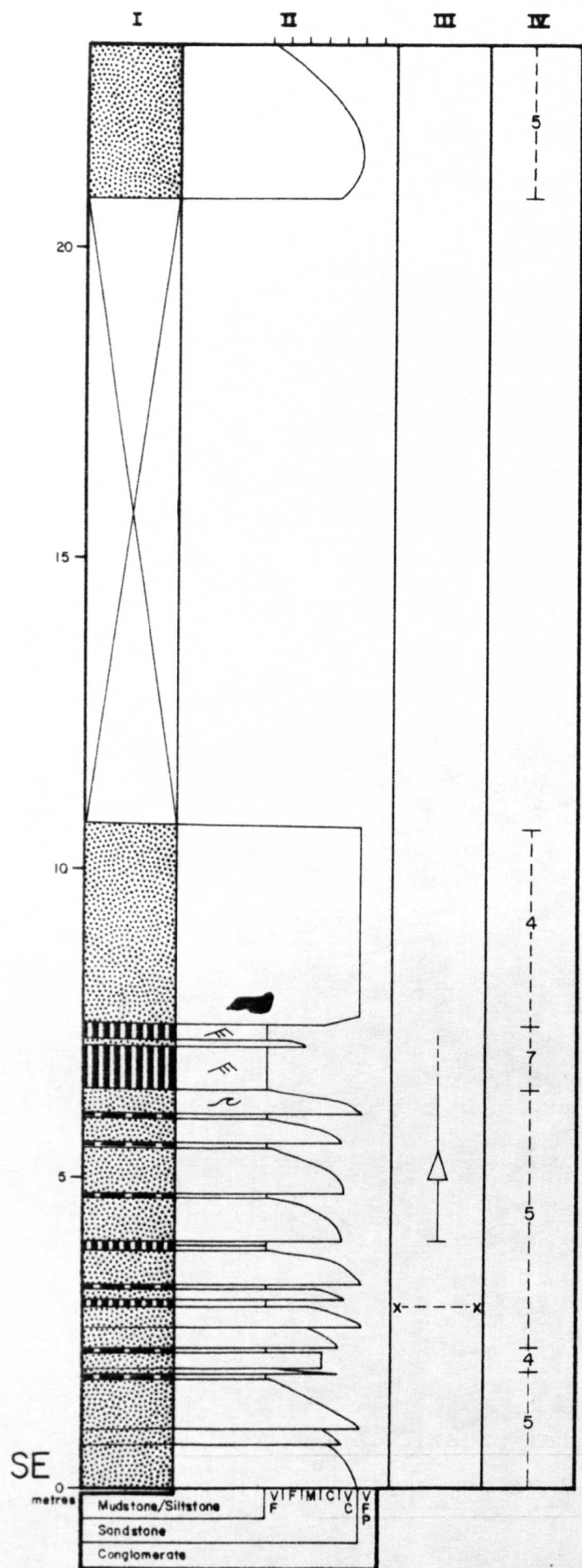
Haggis Rock: K- feldspar, plagioclase, muscovite.

Crawfordjohn Fm.: K- feldspar, plagioclase, muscovite, biotite, chlorite.

Abington Fm.: K- feldspar, plagioclase, microcline, muscovite, biotite, chlorite, garnet, epidote, picotite.

Glencaple Fm.: K- feldspar, plagioclase, microcline, muscovite, biotite, chlorite, epidote, clinoamphibole, clinopyroxene, picotite, prehnite.

Elvan Fm.: K- feldspar, plagioclase, microcline, muscovite, biotite, chlorite, epidote, glaucophane, clinoamphibole, clinopyroxene, olivine.



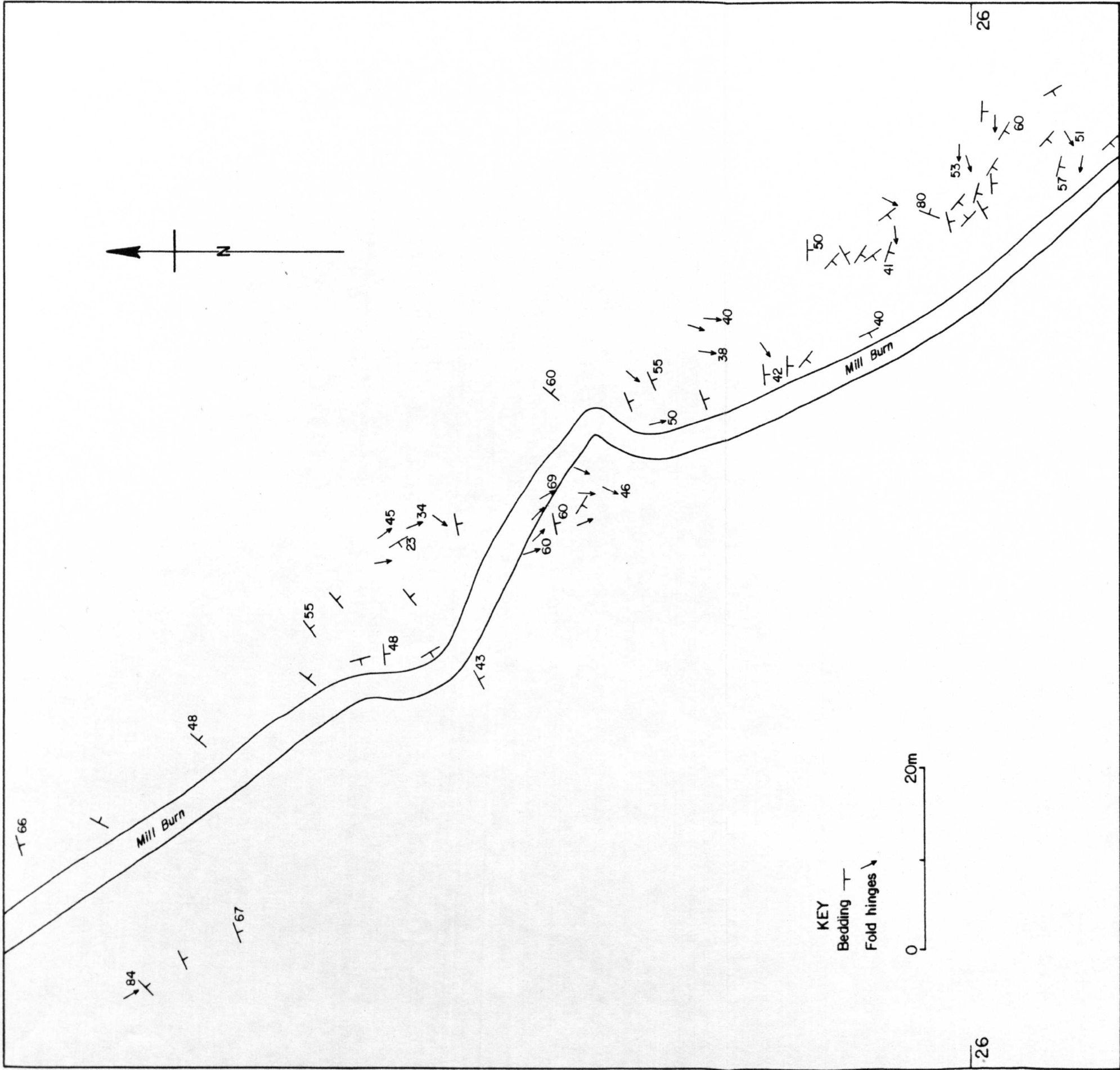
Lithology	I
Sandstone	
Grey mudstone	
Laminite	
Covered	

Structure, grain-size	II
No structure visible	
Ripples	
Parallel lamination	
Flames, load cast	
Intraclasts	
Wentworth scale	

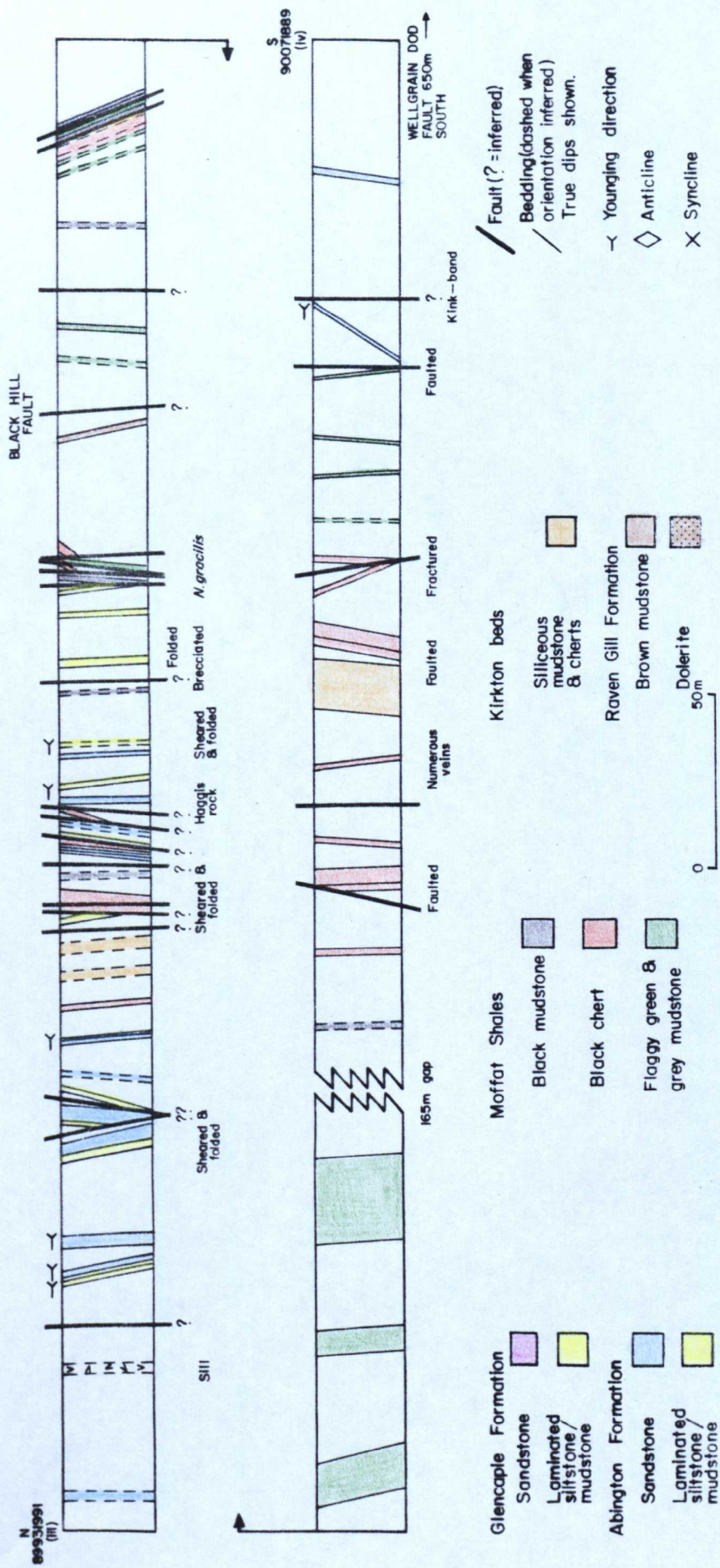
Further observations	III
Thinning and fining upwards sequence	
Fault	

Facies	IV
Organised pebbly sandstone	3
Massive sandstone	4
Graded sandstone	5
Laminite	7

Appendix 6: Sedimentological profile of the Abington Formation in Craighead Quarry

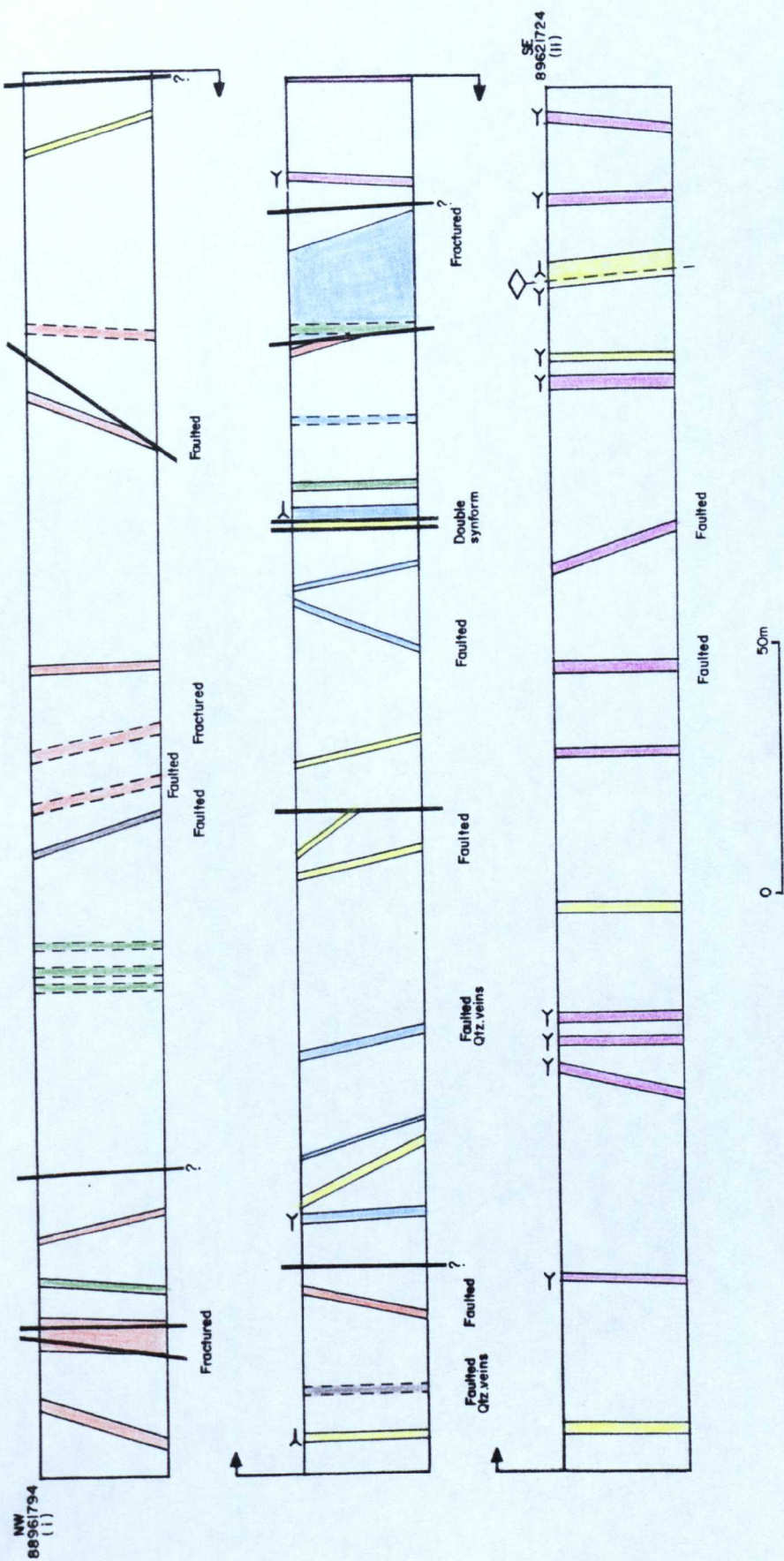


Appendix 7: Field map of structures in Mill Burn



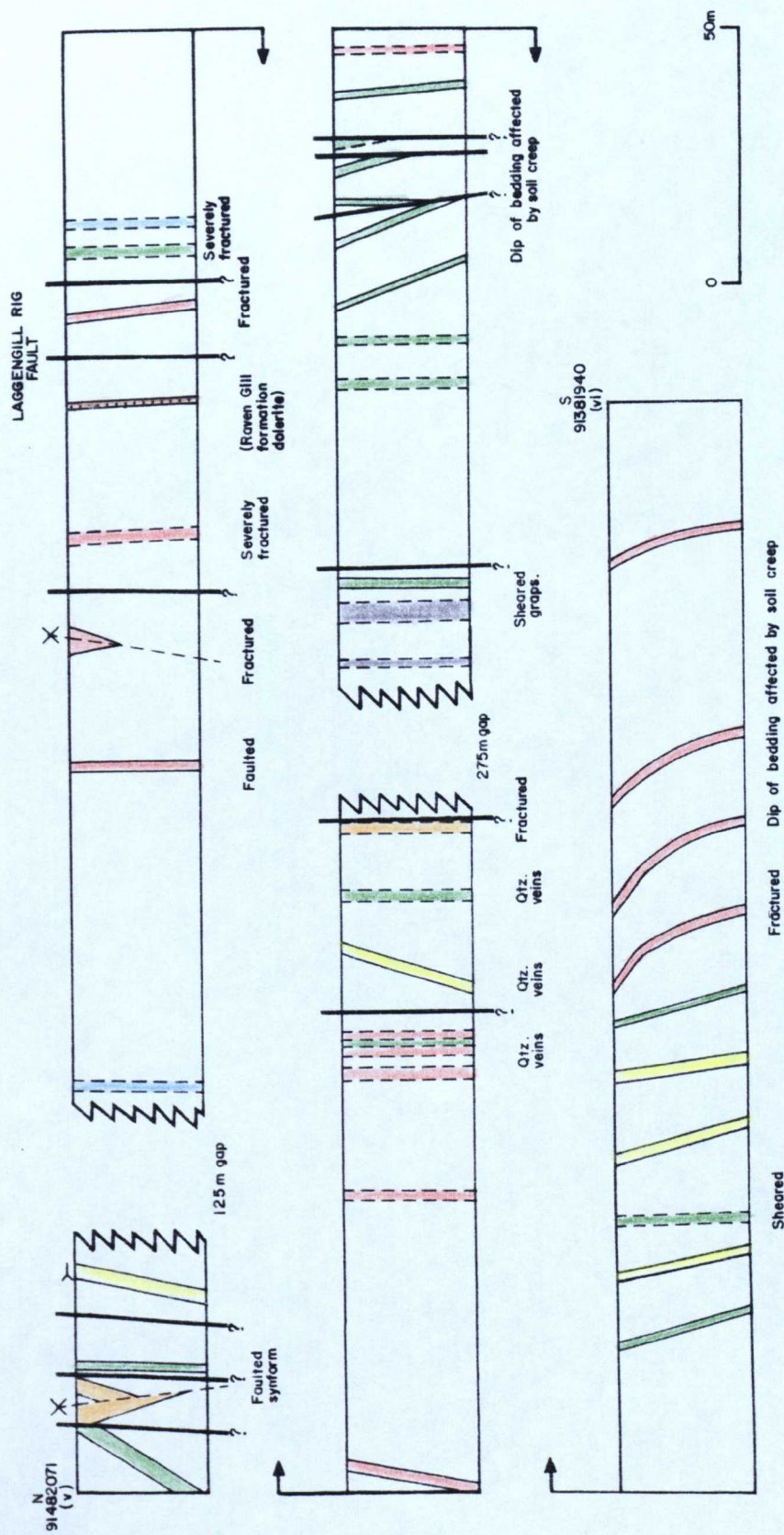
Appendix 8: Structural profile through part of the Leadhills Imbricate Zone in Cleuch Burn.

Location of line of section shown on Fig. 24.



Appendix 9: Structural profile through part of the Leadhills Imbricate Zone in Bellgill Burn and Middle Grain. For key, see Appendix 8. Line of section shown on

Fig. 24.



Appendix 10: Structural profile through part of the Leadhills Imbricate Zone in Kirk Gill.

For key, see Appendix 8. Location of line of section shown on Fig. 24.

Appendix 11: Preparation of -2 μ m fraction for X-ray diffraction studies

Samples (approximately 300 g) of sandstone, laminite or mudstone were chosen for the lack of weathering apparent in hand specimen. Veins and surfaces (usually cleavage or joint planes) showing any visible weathering effects were removed using a 6 inch diamond wheel. Areas of internal weathering were cut away with a saw, and any weathered remnants ground away with diamond rotary lap. Material was crushed to chips (1-2 cm) and washed in distilled water, dried, then ground in a Tema-mill for 1 minute. Further disaggregation was obtained by placing powder/water mixtures in an ultrasonic bath for 20 minutes.

The slurry was then transferred to a water-filled glass cylinder 45 cm in length and shaken to ensure thorough mixing. After 8 hours the suspension (containing -2 μ m fraction) was either siphoned off, or poured directly into an open dish and left to stand for a minimum of 16 hours (Twenhofel & Tyler 1941). The suspension (containing -1 μ m fraction) was removed, leaving a clay slurry representing the 1-2 μ m separate. The paste was then smeared onto a glass slide and air dried.

If the amount of clay produced by this method was not sufficient to coat a glass slide, the entire sedimentation

process was repeated until the required quantity was obtained. This technique was found to be ineffective with certain sandstones and black mudstones.

For analyses involving normal (unorientated), glycolated and heated sample preparations, the above method was inefficient in producing suitable quantities of material, and the $-8\mu\text{m}$ fraction was generally used (sedimentation time 31 minutes).

Appendix 12: Instrumental conditions used for clay mineral determinations

Source $\text{CuK}\alpha$; normal focus ; Ni filter

Slit 1° - 0.2 - 1° : Chart speed 600 mm/h

Angular goniometer speed $0.5^\circ/\text{min}$: Scan 5° - $63^\circ 2\theta$

36kV, 18mA : Time constant 2s : Z = 3

Runs of glycolated and heated specimens were generally made from 5° - $35^\circ 2\theta$. To check for the presence of mixed layering, samples were treated with ethylene glycol for 1 hour, and heated to 550°C for 2 hours. Unorientated powders (dry and heated) were examined using aluminium sample holder; glycolated specimens were mounted on glass slides.

Appendix 13: $d(002)_{2M}$, $d(060)$ and b values of illite. Measurements in Å.

Specimen	Lithology	$d(002)_{2M}$			$d(060)$	b
		Normal	Glycolated	550°C		
21	Bl. mst.	-	10.063	10.018	1.499	8.994
27	Mst.	9.950	9.950/ 10.029*	10.075	1.500	9.000
29c	Bl. mst.	9.995	10.052	10.132	1.503	9.018
29d	Bl. mst.	10.063	-	10.040	1.503	9.018
61	Silty mst.	10.052	10.029	10.018	1.496	8.976
176d	Mst.	9.984	10.018/ 10.029*	10.075	1.501	9.006
189	Sst.	-	9.961	-	-	-
191a	Sst.	9.961	10.006	-	-	-
193	Sst.	10.029	10.029	10.086	1.501	9.006
261	Sst.	9.995	-	10.018	1.504	9.024
272	Silty mst.	10.063	-	10.075	1.501	9.006
281	Pyrit. mst.	-	10.086	10.006	-	-
392	Sst.	9.917	10.040	10.006	-	-
407b	Bl. mst.	9.883	10.029	10.097	1.502	9.012
409	Sst.	-	10.202	-	1.504	9.024
417	Sst.	-	10.063	-	1.502	9.012
421	Sst.	9.984	-	-	-	-
627	Sst.	9.972	-	-	1.506	9.036
702b	Mst.	-	-	-	1.503	9.018
827	Sst.	-	-	-	-	-

* Runs of two separate samples from the same locality.
 Not all specimens contain illite in sufficient quantities for determination of parameters.

Appendix 14: Location of first four basal reflections of chlorite (\AA) and peak position of (001) after ethylene glycol and heat treatments. (Lower sets of figures are intensity values).

Specimen	Lithology	001	002	003	004	001 _{glycol.}	001 _{550°C}
21	Bl. mst.	14.718	7.207	4.741	3.520	14.408	13.951
		63	84	37	100		
27	Mst.	14.040	7.801	4.687	3.531	14.175	14.000
		26	100	31	68		
29c	Bl. mst.	14.130	7.098	4.726	3.535	14.718	14.018
		26	50	31	100		
29d	Bl. mst.	14.173	7.104	4.734	3.542	-	13.951
		50	60	27	100		
61	Silty. mst.	14.040	7.363	4.729	3.535	14.290	13.886
		86	100	43	100		
176d	Mst.	14.130	7.098	4.709	3.538	13.907	13.713
		17	100	30	74		
191a	Sst.	13.864	7.059	4.711	3.535	14.383	-
		15	100	29	73		
193	Sst.	14.198	7.064	4.714	3.537	14.221	13.864
		48	100	38	100		
261	Sst.	14.085	7.104	4.726	3.534	-	13.777
		52	100	30	83		
272	Silty. mst.	14.234	7.109	4.714	3.541	-	14.040
		34	100	27	86		
392	Sst.	14.221	7.115	-	3.550	14.313	13.756
		23	100	26	64		
407b	Bl. mst.	14.359	7.081	4.667	3.523	14.221	?12.083
		100	55	37	80		
409	Sst.	14.175	7.121	4.731	3.543	14.175	13.973
		37	100	28	70		
417	Sst.	14.152	7.075	4.739	3.542	14.267	13.756
		27	100	31	63		
421	Sst.	14.244	7.081	4.726	3.543	14.306	13.791
		35	100	36	84		
627	Sst.	14.290	7.098	4.729	3.541	-	-
		29	99	41	100		
702b	Mst.	14.866	6.959	4.731	3.541	-	-
		41	100	31	82		
827	Sst.	14.062	7.087	4.701	3.537	-	-
		27	100	39	84		

Appendix 15: Chlorite species, as inferred from intensity ratios of (001) to (005) basal reflections

Specimen	Lithology	$\frac{I(002)+I(004)}{I(003)}$	$\frac{I(003)}{I(005)}$	Chlorite ¹ species
21	Bl. mst.	4.97		Ripidolite
27	Mst.	5.42		"
29c	Bl. mst.	4.84	1.47	"
29d	Bl. mst.	5.93		"
61	Silty mst.	4.65	0.50	?
176d	Mst.	5.80	2.50	Ripidolite
191a	Sst.	5.96	1.53	"
193	Sst.	5.26		"
261	Sst.	6.10		"
272	Silty mst.	6.85		?
392	Sst.	6.10	2.25	Ripidolite
407b	Bl. mst	3.65		Sheridanite
409	Sst.	6.07		Ripidolite
417	Sst.	5.26	2.82	"
421	Sst.	5.11		"
627	Sst.	4.85		"
702b	Mst.	5.87		"
827	Sst.	4.72		"

¹ Correspondence between intensity ratios and chlorite species after Post & Plummer (1972), i.e:

Chlorite species	$\frac{I(002)+I(004)}{I(003)}$		$\frac{I(003)}{I(005)}$	
	lowest values	highest values	lowest values	highest values
Ripidolite	4.79	6.53	2.23	3.20
Sheridanite	2.63	3.89	3.13	4.06

Appendix 16: Illite crystallinity: experimental methods
and factors controlling half-peak width

The following sections describe variations in IC according to sample preparation technique (a), grain-size (b) and instrumental conditions (c); instrumental conditions used in the determination of IC throughout the study are given in (d).

(a) Sample Preparation Technique

-2 μ m fraction from one hand specimen mounted for XRD according to three different preparation techniques; variability in half-peak width assessed for 10 \AA mica.

172c(i): -2 μ m fraction allowed to sediment directly onto glass slide (strong preferred orientation of micas).

172c(ii): -2 μ m fraction sedimented onto bottom of glass dish - water poured off after 24 h, then sediment air dried. Sediment scraped from dish and mounted on glass slide with acetone and allowed to dry (moderate preferred orientation of micas).

172c(iii): Sample prepared from same powder as 172c(ii) and placed, loosely packed, into aluminium sample holder (weak preferred orientation of mica).

Time constant:

Specimen	Time constant (TC)					
	0.5	1	2	4	8	16
Kübler 31	0.16	0.19	0.20	0.26	0.37	0.53

Peak width broadens as TC increases.

Voltage:

Voltage	IC($^{\circ}2\theta$)	\bar{X}	s					
Kübler 31	{ 36kV(18mA)	0.24	0.22	0.24	0.18	0.18	0.212	0.03
	{ 40kV(22mA)	0.20	0.20	0.18	0.20	0.20	0.196	0.01
Kübler 33	{ 36kV(18mA)	0.42	0.42	0.40	0.42	0.41	0.414	0.01
	{ 40kV(22mA)	0.42	0.42	0.40	0.40	0.42	0.412	0.01

IC values consistent with those of the Kübler standards were produced at voltages equivalent to those used at Neuchâtel (i.e. 40 kV); less variation between runs occurred at the higher voltage setting.

Divergence slits: Although a 1° divergence slit was used for all sample runs, it was found that a $\frac{1}{2}^{\circ}$ slit consistently produced Hb_{rel} values 3% lower than larger one (L.J. Thomas, pers. comm. 1981). This variation is minimal, and use of different slits by various laboratories would not be expected to augment difficulties in inter-lab. correlations.

Peak width:

Sample	Orientation	IC($^{\circ}2\theta$)					\bar{X}	s
172c(i)	strong	0.28	0.28	0.32	0.28	0.32	0.298	0.02
172c(ii)	moderate	0.50	0.48	0.55	0.60	0.54	0.534	0.05
172c(iii)	weak	0.48	0.83	0.56	0.40	0.60	0.574	0.16

Peak intensity:

Sample	Orientation	Peak Position ($^{\circ}2\theta$)	Counts per second (averaged over 10 sec. interval)						\bar{X}	s
172c(i)	strong	8.80	205	206	207	209	213	208	3.16	
172c(ii)	moderate	8.80	101	99	91	103	101	99	4.69	
172c(iii)	weak	8.78	75	73	75	76	75	75	1.09	

Runs: 40kV22mA; 1200mm/h; scan 7.4° - $10^{\circ}2\theta$; TC = 2;
Z = 3; HV = 408; LL235W140; $2^{\circ}/\text{min}$; 4×10^2

Half-peak width is a function of preparation technique - strongly orientated mount shows more intense and sharper peak, combined with better reproducibility. Weakly orientated mounts confused with background radiation (Bremstrahlung), reducing clarity of peak definition.

(b) Grain-Size

Samples of five grain-size intervals prepared for 20 specimens by sedimentation in glass cylinders. Each IC

value in table below represents mean of a minimum of 5 runs per sample. Samples run in random order, and not in numerical sequence of table below.

Runs: 40kV22mA; 1200mm/h; scan 7.3-10.3°; TC = 2; Z = 3;
 HV = 408; LL235W140; 2°/min; 2×10^2 - 4×10^3

Spec. no.	Lithology	Grain size interval (μm)				
		~ 1-2	2-4	4-8	8-16	16-32
172c	lam.	0.288	0.306	0.264	0.282	0.284
176	mst.	0.292	0.268	0.256	0.236	0.254
178	mst.	0.322	0.260	0.270	0.292	0.254
189	sandst.	0.266	0.264	0.254	0.268	0.200
191	mst.	0.310	0.250	0.264	0.248	0.244
261	mst.	0.318	0.310	0.284	0.282	0.274
272	lam.	0.346	0.320	0.284	0.272	0.258
293	sandst.	0.264	0.228	0.270	0.248	0.286
380	mst.	0.320	0.306	0.272	0.266	0.246
392	sandst.	0.325	0.302	0.280	0.248	-
407	bl. mst.	0.334	0.318	0.320	0.296	0.306
421	sandst.	0.260	0.282	0.304	0.226	0.244
482	sandst.	0.312	0.306	0.302	0.280	0.272
498	sandst.	0.342	0.326	0.280	0.266	-
627	lam.	0.312	0.346	0.296	0.302	0.296
667	mst.	0.374	0.304	0.362	0.324	0.310
688	mst.	0.374	0.334	0.334	0.312	0.306
702	mst.	0.313	0.274	0.280	0.312	0.230
827	mst.	0.298	0.306	0.332	0.332	0.322
837a	mst.	0.276	0.252	0.234	0.252	0.262

mst. = mudstone; bl. mst. = black mudstone; lam. = laminite; sandst. = sandstone.
 IC values in $^{\circ}2\theta$.

IC depends on grain-size; 18 out of 20 specimens give narrower peaks for 16-32 μm fraction when compared to 1-2 μm

fraction. 14 specimens show broadest peak within 1-2 μ m fraction. Values of coarsest-grained separate commonly plot within epizone.

(c) Instrumental Conditions

Variations in IC at different chart speeds can be normalised by measurement in units of $^{\circ}2\theta$ rather than mm (Kisch 1978).

Scanning (goniometer) speed:

Specimen no.	Scanning speed ($^{\circ}2\theta/\text{min}$)					
	4 $^{\circ}$	2 $^{\circ}$	1 $^{\circ}$	0.5 $^{\circ}$	0.25 $^{\circ}$	0.125 $^{\circ}$
(a) Kübler 31	0.24	0.20	0.18	0.16	0.16	0.15
(b) 193	0.62	0.42	0.32	0.29	0.27	0.28

Variation of IC with scanning speed

Runs: 40kV22mA; 1200 mm/h; scan 7.4 $^{\circ}$ -10.2 $^{\circ}2\theta$; Z = 3;
 (a) TC = 2; 4×10^3 ; (b) TC = 4; 2×10^2

Peak width broadens with increasing goniometer speed (in agreement with Kisch 1980, p. 275).

(d) Instrumental Conditions used in Illite Crystallinity Study

Source $\text{CuK}\alpha$: normal focus : Ni filter

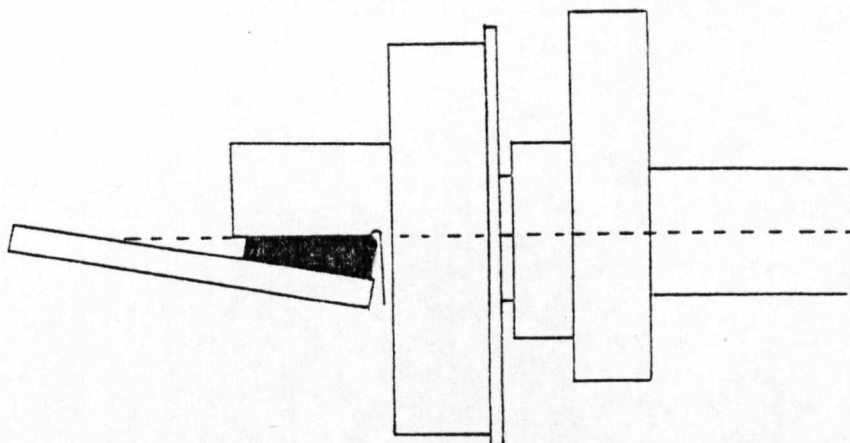
Slit 1° - 0.2 - 1° : Chart speed 1200 mm/h

Angular goniometer speed 2° /min : Scan 7.4° - $10.2^\circ 2\theta$

40kV, 22mA : Time constant 2s : Z = 3

Philips PW1012/20 diffractometer

Appendix 17: Emplacement of wedge-shaped standard
(Kübler 33) on specimen holder



Standard consists of thin section of slate (cut parallel to schistosity) on which metal plate has been glued (black on diagram), allowing an incorrect orientation of approximately 5° with incident X-rays. Illite crystallinity values of slate analagous to epimetamorphic domain.

Appendix 18: Measurement of illite crystallinity

1. At start of run, 5 measurements were taken on the illite (001) peak of Kübler standards 31 and 33 to effect comparability with diffractometer at Neuchâtel.
2. This was repeated for the quartz (100) peak.
3. The sample series was then run, taking at least 5 measurements per specimen from 7.4° - $10.2^{\circ}2\theta$. Each sample series was of approximately $2\frac{1}{2}$ h duration.
4. (1) was repeated to check for possible instrumental fluctuations.
5. At a later period, each specimen was run twice between 7.4° - $10.2^{\circ}2\theta$ and 16.7° - $20.5^{\circ}2\theta$ to determine the illite (002) : illite (001) intensity ratio (Esquevin 1969).

Appendix 19: Accuracy and precision of electron
microprobe data

All analyses were performed at the Grant Institute of Geology, Edinburgh University, using the energy-dispersive electron microprobe. Calibration was monitored by a cobalt standard; accuracy was estimated by analysing a jadeite standard prior to the commencement of each session. Precision is $\pm 1\%$ at the 50% concentration level, $\pm 2\%$ at the 10% level and $\pm 10\%$ at the 2% level (P. G. Hill, pers. comm. 1979).

Appendix 20: Electron probe microanalyses of
pumpellyite

	1	2	3	4
SiO ₂	36.29	36.80	36.34	36.74
Al ₂ O ₃	23.26	22.08	20.17	23.76
FeO *	7.73	8.01	11.70	6.79
MnO	-	-	0.20	-
MgO	1.67	2.09	1.76	1.92
CaO	22.42	22.82	22.12	22.51
Total	92.37	91.80	92.28	91.72
16 cations				
Si	6.11	6.06	6.03	6.03
Al	4.49	4.29	3.95	4.60
Fe ²⁺	1.06	1.10	1.62	0.93
Mn	-	-	0.03	-
Mg	0.41	0.51	0.44	0.47
Ca	3.93	4.03	3.93	3.96
Total	16.00	16.00	16.00	16.00
Al	75.3	72.7	65.8	76.7
Fe	17.8	18.6	26.9	15.5
Mg	6.9	8.6	7.3	7.8

All analyses from Raven Gill Fm. dolerite. 1-2 from veins, 3-4 from amygdale.

* Total iron as Fe²⁺

Appendix 21: Electron probe microanalyses of prehnite

	1	2	3	4	5
SiO ₂	44.85	43.64	43.44	42.41	41.65
Al ₂ O ₃	23.52	24.25	24.28	22.76	21.61
Fe ₂ O ₃ *	0.23	0.36	0.28	1.12	2.74
MnO	0.13	-	-	-	-
CaO	25.98	27.08	26.54	26.95	26.35
Total	94.72	95.33	94.53	93.24	92.35
Number of ions on the basis of 22 oxygens					
Si	6.19	6.02	6.03	6.02	6.03
Al	3.83	3.94	3.97	3.81	3.69
Fe ³⁺	0.03	0.04	0.03	0.13	0.33
Mn	0.02	-	-	-	-
CaO	3.84	4.00	3.95	4.10	4.09
Total	13.90	14.01	13.99	14.07	14.13

All analyses of vein prehnite from Elvan Fm. sandstones.

* Total iron as Fe³⁺

Appendix 22: Electron probe microanalyses of chlorites

	1	2	3	4	5	6	7	8	9	10	11	12	13	14
SiO ₂	31.15	27.35	28.62	25.56	26.52	22.97	26.20	30.41	31.72	29.59	30.27	27.21	24.04	25.65
Al ₂ O ₃	14.22	19.00	11.86	19.10	17.42	20.79	18.57	14.21	14.90	16.96	15.01	19.20	20.71	18.93
Cr ₂ O ₃	-	-	0.24	-	-	-	-	-	-	-	-	-	-	-
FeO*	22.17	26.19	24.89	27.09	29.42	33.38	25.75	22.75	21.24	21.98	22.79	23.30	31.95	32.02
MnO	0.32	0.47	0.32	0.27	0.52	0.33	0.48	0.16	0.44	0.31	0.35	0.51	0.47	0.47
MgO	19.99	15.17	17.96	14.15	12.67	8.52	15.22	18.45	20.00	19.07	18.02	17.47	9.58	11.00
CaO	-	-	0.27	-	-	-	-	-	-	-	-	-	-	-
Total	87.86	88.19	84.17	86.18	86.55	86.00	86.23	85.99	88.31	87.93	86.43	87.69	86.76	88.07
Number of ions on the basis of 28 oxygens														
Si	6.41	5.75	6.33	5.55	5.81	5.20	5.65	6.42	6.45	6.08	6.36	5.67	5.34	5.95
Al	3.45	4.71	3.11	4.89	4.50	5.55	4.72	3.54	3.57	4.11	3.72	4.72	5.43	4.87
Cr	-	-	0.06	-	-	-	-	-	-	-	-	-	-	-
Fe	3.82	4.60	4.62	4.92	5.39	6.32	4.64	4.02	3.61	3.78	4.00	4.06	5.87	5.84
Mn	0.57	0.08	0.08	0.05	0.10	0.06	0.09	0.03	0.08	0.05	0.06	0.09	0.07	0.09
Mg	6.13	4.75	5.94	4.58	4.14	2.88	4.88	5.81	6.06	5.84	5.64	5.43	3.16	3.58
Ca	-	-	0.08	-	-	-	-	-	-	-	-	-	-	-
Total	19.67	19.90	20.30	20.03	19.94	20.02	19.98	19.81	19.77	19.87	19.79	19.97	19.87	19.97

Chlorite Species Dia Pyc Dia Rip Bru Rip Pyc Dia Dia Dia Dia Pyc Rip Bru

1 - 7 Groundmass of spilite (Raven Gill Fm.). 8 - 10 Vein in spilite (Raven Gill Fm.).
 11 - 12 Amygdale in spilite (Raven Gill Fm.). 13 - 14 Detrital chlorite in Elvan Fm. sandstone.

Bru = brunsvigite; Dia = diabantite; Pyc = pycnochlorite; Rip = ripidolite.

* Total iron as Fe²⁺

Appendix 23: Electron probe microanalyses of plagioclase feldspar

	1	2	3	4	5	6	7	8	9	10
SiO ₂	66.17	67.89	68.08	68.32	68.30	67.40	66.96	66.98	67.93	67.57
TiO ₂	-	-	-	-	-	-	-	-	-	-
Al ₂ O ₃	18.28	18.78	19.68	18.47	19.08	19.32	19.10	18.78	19.42	19.18
FeO*	0.79	0.64	0.26	1.09	0.47	0.12	-	-	0.18	0.39
MnO	-	-	-	-	-	-	-	-	-	-
MgO	-	-	-	-	-	-	-	-	-	-
CaO	0.83	0.12	0.35	-	0.21	0.25	0.33	0.24	0.19	0.46
Na ₂ O	11.56	11.41	11.64	11.31	11.18	12.12	11.57	11.72	11.67	11.53
K ₂ O	0.21	0.18	0.14	0.15	0.10	-	-	0.08	-	-
Total	97.84	99.02	100.15	99.34	99.34	99.21	97.96	97.80	99.39	99.13
Number of ions on the basis of 32 oxygens										
Si	11.93	12.01	11.91	12.06	12.02	11.91	11.95	11.98	11.95	11.94
Ti	-	-	-	-	-	-	-	-	-	-
Al	3.88	3.92	4.06	3.84	3.96	4.03	4.02	3.96	4.03	3.98
Fe ²⁺	0.12	0.09	0.04	0.16	0.07	0.02	-	-	0.03	0.06
Mn	-	-	-	-	-	-	-	-	-	-
Mg	-	-	-	-	-	-	-	-	-	-
Ca	0.16	0.02	0.07	-	0.04	0.05	0.06	0.05	0.04	0.09
Na	4.04	3.91	3.95	3.87	3.81	4.15	4.00	4.06	3.98	3.95
K	0.05	0.04	0.03	0.03	0.02	-	-	0.02	-	-
Total	20.18	19.99	20.06	19.96	19.92	20.16	20.03	20.07	20.03	20.02
Mol. % Ab	95.06	98.49	97.53	99.23	98.45	98.81	98.52	98.31	99.01	97.77
An	3.76	0.50	1.73	-	1.03	1.19	1.48	1.21	0.99	2.23
Or	1.18	1.01	0.74	0.77	0.52	-	-	0.48	-	-

1 - 6 Spilite (Raven Gill Fm.). 7 - 8 Veins in spilite (Raven Gill Fm.).
 9 Dolerite (Raven Gill Fm.). 10 Vein in dolerite (Raven Gill Fm.).
 11 Amygdale containing pumpellyite, dolerite (Raven Gill Fm.). 12 - 15
 Detrital fragment in sandstone (Abington Fm.). 16 - 19 Detrital fragment
 in sandstone (Elvan Fm.). 20 Shale raft in sandstone (Elvan Fm.).

* Total iron as Fe²⁺.

cont.

Appendix 23: Electron probe microanalyses of plagioclase feldspar (cont.)

	11	12	13	14	15	16	17	18	19	20
SiO ₂	68.11	66.99	68.77	67.76	68.60	67.25	67.24	67.04	67.01	66.51
TiO ₂	-	-	-	-	-	-	-	-	0.12	-
Al ₂ O ₃	19.39	19.01	19.35	19.43	19.39	18.97	18.97	18.69	18.89	19.36
FeO*	0.30	-	-	0.11	0.20	-	-	-	-	0.19
MnO	-	-	-	-	0.12	-	-	-	-	-
MgO	-	-	-	-	-	-	-	-	-	-
CaO	-	0.96	0.16	0.34	0.19	0.13	0.13	0.22	0.20	1.12
Na ₂ O	12.02	11.22	11.69	11.86	11.53	11.31	11.31	11.55	11.26	11.56
K ₂ O	-	-	-	-	-	0.11	0.11	0.10	0.07	0.07
Total	99.82	98.18	99.97	99.50	100.03	97.77	97.76	97.59	97.56	98.81
Number of ions on the basis of 32 oxygens										
Si	11.95	11.94	12.01	11.92	11.98	12.01	12.00	12.01	11.99	11.83
Ti	-	-	-	-	-	-	-	-	0.02	-
Al	4.01	4.00	3.98	4.03	3.99	3.99	3.99	3.95	3.99	4.06
Fe ²⁺	0.04	-	-	0.02	0.03	-	-	-	-	0.03
Mn	-	-	-	-	0.01	-	-	-	-	-
Mg	-	-	-	-	-	-	-	-	-	-
Ca	-	0.18	0.03	0.06	0.03	0.02	0.02	0.04	0.04	0.21
Na	4.09	3.88	3.96	4.05	3.91	3.91	3.92	4.01	3.91	3.99
K	-	-	-	-	-	0.02	0.04	0.02	0.02	0.02
Total	20.09	20.00	19.98	20.08	19.95	19.98	19.97	20.04	19.96	20.14
Mol. % Ab	100	95.57	99.25	98.54	99.24	98.98	98.50	98.53	98.49	94.55
Mol. % An	-	4.43	0.75	1.46	0.76	0.51	0.50	0.98	1.01	4.98
Mol. % Or	-	-	-	-	-	0.51	1.00	0.49	0.50	0.47

1 - 6 Spilite (Raven Gill Fm.). 7 - 8 Veins in spilite (Raven Gill Fm.).
 9 Dolerite (Raven Gill Fm.). 10 Vein in dolerite (Raven Gill Fm.).
 11 Amygdale containing pumpellyite, dolerite (Raven Gill Fm.). 12 - 15
 Detrital fragment in sandstone (Abington Fm.). 16 - 19 Detrital fragment
 in sandstone (Elvan Fm.). 20 Shale raft in sandstone (Elvan Fm.).

* Total iron as Fe²⁺.

Appendix 24: Electron probe microanalyses of pyroxenes

	1	2	3	4	5	6	7	8	9	10	11
SiO ₂	49.66	49.43	48.68	48.72	48.62	48.54	49.01	51.21	48.59	48.99	47.58
TiO ₂	0.85	0.96	1.32	1.31	1.39	1.12	1.15	0.95	1.50	1.51	1.89
Al ₂ O ₃	3.15	3.37	5.10	4.78	4.42	4.45	2.98	2.10	4.75	4.44	6.04
Cr ₂ O ₃	0.25	0.13	0.33	0.22	0.16	0.33	-	0.15	0.31	-	0.39
FeO*	8.95	8.86	9.87	9.51	10.53	9.48	12.96	9.95	9.12	9.76	9.74
MnO	0.34	0.25	0.25	-	0.20	0.17	0.36	0.27	0.22	-	0.18
MgO	14.80	14.33	13.05	12.46	12.37	13.16	11.85	14.56	13.09	13.23	13.28
CaO	19.68	20.34	21.65	21.71	20.97	21.42	20.46	21.16	21.84	21.50	20.39
Total	97.67	97.67	100.25	99.40	98.68	98.68	98.77	100.37	99.42	99.43	99.63
Number of ions based on 6 oxygens											
Si	1.89	1.88	1.82	1.85	1.85	1.84	1.88	1.91	1.83	1.84	1.79
Al ^{iv}	0.11	0.12	0.18	0.15	0.15	0.16	0.12	0.09	0.17	0.16	0.21
Al ^{vi}	0.03	0.03	0.04	0.06	0.05	0.04	0.02	-	0.04	0.04	0.06
Ti	0.02	0.03	0.04	0.04	0.04	0.03	0.03	0.03	0.04	0.04	0.05
Fe ^{3+***}	0.02	0.02	0.05	-	0.01	0.05	0.03	0.03	0.04	0.03	0.03
Cr	0.01	-	0.01	0.01	0.01	0.01	-	-	0.01	-	0.01
Mg	0.84	0.81	0.73	0.70	0.70	0.74	0.68	0.81	0.73	0.74	0.74
Fe ²⁺	0.26	0.24	0.25	0.30	0.33	0.25	0.38	0.27	0.25	0.28	0.27
Mn	0.01	0.01	0.01	-	0.01	0.01	0.01	0.01	0.01	-	0.01
Ca	0.80	0.83	0.87	0.88	0.86	0.87	0.84	0.84	0.88	0.87	0.82
Total	3.99	3.97	4.00	3.99	4.01	4.00	3.99	3.99	4.00	4.00	3.99
Mg	43.5	42.0	38.0	37.2	36.8	38.7	34.9	41.1	38.2	38.5	39.4
Fe ^{***}	15.0	15.0	16.7	16.0	17.9	15.7	22.0	16.2	15.7	16.1	17.0
Ca	41.4	43.0	45.3	46.8	45.3	45.5	43.1	42.6	46.1	45.3	43.6

1 - 5 Detrital in Elvan Fm. sandstone. 6 - 11 Raven Gill Fm. dolerites.
Pyroxene variety 1 - 2 augite; 3 - 6 salite; 7 - 8 augite; 9 - 10 salite;
 11 augite.

* Total iron as Fe²⁺. ** Structural formulae calculated using charge-
 balance equation of Papike et al. (1974). *** (Fe²⁺+Fe³⁺+Mn).

Appendix 25: Electron Probe Microanalyses of Amphiboles

	1	2	3	4	5	6	7	8	9	10
SiO ₂	42.33	45.97	43.59	42.04	45.56	45.18	45.18	44.31	47.17	44.92
TiO ₂	1.99	1.18	1.20	1.57	1.40	0.79	1.07	0.83	1.29	1.79
Al ₂ O ₃	9.99	7.97	10.54	11.75	8.04	7.53	8.18	11.21	8.78	10.00
FeO*	15.05	13.23	12.02	11.24	13.39	14.22	13.48	11.60	12.73	13.39
MnO	0.27	0.49	0.17	0.12	0.36	0.49	0.32	0.17	0.39	0.26
MgO	12.99	14.65	13.84	14.94	14.13	14.05	13.44	13.65	14.55	13.65
CaO	10.02	10.19	11.74	11.14	10.68	10.74	11.50	12.09	10.74	11.23
Na ₂ O	1.00	0.94	2.77	2.02	1.12	0.80	1.10	1.29	2.80	1.55
K ₂ O	-	0.32	0.41	0.38	0.47	0.37	0.45	0.51	0.40	0.72
Total	93.66	94.95	96.27	95.19	95.15	94.17	94.74	95.66	98.84	97.59
Number of ions based on 23 oxygens										
Si	6.45	6.86	6.51	6.26	6.83	6.82	6.81	6.56	6.83	6.62
Al ^{iv}	1.55	1.14	1.49	1.74	1.17	1.18	1.19	1.44	1.17	1.38
Al ^{vi}	0.24	0.26	0.37	0.32	0.25	0.16	0.26	0.52	0.32	0.35
Ti	0.23	0.13	0.13	0.18	0.16	0.09	0.12	0.09	0.14	0.20
Fe ^{3+*}	0.56	0.27	-	0.42	0.19	0.54	0.28	0.27	-	0.06
Mg	2.95	3.26	3.08	3.31	3.16	3.16	3.02	3.01	3.14	3.00
Fe ²⁺	1.35	1.38	1.50	0.98	1.48	1.25	1.42	1.17	1.54	1.59
Mn	0.03	0.06	0.02	0.01	0.05	0.06	0.04	0.02	0.05	0.03
Ca	1.63	1.63	1.88	1.78	1.71	1.74	1.86	1.92	1.66	1.77
Na	0.29	0.27	0.78	0.58	0.32	0.23	0.32	0.37	0.79	0.44
K	-	0.06	0.08	0.07	0.09	0.07	0.09	0.10	0.07	0.13
$\frac{100 \text{ Mg}}{\text{Mg} + \text{Fe}^{2+} + \text{Fe}^{3+} + \text{Mn}}$	60.33	65.59	66.96	70.13	64.75	63.07	63.44	67.34	66.38	64.10

All analyses of detrital amphibole in Elvan Formation sandstones.
 1 Tschermakitic hornblende. 2 Magnesio-hornblende. 3 Edenitic hornblende.
 4 Magnesio-hastingsitic hornblende. 5 Magnesio-hornblende. 6 Magnesio-hornblende.
 7 Magnesio-hornblende. 8 Magnesio-hornblende. 9 Edenite. 10 Edenitic hornblende.

* Total iron as Fe²⁺. ** Structural formulae calculated using charge-balance equation of Papike et al. (1974).

Appendix 26: Electron probe microanalyses of phengites

	1	2	3	4	5
SiO ₂	46.99	45.45	47.36	45.31	46.03
TiO ₂	0.53	0.84	0.19	1.75	0.97
Al ₂ O ₃	29.44	33.26	33.33	33.97	33.96
FeO*	3.01	1.97	1.11	1.21	1.19
MnO	-	-	-	-	-
MgO	1.73	1.02	0.91	0.31	0.95
CaO	0.08	-	-	-	-
Na ₂ O	1.13	0.48	0.76	0.87	-
K ₂ O	9.01	9.39	9.28	9.34	10.23
Total	91.91	92.42	92.94	92.77	93.33
Number of ions based on 22 oxygens					
Si	6.51	6.23	6.40	6.17	6.23
Ti	0.06	0.09	0.02	0.18	0.10
Al	4.81	5.37	5.31	5.45	5.42
Fe ²⁺	0.35	0.23	0.13	0.14	0.14
Mn	-	-	-	-	-
Mg	0.36	0.21	0.18	0.06	0.19
Ca	0.01	-	-	-	-
Na	0.30	0.13	0.20	0.23	-
K	1.59	1.64	1.60	1.62	1.77
Total	13.99	13.89	13.83	13.86	13.85
Al	87.2	92.4	94.5	96.5	94.3
Fe	6.3	3.9	2.2	2.4	2.4
Mg	6.5	3.7	3.3	1.1	3.3
¹ Si	6.51	6.23	6.40	6.17	6.23
Al	1.49	1.77	1.60	1.83	1.77

* Total iron as Fe²⁺. ¹ Si:Al ratio in tetrahedral site.

All analyses of detrital phengite in Elvan Fm. sandstones.

Appendix 27: Sample preparation techniques for
graptolite reflectance study

The preparation of crushed graptolites or blocks (10-20 mm in length) containing complete specimens as cylindrical casts (30 mm in diameter by 20 mm depth) and subsequent polishing procedures follow methods detailed by Watson (1976, Appendix 4). FIXMA Serifix resin was used to produce casts. Reflectance measurements were obtained with a Leitz MPV microscope photometer connected to a Philips PM 8220 pen-recorder. A 6 volt, 15 watt, tungsten lamp provided light at a chosen wavelength of 546 nm. All reflectance values quoted were measured in Zeiss immersion oil, and calibrated with a diamond standard ($R_{00} = 5.23$).

Th QE660.H4



Fig. 24: Distribution of stratigraphical units (simplified) within the Leadhills Imbricate Zone. Thicknesses of Moffat Shales in excess of 65 m due to repetition by strike faulting. See Appendices 8-10 for geological sections and amounts of exposure in Bellgill Burn, Cleuch Burn and Kirk Gill.

